UNIVERSIDAD COMPLUTENSE DE MADRID
FACULTAD DE CIENCIAS GEOLÓGICAS
Departamento de Petrología y Geoquímica

TESIS DOCTORAL

Geoquímica de series metasedimentarias del Macizo Ibérico: contexto dinámico de la transición Ediacarense- Cámbrico

MEMORIA PARA OPTAR AL GRADO DE DOCTOR

PRESENTADA POR

José Manuel Fuenlabrada Pérez

Directores

Ricardo Arenas Martín
Sonia Sánchez Martínez
Carmen Galindo Francisco

Madrid, 2018

Geoquímica de series metasedimentarias del Macizo Ibérico:
Contexto dinámico de la transición Ediacarense - Cámbrico

Tesis Doctoral

José Manuel Fuenlabrada Pérez

UNIVERSIDAD COMPLUTENSE DE MADRID
FACULTAD DE CIENCIAS GEOLÓGICAS
Departamento de Petrología y Geoquímica

Madrid, 2017

UNIVERSIDAD COMPLUTENSE DE MADRID
Facultad de Ciencias Geológicas
Departamento de Petrología y Geoquímica

TESIS DOCTORAL

Geoquímica de series metasedimentarias del Macizo Ibérico: Contexto dinámico de la transición Ediacarense - Cámbrico

Tesis presentada para optar al grado de

Doctor en Ciencias Geológicas

José Manuel Fuenlabrada Pérez

(Madrid, 2017)

Directores:
Dr. Ricardo Arenas Martín
Dra. Sonia Sánchez Martínez
Dra. Carmen Galindo Francisco

UNIVERSIDAD COMPLUTENSE DE MADRID
Facultad de Ciencias Geológicas
Departamento de Petrología y Geoquímica

TESIS DOCTORAL

Geoquímica de series metasedimentarias del Macizo Ibérico: Contexto dinámico de la transición Ediacarense - Cámbrico

Tesis presentada para optar al grado de

Doctor en Ciencias Geológicas

José Manuel Fuenlabrada Pérez

(Madrid, 2017)

Dr. Ricardo Arenas Martín

Dra. Sonia Sánchez Martínez

Dra. Carmen Galindo Francisco

A Tere
A Laura
A Sergio

Que la fuerza os acompañe

Agradecimientos

A pesar de que mi nombre es seguramente el que más veces aparece a lo largo de toda esta tesis, nada de lo que aquí se presenta hubiera sido posible sin la ayuda de muchas personas que han querido acompañarme a lo largo de este apasionante viaje. A lo largo de estas pocas líneas, deseo expresar mi más sincero agradecimiento a todas esas personas que con su tiempo, dedicación, paciencia, esfuerzo y apoyo han hecho posible que esta tesis haya llegado a su fin.

Quisiera comenzar este capítulo de agradecimientos por las personas que han estado conmigo durante todo el viaje, y a las cuales les debo un reconocimiento muy especial, mis directores.

Gracias Ricardo. Por ese empujón inicial hace unos años, por tu dedicación, por tus explicaciones, por tu paciencia, por todo tu tiempo sin límites, por tus correcciones. Gracias por todas las palabras de aliento, de motivación, sin ellas todo hubiera sido mucho más difícil. Gracias por ser mi guía en esta experiencia, que ten por seguro será muy difícil de superar.

Gracias Sonia. Por animarme a seguir con esta locura, por tu tiempo dedicado a corregir todos los textos y a mejorar todas las figuras. Gracias por las amenas charlas durante todas las salidas de campo, has sido mi conexión con el mundo real entre tanta Geología.

Gracias Carmen. Por confiar en mí para trabajar contigo en el laboratorio. Gracias por enseñarme todo lo que sé de Geoquímica Isotópica, por fomentar desde el primer momento mi curiosidad científica, y por satisfacerla con tus respuestas a mis interminables preguntas. Han sido muchos años juntos y espero que sean muchos más.

Me gustaría igualmente agradecer de una manera especial a Rubén, amigo y compañero en toda esta tesis. Ha sido un verdadero placer coincidir contigo durante todo este tiempo. Desde que empezamos en Malpica, no has dejado de enseñarme cómo disfrutar de la Geología en el campo.

A lo largo de estos últimos años, he tenido la gran oportunidad de trabajar con un numeroso grupo de amigos. Ellos son todos los coautores de los trabajos que aquí se incluyen. Gracias, Ricardo, Sonia, Rubén, Pilar, Agustín, Martim, Francisco, José Brandão, Paco, Luis Miguel, Jerónimo, Alberto, José (Tánago), Antonio, Pedro, Jacobo, Alicia y Floro (te echamos de menos) por haberme permitido trabajar con todos vosotros. Una parte de esta Tesis es también vuestra.

Me gustaría agradecer la ayuda prestada por todo el Departamento de Petrología y Geoquímica de la Universidad Complutense de Madrid, que han puesto a mi servicio todas sus instalaciones, su ayuda y apoyo. Especialmente a Pilar y María José, por compartir mesa conmigo en Filología, por muchos y muy buenos momentos de sobremesa. Gracias Richard por ser un modelo a seguir. ¡No sabes lo que me ha facilitado las cosas que leyeras tu gran Tesis antes que yo! Espero seguir coincidiendo contigo en el futuro. Gracias por supuesto a Irene y Esther. Animaos a recorrer este camino, sin duda merece la pena.

Gracias a toda la gente que trabaja en el sótano. Gracias a mis compañeros del CAI de Técnicas Geológicas por su apoyo constante, especialmente a Isabel, de la que nunca dejará de sorprenderme la cantidad de conocimientos que ha ido acumulando a lo largo de su carrera profesional. A tu lado me siento pequeño. A los grandes profesionales que trabajan en el taller, por ayudarme en la preparación de las muestras. Gracias Carmen, Pedro y Marian. Gracias a Isabel, mi eterna compañera del café, la de charlas y sinsabores que has tenido que soportar. Gracias por tu amistad.

Gracias a Lidia por ayudarme con todo el eterno papeleo, no creo que hubiera logrado enterarme sin su experiencia. Gracias a Beatriz por su ayuda en el CAI, por ese buen rato de conversación amena cada miércoles, que a veces es como un verdadero oasis.

Agradezco también la gran labor realizada por todos y cada uno de los revisores de cada uno de los trabajos incluidos en esta Tesis. Su exhaustiva revisión de los manuscritos ayudó, sin duda, a la mejora del resultado final.

Gracias especiales a mis padres y hermanos. Gracias a ellos sé valorar mejor lo que se consigue con esfuerzo. Y a todos mis amigos, por intentar ocultar sus bostezos (casi no se os notaba) cuando les contaba de qué iba la tesis.

Gracias a mis hijos por su constante apoyo, por animarme en todo momento a ponerme delante del ordenador a expensas de su tiempo. Gracias por sus abrazos y sonrisas cuando no todo iba bien. Si yo he conseguido estar escribiendo este capítulo a mi edad, ¿qué no podréis conseguir vosotros? Os quiero.

Y por último, gracias Tere. Gracias por compartirlo todo, lo bueno y lo no tan bueno. Gracias por tu inagotable paciencia. Este viaje no habría llegado a su destino sin tu ayuda. Gracias por viajar conmigo.

Esta Tesis Doctoral se ha financiado con cargo a los siguientes proyectos del Plan Nacional de I+D+i (Ministerio de Economía y Competitividad): CGL2007-65338-CO2-01/BTE (2007-2012), CGL2012-34618 (2013-2015) y CGL2016-76438-P (2016-2020).

Índice

Resumen

El Macizo Ibérico contiene una excelente representación de la estratigrafía del Paleozoico Inferior, así como de la transición con el Neoproterozoico Superior. La geoquímica de las series siliciclásticas (elementos mayores y trazas) y sus fuentes isotópicas (Sm-Nd) han sido muy poco investigadas hasta tiempos recientes, a pesar de que estos aspectos son importantes a la hora de conocer el contexto dinámico de las cuencas y su ubicación en el paleomargen de Gondwana. En esta tesis se presenta un estudio basado en estas metodologías y tiene como objetivo principal la investigación de las series estratigráficas que definen la transición entre el Cámbrico Inferior y el Ediacarense. Las series estudiadas corresponden a las Unidades Alóctonas Superiores y a las Unidades Alóctonas Basales del NW, al Cámbrico Inferior y Alcudiense del sector meridional de la Zona Centroibérica y a las Unidades Alóctonas Basales del SW. La labor realizada se ha sintetizado en varios trabajos ya publicados, que se han incluido en esta memoria y representan su contenido fundamental. La memoria se ha completado además con unos apartados introductorios de contenido metodológico y un capítulo final que presenta una síntesis de resultados a escala del Macizo Ibérico.

Los resultados obtenidos indican como conclusión general, un cambio significativo en la influencia de un arco volcánico Cadomiense sobre los procesos sedimentarios que tenían lugar en el margen de Gondwana y por consiguiente, sobre la composición química de las secuencias sedimentarias siliciclásticas ediacarenses y cámbricas. Este cambio supuso una evolución progresiva del contexto deposicional, probablemente ligado a la apertura y ensanchamiento de una extensa cuenca *back-arc*. Esta apertura ocasionó durante el Paleozoico más inferior un progresivo alejamiento de las cuencas sedimentarias del foco principal de la actividad magmática, cuya actividad era también aparentemente decreciente, y una evolución muy lenta pero continua hacia un margen pasivo durante la mayor parte del Cámbrico. La transición es especialmente evidente en la geoquímica (elementos mayores y trazas) de las secuencias sedimentarias del Cámbrico Inferior y del Alcudiense (Ediacarense) del sector meridional de la Zona Centroibérica. También es patente en la composición de las secuencias detríticas de las Unidades Alóctonas Basales del NW de Iberia. La investigación de las fuentes isotópicas (Sm-Nd) refleja la misma evolución geodinámica de los terrenos peri-Gondwánicos entre el Ediacarense y el Cámbrico. Es particularmente visible en el caso de las secuencias metasedimentarias de la Zona Centroibérica, donde la evolución de los valores de εNd indican una menor influencia del arco volcánico durante la sedimentación de las series cámbricas. Las T_{DM} más antiguas registradas en estas secuencias del Cámbrico Inferior (1444 - 1657 Ma), son compatibles con un incremento de los aportes desde áreas fuente gondwánicas antiguas y una disminución de los aportes juveniles procedentes del arco volcánico.

Teniendo en cuenta los resultados anteriores y la distribución conocida de los terrenos de edad ediacarense y de las masas cratónicas en el norte de África, en este trabajo se propone un modelo de reconstrucción paleogeográfica, para la posición de los terrenos peri-Gondwánicos representados en el Macizo Ibérico durante la transición Ediacarense - Cámbrico. Según este modelo, los diferentes terrenos que en la actualidad forman parte de un gran apilamiento de mantos de cabalgamiento, ocuparían originalmente posiciones laterales relativas

dentro de una extensa cuenca *back-arc*. Las edades modelo registradas permiten posicionar todos los terrenos entre un arco volcánico activo, que ocuparía la posición más externa en el margen, y diferentes sectores en las proximidades del Cratón del Oeste de África (COA). Las cuencas originarias de las series estudiadas en el Macizo Ibérico pueden posicionarse entre sí con cierta claridad. De este modo, las características geoquímicas e isotópicas han permitido establecer criterios claros de correlación entre las Unidades Alóctonas Basales del NW y SW del Macizo Ibérico. Las T_{DM} observadas en el conjunto de las Unidades Basales son muy antiguas (1499 - 2156 Ma), claramente mayores que las de las secuencias sedimentarias de edad similar de la Zona Centroibérica (1256 - 1334 Ma). Todas las Unidades Basales del Macizo Ibérico proceden pues de un único dominio paleogeográfico muy próximo a Gondwana, del que recibirían un aporte dominante de materiales corticales antiguos. Las cuencas sedimentarias originales debieron situarse en una periferia muy próxima al COA, ya que esta es la unica interpretación posible para explicar los valores muy antiguos de T_{DM} que se han encontrado. Las cuencas sedimentarias donde se depositaron las series del dominio autóctono relativo (Zona Centroibérica), ocuparon posiciones más alejadas en relación al COA, probablemente desplazadas hacia sectores más orientales del paleomargen de Gondwana. Finalmente, los valores de εNd positivos y las T_{DM} bastante más jóvenes de las Unidades Alóctonas Superiores del NW de Iberia (720 - 1215 Ma), sitúan su procedencia en posiciones muy cercanas al arco volcánico activo pero siempre dentro de la cuenca *back-arc*. El arco volcánico sería el área fuente del abundante material juvenil que resulta necesario para explicar los valores de T_{DM} característicos de estas unidades.

Una conclusión fundamental de este trabajo es que la investigación combinada usando geoquímica de elementos mayores y trazas y geoquímica isotópica (Sm-Nd), representa una herramienta siempre útil a la hora de estudiar el contexto dinámico de deposición y las áreas fuente de series siliciclásticas antiguas. El valor de estas metodologías es aun mayor para el estudio de series azoicas, deformadas y metamorfizadas, donde la aplicación de un análisis estratigráfico o paleontológico tradicional es virtualmente imposible.

Abstract

The Iberian Massif contains an excellent representation of the Lower Paleozoic stratigraphy, as well as its transition to the Upper Neoproterozoic. The geochemistry (major and trace elements) of the siliciclastic series and their isotopic sources (Sm-Nd) have been scarcely investigated until recently, even though these aspects are important to infer the geodynamic context of the sedimentary basins and their location along the paleomargin of Gondwana. This PhD Thesis presents a study based on these methodologies, whose main objective is the investigation of the stratigraphic series that define the transition between Lower Cambrian and Ediacaran times. The studied series correspond to the Upper Allochthonous Units and the Basal Allochthonous Units of NW Iberia, the Lower Cambrian and Alcudian series from the southern sector of the Central Iberian Zone and to the SW Basal Allochthonous Units of the Iberian Massif. The whole research has been synthesized in several works already published, which have been included in this PhD Thesis constituting its main content. The document has also been completed with an introductory section incorporating the description of the used methodology and a final chapter that presents a synthesis of the conclusions within the geological frame of the Iberian Massif.

As a general conclusion, the obtained results indicate a significant change in the influence of a Cadomian volcanic arc on the sedimentary processes that took place along the Gondwana margin and consequently, on the chemical composition of the Ediacaran and Cambrian siliciclastic sequences. This change meant a progressive evolution of the depositional context, probably linked to the opening and widening of an extensive back-arc basin. During the Lower Paleozoic, this opening caused a progressive separation of the sedimentary basins from the main focus of the magmatic activity, which apparently was also decreasing, and a very slow but continuous evolution towards a passive margin during most of the Cambrian. The transition is especially evident regarding the geochemistry (major and trace elements) of the Lower Cambrian and Alcudian (Ediacaran) sedimentary sequences of the southern sector of the Central Iberian Zone. It is also very noticeable in the composition of the detrital sequences of the Basal Allochthonous Units of NW of Iberia. The investigation of the isotopic sources (Sm-Nd) reflects the same geodynamic evolution of the peri-Gondwanan terranes between Ediacaran and Cambrian times. It is particularly visible in the case of the metasedimentary sequences of the Central Iberian Zone, where the evolution of εNd values indicates a lower influence of the volcanic arc during the sedimentation of the Cambrian series. The older T_{DM} recorded in the Lower Cambrian sequences (1444 - 1657 Ma), are compatible with an increase in the contributions from older Gondwana sources and a decrease in the juvenile contributions from the volcanic arc.

In the light of former results regarding the known distribution of the Ediacaran terranes and the cratonic masses in North Africa, this PhD Thesis proposes a paleogeographic reconstruction model for the location of the peri-Gondwanan terranes represented in the Iberian Massif during the Ediacaran - Cambrian transition. According to this model, the different terranes, that are currently part of a stack of nappes, would originally occupy lateral positions within an extensive back-arc basin. The recorded model ages allow us to locate all the terranes relative to an active volcanic arc, which would cover the outermost position in the

margin and various sectors in the proximity of the West African Craton (WAC). The original basins of the studied series from the Iberian Massif can be placed with some clarity. In this way, the geochemical and isotopic features have enabled us to establish a clear criterion of correlation between the NW and SW Basal Allochthonous Units in the Iberian Massif. The T_{DM} observed in the Basal Units as a whole are very old (1499 - 2156 Ma), clearly greater than those from sedimentary sequences of similar age from the Central Iberian Zone (1256 - 1334 Ma). Thus, all the Basal Units of the Iberian Massif would come from a single paleogeographic domain, very close to Gondwana, from which they would receive a dominant contribution of old crustal materials. The original sedimentary basins had to be located very close to the WAC, since this is the only possible interpretation to explain the very old T_{DM} that have been found. The sedimentary basins, where the series of the relative Autochthonous domain (Central Iberian Zone) were deposited, occupied more distant positions in relation to the WAC, probably displaced towards more oriental sectors along the paleomargin of Gondwana. Finally, the positive values of εNd and the much younger T_{DM} of the Upper Allochthonous Units of NW Iberia (720 - 1215 Ma), places their origin in positions very close to the active volcanic arc, but always within the back-arc basin. This volcanic arc would be the source of the abundant juvenile material needed to explain the T_{DM} values, typical of these units.

A fundamental conclusion of the present work is that the combined research, using geochemistry of major and trace elements and isotopic geochemistry (Sm-Nd), represents a critical tool when studying the geodynamic context of deposition and the source areas of old siliciclastic series. The value of these methodologies is even greater for the study of azoic, altered and metamorphic series, where the application of a traditional stratigraphic or paleontological analysis is virtually impossible.

Capítulo 1

Introducción y objetivo general

1.1 Introducción

Un procedimiento habitual para investigar la paleogeografía previa a la formación de cualquier orógeno, consiste en estudiar las características de las series sedimentarias involucradas en el mismo (*Pettijohn et al., 1972; Crook, 1974; Dickinson y Suczek, 1979; Bhatia, 1983; Roser y Korsch, 1986, 1988; Floyd et al., 1987; Wronkiewicz y Condie, 1987; Johnsson, 1993*). De manera particular, las series siliciclásticas representan un valioso registro del contexto dinámico existente durante su depósito y también de las fuentes isotópicas implicadas en su formación (áreas fuentes) (*Dickinson et al., 1983; Dickinson, 1985 y 1988; Heller et al., 1985; Bhatia y Crook, 1986; McLennan et al., 1990, 1993 y 1995; Floyd et al., 1991; Maas y McCulloch, 1991; Cullers et al., 1997*). Las rocas siliciclásticas tienen una composición química característica, controlada en general por cuatro factores esenciales: (i) el contexto tectónico en el que se produjo la formación de las cuencas; (ii) la naturaleza de las áreas fuentes; (iii) las características climáticas, que condicionan tanto el volumen erosivo como el tipo e intensidad del transporte sedimentario; y (iv) la naturaleza del sistema sedimentario en general y de los sedimentos de manera particular. Estos factores y sus interacciones condicionan la implicación de las áreas fuentes, los procesos de meteorización (tanto química, como física), la granoclasificación y el grado de reciclado que sufren los sedimentos clásticos durante su transporte desde las áreas fuentes hasta las cuencas sedimentarias, el tamaño de grano y finalmente los posibles procesos de alteración diagenética y/o hidrotermal, capaces de modificar en diferente grado la composición química final (*Nesbitt y Young, 1982 y 1996; Condie et al., 1992; Johnsson, 1993; McLennan et al., 1993; Cullers, 1994 y 1995; Cox et al., 1995; Fedo et al., 1995; Nesbitt et al., 1996; Price et al., 2003*).

Los procesos de interacción entre los factores anteriores son complejos y sus resultados implican una difícil correlación entre las áreas fuente y las características mineralógicas y composicionales observadas en las rocas sedimentarias resultantes (*Jonhsson, 1993*). Sin embargo, varios autores han observado y registrado un evidente paralelismo entre la procedencia, el contexto tectónico en el que se ubican las paleocuencas sedimentarias y la composición química que presentan las series siliciclásticas (*Bhatia y Crook, 1986; Roser y Korsch, 1986; Winchester y Max, 1989; Floyd et al., 1991*). Este hecho sugiere que los procesos de erosión, transporte y sedimentación ligados a contextos tectónicos particulares se comportan de una manera similar, lo que confiere a los sedimentos terrígenos unas características distintivas que varían de un ambiente tectónico a otro (*Bhatia, 1983; Bhatia y Crook, 1986; McLennan et al., 1990; Jonhsson, 1993; McLennan et al., 1993*). Estas singularidades permiten buscar analogías entre series generadas en un ambiente tectónico conocido y otras cuyo origen es incierto y motivo de investigación. El objetivo final de esta comparación es conocer las condiciones en las que se produjo la sedimentación de las series problemáticas investigadas.

La información geoquímica registrada en los sedimentos terrígenos es particularmente relevante a la hora de investigar el ambiente tectónico y las fuentes isotópicas (*Bhatia, 1983 y 1985; Heller et al., 1985; Roser and Korsch, 1986; McLennan et al., 1990 y 1995; Maas y McCulloch, 1991*). Este hecho, bien establecido, hace que estas series tengan una gran importancia para el conocimiento de sistemas muy antiguos, azoicos o intensamente deformados y/o metamorfizados (*O'Nions et al., 1983; Miller y O'Nions, 1984; Nelson y DePaolo, 1988a; Linnemann et al., 2002 y 2004*). *McLennan et al. (1993)* señalaron las ventajas que presenta la aproximación geoquímica para el estudio de las rocas sedimentarias: (i) su aplicabilidad a rocas sedimentarias tanto de grano fino como grueso; (ii) su utilidad en rocas mineralógicamente alteradas, siempre y cuando esta alteración no afecte de modo significativo a la composición química total de la roca, posibilitando la evaluación de procesos sedimentarios secundarios; (iii) la elevada precisión en la determinación y estudio de determinados elementos traza e isótopos, que permite la identificación de componentes menores no reconocibles petrográficamente; (iv) la evaluación del origen y la evolución geoquímica de la roca; y por último (v) la utilización de datos isotópicos permite delimitar la edad de las áreas fuentes y la evolución temporal de los sedimentos.

Debido a las posibilidades que plantea la investigación geoquímica de las series siliciclásticas, son muchos los trabajos que se han centrado en el estudio de las abundancias de determinados elementos traza que muestran un comportamiento relativamente inmóvil en los procesos de meteorización y transporte, con ausencia de alteración en su transferencia desde el área fuente a las cuencas sedimentarias, lo que proporciona una valiosa información acerca de la procedencia y el contexto geodinámico en el que se produjo la sedimentación (*Bhatia y Crook, 1986; Winchester y Max, 1989*). De un modo análogo, otros trabajos han investigado la información que proporcionan determinados isótopos radiogénicos, capaces de delimitar la procedencia primaria de los depósitos siliciclásticos y por tanto de acceder a las claves de la evolución cortical, como ocurre en el caso particular de los isótopos de Nd (*McCulloch and Wasserburg, 1978; O'Nions et al., 1983; Taylor et al., 1983; Miller et al., 1986; McLennan et al., 1989; Gleason et al., 1994; McLennan et al., 1995*). En este caso, es importante tener en cuenta que el fraccionamiento más importante del Sm y el Nd se produce en los procesos de cristalización desde un fundido mantélico, para formar las rocas plutónicas y volcánicas que se exponen posteriormente en la corteza continental (*DePaolo y Wasserburg, 1976; Goldstein et al., 1984; DePaolo, 1988*). La edad modelo de Nd de las rocas siliciclásticas corresponde al promedio de la edad de extracción desde el manto de los diferentes componentes detríticos derivados de los procesos erosivos que afectaron a las áreas fuente (*McLennan et al., 1993*). En términos prácticos, las edades modelo de Nd determinadas nos proporcionan información acerca de la composición isotópica de las rocas investigadas. Estos valores representarían una media de los aportes relativos de materiales juveniles (derivados del manto o de una corteza continental recién formada), en relación con materiales procedentes de una corteza continental más antigua (*O'Nions et al., 1983; Arndt y Goldstein, 1987; Nelson y DePaolo, 1988b; McLennan et al., 1989; McLennan y Hemming, 1992; Murphy y Nance, 2002*).

El Macizo Ibérico está constituido por una gran variedad de series sedimentarias depositadas en los dominios Gondwánicos y peri-Gondwánicos. Las rocas sedimentarias/metasedimentarias son las litologías casi exclusivas en las zonas más externas y su superficie de afloramiento, siempre muy importante, se reduce hacia las zonas internas, donde la presencia de litologías ortoderivadas prevariscas o granitoides variscos se va haciendo progresivamente mayor (*Farias, 1990; Rodríguez Aller, 2005; Díez Montes, 2007; Talavera, 2009; Díez Fernández, 2011; Rubio Pascual, 2013; y referencias en ellas incluidas*). La estratigrafía, paleontología y la evolución tectonometamórfica de estas series son complejas, pero han sido objeto de una intensa investigación, especialmente durante los últimos 50 años. No obstante, el estudio de sus características geoquímicas e isotópicas ha sido escasamente abordado, a pesar de que su potencialidad es muy grande a la hora de avanzar en el conocimiento de la paleogeografia del Paleozoico y de la naturaleza de las áreas fuentes implicadas. Este es especialmente el caso de las series constituidas por rocas sedimentarias siliciclásticas de tipo turbidítico (*Bouma, 1962 y 2004; Zavala y Arcuri, 2016; y referencias incluidas*). La pequeña atención prestada a estas cuestiones queda patente cuando se compara la escasísima bibliografía existente sobre estos aspectos, con la gran cantidad de trabajos que describen la estratigrafía, paleontología, tectónica y/o evolución metamórfica de las series metasedimentarias de las zonas externas e internas del orógeno.

1.2 Objetivo general

Los trabajos incluidos en esta Tesis Doctoral pretenden completar el amplio estudio que se ha venido realizando en las series metasedimentarias del Macizo Ibérico desde otros planteamientos más clásicos. El objetivo general de esta Tesis Doctoral es el estudio de la composición geoquímica convencional e isotópica (Sm-Nd) de las series siliciclásticas que definen la transición Ediacarense – Cámbrico Inferior en diferentes sectores del Macizo Ibérico. Para ello se han seleccionado algunas series poco afectadas por metamorfismo y deformación, evitando en la medida de lo posible la alteración de los sistemas químicos e isotópicos. Estas series afloran en el NW y SW del Macizo Ibérico y también en su dominio más central (*Díaz García, 1990; Ugidos et al., 1997a y 1997b; Valladares et al., 2000; Fernández-Suárez et al., 2003 y 2014; Pereira et al., 2006; Díez Fernández et al., 2010 y 2017; Albert et al., 2015a*). La estructuración del Macizo Ibérico tuvo lugar durante los episodios finales del ensamblado de Pangea, ligados a una colisión con fuerte componente lateral entre Gondwana y Laurussia durante el Devónico y el Carbonífero (*Matte, 1986 y 1991; Stampfli et al., 2002 y 2013; Martínez Catalán et al., 2007 y 2009; Arenas et al., 2009 y 2014;*

Díez Fernández et al., 2012a, 2015 y 2016; y referencias en ellas incluidas). Actualmente, las series seleccionadas forman parte de la extensa zona de sutura existente en el Macizo Ibérico (*Díez Fernández y Arenas, 2015; Arenas et al., 2016a*), definida por varios terrenos alóctonos con ofiolitas (*Sánchez Martínez, 2009; Sánchez Martínez et al., 2009*) y unidades de alta presión, así como de los dominios autóctonos situados estructuralmente más abajo (*Arenas et al., 2016b; y referencias en ella incluidas*). Las conclusiones principales que se han obtenido en esta Tesis indican con claridad que la transición Ediacarense – Cámbrico en el dominio peri-Gondwánico investigado tuvo lugar en un contexto de arco magmático. Distintos aspectos del origen y evolución durante el Neoproterozoico y el Paleozoico más temprano del sistema de arcos y de las secciones próximas del margen de Gondwana, quedan registrados en las series sedimentarias siliciclásticas coetáneas. Sus características geoquímicas e isotópicas particulares ofrecen la posibilidad de delimitar tanto sus áreas fuente, como el contexto geodinámico preciso en el que se produjo la sedimentación, y por consiguiente avanzar en la paleogeografía del Paleozoico en el contexto peri-Gondwánico.

Capítulo 2

Metodología

Los trabajos presentados en esta Tesis Doctoral incorporan una gran cantidad de resultados analíticos, que conforman la base del estudio geoquímico de las series siliciclásticas seleccionadas y proporcionan las claves para las conclusiones obtenidas. Dadas las características de este tipo de técnicas, resulta conveniente describir la metodología utilizada en los trabajos de laboratorio. Por ello, a continuación se incluyen breves descripciones de los procedimientos seguidos para la obtención de los resultados analíticos alcanzados, haciendo especial énfasis en la técnica de análisis isotópico Sm-Nd, realizada por el propio autor, y que conforma la base de muchas de las conclusiones aquí expuestas.

2.1 Preparación de muestras geológicas

Las características petrográficas de las muestras analizadas fueron estudiadas detenidamente, como un paso necesario para conocer sus texturas, mineralogía y otros aspectos de su evolución tectonotermal, así como para descartar la presencia de alteraciones significativas de la composición química original. Para ello, se han preparado secciones delgadas de todas las muestras recogidas, así como se han tenido en cuenta las muestras y trabajos petrográficos previos generados en nuestro equipo de investigación en relación a las series siliciclásticas investigadas.

Previo al tratamiento analítico de las muestras recogidas en las diferentes regiones estudiadas, éstas fueron preparadas en los Laboratorios de Preparación de Muestras del Departamento de Petrología y Geoquímica de la Facultad de Ciencias Geológicas (UCM). La preparación rutinaria de muestras para análisis químicos (elementos mayores y trazas) e isotópicos comprende el lavado y retirada de restos biológicos que puedan existir en el exterior de las rocas, así como la retirada de cualquier parte de la muestra que muestre alteración significativa. A continuación, fragmentos de roca del tamaño aproximado de un puño se trituran en un molino de mandíbulas de acero. Tras este paso, fracciones de la muestra con un tamaño aproximado de entre 2 y 3 centímetros se pasan por un molino de discos de acero de tungsteno, graduando la separación de los discos para conseguir el tamaño de grano deseado. El polvo resultante del paso anterior se cuartea hasta conseguir una fracción representativa del total y posteriormente se pulveriza en un mortero de ágata. El resultado obtenido se pasa por un tamiz de nylon de 100 micras, para recuperar únicamente la fracción con granos menores de ese tamaño y que aseguran posteriormente una buena disolución de la muestra, necesaria para las sistemáticas analíticas utilizadas en esta Tesis.

2.2 Análisis geoquímico de roca total

2.2.1 Introducción

Las rocas siliciclásticas representan un registro temporal completo de la composición química de la corteza continental superior (*Taylor y McLennan, 1985; McLennan y Taylor, 1991; Condie, 1993; McLennan, 2001; Hawkesworth et al., 2010*). Este registro brinda la oportunidad de descifrar las claves que permitan comprender los procesos que tuvieron lugar durante la sedimentación y consolidación de dichas rocas (*McLennan et al., 1993*). Las series metasedimentarias estudiadas presentan un bajo grado de alteración en procesos post-deposicionales, lo que se traduce en la ausencia de modificaciones importantes de las características químicas. Características heredadas desde las áreas fuente gracias a una transferencia química cuantitativa y a la permanencia del sistema químico como un conjunto relativamente hermético (*Bhatia y Crook, 1986; McLennan, 1989; Nesbitt et al., 1996*).

Existe una variabilidad importante en las propiedades relativas a la movilidad de los diferentes elementos químicos, que lógicamente se relaciona con sus características químico-físicas (*Henderson, 1982*). Determinados elementos mayores y menores resultan muy móviles durante los procesos de meteorización, transporte sedimentario, diagénesis y metamorfismo (*Nesbitt et al., 1980; Cullers, 1995*). Por lo tanto, deben utilizarse con cautela en la obtención de conclusiones acerca de la composición química del área fuente o del contexto tectónico en el que tuvo lugar la sedimentación (*Armstrong-Altrin y Verma, 2005; Verma y Armstrong-Altrin, 2016*). Por el contrario, existen numerosas evidencias de una relativa ausencia de modificaciones en las abundancias de algunos elementos menores y traza durante los procesos comentados anteriormente, lo que permite obtener una información precisa de su procedencia (*McLennan et al., 1991 y 1993*). Elementos químicos tales como las Tierras raras (REE: Rare Earth Elements), Hf, Ti, Cr, Co, Zr, Nb, Ta, Y, Th y Sc proporcionan un excelente factor discriminante de la procedencia y del ambiente geodinámico en el que se produjo la sedimentación de las rocas siliciclásticas (*Bhatia y Crook, 1986*). De igual manera, las relaciones entre elementos compatibles o incompatibles nos permiten conocer aspectos importantes acerca de la procedencia de estas rocas (*McLennan et al., 1993*). De un modo análogo, los patrones de distribución de las REE en rocas detríticas indican las afinidades continentales de sus precursores tras la homogenización debida a los procesos erosivos y sedimentarios (*Taylor y McLennan, 1985; McLennan, 1989; McLennan y Hemming, 1992*).

2.2.2 Geoquímica de elementos mayores y trazas

Los análisis químicos de elementos mayores y trazas que se han utilizado en esta Tesis Doctoral (78 muestras) se han realizado en los laboratorios ACTLABS de Ontario, en Canada (*Activation Laboratories Ltd., http://www.actlabs.com/*), siguiendo en su totalidad el método analítico denominado

4Lithores - Lithium Metaborate/Tetraborate Fusion - ICP and ICP/MS. La sistemática analítica utilizada asegura una completa puesta en disolución de las muestras y un preciso análisis de los elementos mayores y traza. El método de disolución utilizado consistió en una fusión con metaborato y tetraborato de litio en un horno de inducción. La mezcla fundida se puso inmediatamente en contacto con una solución de ácido nítrico (5%), que contenía un estándar interno, mezclando continuamente hasta la disolución total de la muestra silicatada (aproximadamente 30 minutos). Las muestran diluidas se analizaron con un equipo de espectrometría de masas con una fuente de ionización por plasma de acoplamiento inductivo (*ICP-MS, modelo Perkin Elmer Sciex ELAN 6000®, 6100® o 9000®*). Durante el proceso completo, se aseguró la bondad de los análisis y la ausencia de contaminación externa al proceso con el análisis simultáneo de blancos de preparación, controles internos, duplicados de muestras seleccionadas y materiales estándar certificados. La calidad de los análisis obtenidos es alta y la precisión general se calcula en aproximadamente 0.01%, con precisiones más altas (ca. 0.001%) para MnO y TiO_2.

2.3 Análisis isotópico (Sm-Nd)

La sistemática isotópica utilizada en esta Tesis ha sido la geoquímica isotópica de Sm y Nd. Esta sistemática se ha llevado a cabo en su totalidad en el Centro de Asistencia a la Investigación de Geocronología y Geoquímica Isotópica de la Universidad Complutense de Madrid (UCM-CEI) (*https://www.ucm.es/geocronologia*). Para ello, se ha empleado la técnica de análisis mediante dilución isotópica por espectrometría de masas de ionización termal (ID-TIMS). Esta técnica sofisticada nos ha permitido conocer las concentraciones precisas de ambos elementos y la composición isotópica del Nd en la misma fracción de la muestra. En esta Tesis Doctoral se presentan los resultados isotópicos Sm-Nd de un total de 78 muestras. A continuación, y previo a la descripción del método analítico seguido, se resumen las bases teóricas de esta sistemática y de los cálculos llevados a cabo para la obtención de los parámetros de utilidad para la consecución de los objetivos planteados en el presente trabajo de Tesis.

2.3.1 Base teórica

Los isótopos radiogénicos se han utilizado ampliamente en los últimos tiempos para llevar a cabo estudios geocronológicos, estratigráficos y de procedencia en rocas sedimentarias, con la intención de ayudar a delimitar los cambios temporales producidos en la superficie terrestre y los procesos que los causan (*O'Nions et al., 1983; Taylor et al., 1983; Miller et al., 1986; McLennan et al., 1989, 1990 y 1995; Gleason et al., 1994; Cullers et al., 1997; Murphy y Nance, 2002*). Esto es debido a que la composición isotópica de los materiales terrestres cambia con el tiempo, lo que está causado en mayor medida por procesos de desintegración radiactiva, interacciones cosmogénicas o fraccionamiento de masas (*Blum, 1995; Dickin, 1995; Dunai, 2010*).

2.3.1.1 Geoquímica Sm-Nd

El Sm y el Nd son elementos que pertenecen al grupo de las REE, con números atómicos (Z) de 62 y 60, respectivamente. Los elementos pertenecientes a este grupo forman generalmente iones con cargas 3+ (con excepciones como Eu^{2+} o Ce^{4+}, bajo determinadas condiciones), y sus radios decrecen proporcionalmente al incremento de su número atómico, desde el Lantano (La, Z=57) con un radio atómico de 1.15 Å, al Lutecio (Lu, Z=71), con un radio atómico de 0.93 Å (*McLennan, 1989; Faure y Mensing, 2005*). El Sm tiene siete isótopos naturales, de los cuales tres son radiactivos. De estos tres isótopos, únicamente el ^{147}Sm sufre una desintegración tipo-α, con una vida media equivalente a una constante de desintegración (λ) de $6.54*10^{-12}$ $años^{-1}$ (*Lugmair y Marti, 1978*), lo suficientemente corta como para producir una variación cuantificable en la abundancia de su isótopo hijo (^{143}Nd) en un periodo de tiempo de 10^8 años o más (*O'Nions et al., 1979*).

El radio iónico de las REE y su relativamente elevada carga hace que estos elementos sean considerados moderadamente incompatibles, siendo el Nd ligeramente más incompatible que el Sm (*Sun y McDonough, 1989*), y que por tanto no se incorporen fácilmente a la red cristalina de algunos minerales. A pesar de todo ello, las REE reemplazan a iones de elementos mayores (*Henderson, 1984; McLennan, 1989*), encontrándose presentes en muchos de los minerales más comunes y formando parte de inclusiones de determinados minerales accesorios (*Faure y Mensing, 2005*). Estos minerales ejercen una importante selectividad a la hora de incluir estos elementos dentro de su estructura cristalina, por lo que determinados minerales, como feldespato, biotita o apatito tienden a concentrar Tierra Raras ligeras (LREE), grupo al cual pertenecen el Sm y Nd; mientras que el piroxeno, anfíbol y granate concentran por el contrario Tierras Raras pesadas (HREE). Esta selectividad a la hora de concentrar ambos tipos de REE tiene un importante reflejo en las abundancias presentes en las rocas que forman dichos minerales, observándose a veces amplias variaciones (*Faure y Mensing, 2005*). El comportamiento geoquímico diferenciado del Sm y Nd es fruto de la denominada "*contracción de los lantánidos*" (*Henderson, 1984*), como resultado de una disminución constante del tamaño, a lo largo de la serie del Lantano al Lutecio, y que tiene su explicación en la distribución de los electrones en el orbital *f* de estos elementos, lo cual dictamina su comportamiento químico. Como consecuencia, el radio iónico del Sm^{3+} (1.04 Å) es menor que el del Nd^{3+} (1.08 Å), aún teniendo este último un número atómico menor. Esto hace que el radio iónico de la mayor parte de las REE trivalentes sea similar al del Ca^{2+}, Th^{4+} y U^{4+}, siendo este hecho clave en el comportamiento de las REE durante los procesos petrogenéticos, al reemplazar a elementos con radio iónico similar. A pesar de que la diferencia en el radio iónico del Sm y Nd es mínima, tiene consecuencias en la química de ambos elementos. El Nd tiende a concentrarse en la fase líquida durante la fusión parcial de los minerales silicatados, mientras que el Sm permanece en los sólidos residuales (*Faure y Mensing, 2005*). Por otra parte, su elevada valencia favorece fuertes enlaces, que junto con su tendencia a rodearse de radicales OH-, hace que este grupo sea relativamente poco soluble y por tanto presente una baja movilidad (*White, 1995*).

2.3.1.2 Notación épsilon-Nd (εNd)

Las propiedades químicas similares del Sm y Nd hacen posible que el fraccionamiento durante los procesos de cristalización y fusión sea relativamente bajo (*Dickin, 2005*), lo que supone bajas desviaciones de la relación $^{143}Nd/^{144}Nd$ con respecto a la elevada pendiente de la línea de evolución de CHUR (*chondritic uniform reservoir - DePaolo y Wasserburg, 1976a*). Esta observación condujo al desarrollo de la notación εNd (*épsilon-Nd*), que representa la desviación de la relación inicial $^{143}Nd/^{144}Nd$ con respecto al valor del condrito (*DePaolo y Wasserburg, 1976b; Jacobsen y Wasserburg, 1980 y 1984*). Debido a que dichas desviaciones son pequeñas, los valores de εNd se expresan como partes por 10.000, definiéndose matemáticamente como:

$$\varepsilon Nd(t) = \left(\frac{(^{143}Nd\ /\ ^{144}Nd)_{muestra}(t)}{(^{143}Nd\ /\ ^{144}Nd)_{CHUR}(t)} - 1 \right) x10^4$$

En esta ecuación, *t* representa el momento para el que se calcula εNd (*DePaolo y Wasserburg, 1976a*), siendo necesario conocer el valor de CHUR para ese tiempo determinado, siempre teniendo en cuenta que los valores actuales de CHUR para las relaciones $^{143}Nd/^{144}Nd$ y $^{147}Sm/^{144}Nd$ son 0.512638 y 0.1967, respectivamente (*Jacobsen and Wasserburg, 1984*).

El uso de la notación εNd, con respecto a la relación isotópica $^{143}Nd/^{144}Nd$, implica el uso de numeraciones más simples, con valores que varían entre +14 y -20 para la mayoría de las rocas terrestres, lo que mejora la comparación entre rocas de diferentes edades (*White, 2015*). Los valores positivos o negativos del εNd nos ayudan a conocer detalles acerca de la procedencia y evolución geológica de las rocas. Un valor positivo de εNd implica una relación $^{147}Sm/^{144}Nd$ mayor que las de CHUR, y por tanto supone una evolución temporal de la relación $^{143}Nd/^{144}Nd$ hacia valores mayores que los del condrito, lo que se explicaría con una fuente dominantemente mantélica, ya que la relación Sm/Nd es mayor en el manto (debido principalmente a la mayor incompatibilidad del Nd, con respecto al Sm). De la misma manera, valores negativos indican rocas derivadas de fuentes con un valor Sm/Nd más bajo que el reservorio condrítico procedentes de rocas corticales antiguas, cuya relación Sm/Nd es menor que la de un reservorio con un patrón condrítico de REE (*Faure y Mensing, 2005*).

2.3.1.3 Edades modelo de Nd

Adicionalmente a las edades modelo de Nd basadas en la evolución condrítica del manto (T_{CHUR} *o también Edad de residencia cortical - DePaolo y Wasserburg, 1976b*), es posible el cálculo de las edades modelo referidas a un manto empobrecido con respecto a

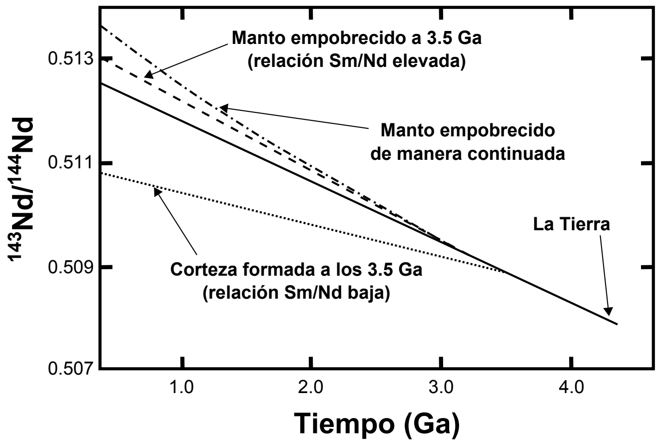

Fig. 2.1- Evolución de la composición isotópica de Nd en el manto y corteza. Se muestran tanto la línea de evolución de la Tierra o CHUR (*chondritic uniform reservoir*), como la evolución de la corteza creada a 3.5 Ga y su manto residual correspondiente, en comparación con la evolución isotópica en el tiempo del manto empobrecido continuamente (Fuente: *White, 2015*).

CHUR. Este cálculo asume la existencia de una corteza enriquecida preferentemente en Nd en relación a Sm, con el progresivo empobrecimiento del manto en Nd, en comparación a su contenido en Sm. Este manto empobrecido presenta una línea de evolución con una pendiente mayor que la del condrito (Fig. 2.1) y al igual que en el caso de la T_{CHUR}, el cálculo matemático de esta edad modelo (T_{DM}) supone llegar a conocer el punto de intersección entre la línea de evolución isotópica de la muestra y la línea de evolución del manto empobrecido, caracterizada por un progresivo aumento en las relaciones, Sm/Nd y $^{143}Nd/^{144}Nd$ (*DePaolo y Wasserburg, 1976b*).

$$T_{DM} = \frac{1}{\lambda}\ln\left(\frac{^{143}Nd/^{144}Nd_{muestra} - ^{143}Nd/^{144}Nd_{DM}}{^{147}Sm/^{144}Nd_{muestra} - ^{147}Sm/^{144}Nd_{DM}} + 1\right)$$

Este punto de intersección representaría la edad a la cual la muestra estudiada tenía una relación $^{143}Nd/^{144}Nd$ igual de la del manto empobrecido, lo que coincidiría con el momento exacto en el que se produjo la extracción desde este manto de los precursores de la muestra estudiada (*Murphy and Nance, 2002*) (Fig. 2.2). Según el modelo utilizado en los trabajos presentados en esta Tesis y propuesto por *DePaolo (1981)*, este punto de intersección vendría definido por la siguiente igualdad:

$$\varepsilon Nd^{ROCA}(t) = \varepsilon Nd^{DM}(t),$$

donde $\varepsilon Nd^{ROCA}(t)$ representa la composición isotópica de Nd en la roca, en un momento determinado del pasado (*t*), y $\varepsilon Nd^{DM}(t)$ la composición del manto empobrecido en relación a CHUR, y que viene dada con suficiente precisión, para un tiempo *t*, por la siguiente ecuación (*DePaolo, 1981*):

$$\varepsilon Nd^{DM}(t) = 0.25t^2 - 3t + 8.5$$

La ausencia de posibles alteraciones en el sistema de Sm-Nd debidas a procesos de erosión, sedimentación, metamorfismo o incluso fusión cortical sugiere que la relación Sm/Nd observada en los sedimentos de grano fino no difiere mucho de la observada en sus precursores, por lo que el sistema nos permite calcular los tiempos de residencia cortical a partir de la los valores observados de T_{DM} y conocer la historia geológica de las rocas seleccionadas (*Dickin, 2005*).

2.3.2 Principios teóricos del método de dilución isotópica

El cálculo cuantitativo de la concentración de un determinado elemento utilizando Espectrometría de Masas con Dilución Isotópica (ID-MS) se basa en el uso de un *spike* como un estándar interno (*Heumann, K.G., 1986*). Para ello es necesaria la adicción de una cantidad precisa del trazador a la muestra y posteriormente, utilizar un espectrómetro de masas para analizar la relación isotópica de una porción de la mezcla de los isótopos con una procedencia diferente. Previo a todo esto, se debe realizar una caracterización del *spike* muy precisa, normalmente con el uso de un estándar en la técnica conocida como

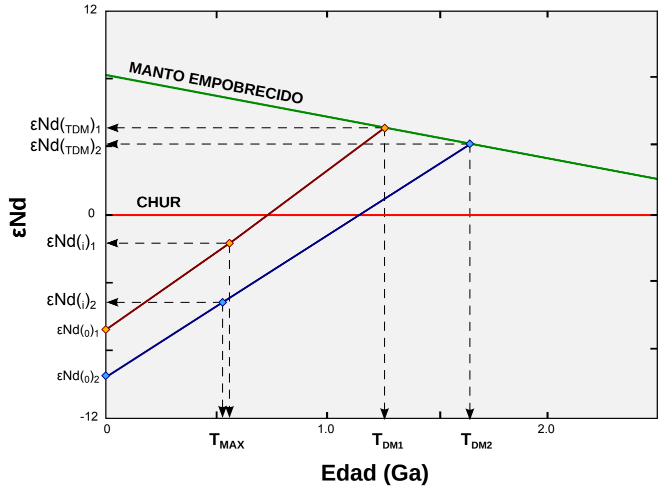

Fig. 2.2- Diagrama Edad vs εNd, donde se muestra la línea de evolución del manto empobrecido según *DePaolo, 1981*. Se incluyen las líneas de evolución de la composición isotópica de Nd de dos rocas, durante el momento de su extracción del reservorio mantélico (T_{DM1} y T_{DM2}), de la cristalización de la roca o de la consolidación de la roca sedimentaria (T_{MAX}) y por último, en la actualidad. Igualmente se reflejan en el eje *y* los valores de la notación épsilon-Nd.

dilución isotópica inversa. Ésto, junto con un conocimiento previo de la composición aproximada de la muestra, ayuda al cálculo preciso de la cantidad de *spike* a añadir, lo que conduce a una minimización en la propagación de errores en el cálculo posterior de la concentración del elemento (*Faure, 1986*).

Es esencial conocer los aspectos críticos del procedimiento experimental, así como conocer las principales fuentes de error para conseguir una elevada exactitud en el cálculo de la concentración de un elemento. Por tanto, es necesario un equilibrio químico completo en la mezcla resultante entre los isótopos del elemento en la muestra y el *spike*. De esta manera se asegura un comportamiento idéntico durante el procedimiento analítico. Para ello, la muestra debe disolverse completamente, y el trazador y muestra ser químicamente equivalentes en la mezcla resultante. Este equilibrio evita que se produzca una separación cromatográfica diferenciada, debida a diferentes eficiencias relativas, relacionadas con las posiblemente distintas formas químicas existentes.

Tras conseguir este equilibrio isotópico, la composición isotópica de la mezcla se analiza por espectrometría de masas, aunque como ya se ha comentado, previamente puede procederse a la separación del elemento con el fin de alcanzar una mayor eficiencia en la ionización del elemento y poder eliminar posibles interferencias isobáricas. Este proceso de separación del analito no es necesario que sea cuantitativo, constituyendo ésta su principal ventaja a la hora de diseñar con una mayor flexibilidad los procesos de purificación (*Makishima, 2016*).

Los principales inconvenientes de esta técnica son el elevado coste y la limitada disponibilidad de soluciones *spike*; los posibles efectos isotópicos debido al desequilibrio de la mezcla en el proceso analítico, la necesidad de un análisis con suficiente exactitud en el espectrómetro de masas y la imposibilidad de utilizar esta técnica con elementos mono-isotópicos. Estas desventajas se compensan en gran medida por el hecho de que hay un número limitado de potenciales fuentes de error: (i) la pureza del spike y el control sobre la concentración y la composición isotópica del mismo, (ii) la ausencia de contaminantes externos a la mezcla muestra-*spike*, lo que se consigue con un control exhaustivo de los blancos de preparación; y por último, (iii) la exactitud en el análisis isotópico en el espectrómetro de masas (*Faure, 1986*).

2.3.3 Metodología específica del análisis isotópico Sm-Nd (ID-TIMS)

De manera rutinaria, el proceso de análisis isotópico de Sm y Nd por espectrometría de masas con ionización termal y dilución isotópica (ID-TIMS) implica la puesta en solución de la muestra sólida pulverizada y la separación cromatográfica de las REE de la matriz de la muestras y de ambos elementos entre sí. Estos procesos son necesarios para conseguir una señal de suficiente intensidad para ambos elementos, que permita su análisis de una manera prolongada en el tiempo alcanzando una precisión estadística satisfactoria.

Previo a la pesada de la muestra, se procede al cálculo preciso de la cantidad de trazador (*spike*) a añadir. Una cantidad demasiado baja o demasiado elevada de esta solución introduciría un error en la precisión analítica final. Para ello, calculamos el peso de *spike* necesario para que, teniendo en cuenta los contenidos observados en los análisis de roca total para las REE, la relación $^{150}Nd/^{144}Nd$ en la mezcla resultante de la muestra y el *spike* sea cercana a la unidad. Una vez calculada esta cantidad, se procede a la pesada en una balanza de precisión de las muestras pulverizadas (ca. 100 mg), junto con la solución de spike mixto (^{149}Sm-^{150}Nd) en recipientes limpios de PFA-Teflon®. Bajo ambiente libre de contaminación se añade una mezcla de 1 mL de HNO_3 y 5 mL de HF ultrapuros (Merck-Suprapur®). Los recipientes cerrados se colocan a alta temperatura (120ºC) durante al menos 48 horas. Tras varios pasos en los que se consigue la evaporación total del SiF_4, las muestras se introducen junto con 5mL de HCl 6N destilado durante 12 horas en una estufa a 120ºC. Este paso asegura la conversión a cloruros y una óptima homogenización química entre las REE de la muestra y la solución de *spike*, necesaria para una separación cromatográfica cuantitativa y lineal (Fig. 2.3).

La primera fase de separación cromatográfica se realiza en una resina DOWEX AG50x8 (200-400 mesh), donde utilizando como eluyentes HCl 2.5N y 6N separamos el grupo completo de las REE del resto de elementos de la matriz de la muestra (Fig. 2.4). En un

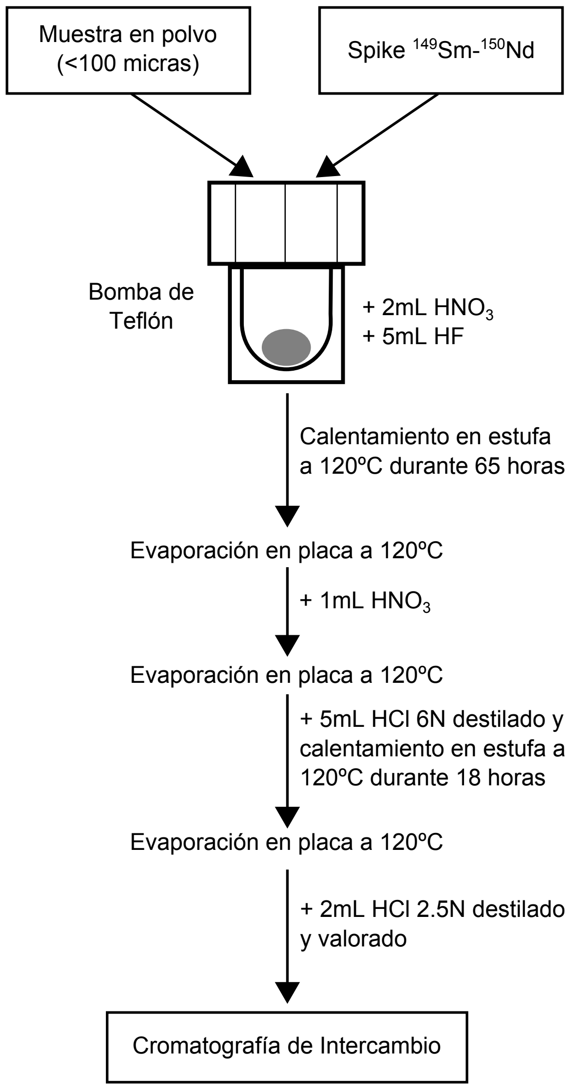

Fig. 2.3- Esquema del protocolo seguido para la disolución química de las rocas metasedimentarias, previo al paso de separación cromatográfica.

segundo paso cromatográfico se utiliza una resina con partículas de Teflon® recubiertas de grupos funcionales formados por HDEHP (*ácido di(2-etilhexil) fosfórico*) (*Richard et al., 1976*). En este caso los ácidos para la elución del Nd y el Sm son HCl 0.3N y 0.6N, respectivamente (Fig. 2.4). La separación de ambos elementos es imprescindible para un análisis preciso, debido a las interferencias isobáricas que presentan ambos elementos. La presencia de Sm en el concentrado de Nd implicaría un análisis no lineal de las abundancias de los isótopos con masas compartidas por ambos elementos, ya que el espectrómetro de masas únicamente discrimina entre masas y no entre elementos.

Ambos elementos se cargan en forma de fosfato sobre un filamento lateral de renio (Re), en lo que se denomina una disposición de triple filamento, formada por tres filamentos de Re, dos laterales y uno central (Fig. 2.5). La conversión a fosfato se consigue al redisolver el residuo seco de la muestras, tras el segundo paso cromatográfico, con ácido fosfórico 0.05M (H_3PO_4). Esta forma química y la disposición de triple filamento, gracias al control electrónico separado de los filamentos laterales y central, aseguran una óptima rotura de los enlaces moleculares del fosfato (evaporación) y de la consiguiente ionización del Nd y Sm metálicos. El elemento metálico liberado del filamento lateral, donde se ha cargado la muestra, se ioniza cerca del filamento central, que permanece durante todo el análisis a una elevada temperatura (≈2000 ºC).

Los filamentos utilizados para la carga de la muestra y el posterior análisis en el espectrómetro de masas han seguido previamente un proceso de limpieza por degasificación. En un equipo degasificador y bajo un vacío de $\approx 1.0*10^{-7}$ bar, se procede a generar una rampa de corriente a través del filamento hasta llegar a los 4A, intensidad que se mantiene durante 30 minutos. Una vez limpios todos los filamentos, se dejan un tiempo en reposo para conseguir su despolarización debida al paso de corriente. En caso contrario podría existir el peligro de una posible repulsión de la gota de muestra disuelta por parte del filamento.

Los análisis de Nd se han llevado a cabo en espectrómetros de masas de ionización térmica, modelos VG Sector-54® y Phoenix-IsotopX® (Fig. 2.6 y 2.7, respectivamente), mediante el método denominado *multicolección dinámica*, en el cual y mediante un cambio

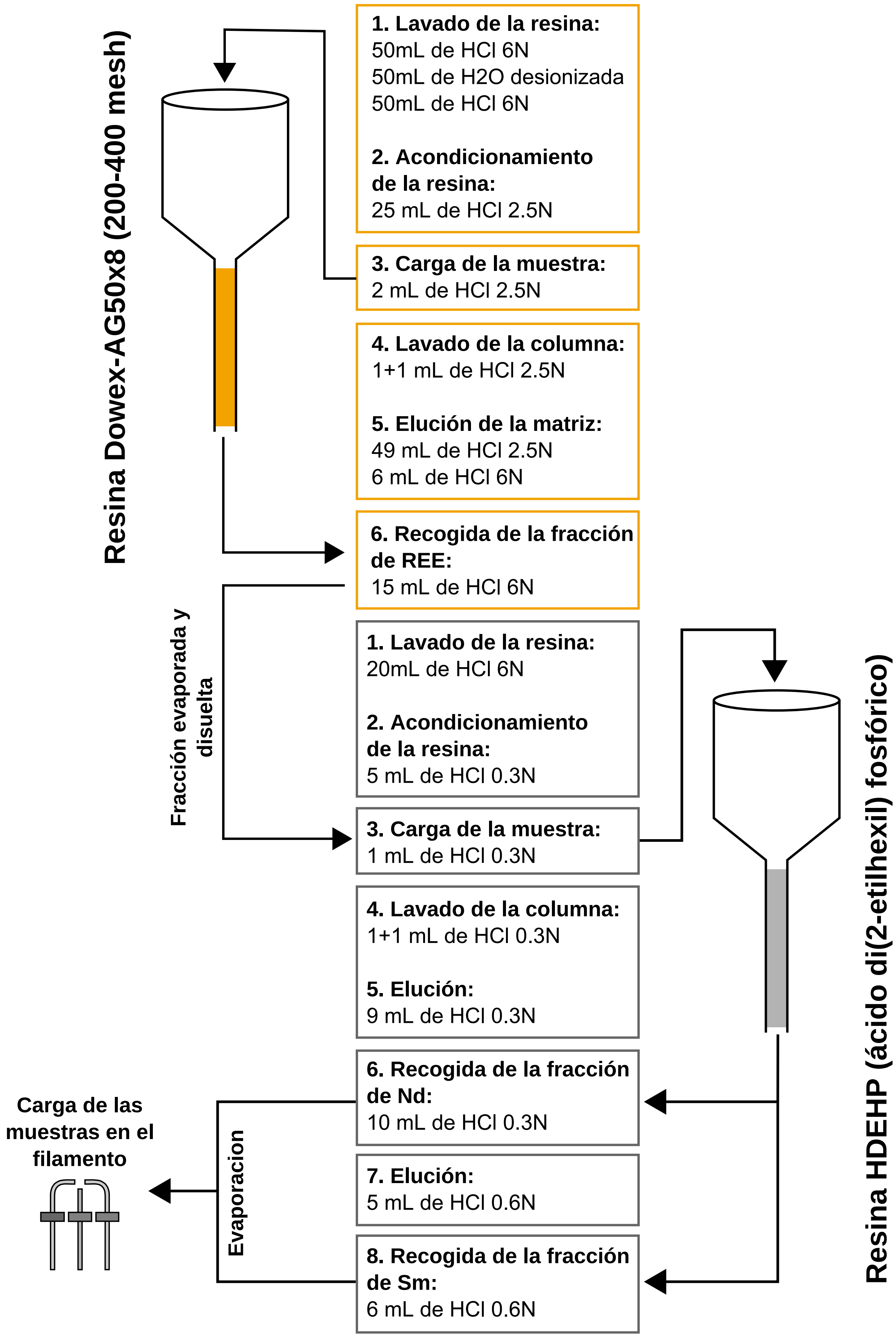

Fig. 2.4- Diagrama esquemático del procedimiento químico de separación cromatográfica del Sm y Nd en las rocas meta-sedimentarias objeto de estudio.

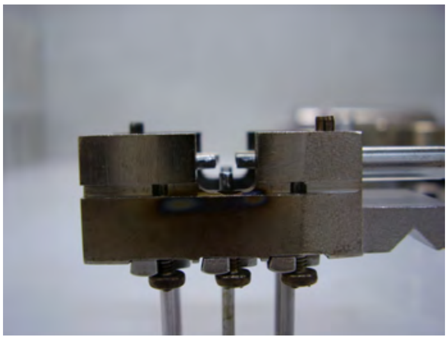

Fig. 2.5- Imagen de una disposición de triple filamento (Re) sobre un bloque de fijación de los mismos, para su unión a la torreta de carga del TIMS.

controlado del campo magnético se automatiza a lo largo de tres secuencias la llegada de diferentes masas a distintos detectores Faraday, consiguiendo una optimización del tiempo de retardo del detector y por consiguiente una reducción en el error estadístico resultante. Esto se consigue gracias a la integración de los valores de las relaciones isotópicas analizadas teniendo en cuenta las intensidades recogidas en tres detectores diferentes. De manera rutinaria en todas las muestras se realizó el análisis de las relaciones isotópicas de Nd durante 160 ciclos de medida, repartidos en 10 bloques de 16 ciclos cada uno. Previo al inicio de un nuevo bloque de medidas, se configuran la intensidad de análisis (1 voltio de intensidad de la masa ^{144}Nd), el campo magnético, los voltajes de focalización, y la línea base de todas las masas. Igualmente, a lo largo de todo el proceso de análisis se recalculan las relaciones de interés teniendo en cuenta la posible existencia de interferencias debidas a la presencia de ^{147}Sm y/o ^{142}Ce, así como para el fraccionamiento de masas debido al proceso físico de calentamiento del filamento metálico. Según este proceso se favorece una ionización fraccionada de los isótopos más ligeros frente a los más pesados, debido a la necesidad de menos energía para la rotura de los enlaces moleculares que implican los primeros. La normalización aplicada en este caso es una corrección exponencial e interna, gracias a la existencia de un par isotópico estable y constante en la naturaleza. Estos isótopos ni se desintegran, ni son fruto de una desintegración radiogénica, por lo que la relación ^{146}Nd/^{144}Nd permanece constante y presenta un valor conocido de 0.7219 (*O'Nions et al., 1979*). Una vez cuantificada la desviación de la relación medida frente a la real y calculado un factor de normalización, se aplica al resto de relaciones analizadas, lo que mejora la precisión en la relación ^{143}Nd/^{144}Nd en un orden de magnitud.

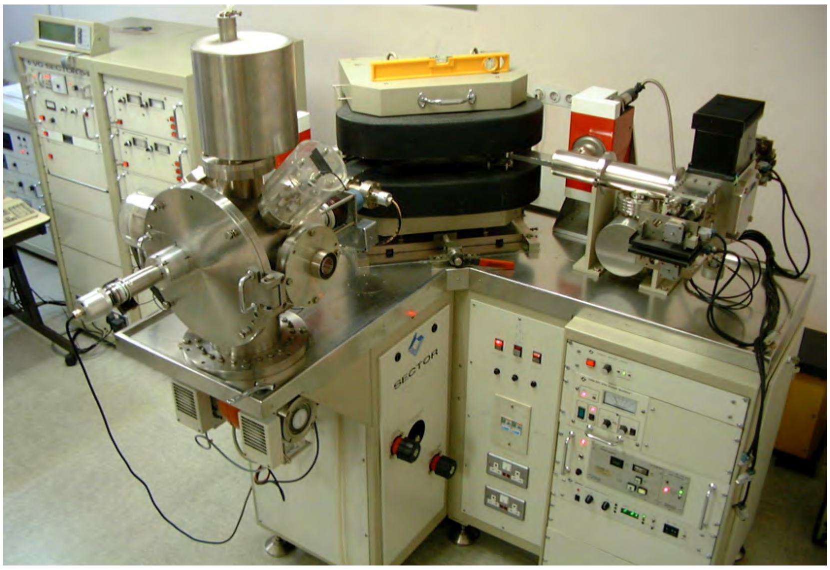

Fig. 2.6- Imagen del espectrómetro de masas de ionización térmica (TIMS) VG-Sector 54® utilizado en este trabajo (CAI de Geocronología y Geoquímica Isotópica - UCM).

Fig. 2.7- Imagen del espectrómetro de masas de ionización térmica (TIMS) IsotopX - Phoenix® utilizado en este trabajo (CAI de Geocronología y Geoquímica Isotópica - UCM).

En el caso del Sm, su análisis se ha llevado a cabo en los mismos espectrómetros que en el caso del Nd, esta vez utilizando un método de *colección simple*. En este método, se programa un cambio en la intensidad del campo magnético, por el cual conseguimos que incidan tres isótopos del Sm en el detector Faraday Axial de una manera secuencial, conservando un tiempo de retardo controlado que impide la existencia de efectos memoria en la señal de amplificación del detector. Durante siete bloques de 16 ciclos cada uno, las intensidades de los isótopos ^{147}Sm, ^{149}Sm y ^{152}Sm se registran en comparación con una línea base y sus relaciones isotópicas obtenidas ($^{149}Sm/^{147}Sm$ y $^{152}Sm/^{147}Sm$) nos permiten, en última instancia, calcular la concentración del Sm en la muestra.

De manera rutinaria se ha comprobado la calidad de los resultados obtenidos, así como la óptima calibración del espectrómetro, analizando repetidamente el estándar isotópico de Nd conocido como *LaJolla* (*Lugmair et al., 1978*). En los respectivos trabajos incluidos en la presente memoria de Tesis, se muestra el número de veces que dicho estándar fue analizado a la vez que las muestras estudiadas, así como el promedio y la doble desviación estándar aplicable a cada grupo de valores. Este valor medio obtenido para el estándar se utilizó para calcular un factor de corrección, que aplicado a las relaciones isotópicas $^{143}Nd/^{144}Nd$ de las muestras, consigue corregir la posible deriva de las mismas con respecto al valor real del estándar. De la misma manera, se analizó el material de referencia BHVO-2 (*USGS - Wilson, 1997; Raczek et al., 2003*), con unas abundancias comparables a las de las muestras analizadas en este trabajo de Tesis, para controlar la óptima homogenización química de la muestra durante el proceso de disolución y tener un control preciso del proceso de dilución isotópica. El basalto de referencia, disuelto y analizado siguiendo el mismo proceso metodológico que las muestras, presenta para un número de análisis de 21 réplicas un valor medio para el Sm y Nd de 5.4 ± 0.8 ppm y 21.8 ± 3.4 ppm, respectivamente. La relación isotópica $^{143}Nd/^{144}Nd$ analizada en un total de 28 réplicas muestra un valor promedio de 0.512994 ± 0.000036. Todos los valores obtenidos son coherentes con los valores certificados del Sm y Nd para el material de referencia analizado en el laboratorio, así como los valores de las relaciones isotópicas, que concuerdan con los valores observados en la bibliografía (*Raczek et al., 2003*).

Capítulo 3

Objetivos específicos

3.1 Objetivos específicos

Como ya se ha comentado en el capítulo inicial, el objetivo general de esta Tesis Doctoral es el estudio de las series siliciclásticas de la transición Ediacarense – Cambrico Inferior del Macizo Ibérico, mediante la utilización de herramientas geoquímicas (elementos mayores y trazas) e isotópicas (Sm-Nd). La formación de estas series tuvo lugar en relación con el desarrollo de un arco magmático, aparentemente activo en el contexto peri-Gondwánico durante la mayor parte del Neoproterozoico y del Cámbrico (*Murphy y Nance, 1987 y 1991; Nance et al., 1991 y 2008; Gutiérrez-Alonso et al., 2003; Murphy et al., 2004; Pereira et al., 2006 y 2012; Linnemann et al., 2007 y 2014; Sánchez Martínez et al., 2009; Albert et al., 2015a; Rubio-Ordóñez et al., 2015; Andonaegui et al., 2016*). Este nuevo enfoque complementa los estudios convencionales que hasta el momento se habían realizado en estas series sedimentarias, y centra sus esfuerzos en: (i) el uso de las abundancias de elementos mayores y trazas para la discriminación del ambiente tectónico concreto en el que tuvo lugar la sedimentación de cada serie; (ii) el análisis de la composición isotópica de Nd (εNd) y el cálculo de las edades modelo (T_{DM}) para la caracterización de las fuentes isotópicas y la procedencia; y (iii) teniendo en cuenta los resultados obtenidos con ambos protocolos analíticos, abordar reconstrucciones paleogeográficas de las cuencas sedimentarias en relación al margen del continente Gondwana, durante la transición entre el Ediacarense Superior y el Cámbrico Inferior.

Para avanzar en el conocimiento sobre la temática general de esta Tesis, se programaron diferentes objetivos específicos basados en investigaciones concretas que se han ido desarrollando a lo largo del tiempo, y sintetizando en los diferentes trabajos publicados que conforman esta memoria. Estos objetivos específicos son los siguientes:

Objetivo 1.- Investigar las características geoquímicas, ambiente geodinámico de sedimentación, fuentes isotópicas y procedencia de las metagrauvacas de las Unidades Alóctonas Superiores del NW del Macizo Ibérico. Estas metagrauvacas afloran de forma excepcional en la sección costera del Complejo de Órdenes, donde han sido investigadas durante la realización de esta Tesis Doctoral. Su edad aproximada es Cámbrico Inferior (edad máxima de sedimentación), de acuerdo con los datos de geocronología U-Pb que aportan sus circones detríticos (*Fernández Suárez et al., 2003*).

Objetivo 2.- Contribuir al análisis estructural de las metagrauvacas culminantes del Complejo de Órdenes y al estudio de geocronología U-Pb de ciertos protolitos implicados en esta serie siliciclástica. Esta información es importante a la hora de interpretar el contexto geodinámico donde se generó la cuenca sedimentaria que se rellenó de sedimentos siliciclásticos, así como para conocer algunos detalles de la paleogeografía durante Cámbrico Inferior y Medio en la periferia de Gondwana.

Objetivo 3.- Investigar las características geoquímicas, ambiente geodinámico de sedimentación, fuentes isotópicas y procedencia de las metagrauvacas y litologías relacionadas de las Unidades Basales del NW del Macizo Ibérico. Estas rocas metasedimentarias tienen buenas condiciones de afloramiento en el Complejo de Malpica-Tui y en menor medida en el oeste del Complejo de Órdenes; en ambos sectores han sido investigadas durante la realización de esta Tesis Doctoral. La edad de las litologías estudiadas se sitúa en el Ediacarense Superior (ca. 560 Ma, secuencia inferior) y en el Cámbrico Medio (ca. 500 Ma, secuencia superior), de acuerdo con los datos de geocronología U-Pb que aportan sus circones detríticos (*Díez Fernández et al., 2010*).

Objetivo 4.- Investigar las características geoquímicas, ambiente geodinámico de sedimentación, fuentes isotópicas y procedencia de las series metasedimentarias que contienen la transición Ediacarense – Cámbrico Inferior en el sector más meridional de la Zona Centroibérica. Esta transición se realiza durante la sedimentación de dos series concretas: la serie grauváquica del Alcudiense Inferior, que ocupa la posición inferior, y las pizarras cámbricas de la Formación Pusa. Para ambas formaciones existe un buen registro cronoestratigráfico (*San José et al., 1990; Vidal et al., 1994a; Jensen et al., 2007*), además de información procedente del estudio de circones detríticos (*Talavera et al., 2012*).

Objetivo 5.- Investigar las características geoquímicas, ambiente geodinámico de sedimentación, fuentes isotópicas y procedencia de las metagrauvacas y litologías relacionadas de las Unidades Basales del SW del Macizo Ibérico. Se han investigado las series metasedimentarias pertenecientes a la Unidad de Escoural, en el Macizo de Évora (*Chichorro, 2006; Pereira et al., 2006, 2007 y 2008*). La Unidad de Escoural está afectada por metamorfismo de alta presión. Estructuralmente se sitúa entre formaciones afines al autóctono de la Zona Centroibérica y otras constituidas por rocas máficas de probable naturaleza ofiolítica. Así pues, resultan en principio correlacionables con las Unidades Basales del NW del Macizo Ibérico. La investigación geoquímica e isotópica en la Unidad de Escoural se planificó también con el objetivo de buscar otros elementos de correlación entre los terrenos del NW y SW del Macizo Ibérico.

Objetivo 6.- Contribuir a avanzar en la reconstrucción de la paleogeografía del margen continental de Gondwana (en el entorno de Iberia) durante la transición Ediacarense – Cámbrico, mediante el estudio e interpretación de las cuencas sedimentarias contemporáneas.

Objetivo 7.- Contribuir a avanzar en la correlación general de los terrenos alóctonos que constituyen el NW y SW del Macizo Ibérico, revisando la zonalidad general que tradicionalmente se ha propuesto para el mismo.

Capítulo 4

Relación de artículos

4.1 Relación de artículos

Esta Tesis Doctoral se presenta según la modalidad basada en el número de artículos indexados publicados. Son seis los artículos que conforman esta Tesis Doctoral, en tres de los cuales el autor de la memoria es el autor principal. Los artículos se han ordenado siguiendo un criterio cronológico, con la excepción del primer artículo presentado, que ofrece un marco geológico regional. Los artículos son los siguientes:

Artículo 1. (Capítulo 5)

ARENAS, R., DÍEZ FERNÁNDEZ, R., RUBIO PASCUAL, F.J., SÁNCHEZ MARTÍNEZ, S., MARTÍN PARRA, L.M., MATAS, J., GONZÁLEZ DEL TÁNAGO, J., JIMÉNEZ-DÍAZ, A., FUENLABRADA, J.M., ANDONAEGUI, P., GARCÍA-CASCO, A. (2016).
The Galicia–Ossa-Morena Zone: Proposal for a new zone of the Iberian Massif. Variscan implications.
Tectonophysics, 681, 135–143.

Artículo 2. (Capítulo 6)

FUENLABRADA, J.M., ARENAS, R., SÁNCHEZ MARTÍNEZ, S., DÍAZ GARCÍA, F., CASTIÑEIRAS, P. (2010).
A peri-Gondwanan arc in NW Iberia I: Isotopic and geochemical constraints on the origin of the arc — A sedimentary approach.
Gondwana Research, 17, 338–351.

Artículo 3. (Capítulo 7)

DÍAZ GARCÍA, F., SÁNCHEZ MARTÍNEZ, S., CASTIÑEIRAS, P., FUENLABRADA, J.M., ARENAS, R. (2010).
A peri-Gondwanan arc in NW Iberia. II: Assessment of the intra-arc tectonothermal evolution through U–Pb SHRIMP dating of mafic dykes.
Gondwana Research, 17, 352–362.

Artículo 4. (Capítulo 8)

FUENLABRADA, J.M., ARENAS, R., DÍEZ FERNÁNDEZ, R., SÁNCHEZ MARTÍNEZ, S., ABATI, J., LÓPEZ CARMONA, A. (2012).
Sm–Nd isotope geochemistry and tectonic setting of the metasedimentary rocks from the basal allochthonous units of NW Iberia (Variscan suture, Galicia).
Lithos, 148, 196–208.

Artículo 5. (Capítulo 9)

FUENLABRADA, J.M., PIEREN, A.P., DÍEZ FERNÁNDEZ, R., SÁNCHEZ MARTÍNEZ, S., ARENAS, R. (2016).
Geochemistry of the Ediacaran–Early Cambrian transition in Central Iberia: Tectonic setting and isotopic sources.
Tectonophysics, 681, 15–30.

Artículo 6. (Capítulo 10)

DÍEZ FERNÁNDEZ, R., FUENLABRADA, J.M., CHICHORRO, M., PEREIRA, M.F., SÁNCHEZ MARTÍNEZ, S., SILVA, J.B., ARENAS, R. (2017).
Geochemistry and tectonostratigraphy of the basal allochthonous units of SW Iberia (Évora Massif, Portugal): Keys to the reconstruction of pre-Pangean paleogeography in southern Europe.
Lithos, 268–271, 285–301.

Capítulo 5

The Galicia–Ossa-Morena Zone: Proposal for a new zone of the Iberian Massif. Variscan implications.

5.1 Introducción

El Macizo Ibérico representa el marco geológico del que forman parte las series siliciclásticas estudiadas. Constituye la sección meridional del Orógeno Varisco, formado durante los episodios finales del ensamblado de Pangea que tuvieron lugar entre el Devónico Inferior y el Carbonífero (Missisipiense) (*Arenas et al., 2014*). Se considera que la formación de Pangea ocurrió tras el cierre de una de las principales cuencas oceánicas Paleozoicas, el Océano Reico (*Nance et al., 2010*), que fue seguido por la colisión progresiva y con una fuerte componente dextral de dos grandes bloques continentales, Laurussia al norte y Gondwana al sur (*Díez Fernández et al., 2012a; Arenas et al., 2014*). Como en otros dominios incluidos dentro de este complejo Orógeno Varisco, el Macizo Ibérico se ha dividido en diferentes zonas geotectónicas o paleogeográficas, siempre de acuerdo a criterios estratigráficos, estructurales, magmáticos y metamórficos (*Lotze, 1945; Julivert et al., 1972*).

La zonalidad geotectónica tradicionalmente establecida en el Macizo Ibérico considera dominios orogénicos externos y otros que representan zonas internas, afectadas por una deformación, metamorfismo y magmatismo de mayor intensidad (*Julivert et al., 1972*). Las zonas internas contienen terrenos con afinidades propias de las cortezas oceánicas (ofiolitas), que junto con otros terrenos afectados por metamorfismo varisco subductivo de alta presión definen la sutura o suturas del orógeno. En el NW del Macizo Ibérico, la denominada Zona de Galicia-Trás-os-Montes contiene una sutura varisca y está constituida por varios Complejos Alóctonos que contienen unidades ofiolíticas y otras de afinidad continental, con una clara impronta heredada de un sistema de arco peri-Gondwánico Ediacarense-Cámbrico (Cadomiense) (*Arenas et al., 2016b*). Los Complejos Alóctonos se encuentran emplazados por encima de un Dominio Parautóctono (también conocido como Dominio Esquistoso de Galicia-Tras-os-Montes), que a su vez está emplazado por cabalgamiento sobre la denominada Zona Centroibérica, considerada como el dominio autóctono de Iberia Central. La zona de sutura del NW del Macizo Ibérico muestra una continuidad limitada y se encuentra aparentemente desenraizada, ya que su contacto basal sale al aire al oeste del denominado Complejo de Malpica-Tui (*Martínez Catalán et al., 2009; Díez Fernández y Arenas, 2015*).

En el suroeste del Macizo Ibérico, en el dominio que se ha definido como Zona de Ossa-Morena, aparecen también unidades ofiolíticas y otras que presentan un metamorfismo de alta presión de edad Varisca (*Díez Fernández y Arenas, 2015; Díez Fernández et al., 2016*). Estas unidades son similares a algunas de las que se han descrito en el NW de Iberia, pese a lo cual la correlación entre ambos dominios nunca pudo ser establecida con claridad. El trabajo que aquí se presenta explora las posibilidades para esta correlación en función de las afinidades litológicas y de las características y cronología de su evolución tectonotermal. La posibilidad de correlación es real, proponiéndose la inclusión de ambos dominios en una nueva zona geotectónica común del Macizo Iberico. Esta nueva zona representaría el dominio más deformado durante la colisión entre Laurussia y Gondwana, tendría un carácter alóctono al haberse emplazado sobre dominios autóctonos más externos y estaría limitada por el suroeste y oeste por el margen meridional de Laurussia, representado por Avalonia (la Zona Sudportuguesa en Iberia).

5.2 Conclusiones parciales

Las afinidades litológicas, la evolución tectonotermal y en particular la cronología y tipo del metamorfismo de alta presión, permiten correlacionar las Unidades Basales alóctonas del NW de Iberia y ciertas unidades de alta presión del SW (Unidad Central y Unidad de Cubito-Moura, en la Zona de Ossa-Morena). Esta correlación define un terreno alóctono basal, que presenta afinidad continental y una continuidad estructural que puede observarse desde el noroeste al suroeste de Iberia. Su posición estructural por debajo de unidades ofiolíticas, así como la edad y el registro metamórfico de alta presión, le identifican como una sección subducida del margen de Gondwana y por tanto parte de una gran zona de sutura Varisca. En el SW de Iberia, por encima de esta sección (constituida por las Unidades Basales y las Unidades Ofiolíticas) se sitúa una potente secuencia metasedimentaria y metaígnea con edades comprendidas entre el Ediacarense y el Devónico, que permite igualmente una correlación coherente entre las Unidades Superiores del NW de Iberia y el sector central de la Zona de Ossa-Morena.

La correlación anterior permite definir un nuevo complejo alóctono, el Complejo de Ossa-Morena, que se añadiría a los previamente considerados dentro del Macizo Ibérico (Cabo Ortegal, Órdenes, Malpica-Tui, Bragança y Morais). La existencia de este nuevo complejo hace posible seguir la sutura desenraizada desde el noroeste de Iberia hacia el sur, hasta el límite con la Zona Sudportuguesa, donde la Ofiolita de Beja-Acebuches define un límite tectónico más joven, que corta los apilamientos previos. La presencia de tres grupos litológicos comunes en los Complejos Alóctonos (las unidades Basales, Ofiolíticas y Superiores), con una disposición estructural similar en el NW y SW del Macizo Ibérico, permite proponer la definición de una nueva zona geotectónica, la Zona de Galicia-Ossa-Morena. Puede definirse también un dominio autóctono relativo para el suroeste del Macizo Ibérico, que ocuparía una posición más externa en el margen de Gondwana que la Zona Centroibérica.

Características tectonoestratigráficas similares y la presencia de unidades ofiolíticas emplazadas sobre otras unidades afectadas por un metamorfismo de alta presión, pueden observarse en otros macizos del Orógeno Varisco (Macizo Armoricano, Macizo Central Francés y Macizo de Bohemia), definiendo una Zona Varisca Interna. Esta zona contiene los restos de un basamento Cadomiense, que representan una sección del margen más externo de Gondwana con un desarrollo importante de un sistema de arcos magmáticos durante la transición entre el Ediacarense y el Cámbrico. Esta sección exterior del margen se vio implicada en dos episodios sucesivos de colisión con Laurussia, con desarrollo de una importante subducción continental marcada por la presencia de dos episodios de metamorfismo de alta-P, datados en ca. 400 Ma y ca. 370 Ma.

Tectonophysics 681 (2016) 135–143

Contents lists available at ScienceDirect

Tectonophysics

journal homepage: www.elsevier.com/locate/tecto

The Galicia–Ossa-Morena Zone: Proposal for a new zone of the Iberian Massif. Variscan implications

Ricardo Arenas [a,*], Rubén Díez Fernández [a], Francisco J. Rubio Pascual [b], Sonia Sánchez Martínez [a], Luis Miguel Martín Parra [b], Jerónimo Matas [b], José González del Tánago [a], Alberto Jiménez-Díaz [c], Jose M. Fuenlabrada [d], Pilar Andonaegui [a], Antonio Garcia-Casco [e,f]

[a] Departamento de Petrología y Geoquímica e Instituto de Geociencias (UCM, CSIC), Universidad Complutense, 28040 Madrid, Spain
[b] Instituto Geológico y Minero de España, 28760, Tres Cantos, Madrid, Spain
[c] Departamento de Geodinámica, Universidad Complutense, 28040 Madrid, Spain
[d] CAI de Geocronología y Geoquímica Isotópica, Universidad Complutense, 28040 Madrid, Spain
[e] Departamento de Mineralogía y Petrología, Universidad de Granada, 18071 Granada, Spain
[f] Instituo Andaluz de Ciencias de la Tierra (CSIC, UGR), E-18100, Armilla, Granada, Spain

ARTICLE INFO

Article history:
Received 25 August 2015
Received in revised form 2 February 2016
Accepted 24 February 2016
Available online 2 March 2016

Keywords:
Galicia–Ossa-Morena Zone
New geotectonic zone
Iberian Massif
Variscan Orogen

ABSTRACT

Correlation of a group of allochthonous terranes (referred to as basal, ophiolitic and upper units) exposed in the NW and SW of the Iberian Massif, is used to propose a new geotectonic zone in the southern branch of the Variscan Orogen: the Galicia–Ossa-Morena Zone. Recent advances in SW Iberia identify most of the former Ossa-Morena Zone as another allochthonous complex of the Iberian Massif, the Ossa-Morena Complex, equivalent to the Cabo Ortegal, Órdenes, Malpica-Tui, Bragança and Morais complexes described in NW Iberia. The new geotectonic zone and its counterparts along the rest of the Variscan Orogen constitute an Internal Variscan Zone with ophiolites and units affected by high-P metamorphism. The Galicia–Ossa-Morena Zone includes a Variscan suture and pieces of continental crust bearing the imprint of Ediacaran–Cambrian events related to the activity of peri-Gondwanan magmatic arcs (Cadomian orogenesis). In the Iberian Massif, the general structure of this geotectonic zone represents a duplication of the Gondwanan platform, the outboard sections being juxtaposed on top of domains located closer to the mainland before amalgamation. This interpretation offers an explanation that overcomes some issues regarding the differences between the stratigraphic and paleontological record of the central and southern sections of the Iberian Massif. Also, equivalent structural relationships between other major geotectonic domains of the rest of the Variscan Orogen are consistent with our interpretation and allow suspecting similar configurations along strike of the orogen. A number of issues may be put forward in this respect that potentially open new lines of thinking about the architecture of the Variscan Orogen.

1. Introduction

The Iberian Massif, like other sectors of the Variscan Orogen, has been classically divided in geotectonic/paleogeographic zones. Although there is no formal definition for a "geotectonic zone" of an orogen, its use is widely accepted to distinguish among orogenic domains with contrasted characteristics regarding their stratigraphy, structure, metamorphism and magmatism (e.g. Hatcher, 1989; Hodges, 2000; Schmid et al., 2004). It is also somewhat diffuse the concept of external and internal zones of orogens, although external domains are generally characterized by thin-skinned tectonics, low-grade regional metamorphism and scarce magmatism, while internal domains are characterized by pervasive ductile deformation, regional foliations and intense metamorphism and magmatism. In addition, internal zones typically contain the suture or sutures of the orogen, which are manifested by the presence of ophiolites and terranes affected by subduction-related high-P metamorphism. In collisional orogens, geotectonic zones can be used to separate different sectors of the colliding continental platforms and tectonic blocks affected by variable intensity of deformation. If well-preserved ophiolites are present, geotectonic zones can also provide information on the oceanic domains closed before collision.

Lotze (1945) and Julivert et al. (1972) made the first geotectonic division of the Iberian Massif, which prevailed for a long time. From northeast to southwest, the Cantabrian, West Asturian-Leonese, Central Iberian, Ossa-Morena and South-Portuguese zones were distinguished.

* Corresponding author at: Departamento de Petrología y Geoquímica e Instituto de Geociencias (UCM, CSIC), Facultad de Geología, Universidad Complutense de Madrid, C/ José Antonio Novais, no. 2, 28040 Madrid, Spain. Tel.: +34 913944904.
E-mail addresses: arenas@geo.ucm.es (R. Arenas), georuben@usal.es (R. Díez Fernández), f.rubio@igme.es (F.J. Rubio Pascual), s.sanchez@geo.ucm.es (S. Sánchez Martínez), lm.martin@igme.es (L.M. Martín Parra), j.matas@telefonica.net (J. Matas), tanago@ucm.es (J. González del Tánago), ajimenezdiaz@geo.ucm.es (A. Jiménez-Díaz), jmfuenla@pdi.ucm.es (J.M. Fuenlabrada), andonaeg@geo.ucm.es (P. Andonaegui), agcasco@ugr.es (A. Garcia-Casco).

http://dx.doi.org/10.1016/j.tecto.2016.02.030
0040-1951/

The Cantabrian and South-Portuguese zones represent foreland (external) domains located at the Gondwanan and Laurussian flanks of the orogen, respectively. The rest of the zones show variable intensity of metamorphism and magmatism and thus make the hinterland (internal zone) of the orogen. More recently, Farias et al. (1987) defined a new geotectonic zone within the hinterland of the Iberian Massif, the Galicia–Trás-os-Montes Zone, with far-travelled character and constituted by a gigantic thrust-sheet overriding the Central Iberian Zone. This zone includes several allochthonous complexes which contain ophiolites and terranes recording high-P metamorphism, and are emplaced on top of a parautochthonous domain also termed Schistose Domain or Parautochthon (Arenas et al., 1988). The Galicia–Trás-os-Montes Zone shows limited continuity, as it can only be followed in Galicia and along the Portuguese region of Trás-os-Montes, although a correlation of the nappe stack in the Ibero-Armorican arc across the Bay of Biscay has been recently proposed (Ballèvre et al., 2014). Importantly, this zone contains a Variscan suture, as suggested by the chronology of its ophiolites (Díaz García et al., 1999; Sánchez Martínez et al., 2011; Arenas et al., 2014a) and the high-P metamorphism experienced by some of its units (Ordóñez Casado et al., 2001; Rodríguez et al., 2003; Fernández-Suárez et al., 2007; Abati et al., 2010). That suture zone is apparently rootless, as its trace lies above bedrock geology of Galicia towards the Atlantic Ocean to the West of the Malpica-Tui Complex (Martínez Catalán et al., 2009).

The aforementioned geotectonic division of the Iberian Massif is built on contrasted differentiation criteria from one region to the other, and so it suffers from significant divergences and inconsistencies. This is mainly due to the large amount of geologic data accumulated since the papers by Lotze (1945) and Julivert et al. (1972) were published. It is hence timely a revision of the subdivision that takes into account new advances in the geology of the Iberian Massif and that is based on uniform criteria. In this regard, perhaps the most important problems faced when subdividing the Iberian Massif concern the interpretation of the geology of its NW and SW sections. The SW Iberian Massif, specifically the Ossa-Morena Zone, is characterized by lithological, structural and metamorphic features that are also representative of the Galicia–Trás-os-Montes Zone (Castro, 1987). For instance, the Ossa-Morena Zone contains ophiolites (e.g. Pedro et al., 2010), and units affected by high-P metamorphism of Variscan age (Azor et al., 1994; Ordóñez Casado, 1998; Moita et al., 2005; Pereira et al., 2010).These high-P units of SW Iberia have been recently correlated with equivalent units located in the NW of the Iberian Massif, allowing the proposal for a continuation of the rootless Variscan suture of NW Iberia and the allochthonous complexes of the same region to the W and SW (Díez Fernández and Arenas, 2015). In this paper, we explore the existing geological data at the regional scale in order to review the subdivision of geotectonic zones of the Iberian Massif in an attempt to reach a simpler though successful scheme. We will mainly consider the new advances in the geology of NW and SW Iberia, specifically the distribution of ophiolites and the units affected by high-P metamorphism together with the geochronology of these events, the interpretation of the autochthonous or allochthonous character of the main geological domains and the correlation along the Iberian Massif of all these first order geological aspects.

Our new approach allows a more integrative view of the geology of the Iberian Massif, which could be eventually considered for a simpler interpretation of the Variscan Orogen and the assembly of Pangea. The whole Variscan Orogen is affected by oroclinal bends, formed after an originally near-linear orogen (Martínez Catalán, 2011; Weil et al., 2012). The Variscan Orogen can be followed from Iberia to the Bohemian Massif, forming also the basement of the Alps, Corsica and Sardinia. It has also continuity in Morocco and eastern North America in the Appalachian-Alleghanian Orogen and defines a long collision zone generated during the main stages of Pangea's assembly (Díez Fernández et al., 2012a; Arenas et al., 2014b). Our aim is also to extrapolate the new correlations proposed for Iberia throughout the Variscan Orogen, and to outline the distribution of the most internal zone of the orogen, the one featured by ophiolites and high-P units. Another consequence of the new correlations across the orogen is a better understanding of the location of the true Rheic suture, which can be clearly distinguished now from other secondary sutures involved in the orogen (Díez Fernández and Arenas, 2015).

2. The NW section of the Iberian Massif: the Galicia–Trás-os-Montes Zone

The NW Iberian Massif contains one of the most complete and representative sections of the Variscan Orogen. From East to West the North Iberia section extends from a foreland thrust and fold belt (Cantabrian Zone) through the external sectors of the hinterland represented by the West Asturian-Leonese and Central Iberian zones, and to the most internal domains well inside the hinterland (Galicia–Trás-os-Montes Zone) (Fig. 1).

The Galicia–Trás-os-Montes Zone includes the allochthonous complexes of the NW Iberian Massif, namely Cabo Ortegal, Órdenes, Mapica-Tui, Bragança and Morais complexes. They are preserved in late upright synforms and represent the remnants of a huge pile of far-travelled terranes, with different origin and tectonothermal evolution. A detailed review of the geology of these allochthonous complexes has been presented by Arenas et al. (submitted for publication). The upper and basal terranes have continental affinity and bear the imprint of two distinct high-P metamorphic events, whereas the intermediate terrane consists of a set of ophiolitic units (Arenas et al., 2014b) (Fig. 1). They also include a thick serpentinitic mélange, the Somozas Mélange, only represented in the eastern part of the Cabo Ortegal Complex, i.e. at the advancing front of the allochthonous complexes (Arenas et al., 2009). Therefore the allochthonous ensemble represents one of the sutures of the Variscan Orogen and contains key units to understand the earliest tectonothermal events related to the assembly of Pangea, and the origin of intervening oceanic domains. The allochthonous complexes are thrust on top of a parautochthonous domain, the so-called Schistose Domain of Galicia–Trás-os-Montes or Parautochthon (Fig. 1). It is formed by Late Cambrian to Devonian metasedimentary rocks, Late Cambrian to Late Ordovician calc-alkaline and alkaline metavolcanics (Valverde-Vaquero et al., 2005; Dias da Silva et al., 2014, in press), and Upper Devonian to Early Carboniferous synorogenic sediments (Martínez Catalán et al., 2016), all of which are tectonically emplaced onto the Central Iberian Zone. According to Piçarra et al. (2006), stratigraphic and faunal affinities of the Silurian sediments of the Parautochthon suggest a more distal palaeogeographic position relative to the Central Iberian Zone. Regarding the allochthonous complexes, the detrital zircon input from both the Parautochthon and the basal units of the allochthonous complexes are almost identical, so they are also considered as neighbouring sections of the same continental margin (Díez Fernández et al., 2012b).

The basal units are formed by metasedimentary rocks (comprising a pile of metagreywackes with alternations of metapelites, graphitic schists, calc-silicate rocks, metacherts and quartzites), calc-alkaline to peralkaline metagranitoids and more scarce mafic rocks. Maximum depositional ages for the metasedimentary rocks range between Ediacaran and Early-Middle Cambrian (Díez Fernández et al., 2010, 2013), while the granitic magmatism developed in the range c. 493–470 Ma, and was followed shortly after by alkaline–peralkaline magmatism (Abati et al., 2010; Díez Fernández et al., 2012c). The basal units have been interpreted as a section of the margin of Gondwana located between the West African Craton (WAC) and the Saharan Craton (SC) (Díez Fernández et al., 2010). The first Variscan tectonothermal event recorded in these units is a high-P and low to intermediate-T (HP-LIT) metamorphic event dated at c. 370 Ma (Rodríguez et al., 2003; Abati et al., 2010). It was generated during oblique subduction of the Gondwana margin under a previously deformed ensemble (upper and ophiolitic units) located to the North (West in present-day coordinates; Díez Fernández et al., 2012a).

R. Arenas et al. / Tectonophysics 681 (2016) 135–143 137

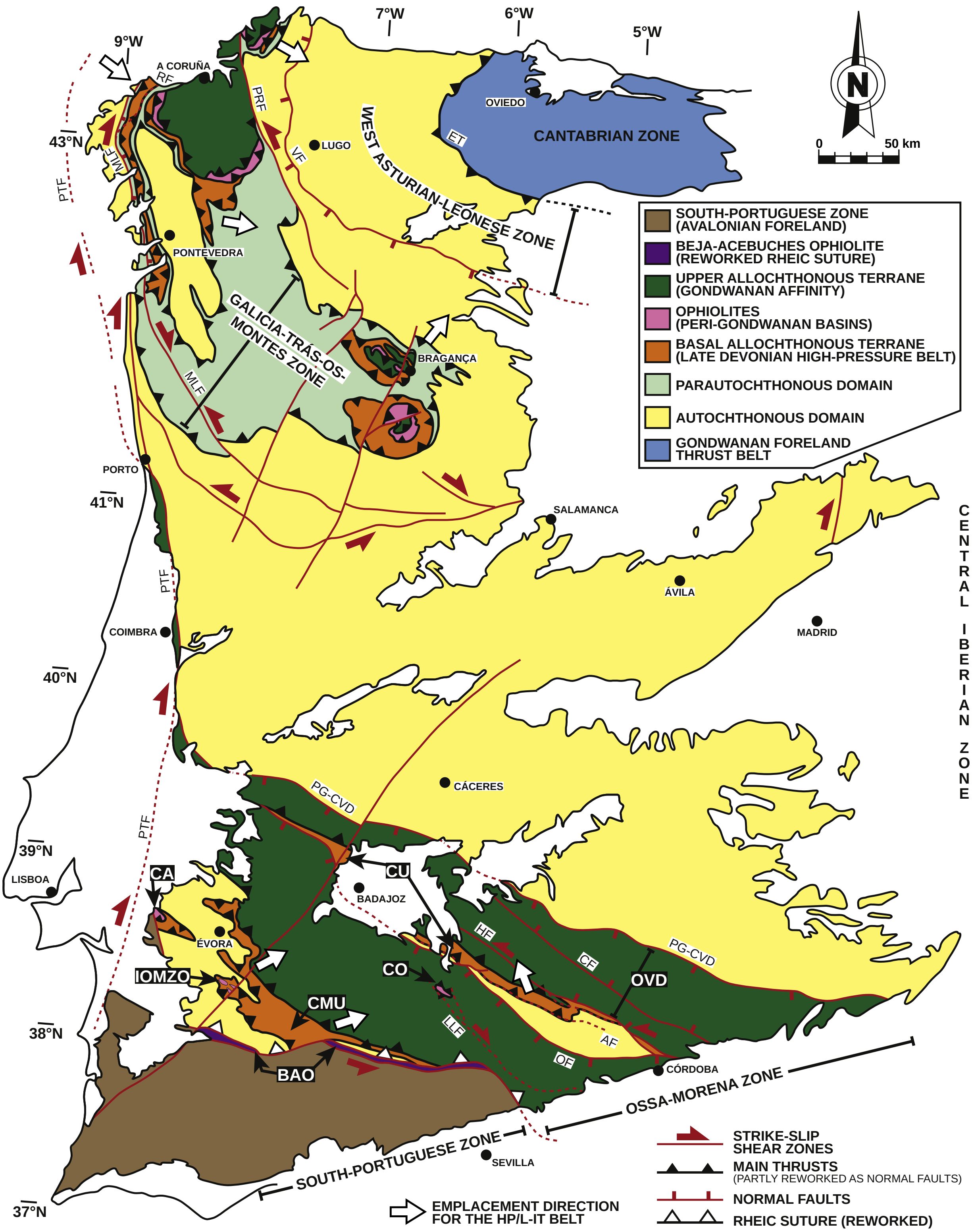

Fig. 1. Geological map of the Iberian Massif and correlation of equivalent allochthonous terranes in NW and SW Iberia. Abbreviations: AF, Azuaga Fault; BAO, Beja-Acebuches Ophiolite; CA, Carvalhal Amphibolites; CF, Canaleja Fault; CMU, Cubito-Moura Unit; CO, Calzadilla Ophiolite; CU, Central Unit; ET, Espina Thrust; HF, Hornachos Fault; IOMZO, Internal Ossa-Morena Zone Ophiolites; LLF, Llanos Fault; MLF, Malpica-Lamego Fault; OF, Onza Fault; OVD, Obejo-Valsequillo Domain; PG-CVD, Puente Génave-Castelo de Vide Detachment; PRF, Palas de Rei Fault; PTF, Porto-Tomar Fault; RF, Riás Fault; VF, Viveiro Fault.
Modified from Díez Fernández and Arenas (2015).

Above the suture zone (ophiolites), the upper units are formed by a 10–12 km thick pile of metasedimentary rocks intruded by large massifs of calc-alkaline granitoids and arc-tholeiitic gabbros. The metasedimentary rocks include a thick greywackic series with Cambrian maximum depositional ages (Albert et al., 2015), while the intrusive igneous massifs have been dated at c. 500 Ma (Andonaegui et al., 2012). The stratigraphic record of the upper units of NW Iberia is not well known, although U–Pb and Lu–Hf isotopic ratios obtained from detrital zircon grains indicate a distinct Gondwanan provenance in the periphery of the WAC (Albert et al., 2015). This origin, together with their lithological constitution and pre-Variscan evolution, indicate that the upper units represent a section of a peri-Gondwanan magmatic arc (Abati et al., 1999). The tectonic fabrics and the tectonothermal events related to the evolution of the arc are dominant features in the higher structural level of the upper units, which shows less penetrative Variscan deformation and metamorphism generally concentrated in discrete shear zones (Abati et al., 1999, 2007; Gómez-Barreiro et al., 2006; González Cuadra, 2007). In contrast, the lower part of the upper units is affected by an eo-Variscan high-P and high-T (HP-HT) metamorphic event, dated at c. 400–390 Ma (Ordóñez Casado et al., 2001; Fernández-Suárez et al., 2007). This high-P event, probably the first and oldest tectonothermal event related to the Variscan cycle, occurred in response to the initial collision between Gondwana and Laurussia (Arenas et al., 2014b).

The ophiolites of NW Iberia have received considerable attention in recent years, when numerous papers have described in detail their lithologies, chemical composition and isotopic geochronology. It is now well-established that their igneous protoliths have a wide age range, what hinders their assignment to a single oceanic domain. Their protoliths do not represent common MORB types, their origin being usually associated with a supra-subduction setting. Two groups of ophiolites have been described (Arenas and Sánchez Martínez, 2015): an older group (lower ophiolitic units) that contains metaigneous rocks of Middle-Late Cambrian age (c. 500–495 Ma), and a younger group (upper ophiolitic units) that includes ultramafic rocks and Devonian gabbros (Emsian-Eifelian; c. 395 Ma; Díaz García et al., 1999; Pin et al., 2002). The lower ophiolites are interpreted to represent the opening of a back-arc basin in the periphery of Gondwana (Vila de Cruces Ophiolite; Arenas et al., 2007), or remnants of a Cambrian peri-Gondwanan ocean tract (Iapetus-Törnquist) accreted to the base of a magmatic arc (Bazar Ophiolite; Sánchez Martínez et al., 2012). Recent isotopic data (Lu–Hf in zircon, whole rock geochemistry and Sm–Nd systematics) indicate that the protoliths of the upper ophiolites (Careón, Purrido and Moeche ophiolites) interacted with isotopic sources of continental nature (Sánchez Martínez et al., 2011; Arenas et al., 2014a). Consequently, their origin is hard to reconcile with wide oceanic domains. The origin of these ophiolites is a key aspect to understand the first tectonothermal events related to the assembly of Pangea. They have been recently interpreted as generated during the opening of an ephemeral pull-apart basin. The inception of this basin occurred in the way of two events of dextral convergence between Gondwana and Laurussia. These two collisional episodes led to different high-P metamorphic events that affected two different sections of the margin of Gondwana at c. 400 Ma (upper units) and c. 370 Ma (basal units) (Arenas et al., 2014b).

3. The SW section of the Iberian Massif: The Ossa-Morena Zone

The SW of the Iberian Massif has been classically divided in two different zones separated by an ophiolite dated at c. 340–332 Ma (Beja-Acebuches Ophiolite; Castro et al., 1999; Díaz-Azpiroz et al., 2006; Azor et al., 2008), the South-Portuguese Zone and the Ossa-Morena Zone (Fig. 1). The South-Portuguese Zone is correlated along the Variscan Orogen with the Rhenohercynian Zone, considered part of Avalonia and hence a section of the southern margin of Laurussia (Franke, 2000; Matte, 2001; Murphy et al., 2011; Linnemann et al., 2012). The Ossa-Morena Zone is part of the peri-Gondwanan realm (López-Guijarro et al., 2008; Pereira et al., 2012), and has been usually considered an autochthonous domain of the Variscan Orogen. New geological data and correlations indicate that rather it should be considered a composite ensemble formed by several different terranes with distinct origin and tectonothermal evolution. In this view most of the previous Ossa-Morena Zone can be interpreted as an allochthonous complex of the Iberian Massif, the Ossa-Morena Complex (Díez Fernández and Arenas, 2015). The arguments for this interpretation are similar to those already used in other parts of the orogen, such as in the NW of the Iberian Massif: the presence of ophiolitic units located on top of continental terranes bearing the imprint of high-P metamorphism and thrust on top of continental units not affected by high-P events. This new interpretation of the geology of the Ossa-Morena Zone presented by Díez Fernández and Arenas (2015), has been the subject of a recent and detailed discussion (Simancas et al., 2016; Díez Fernández and Arenas, 2016). The reader may find in those papers additional information regarding the structure and tectonothermal evolution of the units making the Ossa-Morena Complex. In some sectors of the SW Iberian Massif rocks located below high-P units lack evidence of high-P metamorphism and, consequently, should be considered autochthonous domains in relation to the high-P units (Fig. 1). This SW Iberia autochthon probably represents the continuation of the Central Iberian Zone below the Ossa-Morena allochthonous complex.

The Ossa-Morena Zone contains an uppermost pre-orogenic pile of metasedimentary and metaigneous rocks with ages ranging from Ediacaran to Devonian. Variscan and eo-Variscan deformation shows variable intensity and tectonic polarity (Simancas et al., 2001). This zone also records previous tectonothermal and igneous activity typically referred to as Cadomian, and probably linked to the dynamics of a peri-Gondwanan arc-system that was active during Neoproterozoic and Cambrian times (Linnemann et al., 2008). The Ossa-Morena Zone includes two HP-LIT metamorphic units, the Central Unit (Blastomylonitic Corridor or Coimbra-Córdoba Shear Zone) to the North (Azor et al., 1994) and the Cubito-Moura Unit to the South (Araújo et al., 2005; Booth-Rea et al., 2006; Rubio Pascual et al., 2013) (Fig. 1). The high-P metamorphism is dated at c. 370 Ma in the Cubito-Moura Unit (Moita et al., 2005), and hence its Variscan nature is clear. A less precise Variscan age has been obtained also for the high-P event in the Central Unit (c. 380–340 Ma; Ordóñez Casado, 1998; Pereira et al., 2010). The distribution and extent of the ophiolites of the Ossa-Morena Zone (to the north of Beja-Acebuches) is not well known. However, mafic-ultramafic sequences are located structurally above the high-P units (Fig. 1). These ophiolites are referred to as the internal ophiolitic units of the Ossa-Morena Zone, and some of them have been dated at Cambrian–Ordovician (Pedro et al., 2010). Other ophiolites exposed throughout the Ossa-Morena Zone include the Carvalhal Amphibolites and the Calzadilla Ophiolite (Fig. 1).

The Ossa-Morena Zone is usually considered separated from the Central Iberian Zone by the intermediate Obejo-Valsequillo Domain (Apalategui and Pérez-Lorente, 1983; Martín Parra et al., 2006), with supposedly transitional stratigraphic characteristics (Martínez Poyatos, 2002; San José et al., 2004). However, its paleontological record is somewhat enigmatic and also different of that of the Central Iberian Zone, what has casted doubt on such transitional character (Gutiérrez-Marco et al., 2014). The interpretation of the Ossa-Morena Zone as an allochthonous domain of the Iberian Massif proposed by Díez Fernández and Arenas (2015) overcomes this problem, because the Central Iberian Zone and the Obejo-Valsequillo Domain would be originally located far apart each other. The northern limit of the Ossa-Morena Zone is defined by a large extensional fault, the Puente Génave-Castelo de Vide detachment (Fig. 1; Martín Parra et al., 2006), which subtracts a significant portion from both the overlying Obejo-Valsequillo Domain and the underlying Central Iberian Zone, thus making it difficult to identify a suture zone in this boundary.

4. Equivalence between the NW and SW of the Iberian Massif: the Galicia–Ossa-Morena Zone

The affinity between the continental crusts of NW and SW Iberia was first suggested by Castro (1987). The Ossa-Morena Zone was considered a microcontinent accreted to the Gondwanan margin, represented by

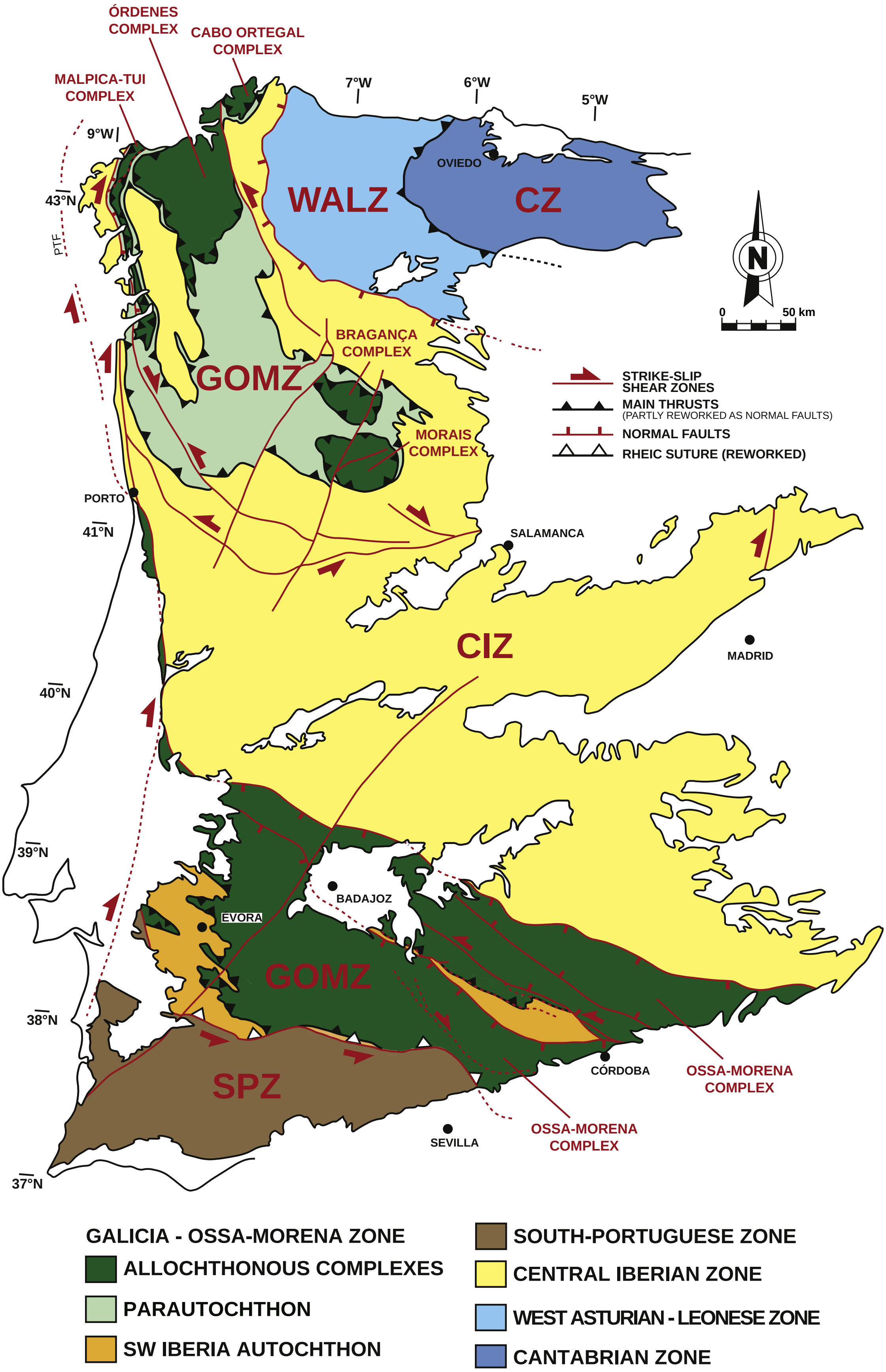

Fig. 2. Geological map of the Iberian Massif showing the distribution of the geotectonic zones in which is divided (Lotze, 1945; Julivert et al., 1972) and the new proposed Galicia–Ossa-Morena Zone. Abbreviations: CZ, Cantabrian Zone; WALZ, West Asturian Leonese Zone; CIZ, Central Iberian Zone; GOMZ, Galicia–Ossa-Morena Zone; SPZ, South Portuguese Zone.

the Central Iberian Zone, during a collision in Cadomian times (Late Proterozoic–Early Cambrian). The allochthonous complexes of NW Iberia would represent transitional parts between the Central Iberian and Ossa-Morena zones, but the Malpica-Tui Complex of NW Iberia and the Central Unit (Badajoz-Cordoba Corridor) were considered parts of a same lithological unit. Following Franke and Engel (1982); Castro (1987) also presented an updated geological map at the scale of the Variscan Orogen showing the location of the Rheic suture, described as the Hercynian suture.

More recently, according to the presence of two high-P belts defining its northern and southern limits, the Ossa-Morena Zone has been interpreted as part of an individual peri-Gondwanan continental microplate, drifted to some extent from the main continent. Such plate was identified as Armorica, a microcontinent that includes sectors of Iberia and Brittany (Matte, 2001; Díaz-Azpiroz et al., 2006; Azor et al., 2008). The two high-P units would represent rooted sutures related to the dynamics of Armorica and its Variscan accretion (Simancas et al., 2001; Azor et al., 2008), but the real significance of the high-P units remain unclear because an integrated model for their subduction and exhumation has not been presented so far. In the case of the Coimbra-Córdoba Shear Zone (Badajoz-Córdoba Corridor), it has also been proposed a Cadomian age for this suture (Abalos et al., 1991).

However, the lithologies and structural evolution as well as the age and type (HP-LIT) of metamorphism are similar in the basal allochthonous units of NW Iberian Massif and in the high-P units of the SW (Central Unit and Cubito-Moura Unit). Hence, these units can be correlated defining a basal allochthonous terrane with continental affinity and structural continuity from NW to SW Iberia. Considering the high-P record of this terrane, the age of metamorphism (c. 370 Ma) and its structural position below ophiolitic units, this basal terrane has been identified as a subducted section of the Gondwanan margin and a marker of a long suture zone of Late Devonian age (Fig. 1; Díez Fernández and Arenas, 2015). The ophiolitic units of the Ossa-Morena Zone are still poorly described although, regardless of their age, their structural position suggests a correlation with their structural equivalents in NW Iberia.

One of the corollaries of the proposed correlation of both groups of allochthonous terranes in NW and SW Iberia is that the largest area of the Ossa-Morena Zone, the thick pile of metasedimentary and metaigneous rocks with Ediacaran-Devonian depositional/crystallization ages, rests on top of a group of units with clear allochthonous nature. The correlations established for the high-P units and the ophiolites, the general synformal structure of the Ossa-Morena Zone (Borrego et al., 2005) and the activity of some significant faults, lead to an important conclusion: most of the central sector of the Ossa-Morena Zone is equivalent to the upper units of NW Iberia, thus representing a large allochthonous unit (Fig. 1; Díez Fernández and Arenas, 2015). Accordingly, most of the Ossa-Morena Zone represents an allochthonous complex of the Iberian Massif, the Ossa-Morena Complex, which should be added to the Cabo Ortegal, Órdenes, Malpica-Tui, Bragança and Morais complexes. The rootless suture of NW Iberia can be therefore followed c. 1000 km south until the limit with the South Portuguese Zone, where the age of the Beja-Acebuches Ophiolite (340–332 Ma) clearly indicates that this is a much younger tectonic limit that transects all the previous nappes (Fig. 1). This interpretation also allows to correlate pre-Variscan events in the upper units of NW Iberia (Abati et al., 1999; Díaz García et al., 2010) and in the central part of the Ossa-Morena Zone (described as Cadomian), where its remarkable bearing has been widely accepted (Galindo, 1989). Moreover, our proposal implies that some sectors usually included in the Ossa-Morena Zone represent the autochthonous domain of the new allochthonus complex. This is the case of the Sierra Albarrana Unit (Azor, 1994; González del Tánago, 1995), and the entire structural domain resting below the Cubito-Moura Unit (Fig. 1).

According to the data and interpretations presented in previous sections, the geology of NW and SW Iberian Massif can be described in terms of the presence of three different groups of allochthonous terranes, the basal, ophiolitic and upper units (Fig. 1). These terranes maintain the same structural arrangement in both sectors of the Massif, and have comparable lithological constitution and tectonothermal evolution. If this correlation holds correct, it should be accepted that the regions of the Iberian Massif where they appear must be interpreted similarly. However this is not the case so far because the structure of the Galicia–Trás-os-Montes Zone and the Ossa-Morena Zone has been interpreted in rather contrasted ways. Based on the structural and tectonostratigraphic correlation of both zones we propose their merging into a single geotectonic zone of the Iberian Massif: the Galicia–Ossa-Morena Zone (Fig. 2). This new zone would be constituted by the allochthonous complexes of the Iberian Massif, from NE to SW, the Cabo Ortegal, Órdenes, Bragança, Morais, Malpica-Tui and Ossa-Morena complexes.

The allochthonous complexes of the Galicia–Ossa-Morena-Zone are emplaced on top of a substrate that apparently shows some different characteristics in NW and SW Iberia. The Parautochthon of the NW section (Fig. 2) does not seem to be represented in the SW, as comparable series have not been described so far. Moreover, sedimentary successions such as the Serie Negra have not been found in the autochthonous sections of Central and NW Iberia, whereas it occurs in the autochthonous domains resting under the Ossa-Morena Complex defined by Díez Fernández and Arenas (2015). On the contrary, some of the metasedimentary series represented in the SW show great lithological similarities with the autochthonous sections of the Central Iberian Zone. In this regard, it is remarkable the presence of quartzitic facies, comparable to the Armorican Quartzite in fossil content and probable

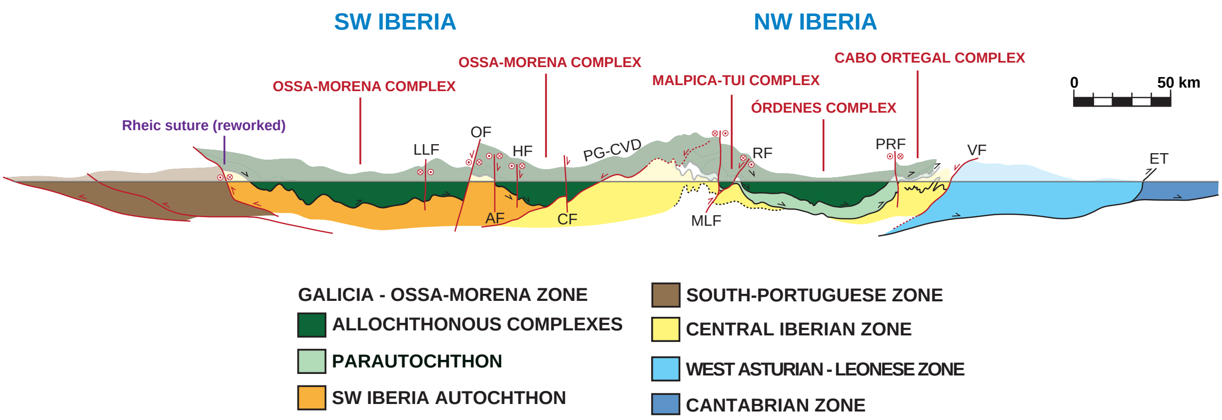

Fig. 3. Composite cross-section showing the general structure of the Galicia–Ossa-Morena Zone and its relationships with the other geotectonic zones of the Iberian Massif. Based on the more detailed sections presented by Díez Fernández and Arenas (2015).

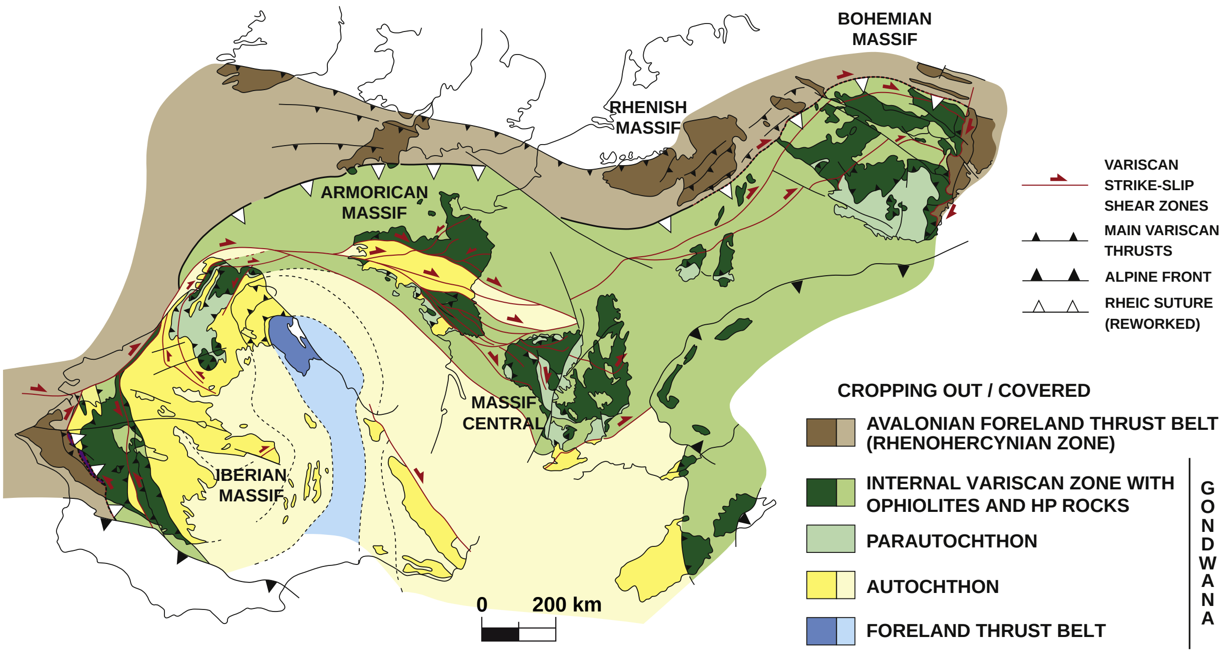

Fig. 4. Zonation of the Variscan Orogen.

age, in Sierra Albarrana Unit (Azor et al., 1991). Therefore, a preliminary distinction could be made between the autochthons of the Galicia–Ossa-Morena Zone, and thence the denomination of SW Iberia Autochthon is proposed for the domains underlying the Ossa-Morena Complex (Fig. 2). The stratigraphic characteristics of this autochthonous domain are not well known at present, but it likely occupied an outboard position across the margin of Gondwana compared to the autochthon of the Central Iberian Zone (Fig. 2).

The general structure of the Galicia–Ossa-Morena Zone is characterized by the presence of a large allochthonous sheet, thrust onto different domains of the continental platform of Gondwana (Fig. 3). This allochthonous sheet includes the most external domains of the margin of Gondwana. Therefore, the geology of the most internal part of the Iberian Massif accounts for a virtual duplication of the Gondwana margin (Fig. 3). The most external domains of this margin were transported during Variscan convergence above other domains of the Gondwana continental platform closer to the mainland, juxtaposing fairly distant regions with different stratigraphic and paleontological features. The stratigraphic and faunal contrast between the Central Iberian Zone and the Obejo-Valsequillo Domain pointed out by Gutiérrez-Marco et al. (2014) highlights these differences.

5. Variscan implications

The most important characteristics of the Galicia–Ossa-Morena Zone of the Iberian Massif can be also found in other massifs of the Variscan Orogen. The presence of ophiolitic units and units affected by Variscan high-P metamorphism is described in the Armorican Massif (Ballèvre et al., 2014), the French Massif Central (Lardeaux et al., 2001), the Bohemian Massif (Kryza and Pin, 2010; Faryad and Kachlík, 2013; Kroner and Romer, 2013) and the basement of the Alps, Corsica and Sardinia (Rossi et al., 2009; Von Raumer et al., 2009, 2015). These domains can be followed along the orogen and appear in the same geotectonic position. They configure an Internal Variscan Zone, limited to the north by the southern margin of Laurussia represented by the Rhenohercynian Zone (Fig. 4). The Internal Variscan Zone includes basement exposures that were previously correlated according to their strong Cadomian imprint (Linnemann et al., 2008; Martínez Catalán, 2011). Therefore it represents the external section of the Gondwanan margin, particularly the one showing the most prominent igneous and tectonothermal activity related to the magmatic arc-system developed in the periphery of Gondwana in Ediacaran-Cambrian times. This is also the most strongly deformed section of the Variscan Orogen. This section of the Gondwanan margin was involved in two continental subduction systems of Variscan age, and the resulting high-P metamorphic belts can be followed along the orogen (Arenas et al., 2014b). The dynamics of this margin is also characterized by the presence of ophiolitic units with similar ages and probably similar tectonic setting along the Variscan orogen (Arenas and Sánchez Martínez, 2015).

The correlations between allochthonous and autochthonous units in Iberia increase the perception of the Variscan Orogen as a markedly linear mountain belt. The Variscan orogeny resulted in a complex suture zone bounded by the southern margin of Laurussia. The duplication of the margin of Gondwana observed in the suture zone exposed in the Iberian Massif has not been described so far in other massifs of the orogen. But the observed analogy between the high-P units and the ophiolites existing throughout the orogen represents a solid argument to search for a similar structural correlation.

Acknowledgements

Insightful reviews by Antonio Castro and Juan Carlos Gutiérrez-Marco are kindly acknowledged. Financial support has been provided by the Spanish project CGL2012-34618 (Ministerio de Economía y Competitividad).

References

Abalos, B., Gil Ibarguchi, J.I., Eguiluz, L., 1991. Cadomian subduction, collision and Variscan transpression in the Badajoz-Cordoba Shear Belt, Southwest Spain. Tectonophysics 199, 51–72.

Abati, J., Castiñeiras, P., Arenas, R., Fernández-Suárez, J., Gómez-Barreiro, J., Wooden, J., 2007. Using SHRIMP zircon dating to unravel tectonothermal events in arc environments. The early Palaeozoic arc of NW Iberia revisited. Terra Nova 19, 432–439.

Abati, J., Dunning, G.R., Arenas, R., Díaz García, F., González Cuadra, P., Martínez Catalán, J.R., Andonaegui, P., 1999. Early Ordovician orogenic event in Galicia (NW Spain): evidence from U–Pb ages in the uppermost unit of the Ordenes complex. Earth Planet. Sci. Lett. 165, 213–228.

Abati, J., Gerdes, A., Fernández-Suárez, J., Arenas, R., Whitehouse, M.J., Díez Fernández, R., 2010. Magmatism and early-Variscan continental subduction in the Northern

Gondwana margin recorded in zircons from the basal units of Galicia, NW Spain. Geol. Soc. Am. Bull. 122, 219–235.

Albert, R., Arenas, R., Gerdes, A., Sánchez Martínez, S., Fernández-Suárez, J., Fuenlabrada, J.M., 2015. Provenance of the Variscan Upper Allochthon (Cabo Ortegal complex, (NW Iberian massif). Gondwana Res. 28, 1434–1448.

Andonaegui, P., Castiñeiras, P., González Cuadra, P., Arenas, R., Sánchez Martínez, S., Abati, J., Díaz García, F., Martínez Catalán, J.R., 2012. The corredoiras orthogneiss (NW Iberian massif): geochemistry and geochronology of the Paleozoic magmatic suite developed in a peri-gondwanan arc. Lithos 128-131, 84–99.

Apalategui, O., Pérez-Lorente, F., 1983. Nuevos datos en el borde meridional de la Zona Centroibérica. El dominio Obejo-Valsequillo-Puebla de la Reina. Stud. Geol. Salmanticensia 18, 193–200.

Araújo, A., Fonseca, P.E., Munhá, J.M., Moita, P., Pedro, J., Ribeiro, A., 2005. The Moura phyllonitic complex: an accretionary complex related with obduction in the Southern Iberia Variscan suture. Geodin. Acta 18, 375–388.

Arenas, R., Sánchez Martínez, S., 2015. Variscan ophiolites in NW Iberia: tracking lost Paleozoic oceans and the assembly of Pangea. Episodes 38, 315–333.

Arenas, R., Díez Fernández, R., Sánchez Martínez, S., Gerdes, A., Fernández-Suárez, J., Albert, R., 2014b. Two-stage collision: exploring the birth of Pangea in the Variscan terranes. Gondwana Res. 25, 756–763.

Arenas, R., Farias, P., Gallastegui, G., Gil Ibarguchi, J.I., González Lodeiro, F., Klein, E., Marquínez, J., Martín Parra, L.M., Martínez Catalán, J.R., Ortega, E., Pablo, Maciá, De, J.G., Peinado, M., Rodríguez Fernández, L.R., 1988. Características geológicas y significado de los dominios que componen la Zona de Galicia–Trás-os-Montes. Actas del II Congreso Geológico de España, v. Simp., pp. 75–84

Arenas, R., Martínez Catalán, J.R., Sánchez Martínez, S., Fernández-Suárez, J., Andonaegui, P., Pearce, J.A., Corfu, F., 2007. The Vila de cruces ophiolite: a remnant of the early Rheic Ocean in the Variscan suture of Galicia (NW Iberian massif). J. Geol. 115, 129–148.

Arenas, R., Sánchez Martínez, S., Castineiras, P., Jeffries, T.E., Díez Fernández, R., Andonaegui, P., 2009. The basal tectonic melange of the Cabo Ortegal complex (NW Iberian massif): a key unit in the suture of Pangea. J. Iber. Geol. 35, 85–125.

Arenas, R., Sánchez Martínez, S., Díez Fernández, R., Gerdes, A., Abati, J., Fernández-Suárez, J., Andonaegui, P., González Cuadra, P., López Carmona, A., Albert, R., Fuenlabrada, J.M., Rubio Pascual, F.J., 2016. Allochthonus terranes involved in the Variscan suture of NW Iberia: a review of their origin and tectonothermal evolution. Earth Sci. Rev. (submitted for publication).

Arenas, R., Sánchez Martínez, S., Gerdes, A., Albert, R., Díez Fernández, R., Andonaegui, P., 2014a. Re-interpreting the Devonian ophiolites involved in the Variscan suture: U–Pb and Lu-Hf zircon data of the Moeche Ophiolite (Cabo Ortegal complex, NW Iberia). Int. J. Earth Sci. 103, 1385–1402.

Azor, A., 1994. Evolución tectonometamórfica del límite entre las zonas Centroibérica y de Ossa-Morena (Cordillera Varisca, SO de España) (PhD thesis) Universidad de Granada, Spain (295 pp).

Azor, A., González Lodeiro, F., Marcos, A., Simancas, J.F., 1991. Edad y estructura de las rocas de sierra albarrana (SW del macizo Hespérico). Implicaciones regionales. Geogaceta 10, 119–124.

Azor, A., Lodeiro, F.G., Simancas, J.F., 1994. Tectonic evolution of the boundary between the Central Iberian and the Ossa-Morena zones (Variscan belt, Southwest Spain). Tectonics 13, 45–61.

Azor, A., Rubatto, D., Simancas, J.F., González Lodeiro, F., Martínez Poyatos, D., Martín Parra, L.M., Matas, J., 2008. Rheic Ocean ophiolitic remnants in southern Iberia questioned by SHRIMP U–Pb zircon ages on the Beja-Acebuches amphibolites. Tectonics 27, TC5006.

Ballèvre, M., Martínez Catalán, J.R., López Carmona, A., Abati, J., Díez Fernández, R., Ducassou, C., Pitra, P., Arenas, R., Bosse, V., Castiñeiras, P., Fernández-Suárez, P., Gómez Barreiro, J., Paquette, J.L., Peucat, J.J., Poujol, M., Ruffet, G., Sánchez Martínez, S., 2014. Correlation of the nappe stack in the Ibero-Armorican Arc across the bay of biscay: a joint French–Spanish Project. In: Schulmann, K., Martínez Catalán, J.R., Lardeaux, J.M., Oggiano, G. (Eds.), The Variscan Orogeny: Extent, Timescale and the Formation of the European Crust. Geological Society, London, Special Publications vol. 405, pp. 77–113.

Booth-Rea, G., Simancas, J.F., Azor, A., Azañón, J.M., González Lodeiro, F., Fonseca, P., 2006. HP-LT Variscan metamorphism in the Cubito-Moura schists (Ossa-Morena zone, southern Iberia). Compt. Rendus Geosci. 338, 1260–1267.

Borrego, J., Araújo, A., Fonseca, P., 2005. A geotraverse through the south and central sectors of the Ossa-Morena Zone in Portugal (Iberian massif). J. Virtual Explor. 19, 1–16.

Castro, A., 1987. Implicaciones de la Zona Ossa-Morena y dominios equivalentes en el modelo geodinámico de la Cadena Hercínica Europea. Estud. Geol. 43, 249–260.

Castro, A., Fernández, C., El-Hmidi, H., El-Biad, M., Díaz, M., de la Rosa, J., Stuart, F., 1999. Age constraints to the relationships between magmatism, metamorphism and tectonism in the Aracena metamorphic belt, Southern Spain. Int. J. Earth Sci. 88, 26–37.

Dias da Silva, I., Díez Fernández, R., Díez Montes, A., González Clavijo, E., Foster, D.A., 2015. Magmatic evolution in the N-gondwana margin related to the opening of the Rheic Ocean — evidence from the upper parautochthon of the Galicia - Trás-os-montes zone and from the Central Iberian zone (NW Iberian massif). Int. J. Earth Sci. http://dx.doi.org/10.1007/s00531-015-1232-9 (in press).

Dias da Silva I, Valverde-Vaquero, P., González Clavijo, E., Díez Montes, A., Martínez Catalán, J.R., Schulmann, K., Martínez Catalán, J.R., Lardeaux, J.M., Janousek, V., Oggiano, G., 2014. Structural and stratigraphical significance of U–Pb ages from the Mora and Saldanha volcanic complexes (NE Portugal, Iberian Variscides). The Variscan Orogeny: Extent, Timescale and the Formation of the European Crust Geological Society of London Special Publication 405, 115–135.

Díaz García, F., Arenas, R., Martínez Catalán, J.R., González del Tánago, J., Dunning, G.R., 1999. Tectonic evolution of the Careón ophiolite (Northwest Spain): a remnant of oceanic lithosphere in the Variscan Belt. J. Geol. 107, 587–605.

Díaz García, F., Sánchez Martínez, S., Castiñeiras, P., Fuenlabrada, J.M., Arenas, R., 2010. A peri-Gondwanan arc in NW Iberia. II: assessment of the intra-arc tectonothermal evolution through U–Pb SHRIMP dating of mafic dykes. Gondwana Res. 17, 352–362.

Díaz-Azpiroz, M., Fernández, C., Castro, A., El-Biad, M., 2006. Tectonometamorphic evolution of the Aracena metamorphic belt (SW Spain) resulting from ridge-trench interaction during Variscan plate convergence. Tectonics 25, TC1001.

Díez Fernández, R., Arenas, R., 2015. The late Devonian Variscan suture of the Iberian Massif: a correlation of high-pressure belts in NW and SW Iberia. Tectonophysics 654, 96–100.

Díez Fernández, R., Arenas, R., 2016. Reply to Comment on “The Late Devonian Variscan suture of the Iberian Massif: a correlation of high-pressure belts in NW and SW Iberia”. Tectonophysics 670, 155–160.

Díez Fernández, R., Martínez Catalán, J.R., Arenas, R., Abati, J., 2012a. The onset of the assembly of Pangaea in NW Iberia: constraints on the kinematics of continental subduction. Gondwana Res. 22, 20–25.

Díez Fernández, R., Martínez Catalán, J.R., Arenas, R., Abati, J., Gerdes, A., Fernández-Suárez, J., 2012b. U–Pb detrital zircon analysis of the lower allochthon of NW Iberia: age constraints, provenance and links with the Variscan mobile belt and Gondwanan cratons. J. Geol. Soc. 169, 655–665.

Díez Fernández, R., Castiñeiras, P., Gómez Barreiro, J., 2012c. Age constraints on lower Paleozoic convection system: magmatic events in the NW Iberian Gondwana margin. Gondwana Res. 21, 1066–1079.

Díez Fernández, R., Foster, D.A., Gómez Barreiro, J., Alonso-García, M., 2013. Rheological control on the tectonic evolution of a continental suture zone: the Variscan example from NW Iberia (Spain). Int. J. Earth Sci. 102, 1305–1319.

Díez Fernández, R., Martínez Catalán, J.R., Gerdes, A., Abati, J., Arenas, R., Fernández-Suárez, J., 2010. U–Pb ages of detrital zircons from the basal allochthonous units of NW Iberia: provenance and paleoposition on the northern margin of Gondwana during the Neoproterozoic and Paleozoic. Gondwana Res. 18, 385–399.

Farias, P., Gallastegui, G., González-Lodeiro, F., Marquínez, J., Martín Parra, L.M., Martínez Catalán, J.R., Pablo Maciá, J.G., de Rodríguez Fernández, L.R., 1987. Aportaciones al conocimiento de la litoestratigrafía y estructura de Galicia central 1. Memórias da Facultade de Ciências, Universidade do Porto, pp. 411–431.

Faryad, S.W., Kachlík, V., 2013. New evidence of blueschist facies rocks and their geoectonic implication for Variscan suture (s) in the Boheman massif. J. Metamorph. Geol. 31, 63–82.

Fernández-Suárez, J., Arenas, R., Abati, J., Martínez Catalán, J.R., Whitehouse, M.J., Jeffries, T.E., 2007. U–Pb Chronometry of Polymetamorphic High-Pressure Granulites: An Example from the Allochthonous Terranes of the NW Iberian Variscan Belt. In: Hatcher Jr., R.D., Carlson, M.P., McBride, J.H., Martínez Catalán, J.R. (Eds.), 4-D Framework of Continental Crust. Geological Society of America Memoir vol. 200, pp. 469–488.

Franke, W., 2000. The Middle-European Segment of the Variscides: Tectonostratigraphic Units, Terrane Boundaries and Plate Tectonic Evolution. In: Franke, W., Haak, U., Oncken, O., Tanner, D. (Eds.), Orogenic Processes: Quantification and Modelling in the Variscan Belt. Geological Society London, Special Publication vol. 179, pp. 3–61.

Franke, W., Engel, W., 1982. Variscan sedimentary basins on the continent and relations with SW England. Proc. Ussher Soc. 5, 259–269.

Galindo, C., 1989. Petrología y geocronología del complejo plutónico Táliga-Barcarrota (Badajoz) (PhD. thesis) Universidad Complutense de Madrid, Spain (378 pp).

Gómez-Barreiro, J., Wijbrans, J.R., Castiñeiras, P., Martínez Catalán, J.R., Arenas, R., Díaz García, F., Abati, J., 2006. $^{40}Ar/^{39}Ar$ laserprobe dating of mylonitic fabrics in a polyorogenic terane of NW Iberia. J. Geol. Soc. Lond. 163, 61–73.

González Cuadra, P., 2007. La Unidad de corredoiras (complejo de Órdenes, Galicia): Evolución estructural y metamórfica. Ediciós do Castro, Sada, serie Nova Terra 33 (254 pp).

González del Tánago, J., 1995. El núcleo metamórfico de sierra albarrana y su campo de pegmatitas graníticas asociado, macizo Ibérico, Córdoba, España. Ediciós do Castro, Sada, serie Nova Terra 12 (511 pp).

Gutiérrez-Marco, J.C., Sarmiento, G., Rábano, I., 2014. Un olistostroma con cantos y bloques del paleozoico inferior en la Cuenca carbonífera del guadalmellato (Córdoba). Parte II: Bioestratigrafía y afinidades paleogeográficas. Rev. Soc. Geol. Esp. 27, 27–45.

Hatcher Jr., R.D., 1989. Tectonic synthesis of the U.S. Appalachians. In: R.D. Jr., Hatcher, Thomas, W.A., Viele, G.W. (Eds.), The Appalachian-Ouachita orogen in the United States. Geological society Of America, Decade of North American Geology v. F-2, pp. 511–531.

Hodges, K.V., 2000. Tectonics of the Himalaya and Southern Tibet from two perspectives. Geol. Soc. Am. Bull. 112, 324–350.

Julivert, M., Fontboté, J.M., Ribeiro, A., Conde, L., 1972. Mapa Tectónico de la Península Ibérica y Baleares E. 1:1.000.000. Instituto Geológico y Minero de España, Madrid.

Kroner, U., Romer, R.L., 2013. Two plates — many subduction zones: the Variscan orogeny reconsidered. Gondwana Res. 24, 298–329.

Kryza, R., Pin, C., 2010. The Central-Sudetic ophiolites (SW Poland): petrogenetic issues, geochronology and palaeotectonic implications. Gondwana Res. 17, 292–305.

Lardeaux, J.M., Ledru, P., Daniel, I., Duchene, S., 2001. The Variscan French massif central-a new addition to the ultra-high pressure metamorphic ‘club’: exhumation processes and geodynamic consequences. Tectonophysics 332, 143–167.

Linnemann, U., Herbosch, A., Liégeois, J.P., Pin, C., Gärtner, A., Hofmann, M., 2012. The Cambrian to Devonian odyssey of the Brabant massif within Avalonia: a review with new zircon ages, geochemistry, Sm-Nd isotopes, stratigraphy and palaeogeography. Earth Sci. Rev. 112, 126–154.

Linnemann, U., Pereira, F., Jeffries, T.E., Drost, K., Gerdes, A., 2008. The cadomian orogeny and the opening of the Rheic Ocean: the diacrony of the geotectonic processes constrained by LA-ICP-MS U–Pb zircon dating (Ossa-Morena and Saxo-Thuringian zones, Iberian and Bohemian massifs). Tectonophysics 461, 21–43.

López-Guijarro, R., Armendariz, M., Quesada, C., Fernández-Suárez, J., Murphy, J.B., Pin, C., Bellido, F., 2008. Ediacaran–Palaeozoic tectonic evolution of the Ossa-Morena and

Central Iberian zones (SW Iberia) as revealed by Sm-Nd isotope systematics. Tectonophysics 461, 202–214.
Lotze, F., 1945. Zur gliederung der varisziden der iberischen meseta. Geotekt. Forsch. 6, 78–92.
Martín Parra, L.M., González Lodeiro, F., Martínez Poyatos, D., Matas, J., 2006. The Puente Génave-Castelo de Vide Shear Zone (southern central Iberian zone, Iberian massif): geometry, kinematics and regional implications. Bull. Soc. Géol. Fr. 177, 191–202.
Martínez Catalán, J.R., 2011. Are the oroclines of the Variscan belt related to late Variscan strike-slip tectonics? Terra Nova 23, 241–247.
Martínez Catalán, J.R., Arenas, R., Abati, J., Sánchez Martínez, S., Díaz García, F., Fernández-Suárez, J., González Cuadra, P., Castiñeiras, P., Gómez Barreiro, J., Díez Montes, A., González Clavijo, E., Rubio Pascual, F.J., Andonaegui, P., Jeffries, T.E., Alcock, J.E., Díez Fernández, R., López Carmona, A., 2009. A rootless suture and the loss of the roots of a mountain chain: the Variscan belt of NW Iberia. Compt. Rendus Geosci. 341, 114–126.
Martínez Catalán, J.R., González Clavijo, E., Meireles, C., Díez Fernández, R., Bevis, J., 2016. Relationships between syn-orogenic sedimentation and nappe emplacement in the hinterland of the Variscan belt in NW Iberia deduced from detrital zircons. Geol. Mag. 153, 38–60.
Martínez Poyatos, D., 2002. Estructura del borde meridional de la zona Centroibérica y su relación con el contacto entre las zonas Centroibérica y de Ossa-Morena. Ediciós do Castro, Sada, serie Nova Terra 18 (295 pp).
Matte, Ph., 2001. The Variscan collage and orogeny (480–290 Ma) and the tectonic definition of the Armorica microplate: a review. Terra Nova 13, 122–128.
Moita, P., Munhá, J., Fonseca, P.E., Pedro, J., Tassinari, C.C.G., Araújo, A., Palacios, T., 2005. Phase equilibria and geochronology of Ossa-Morena eclogites. Abstract, XIV Semana de Geoquímica, VIII Congresso de Geoquímica dos Paises de Lingua Portuguese, Aveiro, Portugal, pp. 463–466.
Murphy, J.B., Cousens, B.L., Braid, J.A., Strachan, R.A., Dostal, J., Keppie, J.D., Nance, R.D., 2011. Highly depleted oceanic lithosphere in the Rheic Ocean: implications for Paleozoic plate reconstructions. Lithos 123, 165–175.
Ordóñez Casado, B., 1998. Geochronological Studies of the Pre-Mesozoic Basement of the Iberian Massif: the Ossa-Morena Zone and the Allochthonous Complexes Within the Central Iberian Zone (PhD thesis) Swiss Federal Institute of Technology, Zürich, Switzerland (235 pp).
Ordóñez Casado, B., Gebauer, D., Schäfer, H.J., Gil Ibarguchi, J.I., Peucat, J.J., 2001. A single Devonian subduction event for the HP/HT metamorphism of the Cabo Ortegal complex within the Iberian massif. Tectonophysics 332, 359–385.
Pedro, J., Araújo, A., Fonseca, P., Tassinari, C., Ribeiro, A., 2010. Geochemistry and U–Pb zircon age of the internal Ossa-Morena zone ophiolites sequences: a remnant of Rheic Ocean in SW Iberia. Ofioliti 35, 117–130.
Pereira, M.F., Apraiz, A., Chichorro, M., Silva, J.B., Armstrong, R.A., 2010. Exhumation of high-pressure rocks in northern Gondwana during the Early Carboniferous (Coimbra-Córdoba shear zone, SW Iberian massif): tectonothermal analysis and U–Th–Pb SHRIMP in-situ zircon geochronology. Gondwana Res. 17, 440–460.
Pereira, M.F., Solá, A.R., Chichorro, M., Lopes, L., Gerdes, A., Silva, J.B., 2012. North Gondwana assembly, break-up and paleogeography: U–Pb isotope evidence from detrital and igneous zircons of Ediacaran and Cambrian rocks of SW Iberia. Gondwana Res. 22, 866–881.
Piçarra, J.M., Gutiérrez-Marco, J.C., Sá, A.A., Meireles, C., González Clavijo, E., 2006. Silurian graptolite biostratigraphy of the Galicia–Trás-os-Montes Zone (Spain and Portugal). J. Geol. Soc. Swed. 128, 185–188.
Pin, C., Paquette, J.L., Santos Zalduegui, J.F., Gil Ibarguchi, J.I., 2002. Early Devonian Supra-Subduction Zone Ophiolite Related to Incipient Collisional Processes in the Western Variscan Belt: The Sierra De Careón Unit, Órdenes Complex, Galicia. In: Martínez Catalán, J.R., Hatcher Jr., R.D., Arenas, R., Díaz García, F. (Eds.), Variscan-Appalachian Dynamics: the Building of the Late Paleozoic Basement. Geological Society of America Special Paper vol. 364, pp. 57–71.
Rodríguez, J., Cosca, M.A., Gil Ibarguchi, J.I., Dallmeyer, R.D., 2003. Strain partitioning and preservation of $^{40}Ar/^{39}Ar$ ages during variscan exhumation of a subducted crust (Malpica-Tui complex, NW Spain). Lithos 70, 111–139.
Rossi, P., Oggiano, G., Cocherie, A., 2009. A restored section of the “southern Variscan realm” across the Corsica–Sardinia microcontinent. Compt. Rendus Geosci. 341, 224–238.
Rubio Pascual, F.J., Matas, J., Martín Parra, L.M., 2013. High-pressure metamorphism in the early Variscan subduction complex of the SW Iberian massif. Tectonophysics 592, 187–199.
San José, M.A., Herranz, P., Pieren, A.P., 2004. A review of the Ossa-Morena Zone and its limits. Implications for the definition of the Lusitan-Marianic Zone. J. Iber. Geol. 30, 7–22.
Sánchez Martínez, S., Arenas, R., Gerdes, A., Castiñeiras, P., Potrel, A., Fernández-Suárez, J., 2011. Isotope geochemistry and revised geochronology of the Purrido Ophiolite (Cabo Ortegal Complex, NW Iberian massif): devonian magmatism with mixed sources and involved Mesoproterozoic basement. J. Geol. Soc. Lond. 168, 733–750.
Sánchez Martínez, S., Gerdes, A., Arenas, R., Abati, J., 2012. The Bazar Ophiolite of NW Iberia: a relict of the Iapetus-Tornquist ocean in the variscan suture. Terra Nova 24, 283–294.
Schmid, S.M., Fügenshuh, B., Kissling, E., Schuster, R., 2004. Tectonic map and overall architecture of the Alpine Orogen. Eclogae Geol. Helv. 97, 93–117.
Simancas, J.F., Azor, A., Martínez Poyatos, D.J., Expósito Ramos, I., Pérez-Cáceres, I., González Lodeiro, F., 2016. Comment on “The Late Devonian Variscan suture of the Iberian Massif: a correlation of high-pressure belts in NW and SW Iberia. Tectonophysics 654, 96-–100” by R. Díez Fernández and R. Arenas 666, 281–284.
Simancas, J.F., Martínez Poyatos, D.J., Expósito, I., Azor, A., González Lodeiro, F., 2001. The structure of a major suture zone in the SW Iberian Massif: the Ossa-Morena/Central Iberian contact. Tectonophysics 332, 295–308.
Valverde-Vaquero, P., Marcos, A., Farias, P., Gallastegui, G., 2005. U–Pb dating of Ordovician felsic vulcanics in the schistose domain of the Galicia–Trás-os-Montes Zone near Cabo Ortegal (NW Spain). Geol. Acta 3, 27–37.
Von Raumer, J.F., Bussy, F., Stampfli, G.M., 2009. The Variscan evolution in the external massifs of the Alps and place in their Variscan framework. Compt. Rendus Geosci. 341, 239–252.
Von Raumer, J.F., Stampfli, G.M., Arenas, R., Sánchez Martínez, S., 2015. Ediacaran to Cambrian oceanic rocks of the Gondwana margin and their tectonic interpretation. Int. J. Earth Sci. 104, 1107–1121.
Weil, A.B., Gutiérrez-Alonso, G., Johnston, S.T., Pastor-Galán, D., 2012. Kinematic constraints on buckling a lithospheric-scale orocline along the northern margin of Gondwana: a geologic synthesis. Tectonophysics 582, 25–49.

Capítulo 6

A peri-Gondwanan arc in NW Iberia I: Isotopic and geochemical constraints on the origin of the arc. A sedimentary approach

6.1 Introducción

En las Unidades Superiores de los Complejos Alóctonos del NW del Macizo Ibérico, los trabajos anteriores a la publicación que se presenta en este capítulo han sido muy numerosos y han abordado una diversidad de aspectos relativos al estudio de la estructura y evolución metamórfica (*Díaz García, 1990; Fernández Rodríguez, 1997; Azcárraga, 2000; Mendia, 2000; Puelles, 2004; Castiñeiras, 2005; Gómez Barreiro, 2007; González Cuadra, 2007; García Izquierdo et al., 2011; y referencias incluidas en ellos*) o de la geocronología de los procesos implicados (*Santos Zalduegui, 1995; Abati, 2002; Albert, 2015b; y referencias incluidas en ellos*). Una síntesis de la geología de estas unidades puede encontrarse en *Arenas et al. (2016)*. Dichos trabajos aportan un gran conocimiento de la historia geológica de las Unidades Superiores y establecen que una parte de la evolución de estas unidades se relaciona con la actividad de un arco magmático peri-gondwánico, activo en el Paleozoico inferior. El margen de Gondwana y los restos de este arco fueron afectados por los episodios principales de la Orogenia Varisca durante el posterior ensamblado de Pangea y la colisión entre Laurussia y Gondwana, durante el Devónico y Carbonífero. Por su parte, el trabajo que aquí se presenta intenta profundizar en el estudio de estas unidades aportando nuevos datos sobre el origen de este arco, de algunas de las series sedimentarias relacionadas y de la naturaleza de sus áreas fuentes.

Para llevar a cabo este estudio se han caracterizado los aspectos geoquímicos e isotópicos de las series grauváquicas culminantes que afloran en las Unidades Superiores del Complejo de Órdenes. Se han estudiado las composiciones de 20 muestras recogidas en la sección costera de la Ría de Ares, entre las localidades de Ares y Redes. Estas series metasedimentarias de bajo grado nos han permitido interpretar, desde un punto de vista geoquímico, el ambiente dinámico de generación de las Unidades Alóctonas Superiores. Por otra parte, la geoquímica isotópica (Sm-Nd) permite también una aproximación precisa al origen de sus áreas fuente (fuentes isotópicas). Los nuevos datos son coherentes con los trabajos previos, pero permiten aumentar el conocimiento sobre la evolución del paleomargen de Gondwana.

6.2 Conclusiones parciales

Los resultados geoquímicos presentados en este trabajo para las series grauváquicas del Complejo de Órdenes, muestran una clara afinidad con una sedimentación relacionada con un arco volcánico altamente evolucionado, con un magmatismo dominantemente félsico. Este arco se habría desarrollado en el contexto de un margen continental activo, como un arco magmático edificado sobre un margen continental adelgazado. Por consiguiente, las abundancias de determinados elementos, que se muestran inmóviles en procesos sedimentarios y metamórficos, se encuentran alejadas de las concentraciones típicas de contextos de márgenes pasivos o de arcos volcánicos construidos sobre cortezas oceánicas (arcos de islas típicos).

Por su parte, las edades modelo de Nd (T_{DM}) varían desde el Neoproterozoico Medio hasta el Mesoproterozoico Superior (720-1215 Ma). Este rango de edad, junto con la ausencia de circones detríticos de estas edades (*Fernández Suárez et al., 2003*), sugiere una participación de diferentes áreas fuentes con mezcla de componentes ediacarenses y paleoproterozoicos y/o más antiguos. Esas edades están ampliamente representadas en las poblaciones de circones detríticos de estas series, y son comunes en áreas cercanas al Cratón del Oeste de África. Esta procedencia parece también confirmada por la ausencia de una población de circones de edad Mesoproterozoica (*Fernández Suárez et al., 2003*). Por otra parte, las poblaciones de circones detríticos de estas grauvacas indican una edad máxima de sedimentación comprendida entre ca. 510 y 530 Ma (Cámbrico Medio - Inferior). La cercanía entre las edades máximas de sedimentación de las metagrauvacas y la edad del magmatismo de las unidades superiores del Complejo de Órdenes (ca. 500-520 Ma; *Andonaegui et al., 2016*), indica que la sedimentación de estas series tuvo lugar coincidiendo con una fase principal de actividad del arco peri-Gondwánico. La probable deposición de las grauvacas sobre una corteza continental adelgazada y la posición actual de las series turbidíticas sobre una serie compleja de rocas metamórficas de alto grado, cuya historia tectonotermal está al menos en parte relacionada con la actividad del arco (*Arenas et al., 2016*), sugiere que su posición refleja la localización originaria. La sedimentación tuvo lugar posiblemente en una cuenca intra-arco, situada sobre complejos metamórficos y plutónicos relacionados con la actividad del arco y con presencia de basamento continental anterior a la formación del sistema de arcos.

Gondwana Research 17 (2010) 338–351

Contents lists available at ScienceDirect

Gondwana Research

journal homepage: www.elsevier.com/locate/gr

A peri-Gondwanan arc in NW Iberia I: Isotopic and geochemical constraints on the origin of the arc—A sedimentary approach

J.M. Fuenlabrada [a], R. Arenas [b,*], S. Sánchez Martínez [c], F. Díaz García [d], P. Castiñeiras [b]

[a] CAI de Geocronología y Geoquímica Isotópica, Facultad de Geología, Universidad Complutense de Madrid, 28040 Madrid, Spain
[b] Departamento de Petrología y Geoquímica e Instituto de Geología Económica (CSIC), Universidad Complutense de Madrid, 28040 Madrid, Spain
[c] Institut für Geowissenschaften, Mineralogie-Petrologie und Geochemie, Goethe-Universität, Altenhöferallee 1, D-60438 Frankfurt am Main, Germany
[d] Departamento de Geología, Universidad de Oviedo, 33005 Oviedo, Spain

A R T I C L E I N F O

Article history:
Received 22 April 2009
Received in revised form 17 September 2009
Accepted 23 September 2009
Available online 6 October 2009

Keywords:
Cambrian turbidites
Sediment geochemistry
Nd isotope composition
Provenance
Peri-Gondwanan arc
Allochthonous complexes
NW Iberia

A B S T R A C T

The arc-derived upper terrane in the NW Iberia Variscan belt contains a 3000 m thick turbiditic formation at its structural top. Most of the sandstones are feldspathic greywackes with a framework of quartz and weakly altered plagioclase. Rock fragments of vitric and microgranular texture are common in polymictic conglomerates and coarse-grained greywackes, together with slates, cherts and bipyramidal volcanic quartz fragments. Although recrystallization under greenschists facies conditions (chlorite and biotite zones) and the presence of two cleavages hinder detailed textural analysis, the sandstones appear to be typically immature, first-cycle sandstones. The metagreywackes have average major and trace element compositions similar to PAAS (Post Archean Australian Shale), which is considered to reflect the composition of the upper continental crust. Their trace element composition is very consistent and records deposition within a convergent tectonic setting, probably in an intra-arc basin located in a volcanic arc built on thinned continental margin. Detrital zircon populations suggest a Middle Cambrian maximum depositional age (530–500 Ma) and a Gondwanan provenance located at the periphery of the West African Craton. Nd isotope data suggest mixing Ediacaran and Paleoproterozoic sources for the provenance of the greywackes, with T_{DM} ranging between 720 and 1215 Ma with an average of 995 Ma ($n = 20$)—an age range unrepresented in the detrital zircon population. The Nd model ages are similar to those exhibited by West Avalonia, Florida or the Carolina terrane, but younger than those of Cambrian and Ordovician sandstones and shales from the autochthonous realm. These data suggest a westernmost location along the Gondwanan margin for the upper terrane of NW Iberia relative to other terranes located in the footwall of the Variscan suture, consistent with several previously proposed paleogeographic models for the NW Iberia terranes.

1. Introduction

The European Variscan Belt and its continuation through the Appalachian Orogen is a major orogenic belt developed during the final stages of the assembly of Pangea as a result of the closure of the Rheic Ocean (Casini and Oggiano, 2008; Nance et al., 2010-this issue; Keppie et al., 2010-this issue; Melleton et al., 2010) and the collision between Gondwana and Laurussia (Matte, 1991; Martínez Catalán et al., 2007), which was probably oblique (Arenas et al., 2009). In Europe, the most internal part of this belt includes a succession of allochthonous complexes that define the main suture zone and are considered to be remant klippen of a large nappe pile (Fig. 1). The allochthonous complexes in the NW Iberian Massif include three main terranes designated, from bottom to top, the basal units, ophiolitic units and upper units (Fig. 2). The basal units are considered to be the most external margin of Gondwana subducted beneath Laurussia at the onset of Variscan deformation (c. 370 Ma; Arenas et al., 1995; Martínez Catalán et al., 1996; Rodríguez et al., 2003; Abati et al., 2010), whereas the upper units are interpreted to be an arc-derived terrane. This arc also has a peri-Gondwanan provenance (Fernández-Suárez et al., 2003), but left the main continent during the Middle Cambrian–Early Ordovician and drifted north contemporaneously with the opening of the Rheic Ocean, which is represented within the stack of allochthonous units by different types of ophiolites (Díaz García et al., 1999; Pin et al., 2002; Arenas et al., 2007; Sánchez Martínez et al., 2007a,b). This rifted arc was finally accreted to the southern margin of Laurussia during the Lower or Middle Devonian (Gómez Barreiro et al., 2007).

* Corresponding author. Departamento de Petrología y Geoquímica, Facultad de Geología, Universidad Complutense de Madrid, C/José Antonio Novais, no. 2, 28040 Madrid, Spain.
E-mail address: arenas@geo.ucm.es (R. Arenas).

1342-937X/$ – see front matter © 2009 International Association for Gondwana Research. Published by Elsevier B.V. All rights reserved.
doi:10.1016/j.gr.2009.09.007

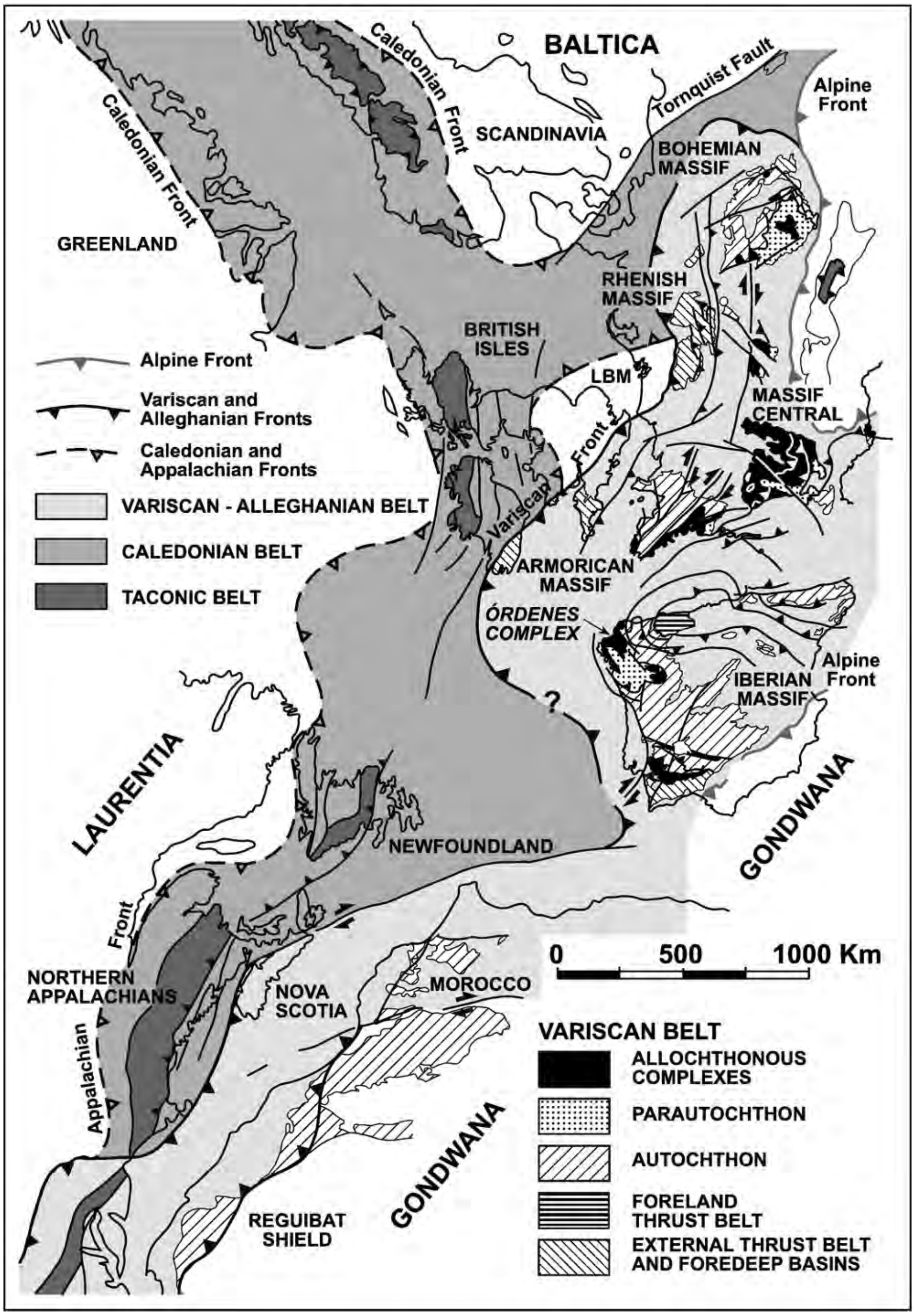

Fig. 1. Sketch showing the distribution of the Paleozoic orogens in a reconstruction of the Baltica–Laurentia–Gondwana junction developed during the assembly of Pangea. The distribution of the most important domains described in the Variscan Belt is also shown, together with the position of the Órdenes Complex in NW Iberia. LBM: London-Brabant Massif. From Martínez Catalán et al. (2002).

Different articles have described the structure and general metamorphic evolution of the arc-derived upper units of the allochthonous complexes of NW Iberia (see Martínez Catalán et al., 2002 and references therein), and data also exist on the geochronology of the tectonothermal events and main magmatic pulses. However, most previous work on the tectonothermal evolution of these units has focussed on events related to the accretion of the arc to Laurussia, and its subsequent Variscan history. Details of the arc's tectonothermal evolution during its development at the periphery of Gondwana are less well known. In addition, the location of the arc within peri-Gondwana and whether it was built on the Gondwanan continental margin or was generated above an intra-oceanic subduction zone at some distance from the margin, remain unknown. To help resolve these issues, we present two consecutive papers on aspects related to the initial development of this magmatic arc. The first paper describes the geochemical features, tectonic setting and provenance of the thick low-grade greywacke series that occupies the uppermost structural position in the upper units of the Órdenes Complex (Figs. 1 and 2) in order to constrain the tectonic setting of the magmatic arc, its internal constitution and its location within peri-Gondwana. The second describes the internal structure of the metagreywacke series and presents new U–Pb age data for a diabasic dyke swarm that intrudes the metasediments (Díaz García et al., 2010-this issue). The new age data constrains the origin of the main fabric at the upper structural levels in the Órdenes Complex and its relationship to magmatic arc dynamics.

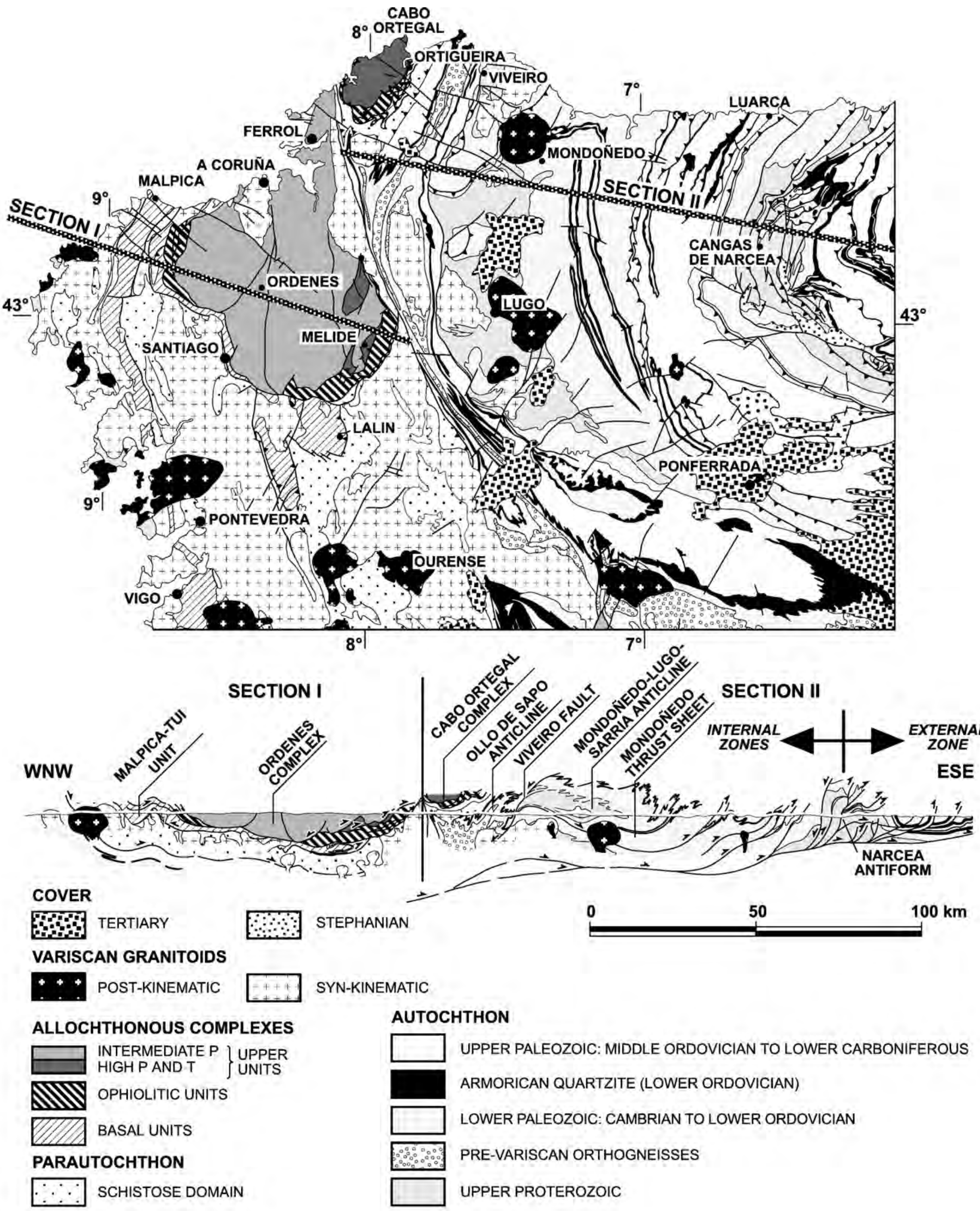

Fig. 2. Geological map of NW Iberia. It shows the distribution of the Autochthon and Parautochthon domains and the main terranes involved in the allochthonous complexes located in the most internal part of the belt.

2. Geological setting of the arc-derived terrane

The upper units of the allochthonous complexes of NW Iberia represent a well-preserved section of a peri-Gondwanan magmatic arc. These units are well exposed in the Cabo Ortegal and Órdenes complexes, and include a large variety of lithologies (Fig. 3). The internal structure of the upper units is characterized by the presence of two sheets that display slightly different tectonothermal histories.

The lower sheet (HP–HT upper units) is a polymetamorphic assemblage affected by a widespread high-pressure and high-temperature metamorphic event, the age of which is estimated to be 410–390 Ma (Ordoñez Casado et al., 2001; Fernández Suárez et al., 2007). This

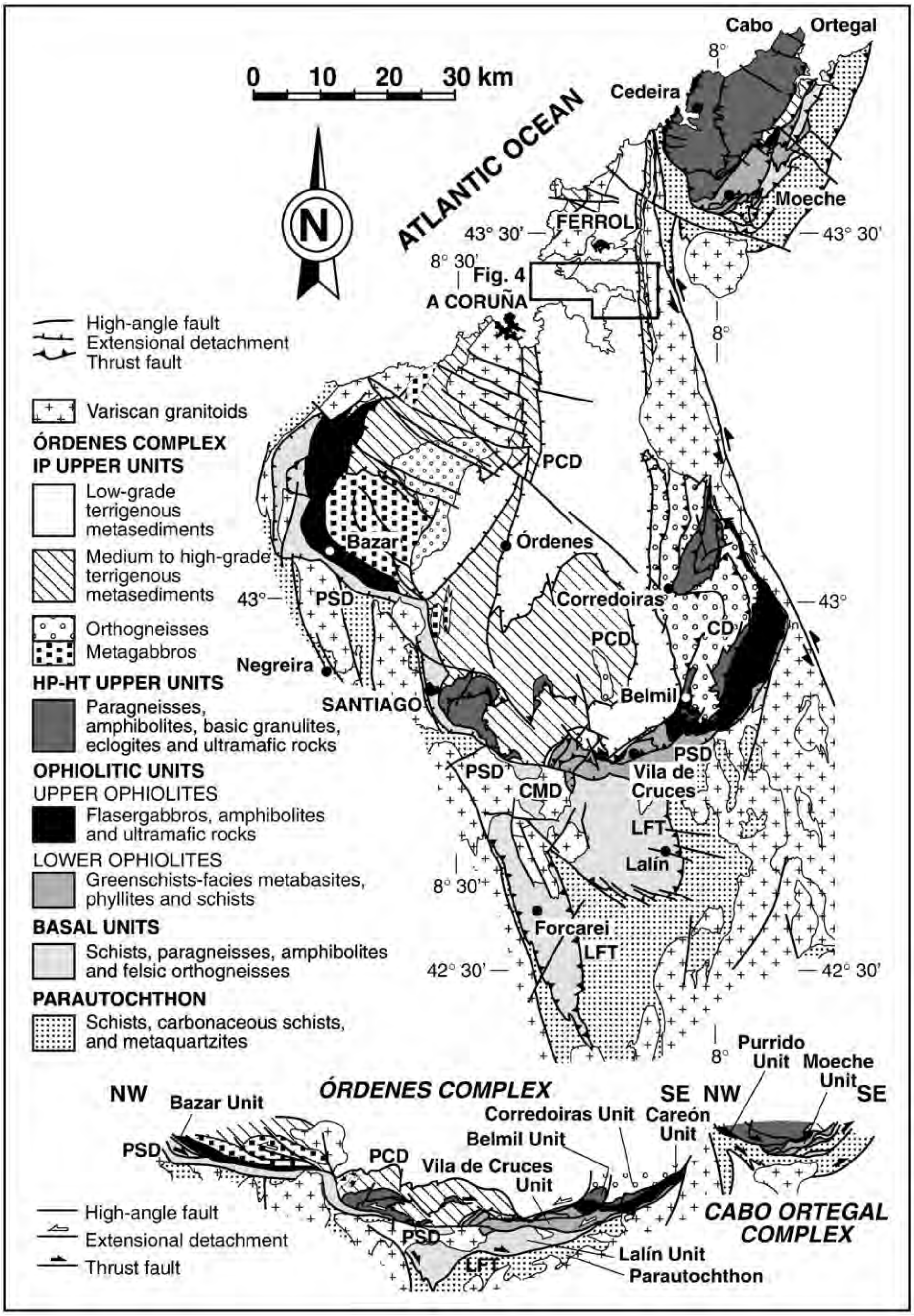

Fig. 3. Geological sketch and cross-section of the Órdenes and Cabo Ortegal complexes (Martínez Catalán et al., 2002; Arenas et al., 2007), with the distribution of the main allochthonous terranes, the basal, ophiolitic and upper units. The position of the area represented in Fig. 4 is also shown. CD, Corredoiras detachment; CMD, Campo Marzo detachment; LFT, Lalín-Forcarei thrust; PCD, Ponte Carreira detachment; PSD, Pico Sacro detachment.

metamorphic event is considered to be related to the accretion of the arc to the southern margin of Laurussia, which facilitated imbrication of a basal sheet that subducted until the development of the HP–HT event. The metamorphic P–T conditions reached around 800 °C and 20–23 kb, obscuring preservation of tectonothermal events prior to the accretion of the arc to Laurussia. Nevertheless, Fernández-Suarez et al. (2002) identified a widespread metamorphic event dated at ca. 490–480 Ma in paragneisses of the lower sheet. This early event reached high-temperature and medium-pressure conditions, but its significance is uncertain. It may be related to the dynamics associated with the magmatic arc while it occupied a position at the periphery of Gondwana.

The upper sheet (intermediate-pressure upper units) consists of medium- to low-grade metasedimentary sequences of problematic age, massifs of variably deformed and metamorphosed gabbros and granitoids, and a thick metagreywacke series occupying the uppermost position (Fig. 3). Both gabbros and granitoids have typical volcanic arc compositions, and have been dated at c. 500 Ma. Abati et al. (1999) have dated (TIMS U–Pb zircons) the Monte Castelo gabbro (western part of the Órdenes Complex) at 499 ± 2 Ma and the Corredoiras orthogneiss (easter part of the same complex) at 500 ± 2 Ma. The upper sheet shows a widespread medium-pressure and variable low- to high-temperature event (see Abati et al., 2003 and references therein), with which most of the regionally distributed fabrics can be associated. The significance of this metamorphic event is uncertain, although it has been repeatedly dated at c. 490–480 Ma (Abati et al., 1999, 2007) and, as in the lower sheet, has been interpreted as related to the earlier dynamics of the peri-Gondwanan arc. The generation of granulitic shear zones that affect the large gabbroic massifs at the base of this sheet has been linked to this event (Abati et al., 2007). In this intermediate-pressure upper unit, it is often difficult to recognize the significance of the tectonothermal evolution subsequent to the development of the dominant regional fabrics, including events associated with the accretion of the arc to Laurussia and those that came later, during the Variscan. As a result, these uppermost units afford an excellent opportunity to investigate the role of the early dynamics of the peri-Gondwanan magmatic arc.

The metagreywacke series, which occupies the uppermost structural levels, is particularly well exposed on the coastline, where it outcrops a schistose formation with frequent recumbent folds, intruded by a swarm of diabasic dykes that, in most cases, clearly cut the regional fabrics. The features and internal structure of this metagreywacke formation were first described by Matte and Capdevila (1978), who identified the presence of large recumbent folds. These folds make it difficult to create detailed stratigraphic columns of the greywacke formation or estimate its true thickness.

3. Lithological and sedimentological features of the top greywacke series

The uppermost series in the intermediate-pressure upper units occupies the central part of the Órdenes Complex (Fig. 3) and is exclusively composed of metasediments intruded by minor gabbroic and diabasic dykes. Intense polyphase deformation precludes precise determination of thickness, but it is roughly estimated to be a maximum of 3 km (Fig. 4). The lower half of this series contains a strong penetrative crenulation cleavage (S_2), with syntectonic garnet and biotite porphyroblasts, the paragenesis of which culminates in the

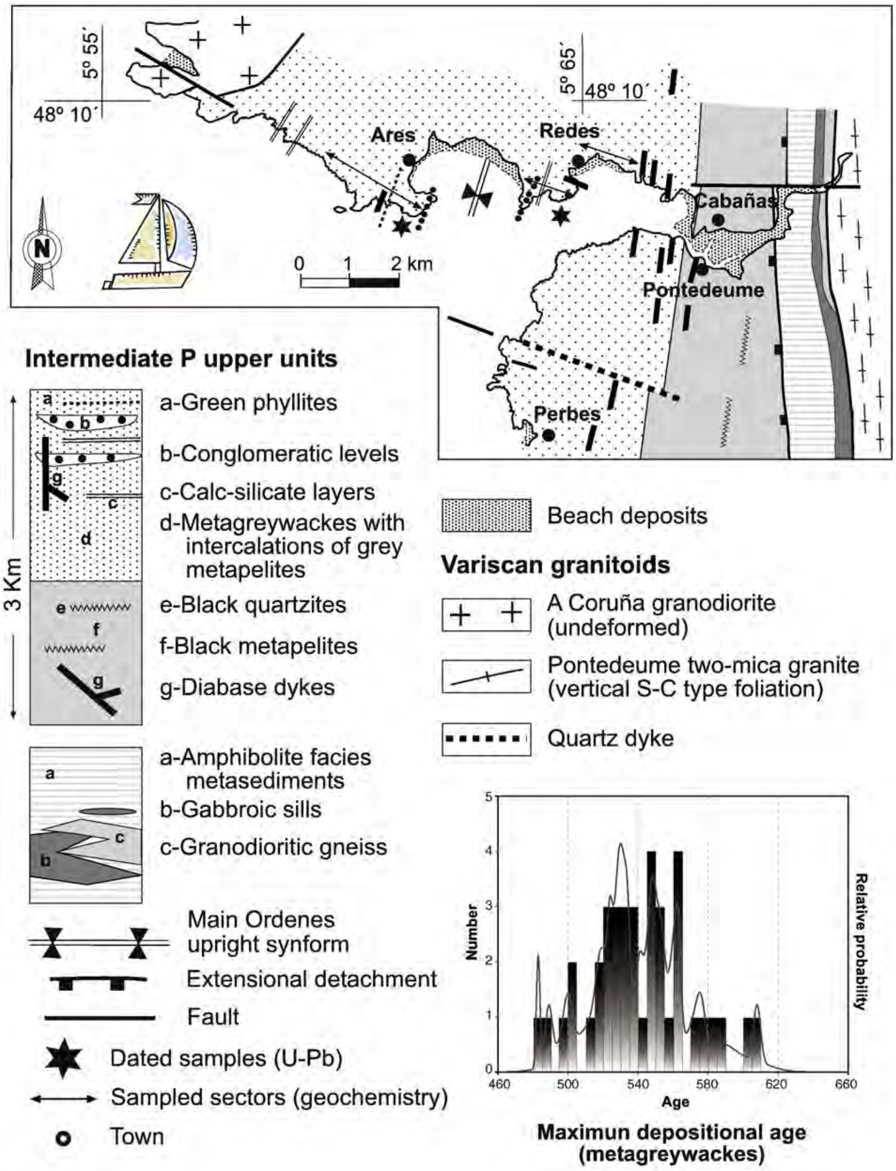

Fig. 4. Sketch showing the geology of the top metagreywackes and related metasediments in the Ares region. A general columnar section of these metasediments is shown, together with the distribution of the most important diabase dykes, the position of the samples dated by U–Pb (detrital zircons in two greywackes; Fernández-Suárez et al., 2003) and the location of the sections sampled for whole rock geochemistry of the metagreywackes. The age diagram used to deduce the maximum sedimentary age of the greywackes is also included (U–Pb ages for the younger group of detrital zircons).

Table 1
Whole rock major and trace element data of the top metagreywackes from the Órdenes Complex.

Sample	SO-1	SO-2	SO-3	SO-4	SO-5	SO-6	SO-7	SO-8	SO-9	SO-10	SO-11	SO-12	SO-13	SO-14	SO-15	SO-16	SO-17	SO-18	SO-19	SO-20
SiO_2	65.54	65.12	62.66	65.33	59.77	63.27	60.90	66.30	65.45	65.05	66.17	63.14	73.07	75.67	75.74	65.44	64.64	62.16	62.21	66.69
Al_2O_3	15.28	15.76	16.80	15.70	17.98	17.00	17.48	14.96	16.09	16.51	16.17	17.41	13.09	11.74	11.35	16.65	16.97	17.17	18.08	15.41
Fe_2O_3	5.85	5.67	7.15	5.90	8.02	7.00	7.59	5.75	5.97	5.89	5.66	6.52	3.86	3.73	3.58	5.93	6.20	6.48	6.56	5.68
MnO	0.122	0.106	0.127	0.128	0.128	0.130	0.135	0.149	0.065	0.054	0.055	0.077	0.040	0.060	0.058	0.084	0.087	0.110	0.078	0.081
MgO	2.15	2.22	2.82	2.23	2.89	2.51	2.56	1.97	1.71	1.63	1.52	2.21	1.05	1.03	0.99	1.80	1.95	2.14	2.17	2.21
CaO	2.22	2.51	3.05	2.60	1.17	1.32	1.23	1.94	0.21	0.15	0.25	0.31	0.12	0.49	0.60	0.60	0.84	0.66	0.59	1.41
Na_2O	2.81	3.57	3.71	3.71	2.48	2.46	2.71	2.92	2.97	2.72	3.38	3.21	3.04	3.26	2.81	2.72	3.14	2.86	3.31	3.86
K_2O	2.81	2.30	1.65	1.82	2.79	2.79	2.93	2.12	2.65	2.86	2.42	2.86	2.11	1.97	2.21	3.12	2.86	3.36	3.03	1.53
TiO_2	0.780	0.801	0.856	0.807	0.892	0.866	0.870	0.808	0.753	0.781	0.773	0.824	0.590	0.566	0.543	0.798	0.813	0.835	0.839	0.765
P_2O_5	0.18	0.17	0.18	0.17	0.13	0.16	0.17	0.16	0.14	0.10	0.14	0.17	0.07	0.09	0.09	0.12	0.14	0.13	0.16	0.16
LOI[a]	1.30	1.03	1.46	1.18	3.28	2.63	2.80	1.76	2.88	3.00	2.51	2.92	1.89	1.23	1.35	2.67	2.58	3.09	3.09	2.07
TOTAL	99.03	99.24	100.50	99.57	99.52	100.10	99.36	98.83	98.88	98.76	99.04	99.65	98.92	99.82	99.31	99.92	100.20	99.00	100.10	99.85
Sc	15	15	19	16	22	19	19	15	15	16	15	18	10	9	8	16	17	18	18	15
V	111	111	116	111	127	121	154	120	138	137	134	144	86	77	73	135	139	160	145	110
Cr	50	50	50	50	50	50	60	50	40	50	40	50	30	30	30	50	50	50	60	50
Co	13	11	15	12	17	13	14	7	6	6	11	14	5	7	7	8	13	11	12	12
Ni	30	30	30	30	40	30	40	<20	20	30	30	30	<20	20	20	30	40	30	30	20
Cu	10	30	40	20	50	30	20	30	30	40	20	30	10	10	10	30	30	30	20	20
Zn	90	90	110	80	120	120	110	90	110	130	110	130	70	70	70	110	130	130	120	80
Ga	19	19	21	19	23	21	22	18	20	21	20	22	15	13	13	21	22	22	23	18
Rb	84	70	47	53	85	92	88	80	88	97	78	93	63	58	68	98	99	100	95	44
Sr	169	252	289	246	217	172	206	231	117	121	145	156	129	139	123	112	138	137	180	295
Y	28.0	20.7	25.3	23.2	34.2	25.0	26.4	19.1	30.0	32.5	31.5	36.7	22.7	21.9	20.7	23.3	34.7	39.3	40.0	23.4
Zr	180	184	180	193	173	171	175	166	194	205	220	195	174	172	164	222	198	197	208	168
Nb	7.5	7.9	10.5	8.2	10.3	10.5	10.1	8.1	9.2	9.7	9.1	10.2	7.0	6.5	6.3	10.0	10.8	10.3	10.7	6.9
Cs	4.8	5.0	3.1	3.5	3.3	4.1	3.9	4.7	4.6	4.5	3.8	4.1	2.5	4.8	6.1	2.7	3.4	2.3	2.4	1.3
Ba	617	758	428	519	689	513	585	468	637	647	574	721	467	573	615	547	597	688	651	449
Hf	4.8	5.3	5.2	5.5	5.1	4.9	5.1	4.5	5.5	5.9	6.2	5.6	4.8	4.7	4.4	6.2	5.8	5.7	6.2	4.5
Ta	0.66	0.70	0.89	0.79	0.92	0.90	0.87	0.68	0.84	0.87	0.85	0.96	0.66	0.64	0.60	0.90	0.95	0.94	0.97	0.60
Pb	15	13	13	13	14	13	11	16	17	17	12	15	13	8	9	14	16	18	9	9
Th	6.63	7.27	8.92	6.81	8.90	7.95	8.70	7.87	8.19	8.79	8.52	9.11	6.44	5.95	5.79	8.60	9.16	9.24	8.96	5.34
U	2.09	2.21	2.91	2.14	2.00	2.10	2.66	2.09	3.33	3.51	3.44	2.96	2.30	1.73	1.93	3.09	3.37	3.17	3.11	1.31
Rb/Sr	0.50	0.28	0.16	0.22	0.39	0.53	0.43	0.35	0.75	0.80	0.54	0.60	0.49	0.42	0.55	0.88	0.72	0.73	0.53	0.15
Ti/Zr	26	26	29	25	31	30	30	29	23	23	21	25	20	20	20	22	25	25	24	27
La/Sc	1.63	1.24	1.35	1.36	1.18	0.83	1.22	1.79	1.62	1.81	1.75	1.74	2.11	2.43	2.24	0.81	1.95	1.27	1.92	1.57
La/Y	0.87	0.90	1.02	0.94	0.76	0.63	0.88	1.41	0.81	0.89	0.83	0.85	0.93	1.00	0.86	0.55	0.95	0.58	0.87	1.01
La/Th	3.68	2.56	2.88	3.20	2.92	1.97	2.67	3.42	2.97	3.30	3.09	3.44	3.28	3.68	3.09	1.50	3.61	2.47	3.86	4.42
Sc/Cr	0.30	0.30	0.38	0.32	0.44	0.38	0.32	0.30	0.38	0.32	0.38	0.36	0.33	0.30	0.27	0.32	0.34	0.36	0.30	0.30
Th/Sc	0.44	0.48	0.47	0.43	0.40	0.42	0.46	0.52	0.55	0.55	0.57	0.51	0.64	0.66	0.72	0.54	0.54	0.51	0.50	0.36

Oxides are in weight percent (wt.%). Trace elements are in parts per million (ppm).
The element concentrations expressed with the < sign are below detection limit.
[a] Loss on ignition.

development of the basal Ponte Carreira detachment (PCD; Fig. 3). This basal extensional detachment prevents the identification of original relationships with the underlying part of the intermediate-pressure upper units.

From a lithological point of view the uppermost terrigenous series can be divided into two members: (1) a lower member with a maximum thickness of c. 1 km consisting of black metapelites with intercalations of grey to black quartzites and lydites of variable thickness; and (2) an upper member, c. 2 km thick, that has a flyschoid appearance and consists of alternations of metagreywackes and grey to black metapelites with conglomeratic intervals and minor green phyllites and calcsilicate layers. The entire succession appears to represent an upward shoaling megasequence. Two detailed partial stratigraphic columns were previously measured and studied by Gutiérrez Alonso et al. (2000), who identified facies indicating various settings within a deep submarine fan model (mainly lower-middle fan and upper fan, with a few facies representing the slope). The identified facies' association suggests a type II turbiditic system (Mutti, 1985), mostly formed by channel and sand lobe complexes.

Conglomeratic levels consist of pebbles of granitic rocks, quartz and greywacke intraclasts. Most of the sandstones can be classified as feldespathic greywackes with a framework of quartz and weakly altered plagioclase. Rock fragments of vitric and microgranular texture are common in polymictic conglomerates and coarse-grained greywackes, together with slates, cherts and bipyramidal volcanic quartz fragments. Although recrystallization under greenschist facies conditions in the chlorite and biotite zones and the presence of two cleavages hinder detailed textural analysis, the sandstones are typical immature, first-cycle sandstones with angular to subangular, poorly sorted grains in a muddy matrix. Heavy minerals are dominated by unabraded zircons and less abundant epidote and rutile.

Detrital zircons of two metagreywacke samples collected near Ares and Redes (Fig. 4) were studied by Fernández-Suárez et al. (2003) in order to constrain the provenance of the greywacke series and its maximum depositional age. The age groups of the zircons (480–610 Ma, 1900–2100 Ma and 2400-2500 Ma) and the absence of Mesoproterozoic zircons suggest an origin in a Neoproterozoic–Early Palaeozoic peri-Gondwanan realm along the periphery of the West African Craton. The maximum depositional age of the greywackes, initially thought to be c. 480 Ma (Early Ordovician), was reassessed in this study. Using only analyses with < 10% discordance (shown in Fig. 4 for the youngest group of detrital zircons), the maximum depositional age can be estimated at c. 530 Ma, based on the average age of the largest group of youngest zircons (Elliot and Fanning, 2008). However, it is possible that the age of the youngest zircon in this group is significant, in which case the maximum age of deposition could be as young as 510–520 Ma.

4. Whole rock geochemistry

The chemical composition of sedimentary rocks depends on numerous factors, including the nature of the source areas, and the subsequent processes, such as weathering, diagenesis or metamorphism. Likewise, the tectonic setting in which the sedimentary basin developed also exerts a significant control over the final composition of the resulting rocks (Bathia, 1983; Bathia and Crook, 1986; Ranjan and Banerjee, 2009; Hegde and Chavadi, 2009). The abundance of some elements, such as rare earth elements (REE), Hf, Ti, Cr, Co, Zr, Nb, Y, Th and Sc, is preserved in sedimentary rocks through the weathering processes. These elements have very low residence times in oceanic waters, being transferred almost quantitatively to sedimentary rocks. Thus, they provide excellent discriminating factors for determining the provenance and tectonic setting of sedimentary rocks in both ancient successions and far travelled terranes.

Twenty metagreywacke samples from the sedimentary series that constitutes the upper levels of the Órdenes Complex (intermediate-

Table 2
Whole rock rare earth element data of the top metagreywackes from the Órdenes Complex.

Sample	SO-1	SO-2	SO-3	SO-4	SO-5	SO-6	SO-7	SO-8	SO-9	SO-10	SO-11	SO-12	SO-13	SO-14	SO-15	SO-16	SO-17	SO-18	SO-19	SO-20
La	24.4	18.6	25.7	21.8	26.0	15.7	23.2	26.9	24.3	29.0	26.3	31.3	21.1	21.9	17.9	12.9	33.1	22.8	34.6	23.6
Ce	50.1	35.2	56.6	41.5	79.6	36.3	49.0	54.9	50.3	61.7	57.2	62.4	43.4	40.2	35.1	29.0	50.6	34.1	49.9	43.6
Pr	6.05	50.70	6.51	5.51	6.69	4.44	5.80	6.05	6.12	7.06	6.62	7.40	4.96	5.26	4.35	3.50	8.51	6.30	8.20	5.67
Nd	24.5	20.1	25.2	22.1	27.0	17.2	22.6	23.2	24.1	28.2	25.9	29.7	19.1	20.6	17.3	14.1	33.0	25.2	31.4	22.1
Sm	5.09	4.18	5.32	4.55	5.84	3.67	4.62	4.53	5.08	5.82	5.45	6.12	3.97	4.00	3.62	3.26	6.88	5.72	6.49	4.53
Eu	1.38	1.19	1.29	1.28	1.48	0.99	1.22	1.20	1.21	1.41	1.32	1.59	1.05	1.04	0.94	0.87	1.74	1.50	1.75	1.30
Gd	4.72	3.49	4.52	3.95	5.52	3.23	3.84	3.92	4.77	5.20	4.87	5.84	3.51	3.59	3.30	3.05	6.43	5.81	6.31	4.04
Tb	0.82	0.62	0.80	0.67	0.98	0.61	0.66	0.67	0.85	0.93	0.90	1.06	0.65	0.62	0.59	0.62	1.11	1.08	1.12	0.71
Dy	4.96	3.88	4.85	4.07	5.99	4.04	4.30	3.80	5.25	5.48	5.39	6.22	4.00	3.75	3.51	4.13	6.74	6.86	6.92	4.32
Ho	0.98	0.77	0.91	0.80	1.19	0.87	0.90	0.72	1.03	1.07	1.05	1.22	0.78	0.72	0.69	0.85	1.26	1.39	1.36	0.85
Er	2.90	2.37	2.79	2.40	3.61	2.74	2.83	2.08	3.11	3.21	3.18	3.64	2.37	2.20	2.13	2.76	3.78	4.22	4.02	2.56
Tm	0.446	0.386	0.455	0.380	0.569	0.449	0.471	0.333	0.482	0.513	0.502	0.558	0.370	0.339	0.345	0.484	0.597	0.686	0.602	0.395
Yb	2.92	2.67	3.11	2.59	3.71	3.05	3.18	2.23	3.17	3.40	3.32	3.70	2.44	2.30	2.30	3.33	3.91	4.54	3.89	2.63
Lu	0.45	0.42	0.5	0.4	0.57	0.48	0.49	0.34	0.51	0.52	0.516	0.589	0.374	0.358	0.348	0.523	0.850	0.670	0.596	0.380
Σ REE	130	99	139	112	169	94	123	131	130	154	143	161	108	107	92	79	158	121	157	117
Eu/Eu*	0.87	0.96	0.81	0.93	0.80	0.88	0.89	0.88	0.76	0.79	0.79	0.82	0.86	0.84	0.84	0.85	0.80	0.80	0.84	0.93
$(La/Sm)_N$	2.96	2.75	2.98	2.96	2.75	2.64	3.10	3.66	2.95	3.07	2.98	3.16	3.28	3.38	3.05	2.44	2.97	2.46	3.29	3.21
$(Gd/Yb)_N$	1.29	1.04	1.16	1.22	1.19	0.84	0.96	1.40	1.20	1.22	1.17	1.26	1.15	1.24	1.14	0.73	1.31	1.02	1.29	1.22
$(La/Yb)_N$	5.59	4.66	5.53	5.63	4.69	3.44	4.88	8.07	5.13	5.7	5.30	5.66	5.78	6.37	5.20	2.59	5.66	3.36	5.95	6.00

Rare earth element data in parts per million (ppm).

pressure upper units) were collected in order to study their geochemistry, provenance and tectonic setting. Samples were collected along three sections on the coastline surrounding Redes and Ares (Fig. 4). Sample preparation was carried out at Universidad Complutense de Madrid, and whole rock major and trace elements analyses were performed at Activation Laboratories Ltd. (Actlabs) in Canada. The method used for sample digestion was fusion with lithium metaborate/tetraborate, and the analytical techniques for major and trace element determination were ICP-OES and ICP-MS, respectively. The chemical analyses of the greywackes are shown in Tables 1 and 2.

4.1. Composition and classification

The analysed greywackes are characterized by variable SiO_2 contents (59.8–75.7 wt.%), with an average of 65.7 wt.%. Only three samples have SiO_2 contents higher than 70 wt.% (SO-13 to SO-15). The grewackes have relatively high, homogeneous Na_2O contents (2.5–3.9 wt.%), with an average of 3.1 wt.%, and relatively low and variable contents in CaO (0.1–3.1 wt.%) and K_2O (1.5–3.4 wt.%), with averages of 1.1 and 2.5 wt.%, respectively. The compositional ranges of the remaining major elements are Al_2O_3 (11.4–18.1 wt.%), Fe_2O_3 (3.6–8.0 wt.%), MnO (0.04–0.15 wt.%), MgO (1.0–2.9 wt.%), TiO_2 (0.54–0.89 wt.%) and P_2O_5 (0.07–0.18 wt.%). Based on the SiO_2 contents and the K_2O/Na_2O ratio (0.4–1.2), most of the greywackes are quartz-intermediate (Crook, 1974). A negative correlation exists between SiO_2 and Fe_2O_3, MgO, MnO, CaO and TiO_2, whereas a positive correlation exists between TiO_2 and Al_2O_3. There is also significant scatter in the SiO_2/K_2O and SiO_2/Na_2O ratios due to the high mobility of Na and K during alteration processes.

The chemical classification of sedimentary rocks differentiates between mature and immature sediments. One of the most widely used parameters is the Fe_2O_3/K_2O ratio (Herron, 1988), which is especially applicable to arkoses. This ratio is better than the Na_2O/K_2O ratio used by Pettijohn et al. (1972), and can be applied to unconsolidated fine- to coarse-grained sediments. Based on the chemical classification diagram by Herron (1988), most of the analysed samples cluster in the greywacke field (Fig. 5a). Only samples SO-14 and SO-15 fall in the field of litharenites. The SiO_2/Al_2O_3 ratio of the samples is low (3.3–6.7), which is indicative of immaturity. The variable K_2O/Na_2O ratio (0.4–1.2) and average value of 0.8, can be interpreted in the same way (Asiedu et al., 2004; Spaletti et al., 2008). The Rb/Sr ratio, which also reflects recycling processes, varies between 0.15 and 0.88, with an average value of 0.5. Weathering processes and, in some cases, diagenesis can lead to an important increase of the Rb/Sr ratio, due largely to Sr loss during plagioclase alteration. Values higher than 0.5 are interpreted by McLennan et al. (1993) as a weathering and sedimentary recycling index. An average value of 0.5 in the greywackes indicates a certain increase relative to the average value of the Rb/Sr ratio in the upper crust (0.32; Taylor and McLennan, 1985). This, in turn, suggests that alteration processes during the sedimentary history of the greywackes were minor.

The effects of homogenization in sedimentary processes result in a relatively uniform distribution of REE in detrital rocks, the pattern reflecting the abundance of REE in the upper crust. REE are generally considered to be immobile, with only slight changes during sedimentation processes. The results of the REE analysis can be seen in Table 2. The analysed greywackes show little variability in ΣREE, with values ranging between 79 (sample SO-16, with a marked depletion in LREE) and 169 (sample SO-5, with a pronounced positive Ce anomaly). The samples also show similar chondrite-normalized (Nakamura, 1974) fractionation patterns, with slight enrichment in LREE (La–Sm) relative to HREE (Fig. 5b). Likewise, the samples show a weak negative Eu anomaly, which varies from 0.76 to 0.96 (calculated according to Taylor and McLennan, 1985). Eu anomalies are usually interpreted in sedimentary rocks as being inherited from the igneous source rocks. The samples also display an unfractionated HREE

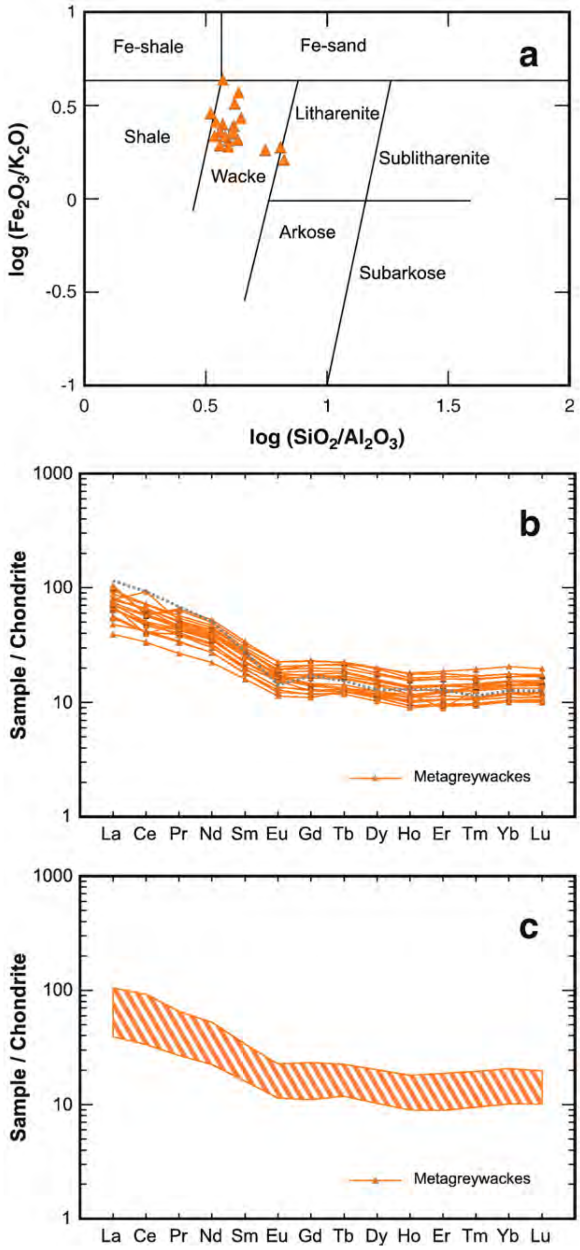

Fig. 5. Chemical diagrams for the metagreywackes from the uppermost levels of the Órdenes Complex. (a) Classification diagram (Herron, 1988). (b) Chondrite-normalized rare earth elements plots; the dotted line corresponds to the PAAS (Post Archean Australian Shale; Taylor and McLennan, 1985). (c) Compositional range of the chondrite-normalized rare earth elements plots.
Normalizing values are from Nakamura (1974).

pattern. As can be seen in Fig. 5b and c, despite some intersample differences in abundance, the REE patterns of the greywackes are similar to those of PAAS (Post Archean Australian Shale; Taylor and McLennan, 1985), which are considered representative of upper continental crust.

The depletion of HREE relative to LREE is usually related to low concentrations of heavy minerals, especially zircon. Here, the low concentration of Zr in the greywackes (average = 187 ppm) is consistent with that interpretation. Almost all the samples have Gd_N/Yb_N values between 1.0 and 2.0 (0.73–1.40) and low Eu/Eu* ratios (0.76–0.96), indicating a provenance from upper continental crust of Post Archean age, based on the similarity of the REE patterns to PAAS. The La_N/Yb_N ratio shows an average value of 5.26 (ranging between 2.59 and 8.07), which is lower than that of PAAS ($La_N/Yb_N = 9.08$) due to a lower La concentration (average La = 24.06 ppm, Yb = 3.12 ppm). The abundance of La agrees with that reported by Bathia and Crook (1986) for igneous terrigenous sediments generated within a volcanic arc built on thinned continental crust, as discussed below.

4.2. Tectonic setting

The geochemistry of major elements has been widely used to establish the tectonic setting of detrital sedimentary rocks (Bathia, 1983; Roser and Korsch 1985, 1986, 1988; Bathia and Crook, 1986; Hegde and Chavadi, 2009). However, diagrams based on the abundance of elements, such as Na or K, must be treated with caution, because of their high mobility during depositional processes. Certain trace elements, such as REE, Cr, Co, Th, Sc, Y, La and Zr, are considered relatively immobile and consequently provide better discrimination of possible tectonic settings (Taylor and McLennan, 1985). Various tectonic discrimination diagrams developed by Bathia and Crook (1986) are shown in Fig. 6. These diagrams allow clear differentiation among the four tectonic settings considered to be the most common sites of greywacke deposition: (A) oceanic island arc, (B) continental island arc, (C) active continental margin, and (D) passive margin. In the Ti/Zr–La/Sc diagram (Fig. 6a), all the samples plot within the continental island arc field. The La/Y–Sc/Cr diagram (Fig. 6b) shows greater scatter due to the variability of the La/Y ratio, the values of which range between 0.55 and 1.41. Nevertheless, all the samples plot in fields related to convergent plate tectonic settings. In the ternary diagrams, La–Th–Sc, Th–Co–Zr and Th–Sc–Zr (Fig. 6c, d and e, respectively), the samples are tightly grouped in the continental island arc fields, with only two samples falling within the field for oceanic island arcs in one of the diagrams. This reflects the low La contents of the two samples relative to the others.

According to Bathia and Crook (1986), the most significant chemical signatures for characterizing greywackes deposited in a continental island arc setting are: La (25 ppm), Th (11 ppm), La/Sc (1.8), Th/Sc (0.85), Ti/Zr (20) and La/Th (2.3). These average values closely match those characteristic of the greywackes of the upper levels of the Órdenes Complex: La (24 ppm), Th (7.86 ppm), La/Sc (1.59), Th/Sc (0.51), Ti/Zr (25) and La/Th (3.1). Hence, according to the concentrations of trace elements with the highest discriminative power, the greywackes were deposited in a sedimentary basin related to a convergent dynamic regime, and in a tectonic setting designated as a continental island arc by Bathia and Crook (1986).

Finally, Fig. 7a and b shows PAAS-normalized plots of the most significant elements for the discrimination of tectonic setting. The figures are plotted according to the criteria of Thompson (1982). The patterns defined by the metagreywackes are very similar to those typical of continental island arcs or active margins (Winchester and Max, 1989). The plots are characterized by depletion in most of the large ion lithophile elements (LILE: Cs, Rb, Th, U, K_2O, La, Ce, and P_2O_5), which deviate slightly from one, whereas the high field strength elements (HSFE: Zr, Hf, HREE, Sm, TiO_2 and Sc)

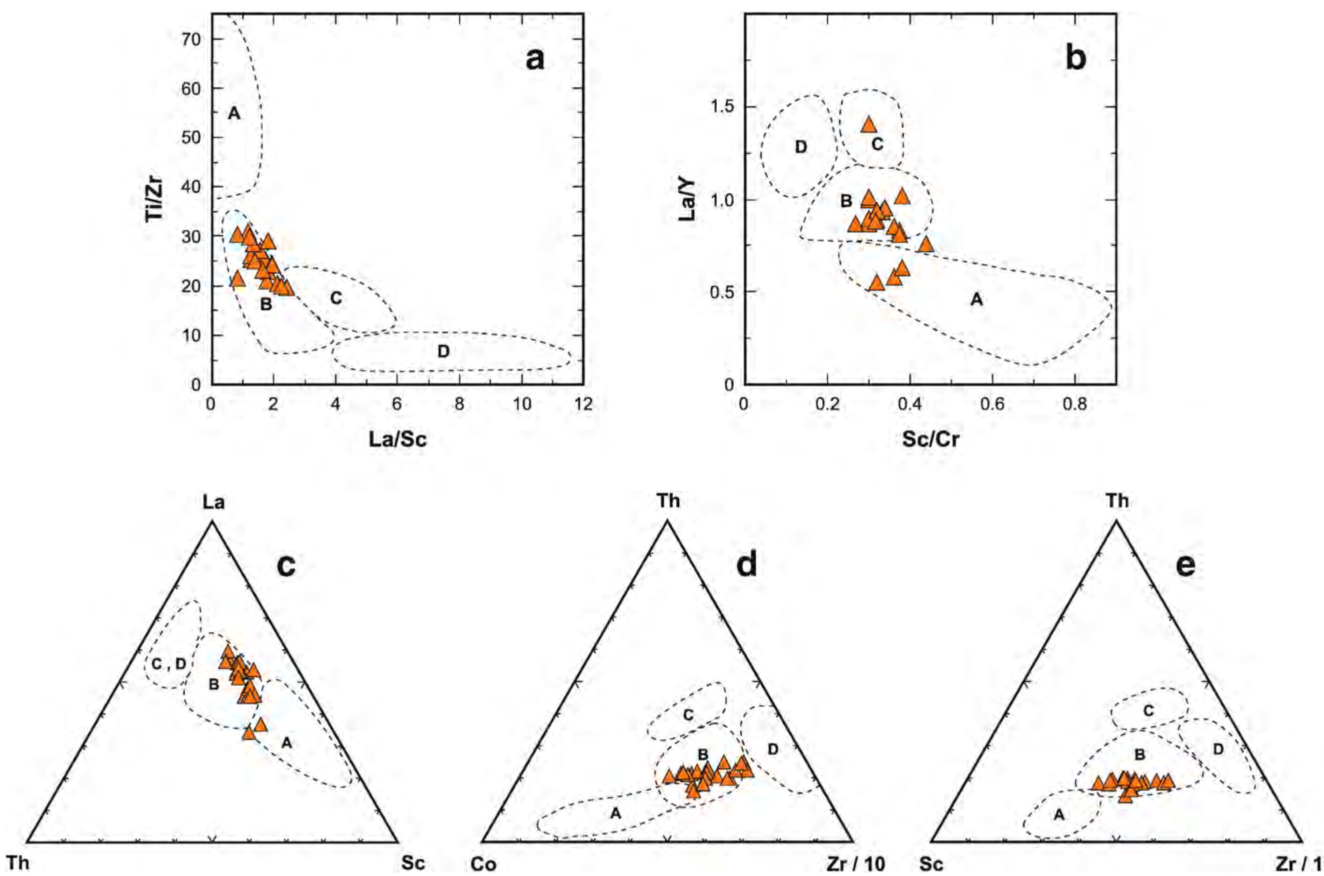

Fig. 6. Trace elements tectonic setting discrimination diagrams for the metagreywackes. A—Oceanic island arc; B—continental island arc; C—active continental margins; D—passive margins.
Diagrams are after Bathia and Crook (1986).

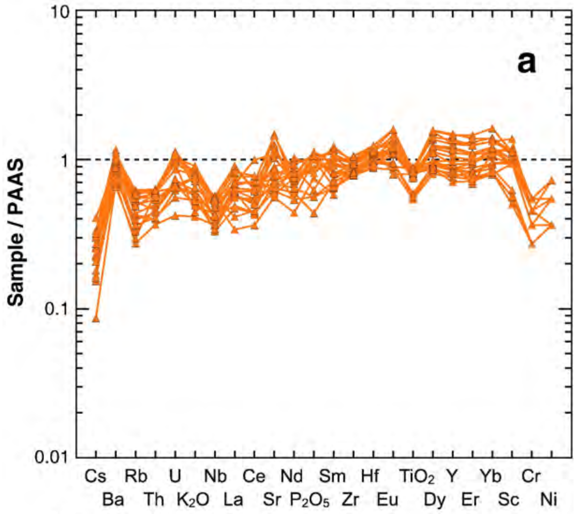

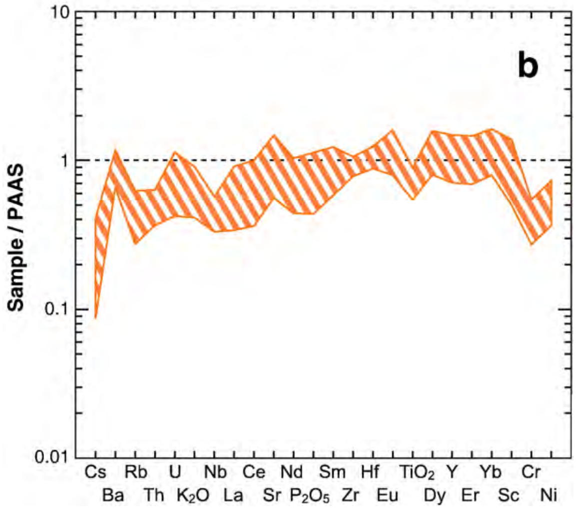

Fig. 7. (a) PAAS-normalized trace elements plots for the metagreywackes. (b) Plot showing the compositional range of the PAAS-normalized trace elements composition of the metagreywackes.
PAAS after Taylor and McLennan, 1985.

Table 3
Whole rock Nd isotope data of the top metagreywackes from the Órdenes Complex.

Muestra	Nd	Sm	$^{147}Sm/^{144}Nd$	$^{143}Nd/^{144}Nd$	2σ	εNd (0)	εNd (500)*	T_{DM} (Ma)[a]
SO-1	22.60	4.93	0.1318	0.512531	3	−2.1	2.0	986
SO-2	18.44	4.22	0.1383	0.512555	4	−1.6	2.1	1017
SO-3	24.49	5.77	0.1425	0.512480	3	−3.1	0.4	1215
SO-4	20.51	4.62	0.1363	0.512633	4	−0.1	3.8	855
SO-5	26.83	5.85	0.1318	0.512456	3	−3.5	0.6	1111
SO-6	16.39	3.78	0.1393	0.512518	3	−2.3	1.3	1098
SO-7	20.64	4.69	0.1373	0.512529	3	−2.1	1.7	1052
SO-8	19.82	4.07	0.1241	0.512589	3	−1.0	3.7	818
SO-9	25.97	4.82	0.1122	0.512482	3	−3.1	2.3	878
SO-10	29.29	6.07	0.1253	0.512497	3	−2.8	1.8	973
SO-11	26.13	5.56	0.1287	0.512518	3	−2.4	2.0	974
SO-12	31.11	6.56	0.1276	0.512537	3	−2.0	2.4	932
SO-13	19.56	4.06	0.1255	0.512587	4	−1.0	3.6	833
SO-14	21.11	4.22	0.1207	0.512636	3	0.0	4.8	720
SO-15	17.66	3.57	0.1224	0.512506	3	−2.6	2.2	930
SO-16	15.76	3.66	0.1402	0.512481	3	−3.1	0.5	1180
SO-17	33.57	7.11	0.1281	0.512427	3	−4.1	0.3	1115
SO-18	26.85	6.20	0.1396	0.512468	3	−3.3	0.3	1194
SO-19	32.82	6.81	0.1254	0.512467	3	−3.3	1.2	1021
SO-20	23.21	4.80	0.1252	0.512476	3	−3.2	1.4	1003

[a] Nd model ages calculated according to DePaolo (1981).
* εNd(t) calculated for 500 Ma.

are generally close to one, with a slight characteristic negative TiO_2 anomaly. In general, a slightly increasing pattern can be observed, culminating in a flat pattern close to one. However, three important differences exist between the diagram for continental island arcs and active margins proposed by Winchester and Max (1989) and that obtained for the analysed greywackes: (1) there is essentially no negative P_2O_5 anomaly, perhaps because of low contents of apatite and monazite; (2) there is a less marked positive Sr anomaly, perhaps as a result of alteration processes; and (3) the Cr and Ni abundances are significantly lower, suggesting an essentially felsic provenance for the greywackes, although the values lie close to the analytical detection limits. The felsic provenance appears to be corroborated by Hf values and La/Th ratio, and is a likely indication of the association of the greywackes with an evolved (mature) volcanic arc.

4.3. Sm–Nd isotope systematics

Isotopic analysis of the greywackes was performed at the Centro de Geocronología y Geoquímica Isotópica at the Universidad Complutense de Madrid. For whole rock Nd isotopic analysis by isotope dilution-thermal ionization mass spectrometry (ID-TIMS), the samples were first dissolved in ultra-pure reagents in order to perform isotope separation by exchange chromatography (Strelow, 1960; Winchester, 1963), and subsequently analysed using a Sector 54 VG-Micromass multicollector spectrometer. The measured $^{143}Nd/^{144}Nd$ isotopic ratios were corrected for possible isobaric interferences from ^{142}Ce and ^{144}Sm (only for samples with $^{147}Sm/^{144}Sm < 0.0001$) and normalized to $^{146}Nd/^{144}Nd = 0.7219$ in order to correct for mass fractionation (Table 3). The La Jolla Nd international isotopic standard was analysed during sample measurement, and gave an average value of $^{143}Nd/^{144}Nd = 0.511859$ for 7 replicas, with an internal precision of ± 0.000015 (2σ). These values were used to correct the measured ratios for possible sample drift. The error estimated for the $^{147}Sm/^{144}Nd$ ratio is 0.1%.

In crustal evolution models based on Nd isotopic composition, the main source of fractionation during the formation and evolution of continental crust takes place during partial melting of lithospheric mantle to generate crustal rocks (McLennan and Hemming, 1992). The εNd model age of a sedimentary rock represents the average age of the extraction of its components from the mantle. In the case of detrital rocks, model ages usually reflect complex mixing based on the different age and provenance of their components. The combined interpretation of model ages and detrital zircon ages has proved to be a powerful tool for investigating the evolution of continental crust, especially in orogenic domains (e.g., Linneman et al., 2004). The Nd model ages calculated for the metagreywackes are included in the εNd vs. the time diagram in Fig. 8. The analysed metagreywackes show $^{147}Sm/^{144}Nd$ ratios <0.145, which is an appropriate ratio for NdT_{DM} calculations. Stern (2002) suggests that a $^{147}Sm/^{144}Nd$ ratio of 0.165 is the upper limit for performing NdT_{DM} calculations. The T_{DM} model ages (DePaolo, 1981) range between 720 and 1215 Ma (Table 3), with an average value of 995 Ma (Fig. 8). εNd (0) values vary from −4.1 to 0, while εNd (500), that is, the εNd value at the time of greywackes sedimentation, ranges between 0.3 and 4.8 (Table 3). A collection of Nd model ages from different regions (Linnemann and Romer, 2002) is also included in Fig. 8. These ages have been divided into two groups according to the age of the dominant source (Grenvillian and post-Grenvillian/pre-Cadomian crust, or pre-Grenvillian, >0.9–1.1 Ga, cratonic crust).

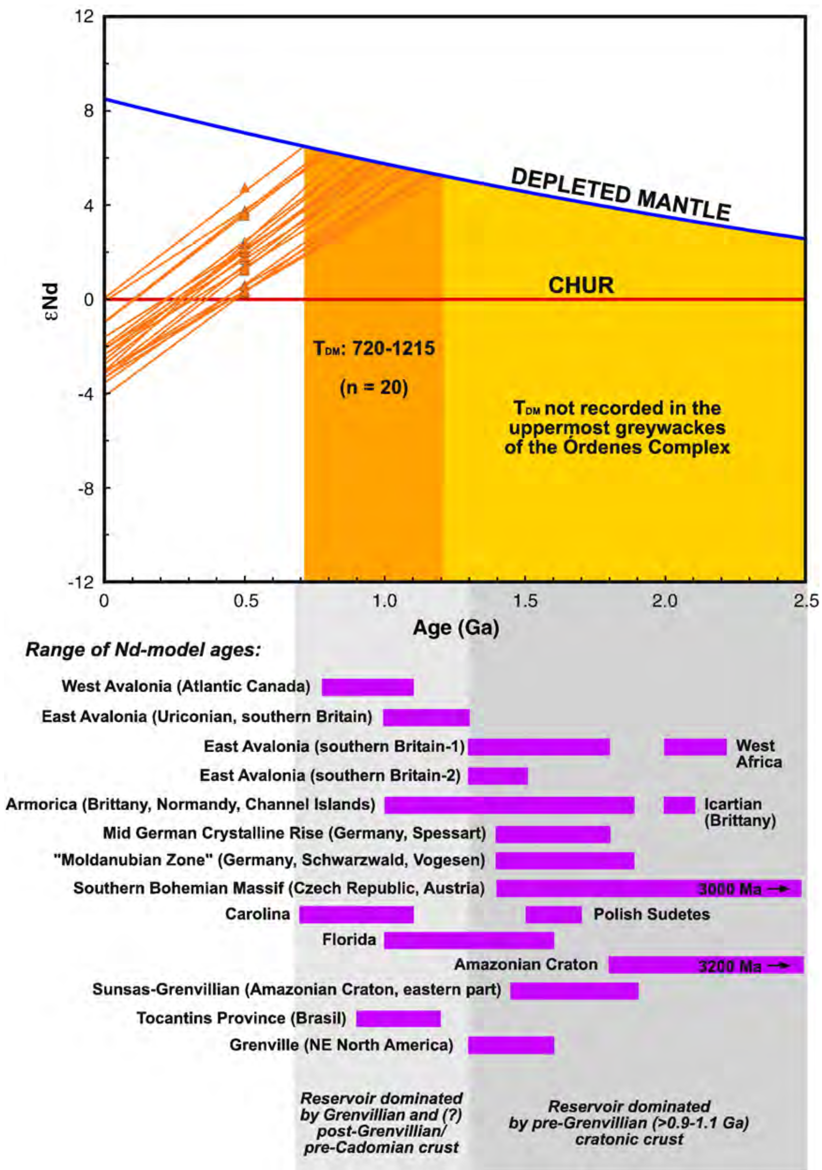

Fig. 8. T_{DM} model ages (DePaolo, 1981) of the top metagreywackes from the Órdenes Complex. Triangles show the εNd values at 500 Ma, a reference age for the deposition of the turbiditic series.
Data source for comparative model ages from different regions taken from Linnemann and Romer (2002).

5. Discussion

According to the age groups recorded by the detrital zircons, the greywackes of the upper levels of the Órdenes Complex have a maximum depositional age of 510–530 Ma (Middle Cambrian). The complete absence of detrital zircons of Mesoproterozoic age (1000–1600 Ma) indicates that the sedimentary basin in which they were deposited was probably located in the peri-Gondwanan realm along the periphery of the West African Craton (Fernández-Suárez et al., 2003). The geochemistry of the greywackes clearly shows that their deposition took place on a convergent margin in a volcanic arc, and specifically (according to the criteria of Bathia and Crook, 1986), in a continental island arc. Within this setting, Bathia and Crook (1986) include sedimentary basins located in the inter-arc, back-arc and fore-arc environments of volcanic arcs developed over thinned continental crust. These arcs have a crystalline continental basement, but lack the thick continental basement of typical arcs generated at active continental margins. The analysed greywackes show very different chemical compositions to those deposited in passive margins or oceanic island arcs. Instead, the geochemical signature of the greywackes indicates deposition in a mature, highly evolved volcanic arc with abundant felsic magmatism.

Pinpointing the location of this sedimentary basin and volcanic arc system turns is more problematic. The similarity in the timing of the greywacke sedimentation (c. 510–530 Ma) and magmatism in the upper units (c. 500-520 Ma; Abati et al., 1999; Fernández Suárez et al., 2007), requires deposition of the turbidites to have taken place during the main phase of volcanic arc activity. Synchronicity of sedimentation with active magmatism is supported by the fact that the greywackes are cross-cut by a coeval diabasic swarm (Díaz-Garcia et al., 2010-this issue). The chemistry of the greywackes also points to the possible presence of thinned continental crust in the root of the arc. Furthermore, the turbiditic series presently forms the upper levels of the arc-derived terrane, and lies structurally above a complex series of high-grade metamorphic rocks (both orthogneisses and paragneisses), the tectonothermal record of which is at least partly

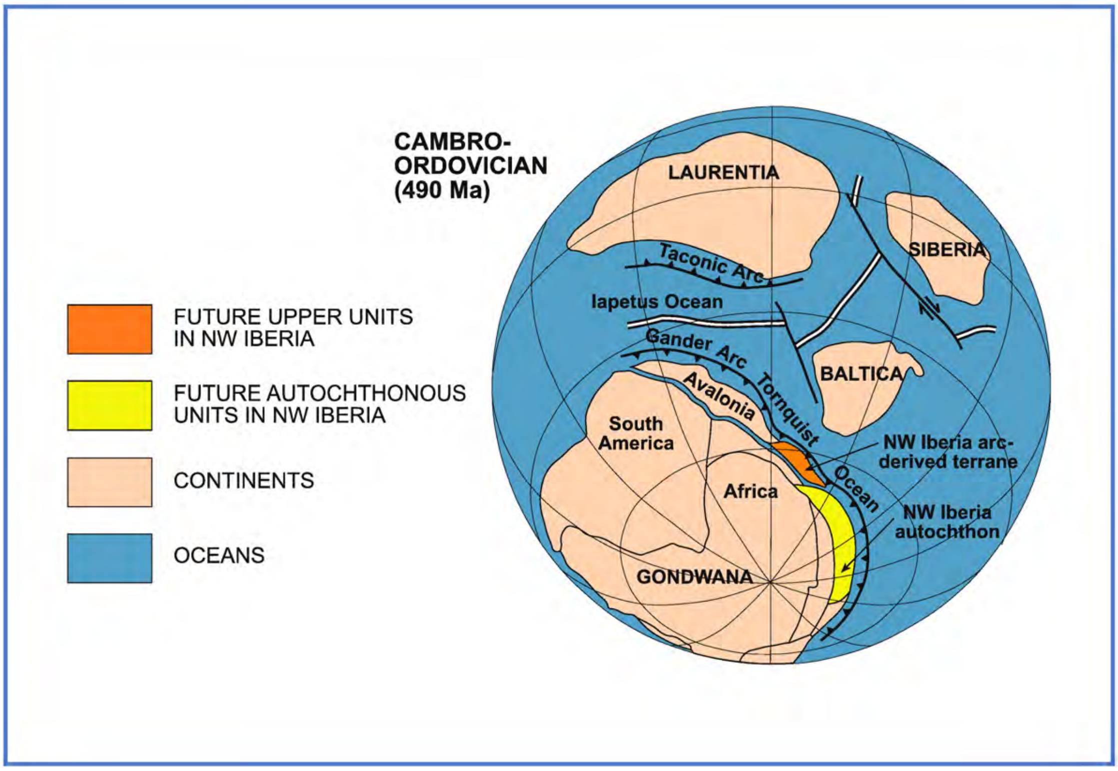

Fig. 9. Paleogeographic reconstruction for the Cambrian–Ordovician limit showing the probable location of the peri-Gondwanan arc where the greywackes were deposited. The figure shows the moment immediately previous to the opening of the Rheic Ocean.
Modified after Arenas et al. (2007).

related to the dynamics of the arc itself. Thus, it is probable that the present position of the turbiditic series partly reflects its primary location (although the contacts with the underlying series are tectonic), and that greywacke deposition took place in an intra-arc basin above thick metamorphic and plutonic complexes and possible pre-arc continental basement, the existence of which has not been investigated in the allochthonous complexes of NW Iberia.

The T_{DM} model ages of the greywackes range from the Middle Neoproterozoic to the Upper Mesoproterozoic (720–1215 Ma, Fig. 8). This, together with the absence of detrital zircons with these ages in the greywackes (Fernández-Suárez et al., 2003), which rules out the presence of Grenvillian terranes in the source area, indicates that the T_{DM} model ages reflect a mixing of components of the Paleoproterozoic and Ediacaran ages. Both sources are represented in the detrital zircon population and are characteristic of the realms bordering the West African Craton.

The presence of Mesoproterozoic basement (1100–1600 Ma) below most of the NW Iberian Massif has been proposed by Murphy et al. (2008). The Paleozoic passive margin sedimentary sequence of the NW Iberian Massif, from the Schistose Domain of the Galicia-Trás-os-Montes Zone to the Cantabrian Zone, may have been deposited on this basement. The combined interpretation of the detrital zircon and Nd model ages from the greywackes of the uppermost levels of the Órdenes Complex, however, indicates a provenance incompatible with the participation of such a basement. If this basement exists, the sedimentary basin in which the greywackes were deposited would have to have been located on a sector of the Gondwanan margin well removed from that represented by the rest of the NW Iberian Massif, although still at the periphery of the West African Craton. A collection of Nd model ages for various terranes of Gondwanan affinity is included in Fig. 8, in addition to the data from the Grenville belt of NE North America (Linnemann and Romer, 2002). Although the ages overlap and the terranes included represent a rather general group, the Nd model ages of the greywackes of the Órdenes Complex compare most closely with those of West Avalonia, Florida and the Carolina terranes, and differ slightly from those of East Avalonia and other terranes, and the domains of the Bohemian Massif. Fig. 9 shows the probable location of the peri-Gondwanan arc immediately prior to the opening of the Rheic Ocean. The opening of this ocean caused the rifting and separation of the external part of the arc, which was transported to the north, carrying with it the sedimentary basin in which the turbiditic series was deposited.

The data obtained from the greywacke provenance of the Órdenes Complex confirm the equivalence of the upper units of the allochthonous complexes of NW Iberia with an arc-derived terrane originally located at the periphery of the West African Craton. This arc was probably generated in the Avalonian peri-Gondwanan realm, in a more westerly position than that occupied by the Lower Paleozoic autochthonous sequence of NW Iberia (Fig. 9). This is consistent with previous data related to the provenance of this allochthonous terrane (Gómez Barreiro et al., 2007). No domain containing the Mesoproterozoic basement was involved in the genesis of the arc. The analysed greywackes were likely deposited adjacent to a mature volcanic arc with abundant felsic magmatism. Although the specific location of the turbidite basin within the volcanic arc is uncertain, the present data suggest deposition in an intra-arc basin generated during the main phase of volcanic arc activity, roughly coincident with the intrusion of the largest plutonic bodies.

Acknowledgements

Financial support for this research has been provided by Spanish project CGL2007-65338-CO2-01/BTE (Ministerio de Ciencia e Innovación). The authors thank Jean Paul Liégeois and an anonymous referee for insightful reviews of the manuscript. This paper is a contribution to IGCP Project 497, "The Rheic Ocean: Origin, evolution and correlatives".

References

Abati, J., Dunning, G.R., Arenas, R., Díaz García, F., González Cuadra, P., Martínez Catalán, J.R., Andonaegui, P., 1999. Early Ordovician orogenic event in Galicia (NW Spain): evidences from U–Pb ages in the uppermost unit of the Órdenes Complex. Earth and Planetary Science Letters 165, 213–228.

Abati, J., Arenas, R., Martínez Catalán, J.R., Díaz García, F., 2003. Anticlockwise P–T path of granulites from the Monte Castelo Gabbro (Órdenes Complex, NW Spain). Journal of Petrology 44, 305–327.

Abati, J., Castiñeiras, P., Arenas, R., Fernández-Suárez, J., Gómez-Barreiro, J., Wooden, J., 2007. Using SHRIMP zircon dating to unravel tectonothermal events in arc environments. The early Palaeozoic arc of NW Iberia revisited. Terra Nova 19, 432–439.

Abati, J., Gerdes, A., Fernández-Suárez, J., Arenas, R., Whitehouse, M.J., Díez Fernández, R., 2010. Magmatism and early-Variscan continental subduction in the northern Gondwana margin recorded in zircons from the basal units of Galicia, NW Spain. Geological Society of America Bulletin 122, 219–235.

Arenas, R., Rubio Pascual, F.J., Díaz García, F., Martínez Catalán, J.R., 1995. High-pressure microinclusions and development of an inverted metamorphic gradient in the Santiago Schists (Órdenes Complex, NW Iberian Massif, Spain): evidence of subduction and syn-collisional decompression. Journal of Metamorphic Geology 13, 141–164.

Arenas, R., Martínez Catalán, J.R., Sánchez Martínez, S., Fernández-Suárez, J., Andonaegui, P., Pearce, J.A., Corfu, F., 2007. The Vila de Cruces Ophiolite: a remnant of the Early Rheic Ocean in the Variscan suture of Galicia (Northwest Iberian Massif). Journal of Geology 115, 129–148.

Arenas, R., Sánchez Martínez, S., Castiñeiras, P., Jeffries, T.E., Díez Fernández, R., Andonaegui, P., 2009. The basal tectonic mélange of the Cabo Ortegal Complex (NW Iberian Massif): a key unit in the suture of Pangea. Journal of Iberian Geology 35, 85–125.

Asiedu, D.K., Dampare, S.B., Asamoah, S.P., Banoeng-Yakubo, B., Osae, S., Nyarko, B.J.B., Many, J., 2004. Geochemistry of Paleoproterozoic metasedimentary rocks from the Birim diamondiferous field, southern Ghana: implications for provenance and crustal evolution at the Archean–Proterozoic boundary. Geochemical Journal 38, 215–228.

Bathia, M.R., 1983. Plate tectonics and geochemical composition of sandstones. Journal of Geology 91, 611–627.

Bathia, M.R., Crook, K.A.W., 1986. Trace elements characteristics of graywackes and tectonic setting discrimination of sedimentary basins. Contributions to Mineralogy and Petrology 92, 181–193.

Casini, L., Oggiano, G., 2008. Late orogenic collapse and thermal doming of the northern Gondwana margin incorporated in the Variscan Chain: a case study from the Ozieri Metamorphic Complex, northern Sardinia, Italy. Gondwana Research 13, 396–406.

Crook, K.A.W., 1974. Lithogenesis and geotectonics: the significance of compositional variations in flysch arenites (greywackes). In: Doti, R.H., Shaver, R.H. (Eds.), Modern and Ancient Geosynclinal Sedimentation: Society of Economic Palaeontologists and Mineralogists Special Publication, vol. 19, pp. 304–310.

DePaolo, D.J., 1981. Neodymium isotopes in the Colorado Front Range and crust–mantle evolution in the Proterozoic. Nature 291, 193–196.

Díaz García, F., Arenas, R., Martínez Catalán, J.R., González del Tánago, J., Dunning, G.R., 1999. Tectonic evolution of the Careón Ophiolite (northwest Spain): a remnant of oceanic lithosphere in the Variscan Belt. Journal of Geology 107, 587–605.

Díaz García, F., Sánchez Martínez, S., Castiñeiras, P., Fuenlabrada, J.M., Arenas, R., 2010. A peri-Gondwanan arc in NW Iberia. II: Assessment of the intra-arc tectonothermal evolution through U–Pb SHRIMP dating of mafic dykes. Gondwana Research 17, 352–362 (this issue).

Elliot, D.H., Fanning, C.M., 2008. Detrital zircons from upper Permian and lower Triassic Victoria Group Sandstones, Shackleton Glacier region, Antarctica: evidence for multiple sources along the Gondwana plate margin. Gondwana Research 13, 259–274.

Fernández Suárez, J., Arenas, R., Abati, J., Martínez Catalán, J.R., Whitehouse, M.J., Jeffries, T.E., 2007. U–Pb chronometry of polymetamorphic high-pressure granulites: an example from the allochthonous terranes of the NW Iberian Variscan belt. In: Hatcher Jr., R.D., Carlson, M.P., McBride, J.H., Martínez Catalán, J.R. (Eds.), 4-D Framework of Continental Crust: Geological Society of America Memoir, vol. 200, pp. 469–488.

Fernández-Suarez, J., Corfu, F., Arenas, R., Marcos, A., Martínez Catalán, J.R., Díaz García, F., Abati, J., Fernández, F.J., 2002. U–Pb evidence for a polymetamorphic evolution of the HP–HT units of the NW Iberia Massif. Contributions to Mineralogy and Petrology 143, 236–253.

Fernández-Suárez, J., Díaz García, F., Jeffries, T.E., Arenas, R., Abati, J., 2003. Constraints on the provenance of the uppermost allochthonous terrane of the NW Iberian Massif: inferences from detrital zircon U–Pb ages. Terra Nova 15, 138–144.

Gómez Barreiro, J., Martínez Catalán, J.R., Arenas, R., Castiñeiras, P., Abati, J., Díaz García, F., Wijbrans, J.R., 2007. Tectonic evolution of the upper allochthon of the Órdenes complex (northwestern Iberian Massif): structural constraints to a polyorogenic peri-Gondwanan terrane. In: Linneman, U., Nance, R.D., Kraft, P., Zulauf, G. (Eds.), The Evolution of the Rheic Ocean: From Avalonian–Cadomian Active Margin to Alleghenian–Variscan Collision: Geological Society of America Special Paper, vol. 423, pp. 315–332.

Gutiérrez Alonso, G., Barba, P., Díaz García, F., 2000. Sedimentology and structure of the low grade uppermost unit of the Órdenes Complex at the coastal section. Superposition of structural trends and processes. In: Diaz García, F., González Cuadra, P., Martínez Catalán, J.R., Arenas, R. (Eds.), Variscan–Appalachian Dynamics: The Building of the Upper Paleozoic Basement. 15th International Conference on Basement Tectonics: A Coruña, Spain, Program and Abstracts Volume, pp. 234–235.

Hegde, V.S., Chavadi, V.C., 2009. Geochemistry of late Archaean metagreywackes from the Western Dharwar Craton, South India: implications for provenance and nature of the late Archaean crust. Gondwana Research 15, 178–187.

Herron, M.M., 1988. Geochemical classification of terrigenous sands and shales from core or log data. Journal of Sedimentary Petrology 58, 820–829.

Keppie, J.D., Nance, R.D., Murphy, J.B., Dostal, J., Briad, J.A., 2010. The high-pressure Iberian-Czech belt in the Variscan orogen: Extrusion into the upper (Gondwanan) plate? Gondwana Research. 17 (2–3), 306–316 (this issue).

Linneman, U., McNaughton, N.J., Romer, R.L., Gehmlich, M., Drost, K., Tonk, C., 2004. West African provenance for Saxo-Thuringia (Bohemian Massif): did Armorica ever leave pre-Pangean Gondwana?—U/Pb-SHRIMP zircon evidence and the Nd-isotopic record. International Journal of Earth Sciences 93, 683–705.

Linnemann, U., Romer, R.L., 2002. The Cadomian Orogeny in Saxo-Thuringia, Germany: geochemical and Nd–Sr–Pb isotopic characterization of marginal basins with constraints to geotectonic setting and provenance. Tectonophysics 352, 33–64.

Martínez Catalán, J.R., Arenas, R., Díaz García, F., Rubio Pascual, F.J., Abati, J., Marquínez, J., 1996. Variscan exhumation of a subducted Paleozoic continental margin: the basal units of the Órdenes Complex, Galicia, NW Spain. Tectonics 15, 106–121.

Martínez Catalán, J.R., Díaz García, F., Arenas, R., Abati, J., Castiñeiras, P., González Cuadra, P., Gómez Barreiro, J., Rubio Pascual, F., 2002. Thrust and detachment systems in the Órdenes Complex (northwestern Spain): implications for the Variscan–Appalachian geodynamics. In: Martínez Catalán, J.R., Hatcher Jr., R.D., Arenas, R., Díaz García, F. (Eds.), Variscan-Appalachian Dynamics: the building of the Late Paleozoic Basement: Geological Society of America Special Paper, vol. 364, pp. 163–182.

Martínez Catalán, J.R., Arenas, R., Díaz García, F., González Cuadra, P., Gómez-Barreiro, J., Abati, J., Castiñeiras, P., Fernández-Suárez, J., Sánchez Martínez, S., Andonaegui, P., González Clavijo, E., Díez Montes, A., Rubio Pascual, F.J., Valle Aguado, B., 2007. Space and time in the tectonic evolution of the northwestern Iberian Massif: implications for the Variscan belt. In: Hatcher Jr., R.D., Carlson, M.P., McBride, J.H., Martínez Catalán, J.R. (Eds.), 4-D Framework of Continental Crust: Geological Society of America Memoir, vol. 200, pp. 403–423.

Matte, Ph., 1991. Accretionary history and crustal evolution of the Variscan belt in Western Europe. Tectonophysics 196, 309–337.

Matte, Ph., Capdevila, R., 1978. Tectonique en grands plis couchés et plissements superposés d´âge hercynien dans la série de Órdenes -Betanzos (Galice Occidentale). Cuadernos del Seminario de Estudios Cerámicos de Sargadelos 27, 193–201.

McLennan, S.M., Hemming, S.R., 1992. Samarium/neodymium elemental and isotopic systematics in sedimentary rocks. Geochimica et Cosmochimica Acta 56, 887–898.

McLennan, S.M., Hemming, S.R., McDaniel, D.K., Hanson, G.N., 1993. Geochemical approaches to sedimentation provenance and tectonics: Geological Society of America Special Paper, vol. 284, pp. 21–40.

Melleton, J., Cocherie, A., Faure, M., Rossi, P., Arenas, R., 2010. Precambrian protoliths and Early Paleozoic magmatism in the French Massif Central: U–Pb data and the North Gondwana connection in the west European Variscan belt. Gondwana Research 17, 13–25.

Murphy, J.B., Gutiérrez-Alonso, G., Fernández-Suárez, J., Braid, J.A., 2008. Probing crustal and mantle lithosphere origin through Ordovician volcanic rocks along the Iberian passive margin of Gondwana. Tectonophysics 461, 166–180.

Mutti, E., 1985. Turbidite systems and their relations to depositional sequences. Provenance of arenites. NATO A.S.I. Series 148, 65–93.

Nakamura, N., 1974. Determination of REE, Ba, Fe, Mg, Na and K in carbonaceous and ordinary chondrites. Geochimica et Cosmochimica Acta 38, 757–775.

Nance, R.D., Gutiérrez-Alonso, G., Keppie, J.D., Linnemann, U., Murphy, J.B., Quesada, C., Strachan, R.A., Woodcock, N.H., 2010. Evolution of the Rheic Ocean. Gondwana Research 17, 194–222 (this issue).

Ordoñez Casado, B., Gebauer, D., Schäfer, H.J., Gil Ibarguchi, J.I., Peucat, J.J., 2001. A single Devonian subduction event for the HP/HT metamorphism of the Cabo Ortegal complex within the Iberian Massif. Tectonophysics 332, 359–385.

Pettijohn, F.H., Potter, P.E., Siever, R., 1972. Sand and Sandstone. Springer-Verlag, New York. 618 p.

Pin, C., Paquette, J.L., Santos Zalduegui, J.F., Gil Ibarguchi, J.I., 2002. Early Devonian suprasubduction-zone ophiolite related to incipient collisional processes in the Western Variscan Belt: the Sierra de Careón unit, Órdenes Complex, Galicia. In: Martínez Catalán, J.R., Hatcher Jr., R.D., Arenas, R., Díaz García, F. (Eds.), Variscan–Appalachian Dynamics: The Building of the Late Paleozoic Basement: Geological Society of America Special Paper, vol. 364, pp. 54–71.

Ranjan, N., Banerjee, D.M., 2009. Central Himalayan crystallines as the primary source for the sandstone–mudstone suites of the Siwalik Group: new geochemical evidence. Gondwana Research 16, 687–696.

Rodríguez, J., Cosca, M.A., Gil Ibarguchi, J.I., Dallmeyer, R.D., 2003. Strain partitioning and preservation of $^{40}Ar/^{39}Ar$ ages during Variscan exhumation of a subducted crust (Malpica-Tui complex, NW Spain). Lithos 70, 111–139.

Roser, B.P., Korsch, R.J., 1985. Plate tectonics and geochemical composition of sandstones: a discussion. Journal of Geology 93, 81–84.

Roser, B.P., Korsch, R.J., 1986. Determination of tectonic setting of sandstone-mudstone suites using SiO_2 content and K_2O/Na_2O ratio. Journal of Geology 94, 635–650.

Roser, B.P., Korsch, R.J., 1988. Provenance signatures of sandstone–mudstone suites determined using discriminant function analysis of major-element data. Chemical Geology 67, 119–139.

Sánchez Martínez, S., Arenas, R., Díaz García, S., Martínez Catalán, J.R., Gómez Barreiro, J., Pearce, J., 2007a. The Careón Ophiolite, NW Spain: supra-subduction zone setting for the youngest Rheic Ocean floor. Geology 35, 53–56.
Sánchez Martínez, S., Arenas, R., Andonaegui, P., Martínez Catalán, J.R., Pearce, J.A., 2007b. Geochemistry of two associated ophiolites from the Cabo Ortegal Complex (Variscan belt of NW Spain). In: Hatcher Jr., R.D., Carlson, M.P., McBride, J.H., Martínez Catalán, J.R. (Eds.), 4-D Framework of Continental Crust: Geological Society of America Memoir, vol. 200, pp. 445–467.
Spaletti, L.A., Queralt, I., Sergio, D.M., Colombo, F., Maggi, J., 2008. Sedimentary petrology and geochemistry of siliciclastic rocks from Upper Jurassic Tordillo Formation (Neuquén Basin, western Argentina): implications for provenance and tectonic setting. Journal of South American Earth Sciences 25, 440–463.
Stern, R.J., 2002. Crustal evolution in the East African Orogen: a neodymiun isotopic perspective. Journal of African Earth Sciences 34, 109–117.
Strelow, F.W.E., 1960. An ion exchange selectivity scale of cations based on equilibrium distributions coefficients. Analytical Chemistry 32, 1185–1188.
Taylor, S.R., McLennan, S.M., 1985. The Continental Crust: Its Composition and Evolution. Blackwell, London. 312 pp.
Thompson, R.N., 1982. Magmatism in the British Tertiary Volcanic Province. Scottish Journal of Geology 19, 49–107.
Winchester, J.W., 1963. Rare earth chromatography using bis-(2-ethylhexyl) (ortho-phosphoric acid). Journal of Chromatography 10, 502–506.
Winchester, J.A., Max, M.D., 1989. Tectonic setting discrimination in clastic sequence: an example from the late proterozoic Erris Group, NW Ireland. Precambrian Research 45, 191–201.

Capítulo 7

A peri-Gondwanan arc in NW Iberia II: Assessment of the intra-arc tectonothermal evolution through U–Pb SHRIMP dating of mafic dykes

7.1 Introducción

El trabajo incluido en este capítulo consiste en un estudio sobre la estructura de las series turbidíticas culminantes del Complejo de Órdenes (Unidades Alóctonas Superiores). La escasa recristalización que afecta a los niveles más altos de esta serie ha favorecido la preservación de determinadas estructuras primarias, que proporcionan información valiosa acerca de las etapas iniciales en la evolución tectónica de las Unidades Alóctonas Superiores.

El trabajo también incluye la datación U-Pb de uno de los diques de diabasas que intruye la serie siliciclástica. Esta datación se había intentado en diferentes ocasiones, pero el problema se mostraba repetidamente refractario al avance del conocimiento, ante la imposibilidad de recuperar los minerales necesarios para realizar la datación. Las relaciones que se establecen entre la edad de las diabasas y las relaciones estructurales de los diques con la fábrica de las grauvacas, permite hacer importantes inferencias sobre la evolución tectonotermal pre-Varisca de las Unidades Superiores.

De acuerdo con las conclusiones presentadas en el capítulo anterior, la secuencia turbidítica culminante del Complejo de Órdenes se generó en un contexto convergente en relación con un importante arco volcánico activo. Probablemente la sedimentación tuvo lugar en una cuenca de intra-arco, desarrollada en la sección más externa del margen de Gondwana y localizada en la cercanía del Cratón del Oeste de África. Este arco se desarrolló sobre una corteza continental adelgazada, y por tanto podría haber incorporado restos de un basamento continental.

Los resultados que se presentan en este trabajo se han obtenido en las mismas series siliciclásticas y también mediante el estudio de los diques de diabasas que intruyen a este conjunto. Por consiguiente, ambos trabajos se complementan y presentan una visión de conjunto de las características geoquímicas, estructurales y geocronológicas de las series grauváquicas culminantes de las Unidades Alóctonas Superiores. El trabajo en su conjunto, es importante para avanzar en el conocimiento de la dinámica asociada al sistema de arcos magmáticos peri-Gondwánicos en el límite Ediacarense – Cámbrico Inferior.

7.2 Conclusiones parciales

Los datos de geocronología U-Pb en circones de uno de los numerosos diques de diabasas que intruyen la secuencia turbidítica culminante del Complejo de Órdenes, proporcionan una edad de ca. 510 Ma, interpretada como la edad de cristalización de los protolitos máficos. Este dato, junto con el análisis de las relaciones estructurales observadas entre los diques de diabasas y las fábricas regionales dominantes en las series encajantes (S1 y S2), indican que las fábricas tectónicas existentes en los niveles más altos en facies de esquistos verdes tienen un claro carácter pre-Varisco. El desarrollo de estas fábricas tuvo lugar muy probablemente, en relación con la dinámica asociada al arco magmático peri-Gondwánico, con el que también se ha relacionado la sedimentación de la serie grauváquica. Así pues, la generación de las fábricas tectónicas, en su mayor parte contemporáneas con la actividad plutónica ligada al arco, la propia sedimentación de las series turbidíticas y la intrusión de los diques diabásicos, indican un ambiente muy dinámico, como se asocia de manera característica a la dinámica de los arcos volcánicos desarrollados en márgenes continentales activos.

En relación a la estructura pre-Varisca concreta de la serie turbidítica, la primera fase de deformación D1 se caracteriza por el desarrollo de grandes pliegues recumbentes vergentes hacia el oeste (coordenadas actuales). Estos pliegues tienen por plano axial la fase esquistosa dominante en los niveles superiores de menor grado (S1). Hacia los niveles inferiores se generaliza la presencia de una segunda esquistosidad, que constituye la fábrica principal (S2). Esta esquistosidad muestra indicadores cinemáticos que indican un movimiento de techo hacia el norte y se considera de carácter extensional. Los diques diabásicos datados en ca. 510 Ma se emplazaron al final de D2, según las indicaciones microestructurales que se han observado, lo que demuestra el carácter pre-Varisco de las dos primeras fábricas. Finalmente, una tercera deformación, de edad ya Varisca, genera pliegues erguidos de tamaño y apretamiento muy variable que pueden observarse afectando a todas las unidades que constituyen el Complejo de Órdenes.

En relación al contexto dinámico y paleogeográfico regional, se interpreta que el desarrollo de la primera deformación (D1) está ligado a un proceso de acreción por debajo del arco volcánico, lo que resulta coherente con el desarrollo de una zona de subducción por debajo del margen externo adelgazado de Gondwana. D2 se desarrolló durante un episodio extensional, probablemente ligado al colapso gravitacional del arco volcánico. La edad obtenida para el protolito de los diques máficos (ca. 510 Ma), cuyo emplazamiento se produjo al final del episodio extensional D2, y la edad máxima de sedimentación calculada para las series turbidíticas (ca. 510-530 Ma), que intruyen estos diques, delimitan la evolución tectónica de los niveles culminantes de las Unidades Alóctonas Superiores.

Gondwana Research 17 (2010) 352–362

Contents lists available at ScienceDirect

Gondwana Research

journal homepage: www.elsevier.com/locate/gr

A peri-Gondwanan arc in NW Iberia. II: Assessment of the intra-arc tectonothermal evolution through U–Pb SHRIMP dating of mafic dykes

F. Díaz García [a], S. Sánchez Martínez [b], P. Castiñeiras [c], J.M. Fuenlabrada [d], R. Arenas [c,*]

[a] Departamento de Geología, Universidad de Oviedo, 33005 Oviedo, Spain
[b] Institut für Geowissenschaften, Mineralogie–Petrologie und Geochemie, Goethe-Universität, Altenhöferallee 1, D-60438 Frankfurt am Main, Germany
[c] Departamento de Petrología y Geoquímica e Instituto de Geología Económica (CSIC), Universidad Complutense de Madrid, 28040 Madrid, Spain
[d] CAI de Geocronología y Geoquímica Isotópica, Facultad de Geología, Universidad Complutense de Madrid, 28040 Madrid, Spain

ARTICLE INFO

Article history:
Received 23 April 2009
Received in revised form 17 September 2009
Accepted 23 September 2009
Available online 5 October 2009

Keywords:
Arc dynamics
Cambrian intra-arc deformation
U–Pb SHRIMP dating
Peri-Gondwanan arc
Allochthonous complexes
NW Iberia

ABSTRACT

The arc-derived upper units of the Órdenes Complex, NW Iberia, are emplaced above the Variscan suture and contain a low-grade metasedimentary uppermost section, with a maximum depositional age of 510–530 Ma, intruded by a number of mafic dykes. Three deformational events affect the metasedimentary section. The youngest deformation event (D_3) is of undifferentiated Variscan age and consists of metre- to decametre-scale, close upright folds with axes plunging gently towards N20°E. The most important D_2 structure is a regional S_2 foliation axial planar of minor folds with dextral asymmetry. The presence of a stretching lineation parallel to the D_2 fold axes is related to a top-to-the-north sense of shearing in a context of regional extension. The oldest meter-scale D_1 folds are developed in suitable greywacke–pelite alternations and consist of tight folds with chevron and similar morphologies, axes plunging gently toward N20°E, and a continuous S_1 axial planar foliation. The essential characteristic of the D_1 deformation event is depicted by a set of west-vergent folds with reverse limbs less than 2 km in wavelength, that are affected in their lower part by the generalised presence of the regional S_2 foliation. The age of D_2 and D_1 structures is not well constrained. The diabase dykes intruding the low-grade turbidites cut the D_1 folds and their field relationships suggest that they were emplaced at the end of the D_2 shearing event and prior to the upright D_3 Variscan folds. Zircon grains obtained from one of the diabase dykes were analysed for U–Pb at the SHRIMP-RG facility at Stanford University. An age of c. 510 Ma, based on the analysis of 31 individual zircon grains, is interpreted to date the crystallization of the Ares dyke. The tectonic and magmatic evolution of the top turbiditic series of the Órdenes Complex is tentatively related to the dynamics of a peri-Gondwanan arc developed during active subduction beneath Gondwana and suggests: (1) accretion beneath the arc during west-vergent (present coordinates) nappe development (D_1); (2) extension of the arc during top-to-the-north shearing (D_2); and (3) final intrusion of the diabasic dykes into an intra-arc turbiditic series. This evolution spans the end of volcanic arc activity and the onset of the opening of the Rheic Ocean.

1. Introduction

The arc-derived upper units of the allochthonous complexes of NW Iberia include a thick turbiditic series that occupies the uppermost structural position. An earlier first companion paper in this issue (Fuenlabrada et al., 2010) describes the geochemistry of the turbidites and their provenance based on new Nd isotope data and a revision of previously published U–Pb ages for detrital zircon grains (Fernández-Suárez et al., 2003). Fuenlabrada et al. (2010) also provide a general description of the tectonothermal evolution of the upper units based on field evidence and U–Pb ages (Abati et al., 1999, 2007; Fernández-Suarez et al., 2002, 2007; Ordoñez Casado et al., 2001). Present data suggest an intra-arc setting for the sedimentary basin in which the turbiditic series was deposited, located in a peri-Gondwanan realm peripheral to the margin of the West African Craton. The volcanic arc was probably built on the most external margin of Gondwana on thinned continental basement. The Nd isotopic data suggest an affinity with West Avalonia, Florida and the Carolina terrane, and a more westerly provenance than that accepted for the Early Paleozoic autochthonous sequence in NW Iberia and its equivalents in the Bohemian Massif (Linnemann and Romer, 2002), largely confirming earlier data on the provenance of this allochthonous terrane (Gómez Barreiro et al., 2007).

This paper presents a detailed structural and microstructural analysis of the turbiditic series from the coastal section of the Ares–Sada region, east of A Coruña city (Fig. 1), and U–Pb age data for diabase dykes intruding the sedimentary succession. Structural analysis of the low-grade uppermost section of the upper units complements the history recorded in the rest of the upper units for two reasons. First, minor recrystallization and grain growth favour the preservation of old

* Corresponding author. Departamento de Petrología y Geoquímica, Facultad de Geología, Universidad Complutense de Madrid, C/ José Antonio Novais, no 2, 28040 Madrid, Spain.
E-mail address: arenas@geo.ucm.es (R. Arenas).

1342-937X/$ – see front matter © 2009 International Association for Gondwana Research. Published by Elsevier B.V. All rights reserved.
doi:10.1016/j.gr.2009.09.010

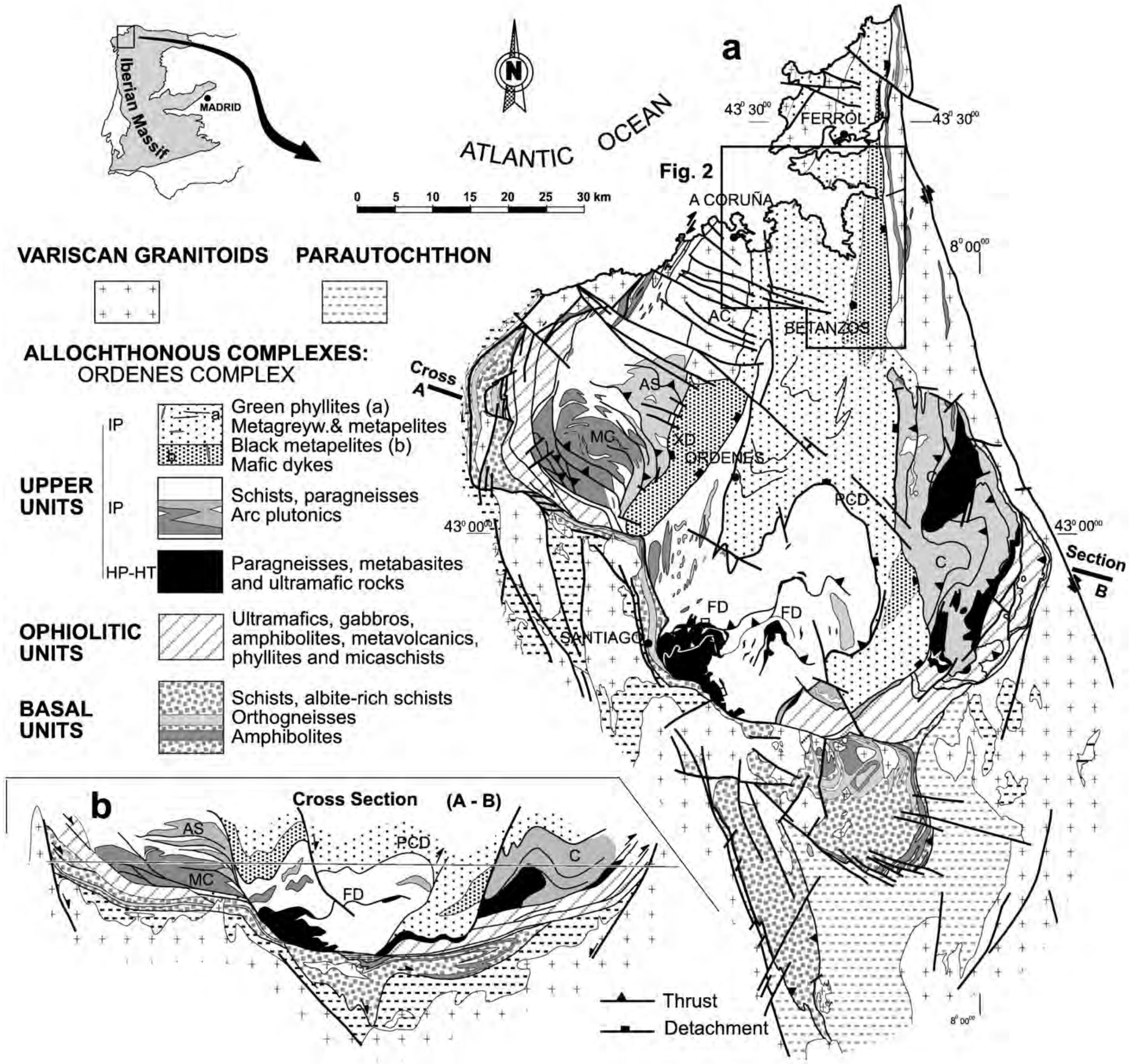

Fig. 1. (a) Structural map, and (b) cross section of the Órdenes Complex showing location of area depicted in Fig. 2. AC, A Coruña granodiorite; AS, A Silva granodiorite; C, Corredoiras granodiorite; CD, Corredoiras detachment; F, Fornás unit; FD, Fornás detachment; MC, Monte Castelo gabbro; PCD, Ponte Carreira detachment; S, Sobrado unit; XD, Xesteda detachment.

structures, such that the unit provides unique information about early stages in the tectonic evolution of the upper units which is usually lost elsewhere as a result of higher grade metamorphic recrystallization. Second, large numbers of mafic dykes intrude the low-grade metasediments and show various relationships with the regional deformation events. The relative timing of mafic dyke emplacement can be established by field relationships, and the new U–Pb age of dyke emplacement can be used to date the structural evolution of this uppermost section. The age data and cross-cutting relationships clearly indicate that this part of the upper units was deformed in Middle Cambrian times. This structural evolution therefore provides important information about the dynamics of the peri-Gondwanan arc represented in the upper allochthonous terrane of NW Iberia, including the structures and kinematics developed during the transition between the contractional and extensional regimes that preceded the Cambro-Ordovician opening of the Rheic Ocean at the periphery of the West African Craton.

2. Structure of the upper units at the Ares–Sada region: the coastal section

In contrast to the rest of the upper units, which are characterized by a pervasive regional S_2 foliation developed under medium- to high-grade conditions that prevents analysis of earlier deformation events, their uppermost low-grade unit can be studied as a typical slate belt by applying classical macroscopic and microscopic geometrical analysis and superpositional criteria. On this basis, three main deformation events can be distinguished, each associated with different structures and kinematics. Hence, the uppermost unit provides a unique opportunity to identify the earliest deformation event in the upper units of the

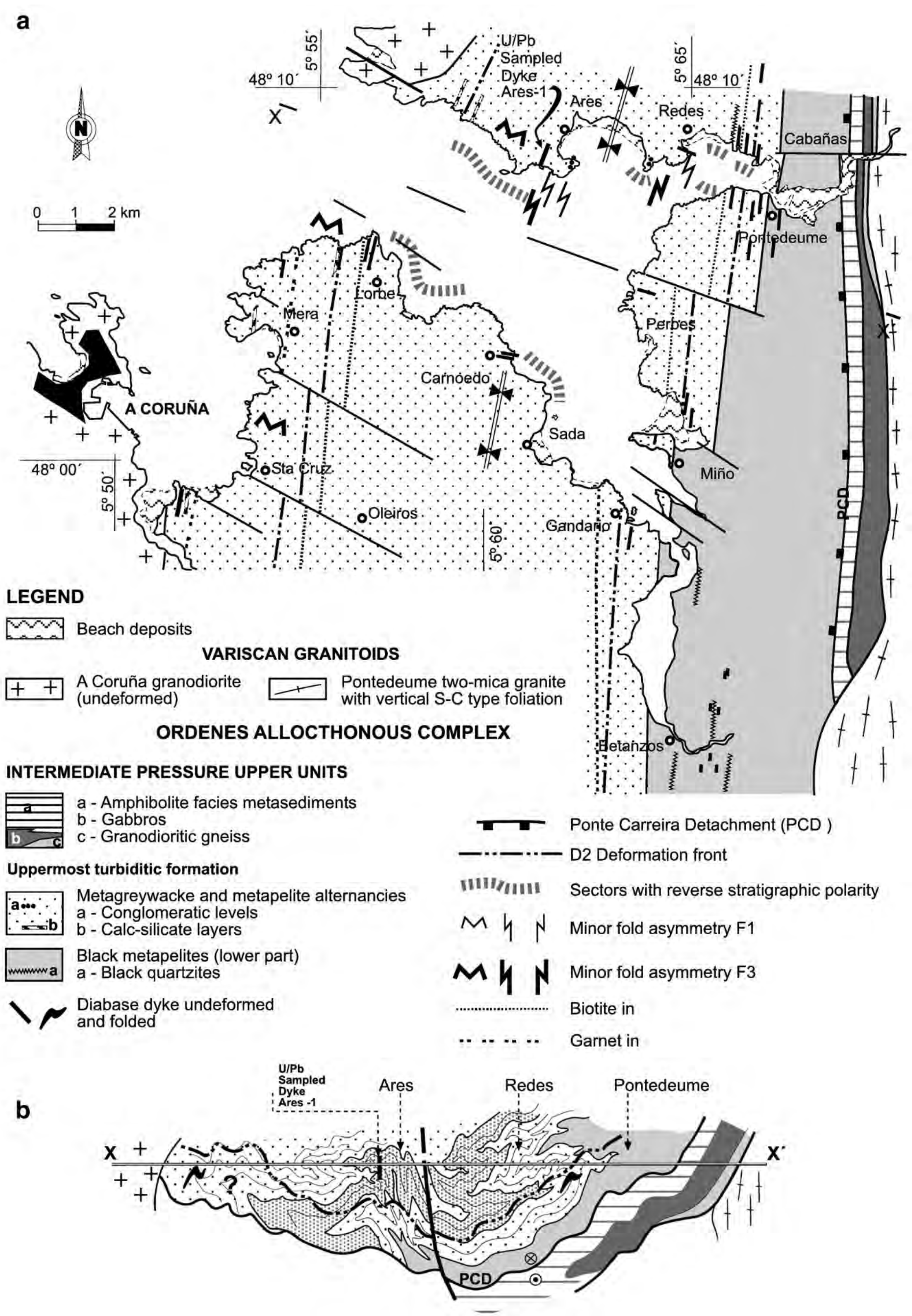

a
U/Pb
Sampled
Dyke
Ares-1
5º 55´
48º 10´
5º 65´
48º 10´
X
X´
Ares
Redes
Cabañas
0 1 2 km
Pontedeume
Lorbe
Mera
Perbes
Carnoedo
A CORUÑA
Sada
Miño
48º 00´
Sta Cruz
5º 50´
Oleiros
Gandario
5º 60´
PCD
Betanzos
LEGEND
Beach deposits
VARISCAN GRANITOIDS
A Coruña granodiorite (undeformed)
Pontedeume two-mica granite with vertical S-C type foliation
ORDENES ALLOCTHONOUS COMPLEX
INTERMEDIATE PRESSURE UPPER UNITS
a - Amphibolite facies metasediments
b - Gabbros
c - Granodioritic gneiss
Uppermost turbiditic formation
Metagreywacke and metapelite alternancies
a - Conglomeratic levels
b - Calc-silicate layers
Black metapelites (lower part)
a - Black quartzites
Diabase dyke undeformed and folded
Ponte Carreira Detachment (PCD)
D2 Deformation front
Sectors with reverse stratigraphic polarity
Minor fold asymmetry F1
Minor fold asymmetry F3
Biotite in
Garnet in
b
U/Pb
Sampled
Dyke
Ares -1
Ares
Redes
Pontedeume
X
X´
PCD

allochthonous complexes. The three deformation events are described below, starting with the most recent.

The youngest deformation event (D_3) consists of metre- to decametre-scale folding developed throughout the entire unit and comprising close, upright structures with axes plunging gently N20°E. Centimetre-wide greywacke layers show flattened parallel folds, sometimes developing cuspate–lobate forms. A near-vertical axial planar crenulation cleavage (S_3) is always present and is better developed in metapelitic beds. These beds sometimes show strong differentiation with a spaced, non-penetrative crenulation cleavage that is less evident, discontinuous or absent, in the metagreywackes. In the coastal section (Figs. 1 and 2) meter-scale D_3 folds show opposite asymmetry, defining a major D_3 synform, the enveloping surface of which is shown in cross-section in Fig. 2b and can be followed inland, where it defines the major Órdenes synform (Fig. 1). This major synform belongs to a widespread Variscan refolding phase in the Órdenes Complex that affected the stacking of allochthonous units and their bounding shear zones (e.g., (Martínez Catalán et al., 1996)).

Structures belonging to the older D_2 deformational event affect almost all the upper units, but in the study area an upper deformation front can be traced parallel to the "biotite in" boundary (Fig. 2). The most important structure of this event is a regional S_2 foliation that shows various microstructures corresponding to early and intermediate stages in the morphological evolution of a crenulation cleavage under increasing deformation and temperature, as proposed by Passchier and Trouw (2005). Although strongly affected by upright folding, it is assumed that S_2 was initially subhorizontal. The foliation is axial planar of minor folds that are dextral in asymmetry, and sometimes non-cylindrical with the intensely sheared short limbs. This feature, together with the presence of a stretching lineation parallel to the fold axes, suggests top-to-the-north sense of shear. At deeper structural levels the S_2 foliation is a highly evolved compositional foliation, the development of which was coeval with amphibolite facies metamorphism (Castiñeiras, 2005). Towards the base of the intermediate pressure upper units, partial melting of the metasediments took place during the final stages of S_2 development, which shows a metatexitic appearance and is locally disaggregated by diatexite. U–Pb analysis of monazites from metatexites has yielded an age of 490 Ma (Abati et al., 1999). This apparently structural continuity is interrupted by the development of a major extensional shear zone, the Ponte Carreira detachment (Martínez Catalán et al., 2002; Gomez Barreiro, 2007) (PCD in Fig. 2), which led to the thinning of the garnet and staurolite zones, strong retrogression and phyllonitization, and the formation of C′ shear bands (Berthé et al., 1979). The mineral stretching lineation parallel to D_2 fold axes is well defined in these rocks where it is aligned north–south and indicates top-to-the-north sense of shear.

The first deformation event (D_1) was probably present throughout the intermediate pressure upper units, although at lower structural levels no major structures have been identified, and D_1 is represented only by an S_1 cleavage strongly overprinted by S_2. In fact, it is only recognizable in relict D_2 fold hinges or as oriented inclusion trails in garnet or staurolite porphyroblasts. The low-grade turbiditic rocks on the coastal section near Ares, however, are devoid of D_2 deformation and so are suitable for the study of minor D_1 fold asymmetries. Combining this with the angular relationships between the existing foliations (S_1 and S_3) and bedding (S_0), and the younging direction of the strata, allows the position of the fold hinges to be located and provides a means of determining fold facing vs. vergence in polyphase folded terrains. Metre-scale folds developed in alternating greywackes and pelites are tight with chevron and similar morphologies. Their axial planes have varying orientations as a consequence of late D_3 folding, but their axes plunge gently towards N20°E. The axial

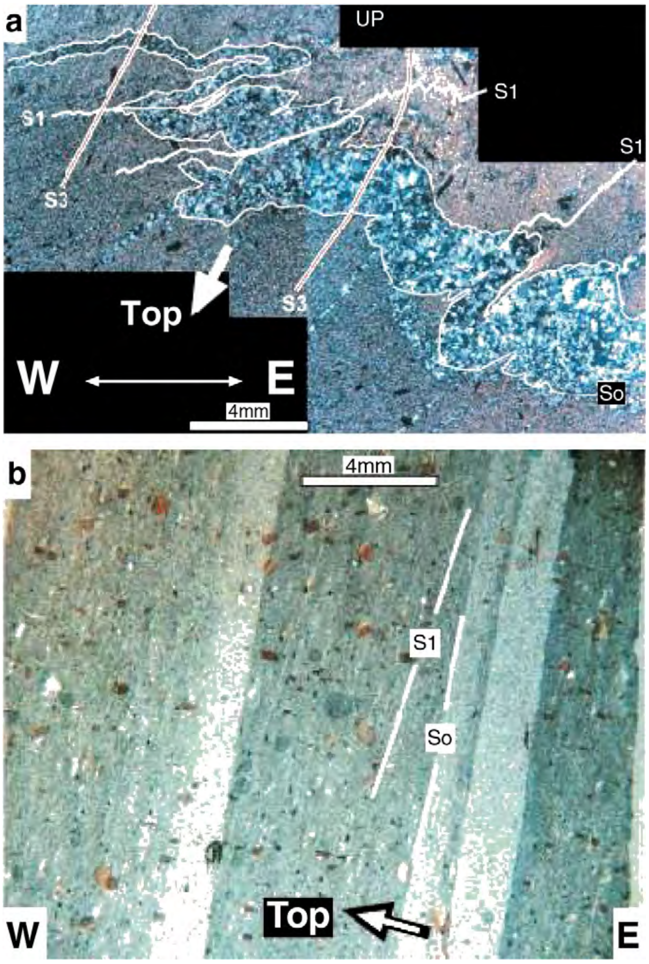

Fig. 3. Microstructural aspects of the different types of foliation in the low-grade part of the upper units and their angular relationships that, together with the presence of graded bedding, suggest a west vergence for the D_1 fold nappe. (a) Minor "Z shaped" folds developed in the reverse limb of a west-vergent D_1 fold that was later affected by a crenulation cleavage (S_3). (b) Angular relationship between bedding (S_0) and slaty cleavage (S_1) within the normal limb of a minor downward facing D_1 fold.

planar S_1 cleavage is a pervasive slaty cleavage at a low angle to the bedding and is well developed in the metapelitic tops of the turbiditic strata. In thin section, S_1 is a continuous foliation (*sensu* (Passchier and Trouw, 2005)) mainly defined by flattened and elongate quartz grains and the non-domainal homogeneous distribution of platy mineral grains with a preferred orientation. The younging direction deduced from graded bedding in greywacke layers shows frequent changes, from which it can be inferred that the largest D_1 reverse limbs never exceed 1 km in wavelength.

Decametre- and centimeter-scale, upward facing D_1 folds can be observed in the western limb of the major Órdenes D3 synform. From these the sinistral asymmetry of a major west-vergent fold can be deduced. In the eastern limb of the Órdenes D_3 synform, suitable minor folds have not been found, but microscopic analysis of oriented samples of S_1, S_3 and S_0 angular relationships suggests a west vergence for this first deformation event (Fig. 3). Thus, the structural and younging criteria discussed above, together with the main stratigraphic features of the area permit the reconstruction of the cross section shown in Fig. 2b. Here, the structural architecture is depicted by a set of west-vergent D_1 folds that have reverse limbs less than 2 km in wavelength and are

Fig. 2. (a) Geological map of the Ares-A Coruña–Betanzos region showing the main lithologies, the sectors with reverse stratigraphic polarity, and the asymmetry of minor folds of the different deformation events. (b) Interpretive cross sections accounting for the presence of several sectors with reverse stratigraphic polarity and S_0/S_1 angular relationships. The structural level with abundant of conglomerates and thick greywacke layers has been highlighted. The location of the dated diabase dyke is also shown.

affected in their lower part by the general presence of the regional S_2 foliation, the development of which culminates in the formation of the Ponte Carreira detachment. The whole package is then overprinted by upright D_3 Variscan folding.

3. Relative timing of dyke emplacement

From a regional point of view, mafic dykes are almost exclusive to the low-grade part of the upper units and are likely linked to the major igneous bodies in the underlying section. Their absence in the remaining part of the orogenic section, however, suggests that they were emplaced prior to the stacking of the allochthonous units. The sills and cross-cutting dykes show a rectilinear geometry and range from 20–30 cm to 20–30 m in thickness, both in map view and in vertical exposures. Individual dyke segments are sub-parallel (from N30°E to N15°W) and perpendicular (N110°E) to the regional foliation (S1 or S2). The dykes are mainly composed of medium-grained gabbro and diabase showing chilled margins, and consist of plagioclase, hornblende, epidote and sphene with minor amounts of quartz and relict pyroxene. The similarity of the macroscopic appearance, phase assemblages, and textures of the gabbroic and diabasic dykes and sills precludes field and petrographic distinction of different magma series. Mafic dykes in the lower part of the study area show clear cross-cutting relationships with the S_2 foliation, but some are boudinaged and sheared at their margins. Syntectonic garnet growth in these sheared margins points to a syn- to post-tectonic intrusion with respect to the regional S_2 foliation. In the uppermost part of the unit, which is devoid of S_2, the mafic dykes are undeformed and transect D_1 folds. Conversely, a number of thin, rectilinear diabase dykes are folded by upright D_3 Variscan folds. In addition, a number of quartz veins were formed at high angles to the S_1 cleavage during D_2. The presence of these veins together with the diabase dyke swarm suggests the existence of a dilational event that may be linked to brittle behaviour during the final stages of D_2.

4. U–Pb dating of the dyke network

4.1. Analytical methods

Zircon crystals from the Ares dyke were separated at Universidad Complutense (Madrid) using conventional gravimetric and magnetic techniques. At the Stanford-US Geological Survey Micro-analytical Center (SUMAC), 39 zircon grains were handpicked under a binocular microscope and mounted on double-sided adhesive on glass slides in 1 × 6 mm parallel rows together with chips of the zircon standard R33 (Black et al., 2004). After being set in epoxy resin, the zircon grains were abraded to expose their central portions by using 1500 grit wet sandpaper, and then polished with 6 µm and 1 µm diamond abrasive on a lap wheel. Prior to isotopic analysis, the internal structure, inclusions, fractures and physical defects were identified with transmitted and reflected light on a petrographic microscope, and with cathodoluminescence (CL) on a JEOL JSM 5600 electron microscope (Fig. 4). Following analysis, secondary electron images were taken to locate the exact position of the spots.

U–Th–Pb analyses of zircon were conducted at the Bay SHRIMP-RG (sensitive high-resolution ion microprobe-reverse geometry) facility operated by SUMAC in a single analytical session in July 2008. Analytical procedures for zircon dating followed methods described in Williams (Williams, 1997). The primary oxygen ion beam operated at 6–7 nA and produced a spot with a diameter of ~25 µm and a depth of 1–2 µm for an analysis time of 12–13 min. Data for each spot were collected in sets of five scans through the mass range. The concentration of U was calibrated using zircon standard CZ3 (550 ppm U; (Pidgeon et al., 1995)), and isotopic compositions were calibrated against R33 ($^{206}Pb^*/^{238}U = 0.06716$, equivalent to an age of 419 Ma; (Black et al., 2004)), which was analyzed every fourth scan.

Data reduction follows the methods described by Williams (1997) and Ireland and Williams (2003), and used SQUID and ISOPLOT software

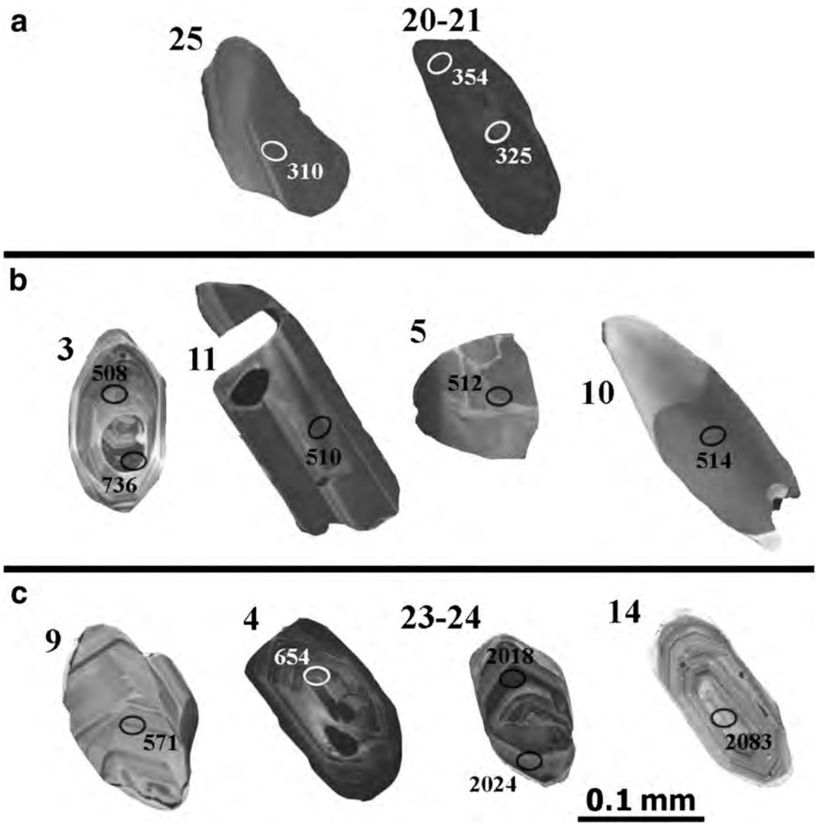

Fig. 4. Cathodoluminescence images of selected zircon crystals from the Ares dyke: (a) Variscan zircons, (b) crystallization age zircons, and (c) inherited zircons.

(Ludwig, 2002, 2003). Ages younger than 1 Ga are reported based on $^{206}Pb/^{238}U$ ratios corrected from common Pb using the ^{207}Pb method. Older ages are reported based on the ^{204}Pb-corrected $^{206}Pb/^{207}Pb$ isotopic ratio. The Pb composition used for initial Pb corrections ($^{204}Pb/^{206}Pb = 0.0554$, $^{207}Pb/^{206}Pb = 0.864$ and $^{208}Pb/^{206}Pb = 2.097$) was estimated using the Stacey and Kramers (1975) model. Analytical results are presented in Table 1 and plotted in Figs. 5 and 6.

La to Yb and Hf were measured concurrently with U–Th–Pb analysis as additional masses on each pass through the mass range. The concentrations of these elements were calibrated against an in-house standard (MAD) and are reproducible at 2–4% (1σ), except for La (15%) because of its typical very low concentration (30 ppb). U, Th, Hf and rare earth element (REE) analyses are listed in Table 2.

4.2. Zircon description and U–Pb results

The analysed zircon grains are colorless with variable length to width ratios (between 1:1 and 3:1). Most are rounded prisms with pitted surfaces, although a few are less rounded with smooth faces. Inclusions are common in all the zircon crystals. Under CL, the zircon grains show an assortment of textures suggesting for most an inherited origin (Fig. 4). Common textures include non-luminescent homogeneous zircon crystals, variably luminescent oscillatory and sector zoning, and complex grains with xenocryst cores mantled by oscillatory zoning and occasionally surrounded by an irregular non-luminescent rim.

Thirty-two analyses were obtained on 31 zircon grains (Fig. 5). The data can be roughly sorted in four age groups, <400 Ma, 480–530 Ma, 545–735 Ma and >2000 Ma (Table 1). In the first group, three scattered ages around 320 Ma could represent metamorphic ages or extreme Pb-loss from older zircon grains during the Variscan orogeny (analyses 20, 21 and 25). Since both the CL images and Th/U ratios are typically magmatic, we favour the latter interpretation. This is also in agreement with the general absence of important tectonothermal events of this age in the Órdenes Complex. From the second group, the best age estimate is obtained by pooling six analyses that yield an age of 510.53 (+8.39, −2.29) Ma using the TuffZirc algorithm (Ludwig and Mundil, 2002). This age is the median obtained from a group of 11 analyses ranging from 480 to 530 Ma, which represent the largest set of internally concordant dates that are statistically coherent, and is interpreted to date the crystallization of the Ares dyke. Ages calculated using this method are reliable provided the data are cogenetic and unaffected by Pb-loss. In this case, we argue for the validity of these assumptions based on the zircon features, namely their homogeneity and sector zoning, which are consistent with zircon growth in mafic

Table 1
SHRIMP Th–U–Pb zircon data from sample GCH-06-2 (dyke Ares-1).

Spot number and description[a]		Common ^{206}Pb (%)	U (ppm)	Th (ppm)	Th/U	$^{238}U/^{206}Pb$[b] (%)	$^{207}Pb/^{206}Pb$[b] (%)	$^{238}U/^{206}Pb^*$[c] (%)	$^{207}Pb^*/^{206}Pb^*$[c] (%)	$^{206}Pb^*/^{238}U$[d]	$^{206}Pb/^{238}U$ age[e,f]
GCH-06-2: Ares dyke											
Variscan ages											
25	m	0.12	521	813	1.61	20.27 ± 0.4	0.0535 ± 1.3	20.25 ± 0.4	0.0541 ± 1.4	0.0493 ± 0.0002	310.1 ± 1.4
21	c	0.13	833	810	1.00	19.32 ± 0.4	0.0540 ± 1.0	19.34 ± 0.4	0.0532 ± 1.2	0.0517 ± 0.0002	324.9 ± 1.2
20	r	<0.01	706	252	0.37	17.76 ± 0.4	0.0528 ± 1.2	17.77 ± 0.4	0.0524 ± 1.3	0.0564 ± 0.0002	353.5 ± 1.5
Magmatic ages											
6	m	0.14	57	48	0.87	12.90 ± 1.3	0.0579 ± 3.2	12.93 ± 1.3	0.0556 ± 3.9	0.0774 ± 0.0010	480.8 ± 6.0
31	m	<0.01	55	41	0.76	12.52 ± 1.2	0.0562 ± 3.4	12.52 ± 1.2	0.0562 ± 3.4	0.0800 ± 0.0010	496.0 ± 6.0
13	m	0.09	200	34	0.17	12.44 ± 0.6	0.0579 ± 1.6	12.46 ± 0.6	0.0567 ± 1.9	0.0803 ± 0.0005	498.1 ± 3.0
18	m	0.01	1163	638	0.57	12.35 ± 0.3	0.0574 ± 0.7	12.35 ± 0.3	0.0577 ± 0.7	0.0809 ± 0.0002	501.7 ± 1.3
22	m	<0.01	37	28	0.78	12.23 ± 1.5	0.0550 ± 3.7	12.23 ± 1.5	0.0550 ± 3.7	0.0820 ± 0.0012	**508.2 ± 7.3**
3.1	m, r	0.06	157	72	0.47	12.18 ± 0.7	0.0580 ± 2.3	12.16 ± 0.7	0.0595 ± 2.6	0.0821 ± 0.0006	**508.4 ± 3.7**
11	m	0.06	150	47	0.32	12.15 ± 0.7	0.0579 ± 1.8	12.16 ± 0.7	0.0574 ± 1.9	0.0823 ± 0.0006	**509.6 ± 3.8**
5	m	<0.01	169	108	0.66	12.11 ± 0.8	0.0574 ± 1.9	12.11 ± 0.8	0.0574 ± 1.9	0.0826 ± 0.0007	**511.5 ± 3.9**
10	m	<0.01	110	49	0.46	12.10 ± 0.8	0.0544 ± 2.1	12.11 ± 0.8	0.0537 ± 2.3	0.0829 ± 0.0007	**513.7 ± 4.3**
1	m	0.16	126	66	0.54	11.91 ± 0.8	0.0590 ± 2.0	11.92 ± 0.8	0.0584 ± 2.2	0.0838 ± 0.0007	**518.9 ± 4.0**
28	m	<0.01	151	93	0.64	11.73 ± 0.8	0.0555 ± 1.9	11.73 ± 0.8	0.0556 ± 1.9	0.0855 ± 0.0007	528.8 ± 4.0
Inherited ages											
29	m	<0.01	195	79	0.42	11.34 ± 0.6	0.0581 ± 1.5	11.35 ± 0.6	0.0571 ± 1.9	0.0882 ± 0.0006	545.1 ± 3.4
17	m	<0.01	118	70	0.61	11.14 ± 0.8	0.0585 ± 1.9	11.14 ± 0.8	0.0585 ± 1.9	0.0898 ± 0.0007	554.3 ± 4.4
27	m	0.13	104	73	0.72	10.98 ± 1.0	0.0599 ± 3.4	11.01 ± 1.0	0.0572 ± 4.2	0.0910 ± 0.0009	561.4 ± 5.5
26	m	<0.01	36	29	0.83	10.96 ± 1.7	0.0588 ± 4.1	10.99 ± 1.7	0.0563 ± 5.1	0.0913 ± 0.0016	563.0 ± 9.4
30	m	0.25	168	61	0.38	10.80 ± 0.7	0.0611 ± 1.6	10.82 ± 0.7	0.0598 ± 1.8	0.0924 ± 0.0006	569.6 ± 3.8
19	m	<0.01	264	103	0.40	10.84 ± 0.5	0.0578 ± 1.3	10.86 ± 0.5	0.0561 ± 1.8	0.0924 ± 0.0005	569.6 ± 3.0
9	m	0.22	69	37	0.55	10.78 ± 1.1	0.0609 ± 2.5	10.78 ± 1.1	0.0609 ± 2.5	0.0926 ± 0.0010	570.9 ± 5.9
32	m	<0.01	207	88	0.44	9.85 ± 0.7	0.0592 ± 1.5	9.83 ± 0.7	0.0607 ± 1.9	0.1017 ± 0.0007	624.5 ± 4.0
16	m	<0.01	302	212	0.73	9.65 ± 0.5	0.0599 ± 1.1	9.65 ± 0.5	0.0599 ± 1.1	0.1037 ± 0.0005	636.3 ± 3.0
4	m	<0.01	185	131	0.73	9.38 ± 0.6	0.0605 ± 1.4	9.37 ± 0.6	0.0612 ± 1.5	0.1067 ± 0.0007	653.8 ± 3.9
7	m	<0.01	178	73	0.43	8.38 ± 0.7	0.0634 ± 1.4	8.38 ± 0.7	0.0634 ± 1.4	0.1194 ± 0.0008	727.1 ± 4.7
3.2	c	<0.01	244	170	0.72	8.27 ± 0.5	0.0636 ± 1.1	8.28 ± 0.5	0.0633 ± 1.1	0.1209 ± 0.0007	735.7 ± 3.8
2	m	0.05	74	59	0.82	2.76 ± 0.8	0.1229 ± 0.8	2.76 ± 0.8	0.1227 ± 0.8	0.3621 ± 0.0034	1996 ± 15
23	m, r	3.14	481	174	0.37	3.50 ± 0.4	0.1244 ± 0.8	3.50 ± 0.4	0.1242 ± 0.8	0.2766 ± 0.0012	2018 ± 14
24	c	1.18	192	75	0.40	2.93 ± 0.6	0.1248 ± 1.9	2.93 ± 0.6	0.1247 ± 2.0	0.3370 ± 0.0025	2024 ± 35
12	m	<0.01	108	51	0.49	2.54 ± 0.7	0.1289 ± 0.7	2.54 ± 0.7	0.1286 ± 0.7	0.3960 ± 0.0034	2079 ± 13
14	m	<0.01	45	21	0.47	2.57 ± 1.1	0.1297 ± 1.1	2.57 ± 1.1	0.1289 ± 1.1	0.3901 ± 0.0051	2083 ± 20
15	m	0.93	142	33	0.24	1.90 ± 0.7	0.1937 ± 0.6	1.90 ± 0.7	0.1936 ± 0.6	0.5207 ± 0.0049	2773 ± 9

Bold ages represent the analyses considered to date the crystallization age of the dyke. All errors are 1σ.
[a] Zircon characterization: m = magmatic; zoned: c = core, r = rim.
[b] Uncorrected ratios.
[c] Radiogenic lead ^{204}Pb corrected for common lead.
[d] Radiogenic lead ^{207}Pb corrected for common lead.
[e] ^{207}Pb corrected for common lead.
[f] Except analyses 2, 23, 24, 12, 14 and 15 ($^{207}Pb/^{206}Pb$ age, ^{204}Pb corrected for common lead).

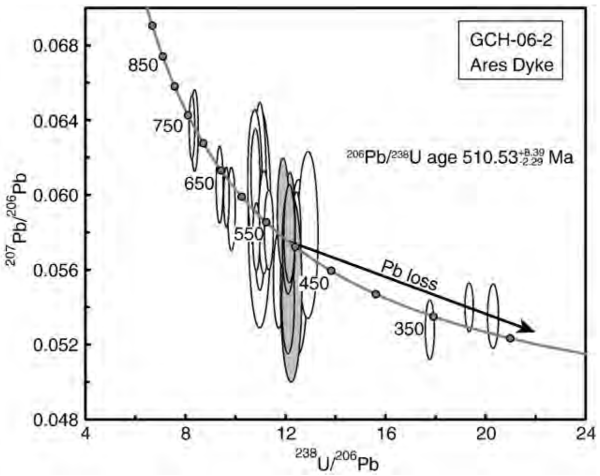

Fig. 5. Tera-Wasserburg plot showing distribution of SHRIMP zircon analyses from sample GCH-06-2. Grey ellipses correspond to analyses considered to date the crystallization age. Error ellipses are $\pm 2\sigma$.

rocks (Corfu et al., 2003). The last two age groups are interpreted as inherited components (Fig. 6) based on the variable morphology and CL features of the zircon grains. There is a cluster of six analyses at ca. 565 Ma; three single analyses between 625 and 650 Ma, and two at ca. 730 Ma. Five analyses reveal a Paleoproterozoic signature at ca. 2010 and 2080 Ma. All of these age groups match ages defined by zircon age spectra for cycles of continental crust production (Condie et al., 2009).

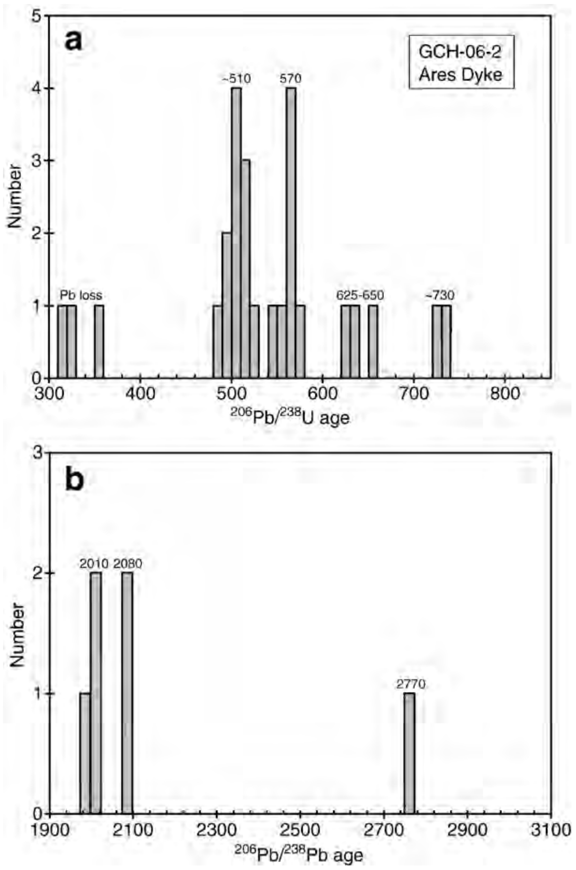

Fig. 6. Diagrams illustrating the distribution of (a) ^{206}Pb/^{238}U ages, and (b) ^{207}Pb/^{206}Pb ages from the Ares dyke zircon grains.

4.3. Trace element data

The magmatic character of the Ares dyke zircon is further supported by their rare earth element (REE) composition. Overall, their REE patterns are typical of magmatic zircon (Hoskin and Schaltegger, 2003), with low light (L) REE contents, a pronounced positive Ce anomaly, a variably negative Eu anomaly, and variable fractionation in the heavy (H) REE (Fig. 7).

Even though inter- and intra-grain compositional variation is usually large in zircons, and thus zircon REE studies should be based on both multiple zircon grains and multiple analyses per grain, some limited petrogenetic information can be suggested for the Ares dyke zircon based on their REE contents and certain elemental ratios. The following section is based on a number of general observations presented by Wooden et al. (2006) using the vast dataset obtained in their laboratory. According to these authors, Yb/Gd, which represents the steepness of the HREE pattern, appears to be an excellent monitor of magma evolution by fractional crystallization during zircon growth. For common magmatic suites, it shows a starting ratio of about 10 and increases rapidly at relatively low temperatures (<750 °C). Conversely, Th/U tends to decrease with zircon crystallization temperature, showing the strongest changes at higher temperature. The Ce/Sm ratio is preferred to that of Ce/Ce* by these authors because it varies more regularly when plotted against a fractionation index, typically showing an increase with increasing fractionation (e.g., Yb/Gd ratio).

These features are illustrated for the Ares dyke zircons in plots of Yb/Gd versus Th/U and Ce/Sm versus Yb/Gd (Fig. 8a and b, respectively). In both diagrams, the low and homogeneous Yb/Gd ratio in the zircon grains used to define the age of the dyke is apparent, consistent with crystallization from a poorly evolved magma such as a mafic dyke. Conversely, the remaining zircon grains usually show higher and more scattered Yb/Gd ratios, consistent with their inherited nature. The homogeneous character of the zircons used to determine the age of the dyke is also evident in their low Ce/Sm ratios compared to the remaining grains.

Hence, given the CL features together and characteristics of the Ares dyke zircons, it can be argued that the grains selected for the age determination represent a homogeneous population of clear magmatic rather than being of metamorphic origin. This population is clearly different from the rest of the zircon grains, which show high variability in their chemical and CL features suggesting an inherited source.

Based on the U–Pb and trace element data, a crystallization age of 510 Ma is proposed for the Ares dyke. However, the possibility that the whole zircon population is inherited cannot be completely discounted since this is a common situation in mafic rocks where the total number of zircon grains is often low. However, even if the zircon grains are inherited, this youngest zircon population would provide a maximum age of intrusion in the same way that detrital zircons provide a maximum depositional age in sedimentary rocks. In this case, the maximum age of intrusion would likely be close to the actual crystallization age. The volcanic arc preserved in the upper units of NW Iberia is characterized by an early intra-arc high-temperature metamorphism dated in the interval 505–483 Ma (Abati et al., 1999, 2007). Moreover, subsequent accretion of the arc to the southern margin of Laurussia at 410–390 Ma (Ordoñez Casado et al., 2001; Fernández Suárez et al., 2007) resulted in high-pressure/high-temperature metamorphism in the lower parts of the upper units. The absence in the dyke of a significant zircon population younger than 510 Ma, and the complete absence of metamorphic zircon grains, consequently provide additional arguments favouring its intrusion at around 510 Ma, even in the case of a completely inherited zircon population.

5. Discussion

Fuenlabrada et al. (2010) show that the sedimentary sequence in the uppermost part of the upper units has a maximum depositional age in the range 510–530 Ma (Middle Cambrian), which overlaps the

Table 2
Th, U, Hf (in ppm) and chondrite-normalized rare earth element data from zircon from sample GCH-06-2 (dyke Ares-1) and zircon standard R33.

Spot number and description		Th	U	Hf	La	Ce	Pr_{calc}	Nd	Sm	Eu	Gd	Dy	Er	Yb	Th/U	Yb/Gd	Ce/Sm	Ce/Ce*	Eu/Eu*
GCH-06-2: Sada Dyke																			
Variscan ages																			
25	m	792	485	9298	0.09	30.6	0.67	1.88	10.4	18.9	53.2	139	320	565	1.63	8.8	12.02	128	0.80
21	c	799	792	10,669	0.72	73.1	3.15	6.59	30.4	25.8	120.2	280	668	1170	1.01	8.1	9.87	48	0.43
20	r	246	662	10,703	0.05	42.1	0.54	1.67	12.4	12.0	69.9	194	561	1111	0.37	13.1	13.93	245	0.41
Ages <500 Ma																			
6	m	48	54	12,696	0.09	11.4	0.34	0.68	5.1	2.2	35.0	123	354	604	0.88	14.3	9.10	65	0.16
31	m	40	52	9877	0.08	2.6	0.79	2.46	20.7	2.2	152.2	462	1165	1781	0.77	9.7	0.50	10	0.04
13	m	34	193	11,897	0.06	1.1	0.45	1.20	17.3	1.1	184.6	1017	3200	5177	0.18	23.2	0.27	7	0.02
18	m	629	1098	11,082	0.10	83.3	1.27	4.54	42.3	10.9	343.7	1271	3338	5018	0.57	12.1	8.08	233	0.09
Dyke crystallization ages																			
22	m	27	34	7967	0.09	3.0	0.60	1.57	9.0	7.4	51.1	126	312	515	0.79	8.3	1.37	13	0.34
3.1	m, r	70	147	10,832	0.06	2.4	0.74	2.55	29.3	1.4	244.7	902	2452	3758	0.48	12.7	0.34	11	0.02
11	m	46	141	10,061	0.08	2.9	0.78	2.48	19.7	6.2	131.1	423	1139	1785	0.33	11.3	0.59	12	0.12
5	m	105	158	11,203	0.08	10.2	0.92	3.17	21.4	11.5	129.6	380	1009	1579	0.67	10.1	1.95	38	0.22
10	m	48	104	7650	0.18	3.4	1.53	4.44	34.4	25.2	225.1	636	1494	2239	0.47	8.2	0.40	6	0.29
1	m	64	118	7960	0.12	11.9	1.11	3.43	20.5	21.4	131.7	413	1177	2133	0.54	13.4	2.38	33	0.41
Inherited ages 510–600 Ma																			
28	m	91	142	10,155	0.09	7.5	1.24	4.57	34.0	6.6	211.8	578	1338	1876	0.64	7.3	0.90	22	0.08
29	m	78	184	10,287	0.18	7.3	0.56	0.98	5.1	9.1	25.4	73	237	532	0.42	17.3	5.92	23	0.80
17	m	69	111	10,793	0.07	21.9	0.39	0.89	8.1	6.2	57.4	197	572	1065	0.62	15.4	11.15	129	0.29
27	m	71	97	10,598	0.08	14.7	0.82	2.64	20.0	14.7	145.0	478	1372	2361	0.73	13.5	3.00	58	0.27
26	m	28	33	8565	0.11	10.5	0.85	2.41	13.0	16.6	61.4	152	426	830	0.84	11.2	3.33	35	0.59
30	m	60	158	10,159	7.50	11.7	2.71	1.63	3.4	4.9	16.8	59	234	654	0.38	32.3	14.07	3	0.65
19	m	101	248	11,034	0.05	22.1	0.32	0.82	7.6	3.4	55.0	198	606	1127	0.41	17.0	11.85	176	0.17
9	m	36	66	10,482	0.03	12.0	0.19	0.47	5.1	3.4	41.4	161	507	952	0.55	19.0	9.68	151	0.24
Inherited ages 600–750 Ma																			
32	m	86	193	11,218	0.11	24.5	0.34	0.58	5.8	3.3	46.6	189	689	1515	0.45	26.9	17.21	126	0.20
16	m	213	291	9917	0.21	39.9	0.89	1.82	11.3	14.1	68.7	223	692	1497	0.73	18.0	14.46	92	0.51
4	m	132	178	7737	0.09	23.6	0.48	1.10	7.5	13.1	44.9	142	426	883	0.74	16.3	12.84	114	0.71
7	m	72	167	10,657	0.05	34.9	0.22	0.47	4.5	2.8	33.6	142	461	981	0.43	24.2	31.67	340	0.23
3.2	c	169	234	10,643	0.05	30.9	0.44	1.31	11.2	8.1	76.9	275	795	1435	0.73	15.4	11.26	205	0.27
Inherited ages >2000 Ma																			
2	m	59	71	9500	0.05	28.5	0.47	1.45	9.9	5.8	58.9	170	427	688	0.83	9.7	11.75	185	0.24
23	m, r	170	448	12,322	1.51	48.6	1.17	1.02	9.2	4.7	75.2	324	1187	2469	0.38	27.2	21.59	37	0.18
24	c	74	181	12,562	0.07	46.1	0.31	0.68	6.6	4.2	53.4	222	792	1717	0.41	26.6	28.62	319	0.22
12	m	50	100	9420	0.08	26.0	0.60	1.61	10.9	7.4	60.4	181	539	1012	0.50	13.9	9.80	118	0.29
14	m	20	42	10,500	0.12	15.7	0.51	1.04	6.6	7.9	35.7	98	284	595	0.48	13.8	9.83	63	0.52
15	m	32	133	11,836	0.03	11.3	0.10	0.17	2.4	2.1	19.6	93	306	645	0.24	27.3	19.71	193	0.30
R-33 zircon standard																			
1	m	184	263	10,312	0.09	8.2	0.87	2.68	16.8	15.6	111.9	416	1384	2700	0.70	20.0	2.01	29	0.36
2	m	117	158	9174	0.13	8.3	1.19	3.64	23.9	18.6	166.0	592	1690	2863	0.74	14.3	1.43	21	0.30
3	m	137	199	10,025	0.06	7.7	0.56	1.76	13.4	13.9	95.0	345	1091	2150	0.69	18.7	2.37	43	0.39
4	m	150	180	8419	0.14	12.2	1.60	5.34	39.0	31.7	282.9	942	2459	3915	0.83	11.5	1.28	26	0.30
5	m	178	273	11,759	0.03	10.6	0.36	1.21	11.2	12.5	86.6	343	1138	2330	0.65	22.3	3.90	98	0.40
6	m	153	203	9262	0.12	9.5	1.30	4.27	26.5	19.8	178.1	675	2045	3520	0.75	16.4	1.47	24	0.29
7	m	129	194	10,484	0.05	7.4	0.69	2.69	18.1	15.4	115.5	427	1353	2565	0.67	18.4	1.68	42	0.34
8	m	95	136	9688	0.06	7.2	0.70	2.47	18.1	14.7	122.6	429	1259	2252	0.70	15.2	1.64	37	0.31
9	m	40	95	9074	0.04	4.6	0.19	0.44	4.3	4.0	36.3	153	542	1161	0.42	26.5	4.35	53	0.32
10	m	136	165	8709	0.05	16.0	0.61	2.13	16.4	13.1	126.8	500	1454	2490	0.83	16.2	4.00	20	0.29
11	m	122	158	8916	0.15	9.0	1.40	4.26	26.8	21.0	191.9	699	1974	3262	0.77	14.1	1.38	71	0.29
12	m	39	93	9252	0.03	6.0	0.25	0.75	6.9	6.1	55.8	232	785	1567	0.42	23.2	3.59	55	0.31
13	m	90	134	9895	0.04	6.7	0.41	1.37	11.9	11.3	90.2	324	989	1837	0.67	16.9	2.31	4	0.34
14	m	78	144	9264	2.37	9.4	2.80	3.05	9.6	9.5	37.4	123	412	918	0.54	20.3	3.99	41	0.50
15	m	12	35	9196	0.04	2.7	0.10	0.16	1.6	1.5	15.1	68	245	501	0.34	27.4	7.00	60	0.30
16	m	269	251	8445	0.08	13.7	0.65	1.84	14.8	12.2	112.0	435	1279	2193	1.07	16.2	3.82	53	0.30
17	m	33	75	9125	0.04	5.7	0.25	0.60	5.7	5.2	47.9	196	667	1322	0.44	22.8	4.07	92	0.32

Some elemental ratios cited in the text are also shown. Pr_N is calculated from La_N and Nd_N contents ($Pr = La_N{}^\wedge 1/3 * Nd_N{}^\wedge 2/3$). Zircon description as in Table 1.

age range of the arc plutonic rocks of the same terrane (500–520 Ma). The turbiditic sequence of the Órdenes Complex was generated in a convergent setting, probably in an intra-arc sedimentary basin developed within a major, active volcanic arc located at the periphery of the West African Craton. This arc was likely built on the most external section of the Gondwanan margin, on thinned continental crust, and may incorporate remnants of the continental basement. The turbiditic sequence is intruded by numerous diabase dykes, one of which (near the village of Ares; Fig. 2), has now yielded a protolith age of c. 510 Ma. The structural relationships between the diabase dykes and the most important regional planar fabrics (S_1 and S_2) show these tectonic fabrics to be pre-Variscan and to have developed in the dynamic setting of the peri-Gondwanan volcanic arc. Moreover, the largely coeval development within the arc of plutonic activity,

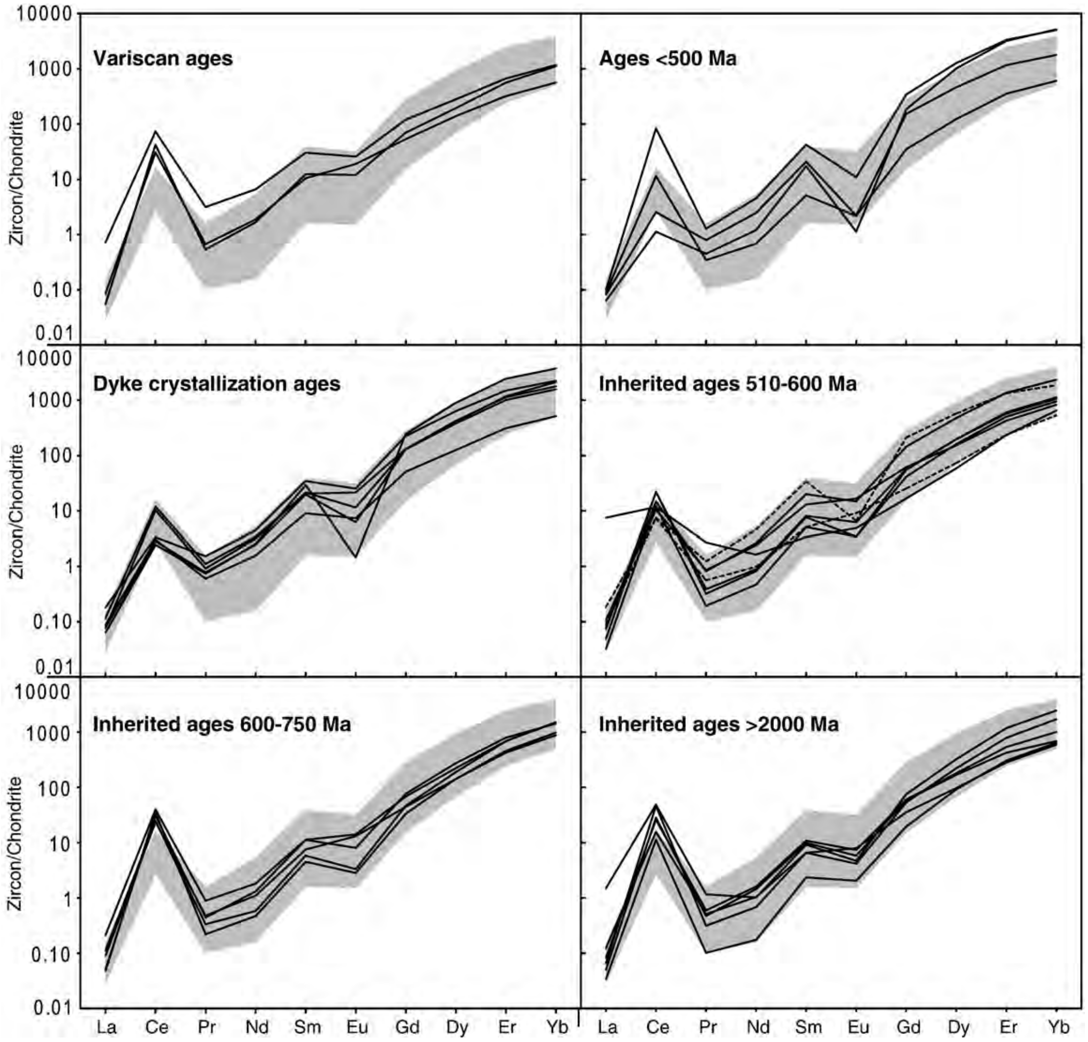

Fig. 7. Rare earth element (REE) patterns for the different age groups defined by the Ares dyke zircon crystals, illustrating their magmatic character. R33 zircon standard patterns are shown for reference (grey area), Chondrite normalization values after Anders and Grevesse (1989) modified by Korotev (1996).

deposition of turbiditic rocks in intra-arc basins, regional deformation, and the intrusion of a swarm of diabase dykes, suggest a very dynamic setting, which is typical of volcanic arcs developed on active continental margins or of island arcs.

Structural analysis of the lowest grade part of the upper unit allows the oldest dynamic history of this terrane to be examined. This study describes the structure of D_1 in the turbiditic series above the D_2 deformation front, and the link between the younger deformation to the pervasive regional

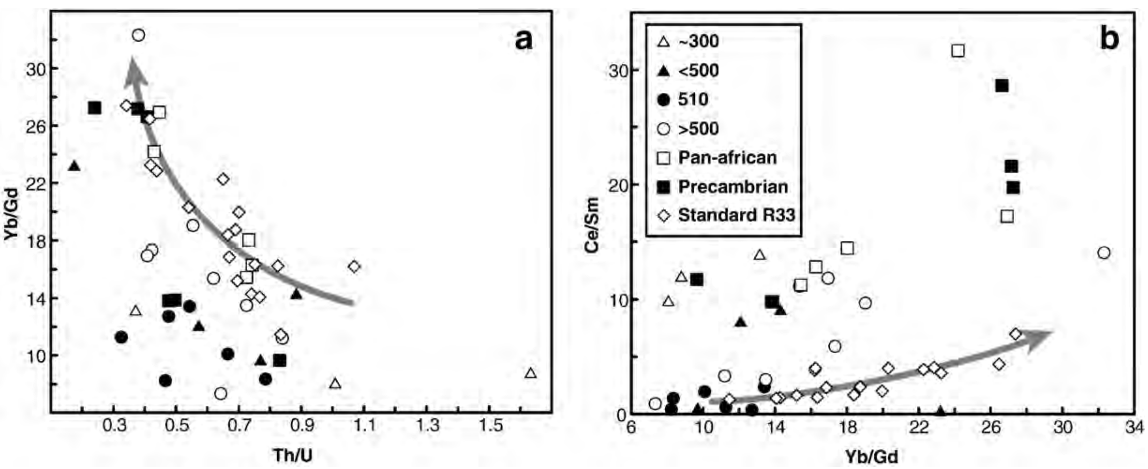

Fig. 8. Plots of (a) Yb/Gd versus Th/U, and (b) Ce/Sm versus Yb/Gd for the zircon grains analyzed in the Ares dyke. Data from R33 zircon standard (open diamonds) are included for comparison and typical magmatic fractionation trends for the standard are shown.

foliation (S_2) that affects the entire intermediate pressure upper units. In addition, the chronology of these two deformational events has been constrained by U–Pb dating of the dyke swarm and reinterpretation of previously reported detrital zircon ages (Fernández-Suárez et al., 2003). As a result, a more complete knowledge of the structural evolution of the upper units has emerged that contributes to a better understanding of the Cambrian subduction processes affecting the margin of Gondwana, and the subsequent rifting associated with the opening of the Rheic Ocean (see (Murphy et al., 2009; Santosh et al., 2009), and references therein). The vergence of the D_1 folds has remained an open question since the visionary paper of Matte and Capdevila (1978), but detailed study of the low-grade sector has revealed the existence of a fold nappe, the basic geometry of which consists of two antiform–synform pairs of west-vergent recumbent folds later folded into an upright Variscan antiform. This D_1 evolution suggests accretion below the volcanic arc, consistent with the development of a subduction zone below the external thinned margin of Gondwana, which has been previously proposed to account for the origin of the volcanic arc itself (Arenas et al., 2007; Martínez Catalán et al., 2007; Abati et al., 2009). Subduction eventually led to the accretion at the base of the arc of oceanic slices, as is suggested by evidence from the western part of the Órdenes Complex, where a thick Cambrian ophiolitic sequence (the Bazar ophiolitic unit) has been emplaced immediately below the arc-related plutonic and metasedimentary successions (Sánchez Martínez, 2009).

The development of the D_1 fold nappes was followed by a general top-to-the-north shearing event (D_2) that, in the study area, is only weakly developed and disappears upwards through a gradual deformation front. Field observations indicate that mafic dykes were emplaced at the end of the D_2 shearing. The 510 Ma protolith age obtained for the mafic dykes and the maximum depositional age obtained for the turbiditic succession (510–530 Ma), restrict the earliest stages of the tectonic evolution of the upper units to a short time interval. The regional S_2 foliation of the uppermost series can be traced downwards into the intermediate pressure upper units, where it developed under increasing temperature conditions with depth, and shows a metatexitic appearance dated at c. 490–500 Ma using U–Pb geochronology in monazites (Abati et al., 1999). This tectonic change is best interpreted in the more general framework of accretion and break up along the northern Gondwana margin. Recently, Nance et al. (2002), Murphy et al. (2006) and Linnemann et al. (2008) proposed a geodynamic model for this margin, in which latest Neoproterozoic to Early Cambrian ridge–trench collision, leads diachronously to the termination of subduction and the generation of a continental transform during the Cambrian, along which the Rheic Ocean later opened. Our data for the arc-derived upper terrane in NW Iberia indicate that accretionary processes, recorded by the D1 west-vergent fold nappes, continued until 510 Ma and that this age marks the change to a period of north-directed extension, anatexis, intrusion of arc plutonics, and emplacement of a mafic dyke swarm, eventually linked to ridge subduction. A similar family of mafic dykes with a comparable age has been described in the tectonic blocks of the Somozas mélange, the basal tectonic mélange of the allochthonous complexes of NW Iberia (Arenas et al., 2009). This mélange includes highly dismembered remnants of a volcanic arc similar to that represented in the upper units. In this case, the diabasic dykes show compositions typical of island-arc tholeiites and intrude submarine volcanic successions with calc-alkaline composition. It has been suggested that the intrusion of the tholeiitic swarm defines the transition to an extensional regime in a mature calc-alkaline arc, which would favour the development of intra-arc basins and marks the onset of the opening of the Rheic Ocean.

Acknowledgements

Financial support for this research was provided by Spanish project CGL2007-65338-CO2/BTE (Ministerio de Ciencia e Innovación). We would like to thank the SUMAC staff at Stanford University, especially Joe Wooden and Ariel Strickland, for their help in operating the SHRIMP instrument and in interpreting the results. P. Castiñeiras's stay at the SUMAC facility was financed with a “Profesores UCM en el extranjero” travel aid. The authors also thank to two anonymous referees for insightful review of the manuscript. This study is a contribution to the IGCP Project 497: “The Rheic Ocean: Origin, evolution and correlatives”.

References

Abati, J., Dunning, G.R., Arenas, R., Díaz García, F., González Cuadra, P., Martínez Catalán, J.R., Andonaegui, P., 1999. Early Ordovician orogenic event in Galicia (NW Spain): evidences from U–Pb ages in the uppermost unit of the Órdenes Complex. Earth and Planetary Science Letters 165, 213–228.

Abati, J., Castiñeiras, P., Arenas, R., Fernández-Suárez, J., Gómez-Barreiro, J., Wooden, J., 2007. Using SHRIMP zircon dating to unravel tectonothermal events in arc environments. The early Palaeozoic arc of NW Iberia revisited. Terra Nova 19, 432–439.

Abati, J., Gerdes, A., Fernández-Suárez, J., Arenas, R., Whitehouse, M.J., Díez Fernández, R., 2009. Magmatism and early-Variscan continental subduction in the northern Gondwana margin recorded in zircons from the basal units of Galicia, NW Spain. Geological Society of America Bulletin 122 (1–2), 219–235.

Anders, E., Grevesse, N., 1989. Abundances of the elements: meteoritic and solar. Geochimica et Cosmochimica Acta 53, 197–204.

Arenas, R., Martínez Catalán, J.R., Sánchez Martínez, S., Fernández-Suárez, J., Andonaegui, P., Pearce, J.A., Corfu, F., 2007. The Vila de Cruces Ophiolite: a remnant of the Early Rheic Ocean in the Variscan suture of Galicia (Northwest Iberian Massif). Journal of Geology 115, 129–148.

Arenas, R., Sánchez Martínez, S., Castiñeiras, P., Jeffries, T.E., Díez Fernández, R., Andonaegui, P., 2009. The basal tectonic mélange of the Cabo Ortegal Complex (NW Iberian Massif): a key unit in the suture of Pangea. Journal of Iberian Geology 35, 85–125.

Berthé, D., Choukroune, P., Jeghouzo, P., 1979. Orthogneiss, mylonite and non coaxial deformation of granites: the example of the South Armorican Shear Zone. Journal of Structural Geology 1, 31–42.

Black, L.P., Kamo, S.L., Allen, C.M., Davis, D.W., Aleinikoff, J.N., Valley, J.W., Mundil, R., Campbell, I.H., Korsch, R.J., Williams, I.S., Foudoulis, C., 2004. Improved $^{206}Pb/^{238}U$ microprobe geochronology by the monitoring of a trace-element-related matrix effect, SHRIMP, ID-TIMS, ELA-ICP-MS and oxygen isotope documentation for a series of zircon standards. Chemical Geology 205, 115–140.

Castiñeiras, P., 2005. Origen y evolución tectonotermal de las unidades de O Pino y Cariño (Complejos Alóctonos de Galicia): Nova Terra, vol. 28. 279 pp.

Condie, K.C., Belousova, E., Griffin, W.L., Sircombe, K.N., 2009. Granitoid events in space and time: constraints from igneous and detrital zircon age spectra. Gondwana Research 15, 228–242.

Corfu, F., Hanchar, J.M., Hoskin, P.W.O., Kinny, P., 2003. Atlas of zircon textures. In: Hanchar, J.M., Hoskin, P.W.O. (Eds.), Zircon. Mineralogical Society of America, Washington: Reviews in Mineralogy and Geochemistry, vol. 53, pp. 468–500.

Fernández Suárez, J., Arenas, R., Abati, J., Martínez Catalán, J.R., Whitehouse, M.J., Jeffries, T.E., 2007. U–Pb chronometry of polymetamorphic high-pressure granulites: an example from the allochthonous terranes of the NW Iberian Variscan belt. In: HatcherJr. Jr., R.D., Carlson, M.P., McBride, J.H., Martínez Catalán, J.R. (Eds.), 4-D framework of continental crust: Geological Society of America Memoir, vol. 200, pp. 469–488.

Fernández-Suarez, J., Corfu, F., Arenas, R., Marcos, A., Martínez Catalán, J.R., Díaz García, F., Abati, J., Fernández, F.J., 2002. U–Pb evidence for a polymetamorphic evolution of the HP–HT units of the NW Iberia Massif. Contributions to Mineralogy and Petrology 143, 236–253.

Fernández-Suárez, J., Díaz García, F., Jeffries, T.E., Arenas, R., Abati, J., 2003. Constraints on the provenance of the uppermost allochthonous terrane of the NW Iberian Massif: inferences from detrital zircon U–Pb ages. Terra Nova 15, 138–144.

Fuenlabrada, J.M., Arenas, R., Sánchez Martínez, S., Díaz García, F., Castiñeiras, P., 2010. A peri-Gondwanan arc in NW Iberia. I: isotopic and geochemical constraints to the origin of the arc — the sedimentary approach. Gondwana Research 17 (2–3), 338–351.

Gomez Barreiro, J., 2007. La Unidad de Fornas: Evolución tectonometamórfica del SO del Complejo de Órdenes: Nova Terra, vol. 32. 334 pp.

Gómez Barreiro, J., Martínez Catalán, J.R., Arenas, R., Castiñeiras, P., Abati, J., Díaz García, F., Wijbrans, J.R., 2007. Tectonic evolution of the upper allochthon of the Órdenes complex (northwestern Iberian Massif): structural constraints to a polyorogenic peri-Gondwanan terrane. In: Linneman, U., Nance, R.D., Kraft, P., Zulauf, G. (Eds.), The evolution of the Rheic Ocean: from Avalonian–Cadomian active margin to Alleghenian–Variscan collision: Geological Society of America Special Paper, vol. 423, pp. 315–332.

Hoskin, P.W.O., Schaltegger, U., 2003. The composition of zircon and igneous and metamorphic petrogenesis. In: Hanchar, J.M., Hoskin, P.W.O. (Eds.), Zircon. Mineralogical Society of America, Washington: Reviews in Mineralogy and Geochemistry, vol. 53, pp. 27–62.

Ireland, T.R., Williams, I.S., 2003. Considerations in zircon geochronology by SIMS. In: Hanchar, J.M., Hoskin, P.W.O. (Eds.), Zircon. Mineralogical Society of America, Washington: Reviews in Mineralogy and Geochemistry, vol. 53, pp. 215–241.

Korotev, R.L., 1996. A self-consistent compilation of elemental concentration data for 93 geochemical reference samples. Geostandards Newsletter 20, 217–245.

Linnemann, U., Romer, R.L., 2002. The Cadomian Orogeny in Saxo-Thuringia, Germany: geochemical and Nd–Sr–Pb isotopic characterization of marginal basins with constraints to geotectonic setting and provenance. Tectonophysics 352, 33–64.

Linnemann, U., Pereira, F., Jeffries, T.E., Drost, K., Gerdes, A., 2008. The Cadomian Orogeny and the opening of the Rheic Ocean: The diacrony of geotectonic processes constrained by LA-ICP-MS U-Pb zircon dating (Ossa-Morena and Saxo-Thuringian Zones, Iberian and Bohemian Massifs). Tectonophysics 352, 11–32.

Ludwig, K.R., 2002. SQUID 1.02, a user's manual: Berkeley Geochronology Center Special Publication, vol. 2. 17 pp.

Ludwig, K.R., 2003. ISOPLOT/Ex, version 3, a geochronological toolkit for Microsoft Excel: Berkeley Geochronology Center Special Publication, vol. 4. 71 pp.

Ludwig, K.R., Mundil, R., 2002. Extracting reliable U–Pb ages and errors from complex populations of zircons from Phanerozoic tuffs. Geochimica et Cosmochimica Acta 66, 463.

Martínez Catalán, J.R., Arenas, R., Díaz García, F., Rubio Pascual, F.J., Abati, J., Marquínez, J., 1996. Variscan exhumation of a subducted Paleozoic continental margin: the basal units of the Órdenes Complex, Galicia, NW Spain. Tectonics 15, 106–121.

Martínez Catalán, J.R., Díaz García, F., Arenas, R., Abati, J., Castiñeiras, P., González Cuadra, P., Gómez Barreiro, J., Rubio Pascual, F., 2002. Thrust and detachment systems in the Órdenes Complex (northwestern Spain): implications for the Variscan–Appalachian geodynamics. In: Martínez Catalán, J.R., HatcherJr. Jr., R.D., Arenas, R., Díaz García, F. (Eds.), Variscan–Appalachian dynamics: the building of the Late Paleozoic Basement: Geological Society of America Special Paper, vol. 364, pp. 163–182.

Martínez Catalán, J.R., Arenas, R., Díaz García, F., González Cuadra, P., Gómez-Barreiro, J., Abati, J., Castiñeiras, P., Fernández-Suárez, J., Sánchez Martínez, S., Andonaegui, P., González Clavijo, E., Díez Montes, A., Rubio Pascual, F.J., Valle Aguado, B., 2007. Space and time in the tectonic evolution of the northwestern Iberian Massif: implications for the Variscan belt. In: HatcherJr. Jr., R.D., Carlson, M.P., McBride, J.H., Martínez Catalán, J.R. (Eds.), 4-D framework of continental crust: Geological Society of America Memoir, vol. 200, pp. 403–423.

Matte, Ph., Capdevila, R., 1978. Tectonique en grands plis couchés et plissements superposés d'âge hercynien dans la série de Ordenes–Betanzos (Galice Occidentale). Cuadernos del Seminario de Estudios Cerámicos de Sargadelos 27, 193–201.

Murphy, J.B., Gutiérrez Alonso, G., Nance, R.D., Fernández-Suárez, J., Keppie, J.D., Quesada, C., Strachan, R.A., Dostal, J., 2006. Origin of the Rheic Ocean: rifting along a Neoproterozoic suture? Geology 34, 325–328.

Murphy, J.B., Nance, R.D., Cawood, P.A., 2009. Contrasting modes of supercontinent formation and the conundrum of Pangea. Gondwana Research 15, 408–420.

Nance, R.D., Murphy, J.B., Keppie, J.D., 2002. A Cordilleran model for the evolution of Avalonia. Tectonophysics 352, 11–32.

Ordoñez Casado, B., Gebauer, D., Schäfer, H.J., Gil Ibarguchi, J.I., Peucat, J.J., 2001. A single Devonian subduction event for the HP/HT metamorphism of the Cabo Ortegal complex within the Iberian Massif. Tectonophysics 332, 359–385.

Passchier, C.W., Trouw, R.A.J., 2005. Microtectonics. Springer-Verlag, Berlin. 366 pp.

Pidgeon, R.T., Furfaro, D., Kennedy, A.K., Nemchin, A.A., van Bronswjk, W., 1995. Calibration of zircon standards for the Curtin SHRIMP II. U.S. Geological Survey Circular 1107, 251.

Sánchez Martínez, S., 2009. Geoquímica y geocronología de las ofiolitas de Galicia. Nova Terra 327, 317–341.

Santosh, M., Maruyama, S., Yamamoto, S., 2009. The making and breaking of supercontinents: some speculations based on superplumes, super downwelling and the role of tectosphere. Gondwana Research 15, 324–341.

Stacey, J.S., Kramers, J.D., 1975. Approximation of terrestrial lead isotope evolution by a two-stage model. Earth and Planetary Science Letters 26, 207–221.

Williams, I.S., 1997. U–Th–Pb geochronology by ion microprobe: not just ages but histories. Economic Geology 7, 1–35.

Wooden, J.L., Mazdab, F.K., Barth, A.P., Miller, C.F., Lowery, L.E., 2006. Temperatures (Ti) and compositional characteristics of zircon: early observations using high mass resolution on the USGS-Stanford SHRIMP-RG. Third SHRIMP workshop, Rottnest Island, Australia. Program and abstracts 64–65.

Capítulo 8

Sm–Nd isotope geochemistry and tectonic setting of the metasedimentary rocks from the basal allochthonous units of NW Iberia (Variscan suture, Galicia)

8.1 Introducción

Las Unidades Basales de los Complejos Alóctonos del NW del Macizo Ibérico han sido objeto de gran atención en los últimos años, cuando se han publicado gran cantidad de trabajos sobre distintos aspectos de su geología. Atendiendo sólo a trabajos monográficos o de síntesis, *Santos Zalduegui (1995), Llana - Fúnez (2001), Rodríguez Aller (2005), Díez Fernández (2011), López Carmona (2015), Arenas et al. (2016) y Díez Fernández et al (2016)* han descrito los aspectos más relevantes de su estructura, evolución metamórfica y geocronología. El trabajo que aquí se presenta, aporta un estudio geoquímico e isotópico (Sm-Nd) de las rocas metasedimentarias que forman parte de las Unidades Basales en el Complejo de Malpica - Tui y en menor medida en el Complejo de Órdenes. Las características composicionales de estas litologías no habían sido investigadas hasta ahora, por lo que este trabajo pretende aportar información sobre el contexto dinámico de generación de las cuencas implicadas y también sobre las áreas fuente. Se han investigado las composiciones de 23 muestras, seleccionadas por su representatividad y escasa modificación química.

En el Complejo de Malpica – Tui, las rocas metasedimentarias definen dos secuencias de características composicionales diferenciadas, que también pueden reconocerse en el Complejo de Órdenes. La secuencia inferior tiene una composición esencialmente siliciclástica y afinidad turbidítica, mientras que la secuencia superior es de composición pelítica. Las edades máximas de sedimentación que se deducen para la secuencia inferior y la superior, mediante geocronología U-Pb de circones detríticos, son de ca. 560 y 500 Ma, respectivamente (*Díez Fernández et al., 2010*). Ambas secuencias aparecen intruidas por una diversidad de rocas graníticas y máficas de afinidad variable entre calcoalcalina y alcalina - peralcalina, datadas en un rango de edad comprendido entre ca. 493 – 470 Ma (*Abati et al., 2010a; Arenas et al., 2016; Díez Fernández et al., 2016; y referencias en ellos incluidas*).

En los sectores que han sido investigados en este trabajo, las Unidades Basales han experimentado una deformación muy intensa (con frecuencia milonítica) y metamorfismo en facies de eclogitas que puede alcanzar unas condiciones P-T de ca. 550 °C y 25 Kb (*López Carmona, 2015*). No obstante, la repartición de la deformación es heterogénea y facilita la conservación de niveles muy escasamente deformados, que en el caso de las rocas siliciclásticas permiten observar series turbidíticas bien preservadas, con estructuras sedimentarias reconocibles e incluso una conservación perfecta de las relaciones entre granos detríticos. Estas características han producido en el pasado una cierta confusión en el Complejo de Malpica - Tui, al ser confundidos con unidades poco metamorfizadas y diferenciadas del resto de las rocas metasedimentarias de este complejo (*Llana – Fúnez, 2001*). Así pues, las condiciones de partida son correctas para acometer un muestreo geoquímico como el que se presenta en este trabajo. A pesar de la intensidad de la deformación y del metamorfismo de alta-P, existen sectores bien conservados que han mantenido intactas sus composiciones químicas originales.

Como en el caso de las Unidades Alóctonas Superiores, el origen de los protolitos de las Unidades Alóctonas Basales se ha relacionado repetidamente con la actividad de un arco magmático peri-Gondwánico (*Rodríguez Aller, 2005; Abati et al., 2010a; Arenas et al., 2016; Díez Fernández et al., 2016*). El magmatimo calcoalcalino se habría originado durante la actividad convergente a la que se liga la formación del propio arco, mientras que el magmatismo alcalino – peralcalino se ha relacionado con el desarrollo de un episodio de rifting en el contexto peri-Gondwánico que favoreció el colapso del propio arco. El trabajo que se incluye en este capítulo complementa los trabajos geoquímicos existentes, que hasta ahora sólo se habían realizado en las rocas metaígneas, y permite ampliar el conocimiento de las series siliciclásticas implicadas y de la dinámica y características del propio sistema de arcos peri-Gondwánico durante la transición Ediacarense – Cámbrico.

8.2 Conclusiones parciales

Los resultados geoquímicos obtenidos para las metagrauvacas y esquistos con albita ediacarenses de las Unidades Basales (secuencia inferior) del Complejo de Malpica-Tui, confirman el carácter inmaduro señalado por un porcentaje dominante de clastos angulares de feldespato y en menor medida de micas. Esta naturaleza conlleva una baja relación SiO_2/Al_2O_3, así como valores de Al_2O_3/Na_2O y Al_2O_3/TiO_2 similares a los de la corteza continental superior. Por su parte, determinados elementos marcadamente inmóviles y con diferente grado de compatibilidad o incompatibilidad, muestran valores para las relaciones Th/Sc, La/Sc, Zr/Sc mayores que las del PAAS, lo que junto con unos bajos contenidos en Cr y Ni, apuntan a unas áreas fuente constituidas por rocas ígneas dominantemente félsicas. Los patrones de REE son similares a los del PAAS, con un ligero enriquecimiento de las LREE con respecto a las HREE, lo que se traduce en una elevada relación La_N/Yb_N, unos patrones casi planos de éstas últimas, con una relación Gd_N/Yb_N muy cercana a la unidad, y una anomalía de Eu ligeramente negativa. Todas estas características sugieren propiedades geoquímicas heredadas de rocas ígneas procedentes de la corteza continental superior. La similitud en los patrones de REE, así como valores de las relaciones Rb/Sr y Th/U, similares a los de la corteza continental superior, sugieren una ausencia de alteración química significativa en los procesos sedimentarios, mientras que el valor medio del índice CIA (*Chemical Index of Alteration - Nesbitt y Young, 1982*) apunta a una baja alteración por meteorización de las rocas fuente.

Por su parte, el carácter dominantemente pelítico de las litologías de la secuencia superior de las Unidades Basales queda confirmado por unos valores de las relaciones SiO_2/Al_2O_3 y K_2O/Na_2O, menores y mayores, respectivamente, que los de las grauvacas de la secuencia inferior, y similares a los del PAAS. Los patrones normalizados de REE muestran en este caso una clara variabilidad. Tres de las rocas estudiadas presentan unos valores similares a los valores medios de la corteza continental superior, representados por el PAAS, mientras que dos de ellas registran patrones fraccionados compatibles con una posible alteración química, como confirman los elevados valores de las relaciones Rb/Sr y Ti/Zr, muy alejados de los valores de referencia de la corteza continental superior. El valor medio del índice CIA para estas muestras, similar al valor del PAAS y claramente superior al de las litologías de la secuencia inferior, resulta compatible con una moderada meteorización química o física, un carácter más maduro y un mayor reciclado de estas rocas metasedimentarias. Otro aspecto diferencial en estos metasedimentos son los mayores contenidos en Cr, Ni, Sc y V, lo que junto con valores de Th y La similares a los de las grauvacas y esquistos con albita de la secuencia inferior, y prácticamente iguales a los valores del PAAS, sugieren un área fuente de composición intermedia, con un mayor aporte de rocas ígneas máficas que las observadas en el caso de las rocas siliciclásticas de la secuencia inferior.

De acuerdo con los diagramas de *Bhatia y Crook (1986)*, en el origen de los sedimentos siliciclásticos de la secuencia inferior es clara la implicación de un margen convergente ediacarense. Así lo indican las abundancias medias de elementos como el Th, Co, y Zr, y los valores medios de las relaciones Th/Sc, Zr/Th y Ba/Rb. Estos valores apuntan a la participación de un arco magmático evolucionado. En estos diagramas se evidencia también que el desarrollo del arco tuvo lugar sobre una corteza continental engrosada y la posible existencia de una cuenca asociada de tipo marginal (*back-arc*) evolucionando hacia un margen pasivo. Las elevadas abundancias de los grandes cationes (Rb, Ba y K), La y Ce, el bajo contenido en Sc, y los valores medios para las relaciones Ti/Zr, Sc/Cr y La/Sc parecen confirmar esta tendencia.

Por su parte, las litologías estudiadas en la secuencia superior cámbrica no permiten un tratamiento análogo utilizando los diagramas anteriormente comentados. Dichos diagramas son aplicables sólo a series grauváquicas inmaduras, lo que excluye a los micaesquitos de esta secuencia. Sin embargo, sí es posible una comparación geoquímica de las litologías de las dos secuencias atendiendo a los contenidos de una selección de elementos mayores y traza normalizados a los valores del PAAS, recogidos en un diagrama propuesto por *Winchester y Max (1989)*. Estos patrones muestran una serie de características discriminantes que los autores asocian a contextos tectónicos concretos. Según estos criterios, las series siliciclásticas ediacarenses-cámbricas de la secuencia inferior presentan un patrón característico de un margen continental activo: (i) la aparente variabilidad en los contenidos de los elementos utilizados, propios de sedimentos inmaduros, con un grado de reciclaje limitado; (ii) los contenidos relativamente elevados de los grandes cationes (LILE), los cuales muestran un patrón casi plano, con una clara tendencia hacia la unidad; (iii) la ausencia de una clara anomalía negativa de Sr; y por último (iv) la presencia de una anomalía negativa del TiO_2, típica de sedimentos depositados en este tipo de contextos. De igual manera, también se observan determinados aspectos que indican la posible existencia de una cuenca asociada de tipo *back-arc*. El patrón normalizado presenta en su parte intermedia unos valores medios más elevados de lo esperable, como sucede en el caso de los HFSE, especialmente en relación con las abundancias de Zr, Hf, Sc, La y Nd; así como en el caso del P_2O_5, con un valor medio muy similar al del PAAS.

La tendencia hacia un patrón más propio de una sedimentación en el marco de un posible margen pasivo se continúa de manera más patente en los micaesquistos Cámbricos analizados en la secuencia superior. En este caso no se han tenido en cuenta las dos muestras que presentan indicios de una posible alteración química, por lo que el número de muestras es limitado. En el caso de las tres muestras restantes, el patrón que observamos es prácticamente similar, lo que sugiere un comportamiento análogo de las mismas en los procesos sedimentarios. Estas rocas no evidencian la variabilidad hallada en los patrones de la secuencia inferior, como ya se ha comentado con anterioridad, posiblemente debido a un mayor grado de madurez y reciclaje sedimentario. Los LILE muestran una clara cercanía a la unidad, sin una disminución en sus abundancias con respecto al PAAS, característica de contextos activos. En general, el patrón de estas tres muestras es casi plano, y presenta anomalías negativas, en diferentes grados para el Sr, U y TiO_2, muy comunes en sedimentos depositados en un contexto de margen pasivo, debidos al aumento de la movilidad e intercambio de los mismos en procesos de reciclaje sedimentario. Es llamativo el hecho de que los micaesquistos de la secuencia superior muestren, al contrario de lo esperable, abundancias de Zr y Hf menores que los metasedimentos de la secuencia inferior. Estos elementos habitualmente se encuentran presentes en minerales pesados, más resistentes a un cierto grado de reciclaje sedimentario, coherente con una sedimentación en el marco de un margen pasivo. Esta característica posiblemente tiene su explicación en una procedencia de áreas fuentes más máficas. Otro aspecto a tener en cuenta, y que se repite en ambos grupos de muestras, es la ausencia de la anomalía negativa de P_2O_5. De acuerdo con los diagramas propuestos por *Winchester y Max (1989)*, la presencia de esta fuerte anomalía es común para rocas depositadas en contextos de margen activo y pasivo. El contenido en fósforo está estrechamente relacionado con la proporción de determinadas fases minerales como apatito, monacita y/o xenotima. La presencia habitual de estos minerales, incluso como inclusiones, ejerce una fuerte influencia en la abundancia de este elemento, limitando posiblemente el uso del mismo como un factor discriminante del contexto tectónico de sedimentación.

Los análisis isotópicos según la sistemática Sm-Nd no han proporcionado una discriminación evidente en las fuentes isotópicas de ambas secuencias. Los valores de εNd inicial de las litologías de la secuencia inferior, calculados para una edad de ca. 560Ma, varían entre -8.1 y -13.1. En la secuencia superior, los valores de εNd inicial calculados para una edad de ca. 500 Ma, varían entre -8.5 y -10.1. De igual manera, los valores registrados de edades modelo de Nd (T_{DM}) para ambas secuencias no indican una diferenciación clara entre ambos grupos de rocas, definiendo más bien una única población de edades. Estas T_{DM}, calculadas según el método de *DePaolo (1981)*, se distribuyen a través del Paleoproterozoico en el rango 1743 - 2223 Ma. Este dato sugiere que la deposición de ambas secuencias tuvo lugar en una misma cuenca sedimentaria y que sus fuentes isotópicas no experimentaron cambios significativos durante la transición entre el Neoproterozoico y el Cámbrico.

Los resultados geoquímicos obtenidos para las rocas metasedimentarias de ambas secuencias litológicas, indican un cambio en el contexto tectónico de su sedimentación. A pesar de que la secuencia inferior muestra una cierta afinidad por un contexto relacionado con un arco volcánico altamente evolucionado, desarrollado sobre una corteza continental adelgazada, las abundancias de algunos de sus elementos químicos discriminantes se comportan más acordes con contextos más pasivos. Esta tendencia se continúa en la secuencia superior, donde es clara la transición hacia un contexto de margen pasivo durante el Cámbrico. A pesar de que la influencia del arco Cadomiense es clara en los aportes terrígenos recibidos por la secuencia inferior, las evidencias geoquímicas comentadas anteriormente permiten concluir que esta secuencia se depositó dentro de una gran cuenca *back-arc* entre el Ediacarense y el Cámbrico Inferior. Esta cuenca se situaría cercana al margen externo de Gondwana y en una posición donde los aportes sedimentarios dominantes llegarían desde el dominio continental. Por su parte y de acuerdo con los resultados geoquímicos obtenidos, la sedimentación durante el Cámbrico Superior de la secuencia suprayacente se realizó en un contexto de margen pasivo. La transición observada entre un contexto de cuenca tipo *back-arc* y uno de margen pasivo es coherente con la apertura del Océano Reico entre el Cámbrico Medio y el Ordovícico Inferior (*Arenas et al., 2007; Nance et al., 2010*), y explicaría la mayor proporción de los aportes desde fuentes máficas a la secuencia superior. La sedimentación de la secuencia superior, teniendo en cuenta posibles variaciones laterales de la cuenca a lo largo del margen de Gondwana con respecto a la posición de la secuencia inferior, se habría producido muy cercana a la plataforma continental.

Las conclusiones anteriores se basan igualmente en los valores muy negativos de εNd para ambas secuencias. Estos valores de εNd, junto con una ligera anomalía de Eu, y los valores de las relaciones Th/Sc (igual o ligeramente superior a la unidad) y Th/U (valores superiores a los valores de la corteza continental superior), apuntan a una procedencia relacionada con una corteza continental superior antigua y un cierto grado de reciclaje sedimentario (*McLennan et al., 1993*). Esta procedencia parece confirmada también por unos valores de T_{DM} muy antiguos, únicamente compatibles con áreas fuente Paleoproterozoicas y Arcaicas, que permiten situar a la cuenca sedimentaria en el margen Gondwánico contiguo al Cratón del Oeste de África (Cratón de Reguibad). La contribución de fuentes juveniles de edad Ediacarense fue extremadamente reducida, ya que de otro modo se habría producido una dilución isotópica importante de una señal de procedencia tan antigua.

Lithos 148 (2012) 196–208

Contents lists available at SciVerse ScienceDirect

Lithos

journal homepage: www.elsevier.com/locate/lithos

Sm–Nd isotope geochemistry and tectonic setting of the metasedimentary rocks from the basal allochthonous units of NW Iberia (Variscan suture, Galicia)

José Manuel Fuenlabrada [a], Ricardo Arenas [b,*], Rubén Díez Fernández [c], Sonia Sánchez Martínez [b], Jacobo Abati [b], Alicia López Carmona [b]

[a] CAI de Geocronología y Geoquímica Isotópica, Facultad de Geología, Universidad Complutense de Madrid, 28040 Madrid, Spain
[b] Departamento de Petrología y Geoquímica e Instituto de Geociencias (UCM-CSIC), Universidad Complutense de Madrid. 28040 Madrid, Spain
[c] Departamento de Geología, Universidad de Salamanca, 37008 Salamanca, Spain

A R T I C L E I N F O

Article history:
Received 12 November 2011
Accepted 2 June 2012
Available online 9 June 2012

Keywords:
Metasedimentary rocks
Tectonic setting
Sm–Nd isotope geochemistry
Allochthonous complexes
Variscan belt
NW Iberia

A B S T R A C T

The basal units of the allochthonous complexes of NW Iberia are formed by thick metasedimentary rock sequences intruded by granitoids, ranging in composition from calc-alkaline (c. 493 Ma) to minor alkaline–peralkaline massifs (c. 475–470 Ma), and mafic rocks. The granitoids were transformed into variably deformed othogneisses and the associated mafic rocks were transformed into amphibolites, blueschists and eclogites during eo-Variscan high-P metamorphism dated at c. 370 Ma. Two different superimposed metasedimentary rock sequences can be distinguished. The lower sequence (maximum depositional age at c. 560 Ma) is mainly composed of metagreywackes, while the upper sequence (maximum depositional age at c. 500 Ma) consists of mica schists and other minor types. Major and trace element geochemistry of the metagreywackes of the lower sequence suggests that they were generated in relation to a peri-Gondwanan arc system built on the thinned continental margin, although some chemical transition to passive margin greywackes is also observed. This sedimentary sequence was probably deposited in an Ediacaran–Early Cambrian back-arc setting or retro-arc setting, closer to the thinned platform of the continental margin. The geochemical features of the sedimentary rocks of the upper sequence suggest some affinity with passive margin sediments; they were probably deposited closer to the continental domain and to certain distance from the most active zones of the magmatic arc. The Nd model ages of 23 analysed samples are Paleoproterozoic and range between 1782 Ma and 2223 Ma (average value 1919 Ma). The Nd model ages are slightly younger in the upper sequence than in the lower sequence, but altogether they define a single population, and therefore the two metasedimentary rock sequences can be clearly related. Sedimentation probably took place within the same basin located in the continental platform of Gondwana, the main source areas of these sedimentary rocks did not change during the Late Neoproterozoic and Cambrian times. The Nd model ages are very old and they seem to be compatible with Paleoproterozoic or Archean source areas, with only minor participation of younger sources probably represented by intrusive Cadomian–Pan-African granitoids.

1. Introduction

The interpretation of metasedimentary series involved in the suture zone of mountain belts is a key issue to unravel the origin of the most relevant terranes, frequently with different tectonic settings and sometimes characterized by an important exoticism (Hatcher et al., 2007; Merschat and Hatcher, 2007; Searle, 2007). These are generally highly deformed and variably metamorphosed azoic metasedimentary series; consequently little information can be obtained from traditional studies based in paleontology or stratigraphy. In these cases, provenance analysis based in U–Pb dating of detrital zircons can be a complement to major and trace element geochemistry and Sm–Nd systematics (Díez Fernández et al., 2010; Drost et al., 2004; Linnemann and Romer, 2002; Linnemann et al., 2004). In favourable situations, these data allow to determine the tectonic setting and location of the sedimentary paleo-basins. Sedimentary series formed by greywackes are particularly useful for these studies since the analysis of immobile elements during post-sedimentary and orogenic processes has been proven to be suitable for constraining the tectonic setting (Bathia and Crook, 1986).

This paper presents a case-study of the metasedimentary rocks from the basal units of the allochthonous complexes of NW Iberia, one of the far-travelled terranes involved in the Variscan suture that are exposed in southern Europe (Martínez Catalán et al., 2009). The structural and metamorphic characteristics of this crustal-derived terrane indicate

* Corresponding author at: Departamento de Petrología y Geoquímica e Instituto de Geociencias (UCM-CSIC). Facultad de Geología, Universidad Complutense de Madrid, C/ José Antonio Novais, no 2, 28040 Madrid, Spain. Tel.: +34 639601919; fax: +34 915442535.
E-mail addresses: jmfuenla@pas.ucm.es (J.M. Fuenlabrada), arenas@geo.ucm.es (R. Arenas), georuben@usal.es (R. Díez Fernández), s.sanchez@geo.ucm.es (S. Sánchez Martínez), abati@geo.ucm.es (J. Abati), alcarmona@geo.ucm.es (A. López Carmona).

0024-4937/$ – see front matter © 2012 Elsevier B.V. All rights reserved.
doi:10.1016/j.lithos.2012.06.002

that it was affected by high-P and low-to-intermediate-T eo-Variscan metamorphism reaching the blueschist and eclogite facies. The origin and geological history of this terrane are still under discussion, and the complex tectonothermal evolution makes difficult to deduce the original setting and provenance of the protoliths of these metasedimentary rock series using traditional techniques. These series include clastic rocks suitable for a provenance study based on geochemical methods. Only few works have applied so far this methodology in the metasedimentary rocks of the Variscan Belt (Fuenlabada et al., 2010; Linnemann et al., 2004, 2007; Ugidos et al., 2003). Moreover, the progressive incoming and comparison of this kind of data may help to correlate the terranes that bound the suture zone of the Variscan Belt.

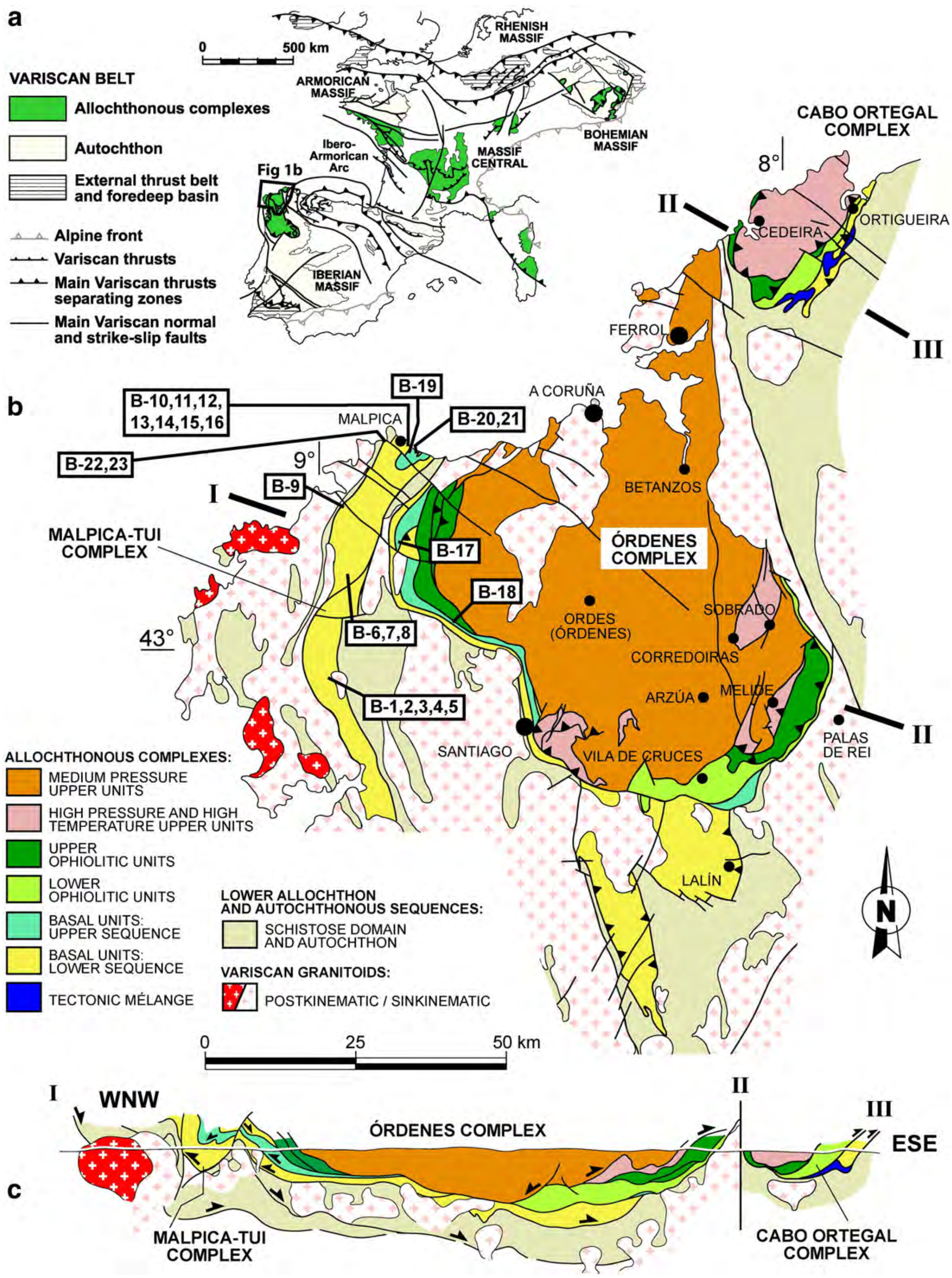

Fig. 1. (a) Location of the study area in the Variscan belt. (b) Map showing the terranes involved in the Variscan suture exposed in NW Iberia and the location of the analysed samples. (c) Representative cross section showing the general structure. Note the nappe stacking and the position of the lower and upper metasedimentary rock sequences. Top-to-the-ESE kinematics often represents thrusting, whereas top-to-the-WNW movements are related to post-nappe stacking gravitational extension. The general map and section of NW Iberia are based in previous data and maps by Díaz Garcia et al. (1999), Arenas et al. (2009), Martínez Catalán et al. (2009) and Díez Fernández et al. (2010).

2. Geological setting

The NW Iberian section of the Variscan Belt contains a set of allochthonous terranes thrust over an autochthonous domain representing the margin of Gondwana (Fig. 1a). It is generally accepted that the lowermost allochthonous terrane (Parautochthon), mainly constituted by metasedimentary rocks, represents an external section of the Paleozoic Gondwana margin. However, the interpretation of those terranes located either in the hanging wall or in the footwall to the Variscan suture zone is more complex, as they are probably affected by important displacements and may have an exotic nature (Martínez Catalán et al., 2007, 2009). In the NW Iberian Massif, the suture zone is marked by several ophiolitic units (Fig. 1b and c) different in age and likely related to different geodynamic settings, but considered as a whole formed during different evolutionary stages of the Rheic Ocean. These units were obducted over the most external margin of Gondwana at the onset of the Variscan collision, after closure of this ocean at the end of Devonian times (Arenas et al., 2007; Díaz García et al., 1999; Gómez Barreiro et al., 2010; Sánchez Martínez et al., 2007).

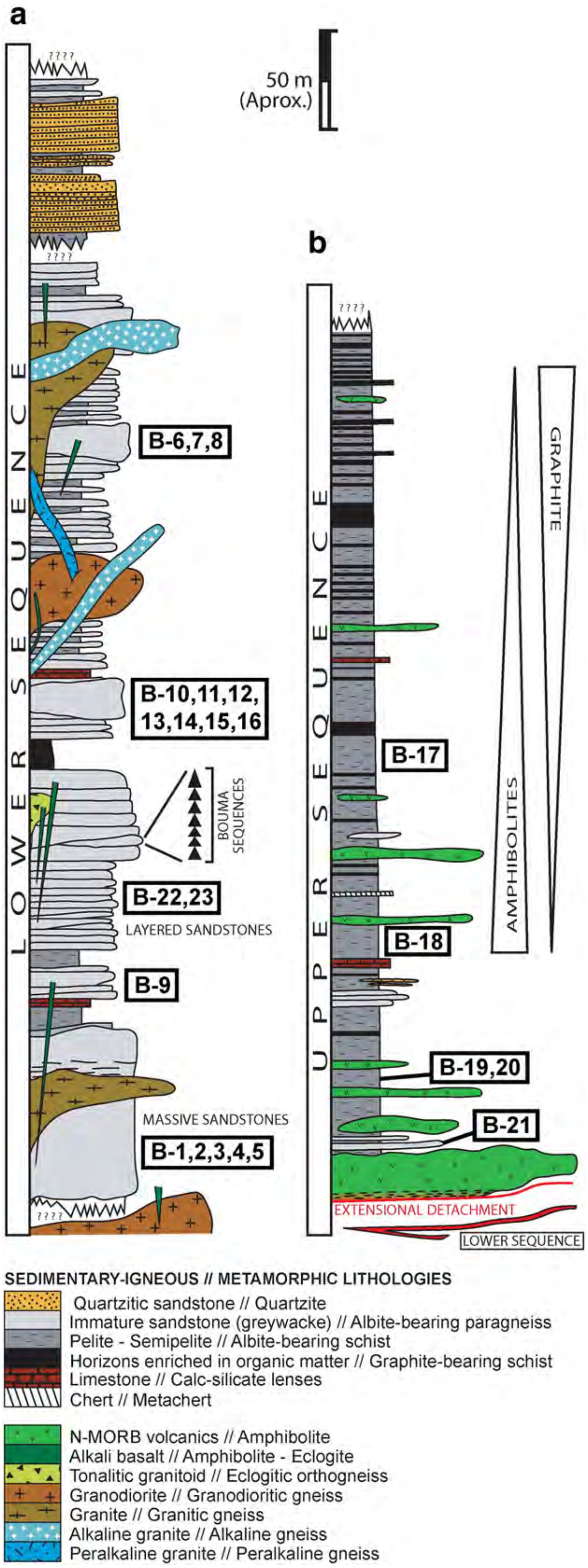

Fig. 2. Idealized stratigraphic columns summarizing the main sedimentological features observed in the lower (a) and upper (b) sequences. The position of the analysed samples is also shown. Due to strong Variscan deformation, the vertical distribution of the facies of the lower sequence shown in this figure is approximate.

The upper section of the allochthonous pile (upper units) rests over the ophiolites and contains an intricate succession of siliciclastic metasedimentary rocks intruded by large massifs of granitoids and gabbros (Fig. 1b and c). This terrane has a polymetamorphic tectonothermal evolution developed during two consecutive Middle Cambrian and Late Silurian–Middle Devonian events (Abati et al., 1999, 2007; Fernández-Suárez et al., 2002, 2007). The upper units are considered a section of a Cambrian peri-Gondwanan magmatic arc, some of these units show a counter-clockwise P–T evolution associated to magmatic underplating (Abati et al., 2003). In a subsequent event, the arc drifted away from Gondwana leaving the Rheic Ocean at its tail, being accreted to the southern margin of Laurussia afterwards (Gómez Barreiro et al., 2007). The uppermost sequence of this terrane is constituted by a low grade thick sequence of metagreywackes intruded by a network of diabasic dikes. These metagreywackes are Middle Cambrian in age, and their tectonic setting was revealed using major and trace element geochemistry and Sm–Nd systematics (Fuenlabrada et al., 2010).

The basal units of the allochthonous complexes define a crustal accretionary complex stacked below the ophiolites (Fig. 1c). They are formed by thick metasedimentary rock sequences intruded by calc-alkaline granitoids (c. 493 Ma; Abati et al., 2010b; Díez Fernández et al., 2012) and minor alkaline to peralkaline massifs (c. 475–470 Ma; Díez Fernández et al., 2012; Rodríguez Aller, 2005; Rodríguez et al., 2007), both transformed in variably deformed orthogneisses, as well as mafic rocks transformed in amphibolites, blueschists and eclogites (Gil Ibarguchi and Ortega Gironés, 1985). These units are considered to represent a section of the most external margin of Gondwana (Arenas et al., 1986; Díez Fernández et al., 2011; Martínez Catalán et al., 1996). According to the chemical composition of the orthogneisses, the protoliths of the basal units were formed in the context of a peri-Gondwanan magmatic arc (calc-alkaline granitoids), affected by subsequent rifting during the opening of the Rheic Ocean (alkaline-peralkaline granitoids; Abati et al., 2010b). However, any description of the compositional characteristics of the metasedimentary rocks did not exist until now, although these are the oldest lithologies and they can be used to deduce the initial tectonic setting. This margin was subsequently affected by eo-Variscan high-P low-to-intermediate-T metamorphism, developed at c. 370 Ma during subduction beneath Laurussia at the onset of the Variscan collision, in the main stage of the Pangea assembly (Abati et al., 2010b; Rodríguez et al., 2003).

3. The sedimentary record of the basal units

Two different and superimposed metasedimentary rock sequences can be distinguished in the basal units. The deformation shows an heterogeneous character with important partitioning, which allows the preservation of low to very low deformed sections, sometimes almost intact and even preserving the original sedimentary features (Díez Fernández, 2011). In the low deformed sections, the lower metasedimentary sequence consists of a thick pile of metagreywackes alternating with minor layers of metapelites, graphitic schists, calc-silicate lenses and quartzites (Fig. 2a). The metagreywackes preserve Bouma sequences, crossed bedding, erosive contacts and normal graded bedding. Their protoliths were clast-supported sedimentary rocks containing angular feldspar fragments (the most abundant clasts), quartz and detrital micas in a clay rich matrix with carbonaceous material. No conglomeratic levels have been found. Metapelitic horizons are common, and carbonaceous matter within them can be so abundant as to form graphitic horizons. Quartzite layers occur in the upper part of the sequence (Fig. 2a). The original thickness of the lower sequence cannot be calculated due to the intense ductile deformation accompanying the Variscan subduction and subsequent exhumation, but a minimum present thickness of 4 km can be estimated, although this value probably represents less than half of the original thickness. The maximum depositional age, as revealed by the detrital zircon input, is latest Neoproterozoic (c. 560 Ma; Díez Fernández et al., 2010).

The upper sequence appears strongly deformed. No significant deformation partitioning associated with the subduction–exhumation process can be seen in this series during the subduction–exhumation process. This sequence consists of mica schists alternating with minor lenses of amphibolites, graphite schists, metacherts, calc-silicate lenses, metagreywackes and quartzites (Fig. 2b). The maximum depositional age of this sequence is Late Cambrian (c. 500 Ma; Díez Fernández et al., 2010).

4. Whole rock geochemistry

The chemical composition of sedimentary rocks depends on numerous factors, including the nature of the source areas and the subsequent processes affecting them, such as weathering, diagenesis or metamorphism. Likewise, the abundance of some elements, such as rare earth elements (REE), Hf, Ti, Cr, Co, Zr, Nb, Ta, Y, Th and Sc, is preserved in sedimentary rocks in spite of the weathering processes. These elements have very low residence times in oceanic waters, being transferred almost quantitatively to sedimentary rocks. Thus, they provide excellent discriminating factors for determining the provenance and tectonic setting of sedimentary rocks (Bathia, 1983; Bathia and Crook, 1986; Hegde and Chavadi, 2009; Roser and Korsch, 1986, 1988; Taylor and McLennan, 1985). The effects of homogenization in sedimentary processes result in a relatively uniform distribution of REE in detrital rocks, whose pattern reflects the REE abundance in the upper crust. Moreover, the Th/Sc, La/Sc, Ti/Zr, Zr/Sc and La/Th ratios has been frequently used to investigate provenance according to the different compatibility of these elements during magmatic crystallization (McLennan et al., 1993), and also in relation to the PAAS abundances (Post Archean Australian Shale; Taylor and McLennan, 1985).

Twenty three samples from the sedimentary series that constitutes the basal units of the allochthonous complexes of NW Iberia were collected in order to study their geochemistry, provenance and tectonic setting. Samples were collected mainly along the northern sector of the Malpica–Tui Complex although a few samples were taken in the NW part of the Órdenes Complex (see location of the samples in Figs. 1b and 2). Eighteen samples belong to the lower sequence and they include weakly sheared metagreywackes and some albite schists developed after intense deformation and metamorphism of the greywackic types. Five samples represent the upper sequence including the Cean schists (Malpica–Tui Complex) and the Santiago schists (NW Órdenes Complex).

Sample preparation was carried out at Universidad Complutense de Madrid, and whole rock major and trace elements analyses were performed at Activation Laboratories Ltd (Actlabs) in Canada. Fusion with lithium metaborate/tetraborate was used for sample digestion, and the analytical techniques for major and trace element determination were ICP-OES and ICP-MS, respectively. The chemical analyses results are shown in Tables 1 and 2.

4.1. Composition and classification

4.1.1. Lower sequence

The greywackes and albitic schists show a homogeneous major element composition (Table 1). The SiO_2 content shows the largest variation (60.3–74.9 wt.%), with average value of 70.65 wt.%. Only 4 samples have SiO_2 contents lower than 70 wt.% (B-3, B-5, B-9, B-23), mainly compensated by larger values of Al_2O_3 and MgO. The Na_2O content is relatively high and homogeneous (2.5–4.1 wt.%; average 2.9 wt.%), and also can be considered homogeneous the content in K_2O (2.0–3.4 wt.%; average 2.6 wt.%) and MgO (1.1–3.4 wt.%; average 1.7 wt.%). The compositional range of the other major elements is: CaO (0.5–2.9 wt.%; average 1.0 wt.%), Al_2O_3 (11.0–17.8 wt.%; average 13.3 wt.%), Fe_2O_3 (3.3–6.8 wt.%; average 4.32 wt.%), MnO (0.03–0.14 wt.%), TiO_2 (0.50–0.83 wt.%) and P_2O_5 (0.13–0.20 wt.%). SiO_2 shows marked negative correlation with Al_2O_3, Fe_2O_3, MnO and MgO, and moderate negative correlation with CaO, Na_2O, K_2O, TiO_2 and P_2O_5. The relatively low SiO_2/Al_2O_3 ratio of these rocks indicates an immature character, as confirmed by the Al_2O_3/Na_2O (3.6–5.8) and Al_2O_3/TiO_2 (16.8–23.9) ratios, which lay within the typical range of the upper continental crust (3.9 and 30.4, respectively; Taylor and McLennam, 1985).

The Fe_2O_3/K_2O ratio can be applied to distinguish between mature and immature compositions of unconsolidated fine- to coarse-grained sediments (particularly in arkoses). According to the chemical classification diagram published by Herron (1988), most of the protoliths of the metasedimentary rocks of the lower sequence can be classified as greywackes, but some few samples (Xareira metagreywackes; Díez Fernández, 2011) plot in the boundary with the litharenite field (Fig. 3a). According to the K_2O/Na_2O ratio, most of the analysed rocks have quartz-intermediate compositions (Crook, 1974).

Table 2 shows the results of the REE analyses. The samples have similar REE contents, with ΣREE values ranging between 112 ppm (sample B-22, with marked depletion in LREE) and 213 ppm (the highest values in some samples with the highest contents in La and Ce). The samples also show similar chondrite-normalized (Nakamura, 1974) fractionation patterns (Fig. 3b), with a $(La/Yb)_N$ ratio ranging between 7.1 and 14.4. The LREE (La–Sm) show a moderate enrichment in relation to the HREE, which display almost flat patterns with $(Gd/Yb)_N$ ratios ranging between 1.0 and 1.7. All the samples show slight but significant negative Eu anomaly, variable between 0.57 and 0.77 (calculated according to Taylor and McLennan, 1985). Eu anomalies in sedimentary rocks are usually interpreted as inheritance from the igneous rock source. Despite some differences in abundance between samples, the REE patterns of the greywackes are similar to those of PAAS, which are considered representative of upper continental crust.

The analysed samples show an average Th/Sc value of 1.2, larger than the PAAS value (Th/Sc = 0.9) and probably suggesting a source area with predominance of felsic rocks. This interpretation is also based in the high La contents in relation to Sc, with average La/Sc = 4.27 above the PAAS ratio (La/Sc = 2.4). The same interpretation can be obtained from the Ti/Zr and Zr/Sc ratios, respectively lower and higher than PAAS, and also from the low contents in Cr (average 73 ppm) and Ni (average 26 ppm). Moreover, the La/Th ratio ranging from 2.4 to 4.7 with an average value of 3.5, higher than PAAS (2.6), also suggests the abundance of felsic rocks in the source areas. The relatively high Hf contents (average 6.2; PAAS = 5) can be also considered an indication of source areas located in the surrounding area of a passive margin (Hegde and Chavadi, 2009).

Table 1
Whole rock major and trace element data of metasedimentary rocks.

Lower sedimentary sequence.											
Sample	B-1	B-2	B-3	B-4	B-5	B-6	B-7	B-8	B-9	B-10	B-11
SiO_2	73.83	73.94	60.34	71.77	64.50	70.81	70.51	70.14	61.40	73.12	74.40
Al_2O_3	12.62	12.36	16.77	12.97	15.85	13.22	13.52	13.52	17.85	12.06	11.24
Fe_2O_3	3.36	3.38	6.82	4.46	5.60	4.00	4.29	4.85	5.92	3.46	3.96
MnO	0.049	0.047	0.077	0.058	0.068	0.048	0.049	0.055	0.149	0.033	0.042
MgO	1.21	1.13	3.38	1.72	2.45	1.55	1.74	1.80	2.47	1.24	1.23
CaO	1.83	1.50	2.85	1.55	1.33	0.88	0.63	0.76	1.63	0.61	0.52
Na_2O	3.09	2.91	4.13	3.35	2.79	3.64	2.73	3.07	2.56	2.86	2.79
K_2O	2.01	2.10	2.48	2.15	3.42	2.02	2.66	2.66	2.88	2.94	2.52
TiO_2	0.557	0.563	0.834	0.542	0.725	0.576	0.583	0.768	0.777	0.509	0.659
P_2O_5	0.15	0.17	0.16	0.13	0.16	0.14	0.15	0.20	0.18	0.13	0.15
LOI[a]	0.9	0.8	1.4	0.8	1.5	1.8	2.5	1.9	2.4	1.4	1.8
Total	99.62	98.93	99.19	99.51	98.36	98.71	99.30	99.75	98.23	98.35	99.25
Sc	8	8	19	9	14	9	10	11	15	7	8
V	58	58	133	62	92	65	65	81	105	56	71
Cr	80	60	100	80	90	60	60	80	90	70	140
Co	15	12	26	15	15	7	9	9	11	10	11
Ni	30	20	50	30	40	20	20	20	30	30	30
Cu	20	<10	20	30	20	<10	<10	<10	40	20	20
Zn	50	50	90	80	80	50	50	60	90	50	70
Ga	15	14	23	15	20	16	16	17	22	14	14
Rb	73	79	99	89	131	83	89	100	87	94	88
Sr	153	121	207	164	133	164	125	135	198	144	117
Y	22.9	23.1	28.9	22.9	22.7	20.2	17.9	25.8	32.1	17.8	21.4
Zr	268	315	167	166	200	250	182	430	234	214	381
Nb	11.2	9.7	12.9	10.8	13.7	10.1	9.0	12.6	14.0	9.4	12.4
Cs	5.4	5.8	12.1	8.1	7.1	5.2	5.0	6.4	9.6	4.9	4.7
Ba	584	453	963	466	716	629	881	903	999	1004	838
Hf	6.5	7.2	4.3	4.1	5.0	5.9	4.2	10.0	5.6	5.1	9
Ta	0.94	0.91	1.11	0.90	1.19	0.92	0.92	1.15	1.33	0.84	1.05
Pb	28	18	32	18	12	9	7	11	15	23	22
Th	9.88	11.20	11.10	7.92	10.50	10.70	9.36	14.30	12.90	9.26	14.3
U	2.92	2.93	3.26	2.42	3.13	2.59	2.36	3.55	3.97	2.63	3.43
Rb/Sr	0.48	0.65	0.48	0.54	0.98	0.51	0.71	0.74	0.44	0.65	0.75
Ti/Zr	12.46	10.71	29.94	19.57	21.73	13.81	19.20	10.71	19.91	14.26	10.7
La/Sc	4.91	5.46	2.23	4.11	2.81	4.28	2.64	4.54	3.85	4.94	6.43
La/Y	1.72	1.89	1.46	1.62	1.73	1.91	1.47	1.93	1.80	1.94	2.4
La/Th	3.98	3.90	3.81	4.67	3.74	3.60	2.82	3.49	4.48	3.74	3.59
Sc/Cr	0.10	0.13	0.19	0.11	0.16	0.15	0.17	0.14	0.17	0.10	0.06
Th/Sc	1.24	1.40	0.58	0.88	0.75	1.19	0.94	1.30	0.86	1.32	1.79

Oxides are in weight percent (wt.%).
Trace elements are in parts per million (ppm).
The element concentrations expressed with the < sign are below detection limit.
[a] Loss on ignition.

Table 2
Whole rock rare earth element data of metasedimentary rocks.

Lower sedimentary sequence											
	B-1	B-2	B-3	B-4	B-5	B-6	B-7	B-8	B-9	B-10	B-11
La	39.3	43.7	42.3	37	39.3	38.5	26.4	49.9	57.8	34.6	51.4
Ce	71.5	80.5	79.4	65.9	73.7	59.3	48.3	87.6	70.6	61.7	94.5
Pr	8.05	9.03	9.23	7.47	8.41	8.14	5.97	10.7	11.4	7.2	10.4
Nd	27.9	32.3	32.5	26.6	29.6	29.4	21.7	38.1	41.5	24.7	34.5
Sm	5.28	6.11	6.66	5.13	5.88	5.48	4.39	7.04	7.95	4.61	6.07
Eu	1.10	1.10	1.29	1.15	1.16	1.08	0.92	1.27	1.64	0.95	0.98
Gd	4.46	4.74	5.88	4.34	4.95	4.27	3.38	5.33	6.58	3.62	4.64
Tb	0.73	0.76	0.97	0.71	0.78	0.67	0.56	0.86	1.03	0.59	0.71
Dy	4.01	4.3	5.35	3.85	4.19	3.81	3.33	4.89	5.83	3.27	3.97
Ho	0.79	0.83	1.01	0.77	0.82	0.74	0.66	0.95	1.12	0.62	0.78
Er	2.3	2.41	2.97	2.24	2.43	2.18	1.95	2.8	3.32	1.85	2.27
Tm	0.373	0.372	0.466	0.345	0.380	0.328	0.309	0.442	0.512	0.309	0.364
Yb	2.4	2.5	2.9	2.2	2.5	2.2	2.0	2.9	3.3	2.0	2.38
Lu	0.344	0.347	0.416	0.308	0.358	0.322	0.282	0.423	0.469	0.287	0.364
Σ REE	168.50	188.97	191.31	158.01	174.42	156.44	120.16	213.18	213.05	146.31	213.33
Eu/Eu^*	0.70	0.63	0.63	0.75	0.66	0.69	0.73	0.64	0.70	0.72	0.57
(La/Sm)N	4.59	4.41	3.92	4.45	4.12	4.33	3.71	4.37	4.49	4.63	5.22
$(Gd/Yb)_N$	1.51	1.53	1.63	1.57	1.6	1.53	1.34	1.48	1.59	1.44	1.55
$(La/Yb)_N$	11.14	11.83	9.86	11.25	10.68	11.6	8.78	11.63	11.71	11.57	14.44

Rare earth elements data in parts per million (ppm).

							Upper sedimentary sequence				
B-12	B-13	B-14	B-15	B-16	B-22	B-23	B-17	B-18	B-19	B-20	B-21
73.36	73.23	74.89	72.50	73.84	73.27	65.94	59.77	59.59	57.63	58.87	72.9
11.73	12.05	11.08	12.55	11.82	12.83	16.05	19.82	19.59	19.59	18.86	14.58
3.77	3.67	3.74	3.73	3.57	3.72	5.62	7.73	7.51	8.33	8.58	1.53
0.038	0.033	0.039	0.036	0.032	0.05	0.042	0.511	0.222	0.272	0.414	0.025
1.32	1.32	1.23	1.38	1.30	1.47	2.31	2.23	1.97	2.50	1.91	0.28
0.64	0.49	0.71	0.58	0.62	1	0.78	0.32	0.36	0.45	1.01	0.33
2.74	2.65	3.00	2.78	3.02	3.3	2.51	0.70	0.66	1.05	1.06	2.61
2.78	2.85	2.19	3.09	2.45	2.32	3.2	3.77	4.04	3.52	4.48	4.77
0.581	0.539	0.660	0.549	0.533	0.566	0.683	0.817	0.891	0.926	0.719	0.205
0.14	0.14	0.14	0.14	0.15	0.15	0.13	0.13	0.14	0.18	0.09	0.27
1.3	1.4	1.6	1.5	1.2	1.12	2.48	3.5	3.7	4.1	3.1	1.89
98.37	98.33	99.26	98.80	98.52	99.8	99.74	99.27	98.62	98.55	99.05	99.39
8	8	8	8	8	8	13	19	20	20	20	3
61	60	71	61	60	64	96	164	132	124	131	8
60	60	60	50	60	50	70	100	90	140	100	<20
8	9	8	11	14	13	12	16	15	25	25	3
<20	<20	<20	20	<20	20	30	50	40	70	50	<20
10	10	10	20	10	10	20	20	20	400	140	60
30	40	50	50	60	50	70	110	100	130	100	100
13	14	12	15	13	15	20	26	26	25	24	24
94	100	85	105	94	84	114	144	162	153	144	408
136	115	133	123	146	163	158	118	96	122	121	28
20.4	18.7	20.8	20.9	22.2	19.6	27.1	27.4	28.6	30.9	24.5	8.7
278	238	390	272	267	248	189	119	172	121	110	68
9.5	8.4	10.7	8.9	9.9	9.1	11.5	16.1	13.8	16.2	12.4	16.1
4.7	5.2	4.5	5.1	5.7	5.2	8.9	4.9	6	8.8	5.3	30
966	1039	765	1132	828	651	773	609	657	541	677	62
6.6	5.4	8.9	6.5	6.3	5.8	4.6	3.1	4.2	3.2	2.9	2.1
0.96	0.87	1.04	0.92	0.91	0.96	1.09	1.26	1.32	1.24	1.05	2.64
18	14	20	17	18	13	15	33	27	32	19	33
12.2	9.47	13.3	12	15.2	10	10.9	14.5	16.7	14.2	12.5	14.7
2.88	2.55	3.14	2.8	2.78	2.23	2.83	2.76	1.98	2.47	3.78	10.5
0.69	0.87	0.64	0.85	0.64	0.52	0.72	1.22	1.69	1.25	1.19	14.57
12.53	13.58	10.15	12.1	11.97	13.68	21.66	41.16	31.06	45.88	39.19	18.07
5.06	4.48	5.13	5.08	5.00	2.95	2.93	2.84	2.58	2.56	0.81	7.1
1.99	1.91	1.97	1.94	1.8	1.20	1.41	1.97	1.8	1.66	0.66	2.45
3.32	3.78	3.08	3.38	2.63	2.36	3.50	3.72	3.09	3.61	1.29	1.45
0.13	0.13	0.13	0.16	0.13	0.16	0.19	0.19	0.22	0.14	0.20	
1.53	1.18	1.66	1.5	1.9	1.25	0.84	0.76	0.84	0.71	0.63	4.9

							Upper sedimentary sequence				
B-12	B-13	B-14	B-15	B-16	B-22	B-23	B-17	B-18	B-19	B-20	B-21
40.5	35.8	41.0	40.6	40.0	23.6	38.1	53.9	51.6	51.2	16.1	21.3
76.1	66.0	79.0	74.3	74.8	47.2	72.7	108.0	99.9	93.8	39.9	46.8
8.6	7.5	8.9	8.4	8.3	5.34	8.61	10.6	11.1	10.5	3.6	5.84
31.1	26.4	31.1	29.8	29.4	18.9	31.4	35.5	39.1	37.4	12.3	20.2
5.83	4.80	6.05	5.47	5.58	3.65	6.47	6.44	7.54	7.36	2.37	4.6
1.08	0.97	1.15	1.14	1.25	0.744	1.31	1.35	1.39	1.53	0.55	0.247
4.54	3.67	4.62	4.24	4.48	2.9	5.12	5.32	5.71	6.13	2.44	3.09
0.68	0.59	0.69	0.68	0.70	0.53	0.83	0.92	0.93	0.99	0.57	0.47
3.82	3.39	3.92	3.85	3.98	3.26	4.88	5.35	5.44	5.61	4.04	2.08
0.74	0.67	0.75	0.76	0.79	0.67	0.92	1.04	1.03	1.09	0.88	0.3
2.15	1.98	2.15	2.26	2.29	2.09	2.61	3.02	2.93	3.15	2.66	0.71
0.331	0.308	0.329	0.348	0.355	0.326	0.384	0.466	0.446	0.489	0.399	0.099
2.26	2.07	2.18	2.33	2.36	2.23	2.54	2.92	2.77	3.06	2.55	0.56
0.342	0.313	0.327	0.348	0.353	0.316	0.357	0.396	0.38	0.429	0.363	0.072
178.09	154.47	182.20	174.51	174.60	111.76	176.23	235.22	230.27	222.74	88.69	106.37
0.65	0.71	0.67	0.73	0.77	0.70	0.70	0.71	0.65	0.7	0.7	0.20
4.29	4.6	4.18	4.58	4.42	3.99	3.63	5.16	4.22	4.29	4.19	2.86
1.60	1.41	1.69	1.45	1.51	1.04	1.61	1.45	1.64	1.60	0.76	4.4
11.98	11.56	12.58	11.65	11.33	7.08	10.03	12.34	12.46	11.19	4.22	25.43

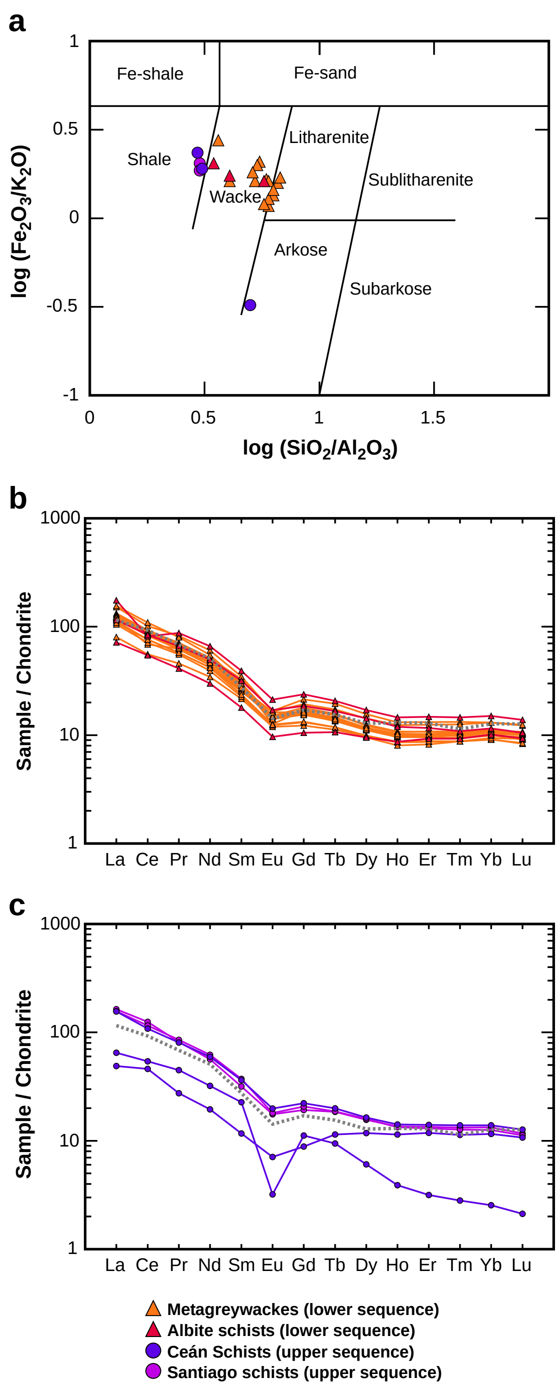

Fig. 3. Chemical diagrams for the metasedimentary rocks from the basal units of NW Iberian Massif. (a) Classification diagram (Herron, 1988). (b, c) Chondrite-normalized rare earth elements plots for the metasedimentary rocks of the lower and upper sequences, respectively; the dotted line corresponds to the PAAS (Post Archean Australian Shale; Taylor and McLennan, 1985). Normalizing values are from Nakamura (1974).

4.1.2. Upper sequence

The metapelitic schists of this sequence show less silicic (SiO_2 = 57.63–59.77) and more aluminic (Al_2O_3 = 14.58–19.82 wt.%) compositions than the detrital rocks from the lower sequence. They also have higher contents in K_2O, Fe_2O_3, MgO, MnO and TiO_2, and lower values in Na_2O and CaO (Table 1). The SiO_2/Al_2O_3 (2.9–3.1) and Al_2O_3/TiO_2 (21.1–26.2) ratios fit those of the upper continental crust (McLennan, 2001). The schists are classified as shales in the diagram of Herron (1988). Sample B-21 is an arkose, but this is a local and very restricted composition in the upper sequence (Fig. 3a), and it is shown in Fig. 2b.

The total REE content (ΣREE) ranges between 88 and 235 ppm, with moderately to highly (sample B-21) fractionated chondrite-normalized patterns (Fig. 3c). The schist samples B-17, B-18 and B-19 show REE patterns almost identical to those of the greywackes of the lower sequence, in turn similar to the average composition of the upper continental crust represented by the PAAS (Taylor and McLennan, 1985). All the samples show a slight to pronounced Eu anomaly (Eu/Eu^* = 0.71–0.20). The samples with shale composition have an average Th/Sc value of 0.7, slightly lower than PAAS and probably suggesting the presence of an important volume of mafic rocks in the source area. This conclusion is also based on the Ti/Zr (39.3; PAAS = 28.2) and Zr/Sc (6.6; PAAS = 13.1) ratios, as well as on the high V contents (124–164 ppm).

4.2. Tectonic setting

The tectonic discrimination diagrams developed by Bathia and Crook (1986) allow to distinguish clearly among the four tectonic settings considered to be the most common environments for greywacke deposition: (A) oceanic island arc, (B) continental island arc, (C) active continental margin, and (D) passive margin. Only siliciclastic rocks from the lower sequence showing greywacke compositions were plotted in these diagrams (Fig. 4). The schists from the upper sequence do not meet the requirements (pelitic composition) to be plotted in them, and were consequently ruled out for tectonic discrimination studies.

The diagrams presented in Fig. 4 allow to discard the type-A setting for the sedimentation of these greywackes, as their origin seems clearly related to a tectonic setting with the presence of an older continental crust. In the Th-Co-Zr diagram the metagreywackes generally plot in the B field, which points to a basin located either in an island arc built on a mature continental crust, or in a magmatic arc built on a thinned continental margin. On the other hand, the Th-Sc-Zr and La-Th-Sc diagrams suggest some passive margin affinity. This affinity is especially clear in Fig. 4b, but can be also deduced from the diagram 4c where it is not possible to differentiate type-C or type-D greywackes, although the incompatibility with type-C is clear after projections in Fig. 4a and b. In summary and according to the diagrams of Bathia and Crook (1986), the metagreywackes from the lower sequence were generated in relation to a magmatic arc built on a thinned continental margin, but probably closer to the main continental domain and to certain distance from the areas with the most important magmatic activity. This setting would probably explain the observed relative affinity to passive margins. A back-arc setting or a retro-arc setting would explain the compositions observed in the metagreywackes, as well as the whole sedimentary characteristics of the lower sequence. This tectonic setting was previously suggested by Díez Fernández et al. (2010) and it will be examined in more detail in a next section.

Fig. 5 shows PAAS-normalized plots of the most significant elements for tectonic setting discrimination. The diagrams are plotted according to the criteria of Thompson (1982). The patterns defined by the metagreywackes (Fig. 5a) are quite similar to those typical of continental island arc or active margins (Winchester and Max, 1989). The plots are characterized by depletion in most of the large ion lithophile elements (LILE: Cs, Rb, Th, Ce and K_2O), which deviate slightly from 1, with the exception of La, U and P_2O_5. The high field strength elements (HFSE: Zr, Hf, HREE, Sm, TiO_2 and Sc) are generally close to 1, with a slight characteristic negative TiO_2 anomaly, typical of this type of greywackes (Winchester and Max, 1989). In general a flat pattern is observed, with an average close or below 1. It can be also stressed the general absence of a pronounced Sr anomaly, typical of the most characteristic passive margins. The schists of the upper sequence show more variable patterns, specially when the anomalous

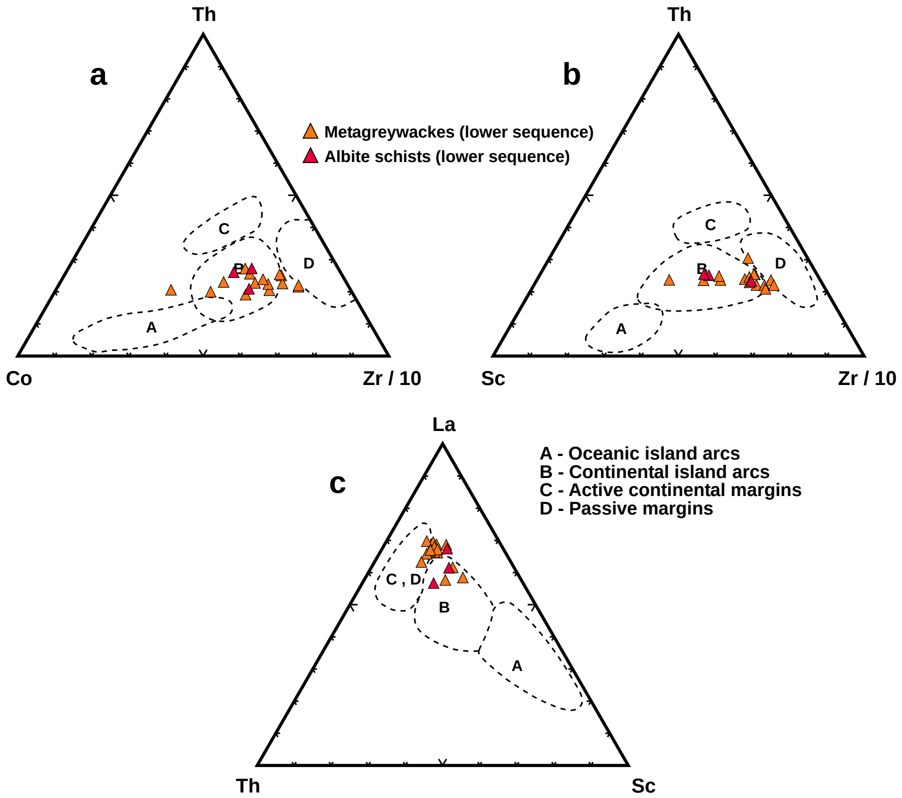

Fig. 4. Trace element tectonic setting diagrams for the greywackes from the lower metasedimentary rock sequence. The analysed schists from the upper sedimentary sequence are not included in these diagrams, as they show a scattered projection due to compositions different from typical greywackes. Diagrams are after Bathia and Crook (1986).

sample B-21 (arkose) is considered. However, samples B-17, B-18 and B-19 show patterns close to 1 with some differences in relation to the metagreywackes from the lower sequence. They do not show depletion in some LILE elements (Rb, Th, Ce, K_2O) although negative anomalies exist for U, Sr, Hf and TiO_2, which could suggest passive margin affinity (Fig. 5b).

4.3. Sm–Nd isotope systematics

The Sm–Nd isotopic analyses were performed at the Centro de Geocronología y Geoquímica Isotópica from the Universidad Complutense de Madrid. They were carried out in whole-rock powders using a ^{150}Nd-^{149}Sm tracer by isotope dilution-thermal ionization mass spectrometry (ID-TIMS). The samples were first dissolved through oven digestion in sealed Teflon bombs with ultra pure reagents to perform two-stage conventional cation-exchange chromatography for separation of Sm and Nd (Strelow, 1960; Winchester, 1963), and subsequently analysed using a Sector 54 VG-Micromass multicollector spectrometer. The measured ^{143}Nd/^{144}Nd isotopic ratios were corrected for possible isobaric interferences from ^{142}Ce and ^{144}Sm (only for samples with ^{147}Sm/^{144}Sm $<$ 0.0001) and normalized to ^{146}Nd/^{144}Nd = 0.7219 to correct for mass fractionation (Table 3). The LaJolla Nd international isotopic standard was analysed during sample measurement, and gave an average value of ^{143}Nd/^{144}Nd = 0.5114840 for 9 replicas, with an internal precision of $\pm$0.000032 (2σ). These values were used to correct the measured ratios for possible sample drift. The estimated error for the ^{147}Sm/^{144}Nd ratio is 0.1%.

In crustal evolution models based on Nd isotopic composition, the main fractionation event during the formation and evolution of continental crust takes place during partial melting of lithospheric mantle to generate crustal rocks (McLennan and Hemming, 1992). The εNd model age of a sedimentary rock represents the average age of the extraction of its components from the mantle. In the case of detrital rocks, model ages usually reflect complex mixing based on the different age and provenance of their components. The combined interpretation of Nd model ages and detrital zircon ages has proven to be a powerful tool for investigating the evolution of continental crust, especially in orogenic belts (e.g., Linnemann et al., 2004). The investigated metasedimentary rocks show relatively uniform εNd(0) values, ranging between −19.0 and −12.3 (average −16.4; Table 3). εNd(T) ranges −13.1 to −8.1 in the lower sequence (maximum depositional age of 560 Ma; Díez Fernández et al., 2010) and −10.1 to −8.5 in the upper sequence (maximum depositional age of 500 Ma; Díez Fernández et al., 2010). The analysed metasedimentary rocks show ^{147}Sm/^{144}Sm ratios ranging between 0.1055 and 0.1464, with average at 0.1174. This is a ratio below the upper limit of ^{147}Sm/^{144}Sm = 0.165 suggested by Stern (2002) appropriate to perform NdT_{DM} calculations. The T_{DM} model ages (DePaolo, 1981) are Paleoproterozoic and range between 2223 and 1782 Ma, with an average value of 1919 Ma (Fig. 6). A collection of Nd model ages from different regions (Linnemann and Romer, 2002) is also included in Fig. 6. These ages have been divided into two groups according to the age of the dominant source (Grenvillian and post-Grenvillian/pre-Cadomian crust, or pre-Grenvillian, >0.9–1.1 Ga. cratonic crust). In this collection of Nd model ages, similar Paleoproterozoic ages are only reported in elements of the West African Craton, the Amazonian Craton and the Icartian gneisses of Brittany. The rest of terranes included in this collection show younger Nd model ages. Moreover, Fig. 6 also includes for comparison Nd data of the uppermost greywackes of the Órdenes Complex (upper units; Fuenlabrada et al., 2010). These Cambrian greywackes (maximum age of sedimentation at 530–500 Ma) have much younger model ages ranging between 1215 and 720 Ma.

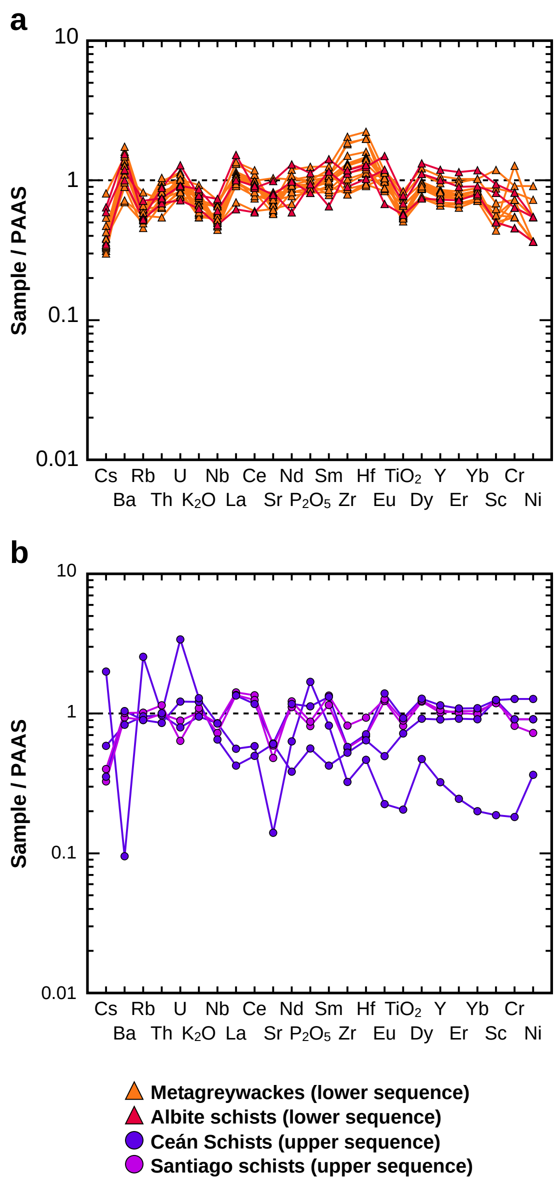

Fig. 5. (a, b) PAAS-normalized trace elements plots for the metasedimentary rocks from the lower and upper sequences, respectively. PAAS after Taylor and McLennan (1985).

5. Discussion

Different paleogeographic models have shown that large magmatic arcs developed in the peri–Gondwanan realm. Their activity took place between Neoproterozoic (Cadomian–Pan-African cycle) and Early Ordovician times (Murphy and Nance, 2002; Stampfli and Borel, 2002), and they left an imprint in the sedimentological and magmatic record of many of the terranes forming part of the Variscan Belt (Linnemann et al., 2004, 2007; Rodríguez Alonso et al., 2004; Ugidos et al., 2003). The geochemical features of the metagreywackes of the lower sequence suggest that they were generated in relation to an arc system built on a thinned continental margin, although they also record certain chemical transition to passive margin greywackes. A back-arc setting or a retro-arc setting as those presented in the models of Fig. 7 (a, b), would explain most of the geochemical features observed in these lithologies. The lower sequence of the basal units was probably deposited in an Ediacaran–Early Cambrian back-arc/retro-arc setting, closer to the external platform of the Gondwana Mainland, in a region where the most important sedimentary supplies would come from source areas located in the interior of the continental domain. The influence of the Cadomian magmatic arc on the composition of the greywackes is clear, as indicated by their detrital zircon age populations (Díez Fernández et al., 2010). However, the sedimentary basin was apparently located far away from the region with the most important igneous activity, because the oldest igneous rocks intruding the greywackic sequence are Middle Cambrian.

The origin of the Cambrian sedimentary rocks of the upper sequence is more uncertain, as they are mainly constituted by metapelitic schists whose compositions are not ideal for tectonic setting discrimination. The available geochemical data are not abundant, but they seem to suggest some affinity with passive margin sediments; i.e., these sediments were probably deposited close to the continental domain and to certain distance from the most active zones in the magmatic arc. The absence of intrusive granitic rocks, which are widespread in the lower sequence, supports this interpretation (Fig. 2b). It is likely that during Late Cambrian times the previously deposited series of the lower sequence were located towards the most active part of the arc system, while the sediments of the upper sequence were deposited closer to the continental platform. In addition, it is important to consider that the contact between upper and lower metasedimentary sequences is a low-angle fault (extensional detachment), so these series could have been located at different positions along the margin. On the other hand, opening of the Rheic Ocean and transition of the Gondwana margin to a typical passive margin setting occurred between the Middle Cambrian and the Early Ordovician (Arenas et al., 2007; Murphy et al., 2010; Nance et al., 2010). This agrees with the observed sedimentary evolution and explains the presence of N-MORB mafic rocks in the sedimentary series (Rodríguez Aller, 2005), which are particularly more abundant in the upper sequence (Fig. 2b). Although there are not many geochemical data about the metasedimentary rocks of the upper sequence, the compositional patterns (PAAS-normalized plots) of some samples (Fig. 5b) could indicate an evolution from a back-arc setting to a passive margin. This transition might be related either with the

Table 3
Whole rock Nd isotope data of metasedimentary rocks.

Sample	Sm	Nd	$^{147}Sm/^{144}Nd$	$^{143}Nd/^{144}Nd$	2σ	εNd(0)	εNd(560)[a]	TDM (Ma)[b]
B-1	4.00	20.67	0.1169	0.511676	3	−18.8	−13.1	2078
B-2	4.14	21.83	0.1146	0.511670	3	−18.9	−13.0	2041
B-3	4.75	23.42	0.1227	0.511950	3	−13.4	−8.1	1782
B-4	4.10	21.31	0.1164	0.511852	3	−15.3	−9.6	1817
B-5	4.49	22.80	0.1191	0.511800	4	−16.3	−10.8	1940
B-6	3.73	19.69	0.1146	0.511731	3	−17.7	−11.8	1956
B-7	3.03	14.81	0.1239	0.511809	4	−16.2	−11.0	2020
B-8	5.58	30.14	0.1118	0.511712	3	−18.1	−12.0	1934
B-9	5.62	29.26	0.1162	0.511844	4	−15.5	−9.7	1824
B-10	3.33	17.93	0.1123	0.511727	6	−17.8	−11.7	1921
B-11	6.24	35.72	0.1055	0.511663	3	−19.0	−12.5	1893
B-12	4.41	22.83	0.1167	0.511728	3	−17.7	−12.0	1999
B-13	3.61	19.94	0.1095	0.511708	3	−18.1	−11.9	1898
B-14	4.05	21.25	0.1152	0.511729	3	−17.7	−11.9	1971
B-15	3.71	19.80	0.1133	0.511753	3	−17.3	−11.3	1902
B-16	4.04	21.90	0.1115	0.511700	3	−18.3	−12.2	1946
B-22	2.46	12.91	0.1150	0.511771	3	−16.9	−11.1	1906
B-23	4.55	22.19	0.1238	0.511885	3	−14.7	−9.5	1902
B-17	4.84	26.06	0.1123	0.511846	4	−15.4	−10.1	1756
B-18	5.19	26.38	0.1189	0.511877	3	−14.9	−9.9	1824
B-19	5.33	26.66	0.1208	0.511954	4	−13.3	−8.5	1743
B-20	1.87	9.26	0.1223	0.511892	3	−14.6	−9.8	1863
B-21	3.05	12.60	0.1464	0.512007	3	−12.3	−9.1	2223

[a] εNd(t) calculated for 560 Ma.
[b] Nd model ages calculated according to DePaolo (1981).

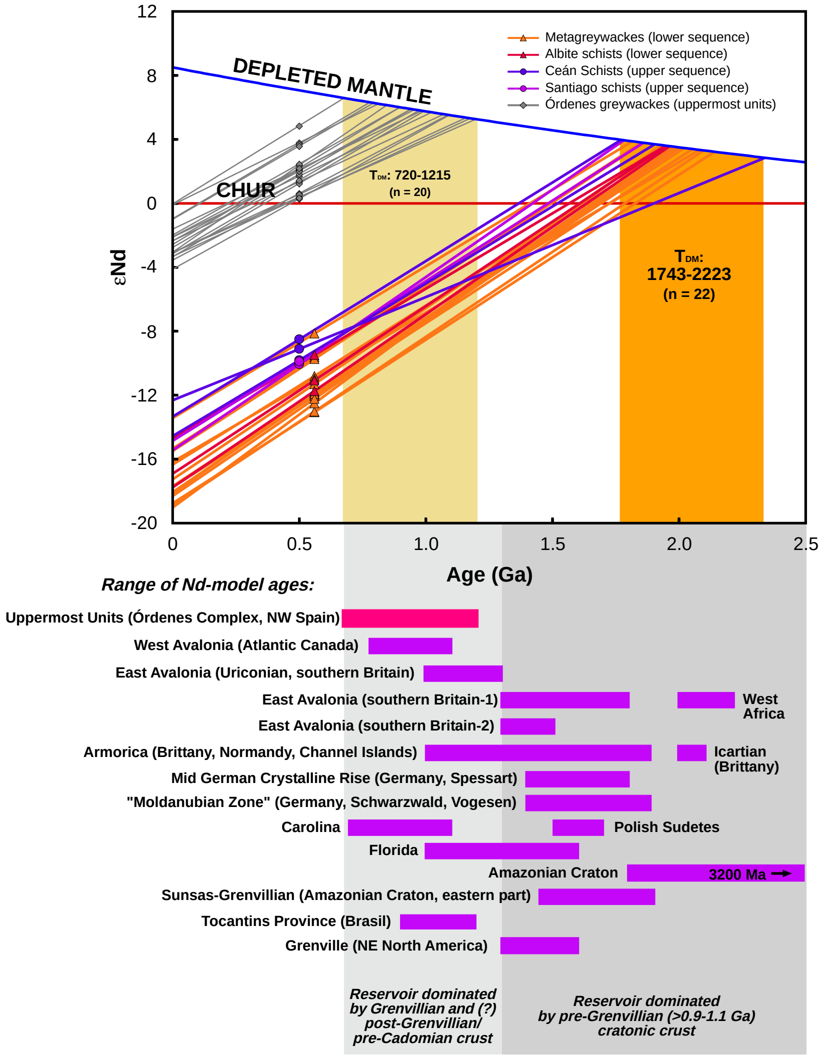

Fig. 6. T_{DM} model ages (DePaolo, 1981) of the metasedimentary rocks from the basal units of the allochthonous complexes of NW Iberian Massif. Triangles and circles show the εNd values at 560 Ma and 500 Ma, reference ages for the deposition of the lower and upper sequences, respectively (Díez Fernández et al., 2010). Nd data of the uppermost greywackes of the Órdenes Complex (upper units; Fuenlabrada et al., 2010) are included for comparison. Data source for comparative model ages from different regions taken from Linnemann and Romer (2002).

attenuation of the magmatic activity in the arc, or the progressive ocean ward translation of this activity, or the drifting of the whole arc system away from the continental margin.

The Nd model ages of the 23 analysed samples are Paleoproterozoic and range between 1782 Ma and 2223 Ma (average value 1919; Fig. 6). The Nd model ages are slightly younger in the upper sequence than in the lower sequence, but altogether they define a single population. Therefore the two metasedimentary rock sequences can be clearly related. Sedimentation probably took place in the same basin located in the continental platform of Gondwana, whose main source areas did not change during the Late Neoproterozoic and Cambrian times. The Nd model ages are very old and they seem to be only compatible with Paleoproterozoic–Archean source areas. The participation of younger sources was probably limited, although both the metagreywackes and the metapelitic rocks contain Mesoproterozoic and Neoproterozoic (actually the most abundant grains) detrital zircon populations (Díez Fernández et al., 2010). The chronology recorded by the main detrital zircon population and by the NdT_{DM} is not contradictory as each method supplies a different information (Liégeois and Stern, 2010). Source areas dominated by Paleoproterozoic–Archean materials intruded by Pan-African granitoids, and with variable participation of detrital sedimentary rock series through time, explain the Sm–Nd isotopic data and the age populations of detrital zircons (see Liégeois and Stern, 2010, and references therein). The significant difference between the ages reported by the two methods suggests that the involved Pan-African granitoids were the result of partial melting of Paleoproterozoic–Archean basement and its erosion products, and consequently they share a same Sm–Nd isotope signature. The important participation of Neoproterozoic zircons can be explained by the high abundance of zircons in the Cadomian–Pan-African granitoids (750–550 Ma), as it is known that granitoids are the most important source for detrital zircons. The North African margin of Gondwana shows suitable features to be considered the source area for these sedimentary rocks. It is difficult to ascertain the precise location of the sedimentary basin, because its position can only be determined presently using provenance studies based in U–Pb geochronology of detrital zircons. In the context of North Africa a key element is the presence/absence of a Stenian–Tonian population of detrital zircons (750–1150 Ma), which it is also present in the sedimentary series of the basal units. Avigad et al. (2012) suggested that Gondwanan series

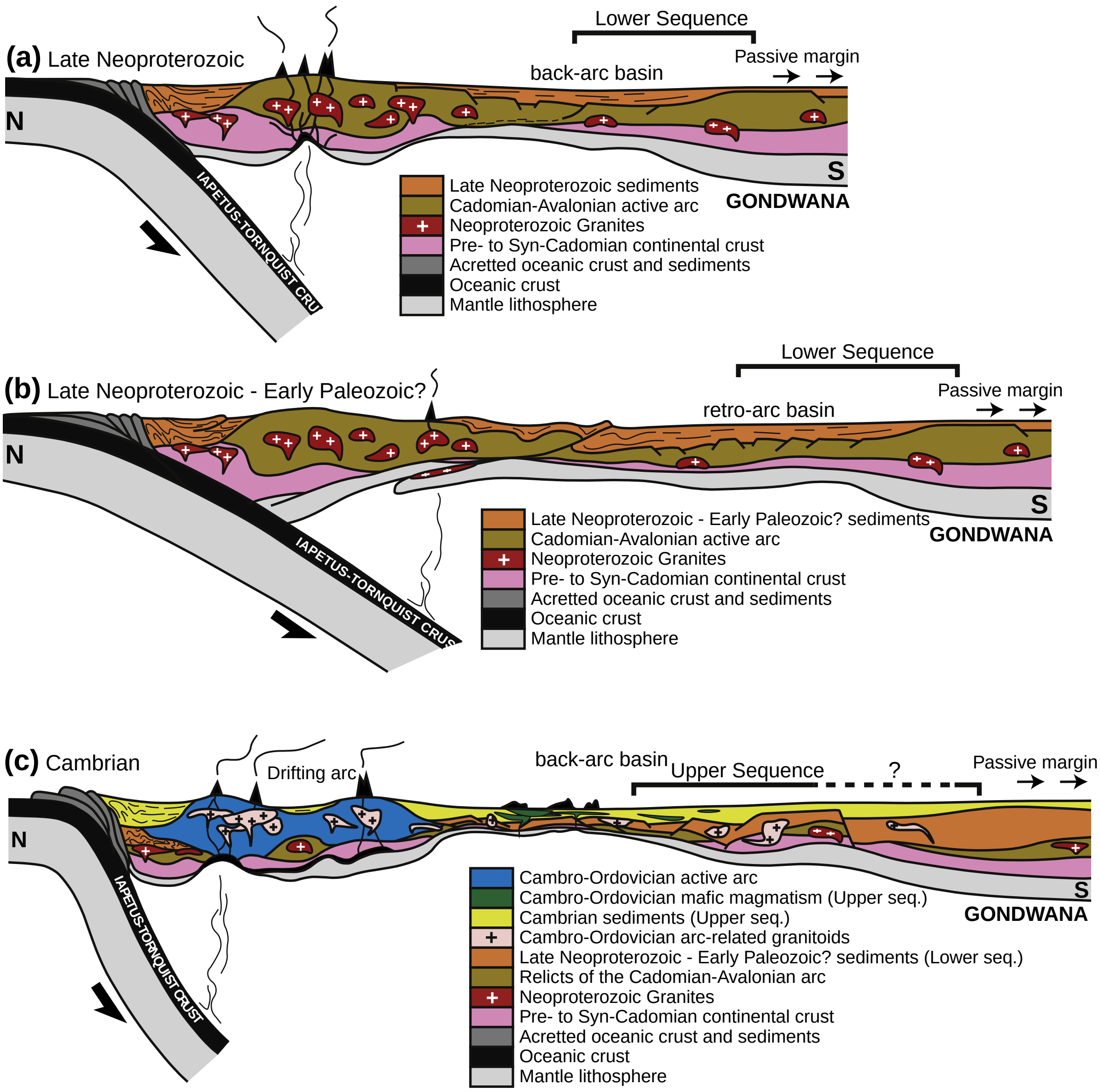

Fig. 7. Cartoon showing the tectonic setting for the lower (Late Neoproterozoic) and upper (Middle–Late Cambrian) sequences of the basal units of the allochthonous complexes of NW Iberia. In (a) and (b), the lower sequence is a greywacke series deposited near the main continent, where the most important supplies come from the interior of Gondwana. In (c), the Cambrian sediments fill a back-arc related to the drifting of an ensialic arc; they are being deposited close to the continental edge. Cambro-Ordovician calc-alkaline magmatism is intruding the Neoproterozoic sediments, while the roll-back of the oceanic slab is forcing the active arc to migrate oceanward, leaving behind synchronous deposits in the back-arc and a tail of Cambro-Ordovician plutons. The Nd model ages of the clastic sediments derived from this rifted arc (the greywackes from the uppermost Allochthon in Fig. 6) indicates contribution from juvenile sources. These models refine previous interpretations presented by Díez Fernández et al. (2010).

from Morocco include these zircons only since Middle Cambrian times, without any significant presence before this period (see also Ábalos et al., 2012; Abati et al., 2010a; Boher et al., 1992; Potrel et al., 1998). The presence of Stenian–Tonian detrital zircons is more common in the Saharan Craton, also in Lower Cambrian–Neoproterozoic sedimentary series (Avigad et al., 2003, 2012). Anyway the existence of large outcrops of primary Stenian–Tonian materials is unknown in North Africa, and thence the actual source of these zircons is enigmatic suggesting long transport from source areas located far away. Using this information, Díez Fernández et al. (2010) suggested that sediments from the basal units were deposited in basins probably located in an intermediate position between the West African Craton and the Saharan Craton. This interpretation is very sensitive to the actual age of the studied series, to which only a maximum depositional age approach based in detrital zircons is available, but it is coherent with a provenance not too far from the present location of the investigated allochthonous sedimentary rock series.

The Nd model ages of the sedimentary sequences of the basal units are considerably older than those of the Cambrian greywackes (530–500 Ma) of the upper units of the same region, which range between 720 Ma and 1215 Ma (Fuenlabrada et al., 2010; Fig. 6). Separated from the basal units by ophiolites, the upper units have been repeatedly interpreted as a well-preserved section of a peri-Gondwanan arc (Abati et al., 2003, 2007; Díaz García et al., 2010; Fuenlabrada et al., 2010), what suggests that these relatively young Nd model ages are influenced by abundant supplies of juvenile material generated in relation to the magmatic activity of the arc (see Fig. 7c).

Comparison of the Sm–Nd geochemistry of metasedimentary rocks from terranes located in the footwall and hanging wall to the Variscan suture, may help to reconstruct the paleogeography of the peri-Gondwanan domain during Ediacaran–Early Paleozoic times. This information can also be valuable in order to recognize and correlate the allochthonous terranes located to both sides of the suture zone in central and Western Europe, especially in regions where the position of the suture is not clear or the structural relationships are under discussion.

Acknowledgments

Financial support for this research has been provided by the Spanish project CGL2007-65338-CO2/BTE (Ministerio de Ciencia e Innovación). Insightful reviews of the manuscript performed by Ulf Linnemann and an anonymous referee are gratefully acknowledged, as well as the important editorial work of Marco Scambelluri that significantly improved the final version of the manuscript.

References

Ábalos, B., Gil Ibarguchi, J.I., Sánchez-Lorda, M.E., Paquette, J.L., 2012. African/Amazonian Proterozoic correlations of Iberia: A detrital zircon U–Pb study of early Cambrian conglomerates from the Sierra de la Demanda (northern Spain). Tectonics 31, TC3003.

Abati, J., Dunning, G.R., Arenas, R., Díaz García, F., González Cuadra, P., Martínez Catalán, J.R., Andonaegui, P., 1999. Early Ordovician orogenic event in Galicia (NW Spain): evidences from U–Pb ages in the uppermost unit of the Órdenes Complex. Earth and Planetary Science Letters 165, 213–228.

Abati, J., Arenas, R., Martínez Catalán, J.R., Díaz García, F., 2003. Anticlockwise P–T path of granulites from the Monte Castelo Gabbro (Órdenes Complex, NW Spain). Journal of Petrology 44, 305–327.

Abati, J., Castiñeiras, P., Arenas, R., Fernández-Suárez, J., Gómez Barreiro, J., Wooden, J., 2007. Using SHRIMP-RG U–Pb zircon dating to unravel tectonomagmatic events in arc environments. A new peri-Gondwanan terrane in Iberia? Terra Nova 19, 432–439.

Abati, J., Aghzer, A.M., Gerdes, A., Ennih, N., 2010a. Detrital zircon ages of Neoproterozoic sequences of the Moroccan Anti-Atlas belt. Precambrian Research 181, 115–128.

Abati, J., Gerdes, A., Fernández-Suárez, J., Arenas, R., Whitehouse, M.J., Díez Fernández, R., 2010b. Magmatism and early-Variscan continental subduction in the northern Gondwana margin recorded in zircons from the basal units of Galicia, NW Spain. Geological Society of America Bulletin 122, 219–235.

Arenas, R., Gil Ibarguchi, J.I., González Lodeiro, F., Klein, E., Martínez Catalán, J.R., Ortega Gironés, E., de Pablo Maciá, J.G., Peinado, M., 1986. Tectonostratigraphic units in the complexes with mafic and related rocks of the Iberian Massif. Hercynica 2, 87–110.

Arenas, R., Martínez Catalán, J.R., Sánchez Martínez, S., Fernández-Suárez, J., Andonaegui, P., Pearce, J.A., Corfu, F., 2007. The Vila de Cruces Ophiolite: A remnant of the Early Rheic Ocean in the Variscan suture of Galicia (Northwest Iberian Massif). Journal of Geology 115, 129–148.

Arenas, R., Sánchez Martínez, S., Castiñeiras, P., Jeffries, T.E., Díez Fernández, R., Andonaegui, P., 2009. The basal tectonic mélange of the Cabo Ortegal Complex (NW Iberian Massif): a key unit in the suture of Pangea. Journal of Iberian Geology 35, 85–125.

Avigad, D., Kolodner, K., McWilliams, M., Persing, H., Weissbrod, T., 2003. Origin of northern Gondwana Cambrian sandstone revealed by detrital zircon SHRIMP dating. Geology 31, 227–230.

Avigad, D., Gerdes, A., Morag, N., Bechstädt, T., 2012. Coupled U–Pb-Hf of detrital zircons of Cambrian sandstones from Morocco and Sardinia: Implications for provenance and Precambrian crustal evolution of North Africa. Gondwana Research 21, 690–703.

Bathia, M.R., 1983. Plate tectonics and geochemical composition of sandstones. Journal of Geology 91, 611–627.

Bathia, M.R., Crook, K.A.W., 1986. Trace elements characteristics of greywackes and tectonic setting discrimination of sedimentary basins. Contributions to Mineralogy and Petrology 92, 181–193.

Boher, M., Abouchami, W., Michard, A., Albarede, F., Arndt, N.T., 1992. Crustal growth in West Africa at 2.1 Ga. Journal of Geophysical Research 97, 345–369.

Crook, K.A.W., 1974. Lithogenesis and geotectonics: the significance of compositional variations in flysch arenites (greywackes). In: Doti, R.H., Shaver, R.H. (Eds.), Modern and ancient geosynclinal sedimentationSociety of Economic Palaeontologists and Mineralogists Special Publication 19, 304–310.

DePaolo, D.J., 1981. Neodymium isotopes in the Colorado Front Range and crust-mantle evolution in the Proterozoic. Nature 291, 193–196.

Díaz García, F., Arenas, R., Martínez Catalán, J.R., González del Tánago, J., Dunning, G.R., 1999. Tectonic evolution of the Careón Ophiolite (northwest Spain): a remnant of oceanic lithosphere in the Variscan Belt. Journal of Geology 107, 587–605.

Díaz García, F., Sánchez Martínez, S., Castiñeiras, P., Fuenlabrada, J.M., Arenas, R., 2010. A peri-Gondwanan arc in NW Iberia. II: Assessment of the intra-arc tectonothermal evolution through U–Pb SHRIMP dating of mafic dykes. Gondwana Research 17, 352–362.

Díez Fernández, R., 2011. Evolución estructural y cinemática de una corteza continental subducida: la unidad de Malpica-Tui (NO del Macizo Ibérico). Nova Terra 40 228 pp..

Díez Fernández, R., Martínez Catalán, J.R., Gerdes, A., Abati, J., Arenas, R., Fernández-Suárez, J., 2010. U–Pb ages of detrital zircons from the basal allochthonous units of NW Iberia: Provenance and paleoposition on the northern margin of Gondwana during the Neoproterozoic and Paleozoic. Gondwana Research 18, 385–399.

Díez Fernández, R., Martínez Catalán, J.R., Arenas, R., Abati, J., 2011. Tectonic evolution of a continental subduction-exhumation channel: Variscan structure of the basal allochthonous units in NW Spain. Tectonics 30, TC3009.

Díez Fernández, R., Castiñeiras, P., Gómez Barreiro, J., 2012. Age constraints on Lower Paleozoic convection system: magmatic events in the NW Iberian Gondwana margin. Gondwana Research 21, 1066–1079.

Drost, K., Linnemann, U., McNaughton, N., Fatka, O., Kraft, P., Gehmlich, M., Tonk, C., Marek, J., 2004. New data on the Neoproterozoic–Cambrian geotectonic setting of the Teplá-Barrandian volcano-sedimentary succesions: geochemistry, U–Pb zircon ages, and provenance (Bohemian Massif, Czech Republic). International Journal of Earth Sciences 93, 742–757.

Fernández-Suarez, J., Corfu, F., Arenas, R., Marcos, A., Martínez Catalán, J.R., Díaz García, F., Abati, J., Fernández, F.J., 2002. U–Pb evidence for a polymetamorphic evolution of the HP-HT units of the NW Iberia Massif. Contributions to Mineralogy and Petrology 143, 236–253.

Fernández-Suárez, J., Arenas, R., Abati, J., Martínez Catalán, J.R., Whitehouse, M.J., Jeffries, T.E., 2007. U-Pb chronometry of polymetamorphic high-pressure granulites: An example from the allochthonous terranes of the NW Iberian Variscan belt. In: Hatcher Jr., R.D., Carlson, M.P., McBride, J.H., Martínez Catalán, J.R. (Eds.), 4-D Framework of continental crustGeological Society of America Memoir 200, 469–488.

Fuenlabrada, J.M., Arenas, R., Sánchez Martínez, S., Díaz García, F., Castiñeiras, P., 2010. A peri-Gondwanan arc in NW Iberia. I: Isotopic and geochemical constraints on the origin of the arc–A sedimentary approach. Gondwana Research 17, 338–351.

Gil Ibarguchi, J.I., Ortega Gironés, E., 1985. Petrology, structure and geotectonic implications of glaucophane-bearing eclogites and related rocks from the Malpica-Tuy (MT) unit, Galicia, Nortwest Spain. Chemical Geology 50, 145–162.

Gómez Barreiro, J., Martínez Catalán, J.R., Arenas, R., Castiñeiras, P., Abati, J., Díaz García, F., Wijbrans, J.R., 2007. Tectonic evolution of the upper allochthon of the Órdenes complex (northwestern Iberian Massif): Structural constraints to a polyorogenic peri-Gondwanan terrane. In: Linneman, U., Nance, R.D., Kraft, P., Zulauf, G. (Eds.), The evolution of the Rheic Ocean: From Avalonian-Cadomian active margin to Alleghenian-Variscan collisionGeological Society of America Special Paper 423, 315–332.

Gómez Barreiro, J., Martínez Catalán, J.R., Prior, D., Wenk, H.-R., Vogel, S., Díaz García, F., Arenas, R., Sánchez Martínez, S., Lonardelli, I., 2010. Fabric development in a Middle Devonian intra-oceanic subduction regime: the Careón ophiolite (NW Spain). Journal of Geology 118, 163–186.

Hatcher Jr., R.D., Bream, B.R., Merschat, A.J., 2007. Tectonic map of the southern and central Appalachians: A tale of three orogens and a complete Wilson cycle. In: Hatcher Jr., R.D., Carlson, M.P., McBride, J.H., Martínez Catalán, J.R. (Eds.), 4-D Framework of continental crustGeological Society of America Memoir 200, 595–632.

Hegde, V.S., Chavadi, V.C., 2009. Geochemistry of Late Archaean metagreywackes from the Western Dharwar Craton, South India: Implications for provenance and nature of the Late Archaean crust. Gondwana Research 15, 178–187.

Herron, M.M., 1988. Geochemical classification of terrigenous sands and shales from core or log data. Journal of Sedimentary Petrology 58, 820–829.

Liégeois, J.P., Stern, R.J., 2010. Sr-Nd isotopes and geochemistry of granite-gneiss complexes from the Meatiq and Hafafit domes, Eastern Desert, Egypt: No evidence for pre-Neoproterozoic crust. Gondwana Research 57, 31–40.

Linneman, U., McNaughton, N.J., Romer, R.L., Gehmlich, M., Drost, K., Tonk, C., 2004. West African provenance for Saxo-Thuringia (Bohemian Massif): Did Armorica ever leave pre-Pangean Gondwana?–U/Pb-SHRIMP zircon evidence and the Nd-isotopic record. International Journal of Earth Sciences 93, 683–705.

Linnemann, U., Romer, R.L., 2002. The Cadomian Orogeny in Saxo-Thuringia, Germany: geochemical and Nd-Sr-Pb isotopic characterization of marginal basins with constraints to geotectonic setting and provenance. Tectonophysics 352, 33–64.

Linnemann, U., Gerdes, A., Drost, K., Buschmann, B., 2007. The continuum between Cadomian orogenesis and opening of the Rheic Ocean: Constraints from LA-ICP-MS U–Pb zircon dating and analysis of plate-tectonic setting (Saxo-Thuringian zone, northeastern Bohemian Massif, Germany). In: Linnemann, U., Nance, R.D., Kraft, P., Zulauf, G. (Eds.), The evolution of the Rheic Ocean: From Avalonian-Cadomian active margin to Alleghenian-Variscan collisionGeological Society of America Special Paper 423, 61–96.

Martínez Catalán, J.R., Arenas, R., Díaz García, F., Rubio Pascual, F.J., Abati, J., Marquínez, J., 1996. Variscan exhumation of a subducted Paleozoic continental margin: The basal units of the Órdenes Complex, Galicia, NW Spain. Tectonics 15, 106–121.

Martínez Catalán, J.R., Arenas, R., Díaz García, F., González Cuadra, P., Gómez-Barreiro, J., Abati, J., Castiñeiras, P., Fernández-Suárez, J., Sánchez Martínez, S., Andonaegui, P., González Clavijo, E., Díez Montes, A., Rubio Pascual, F.J., Valle Aguado, B., 2007. Space and time in the tectonic evolution of the northwestern Iberian Massif: Implications for the Variscan belt. In: Hatcher Jr., R.D., Carlson, M.P., McBride, J.H., Martínez Catalán, J.R. (Eds.), 4-D Framework of continental crustGeological Society of America Memoir 200, 403–423.

Martínez Catalán, J.R., Arenas, R., Abati, J., Sánchez Martínez, S., Díaz García, F., Fernández-Suárez, J., González Cuadra, P., Castiñeiras, P., Gómez Barreiro, J., Díez Montes, A., González Clavijo, E., Rubio Pascual, F.J., Andonaegui, P., Jeffries, T.E., Alcock, J.E., Díez Fernández, R., López Carmona, A., 2009. A rootless suture and the loss of the roots of a mountain chain: The Variscan belt of NW Iberia. Comptes Rendus 341, 114–126.

McLennan, S.M., 2001. Relationships between the trace element composition of sedimentary rocks and upper continental crust. Geochemistry, Geophysics, Geosystems 2 art. no. 2000GC000109.

McLennan, S.M., Hemming, S.R., 1992. Samarium/neodymium elemental and isotopic systematics in sedimentary rocks. Geochimica et Cosmochimica Acta 56, 887–898.

McLennan, S.M., Hemming, S.R., McDaniel, D.K., Hanson, G.N., 1993. Geochemical approaches to sedimentation, provenance and tectonics. In: Johnssons, M.J., Basu, A. (Eds.), Processes controlling the composition of clastic sedimentsGeological Society of America Special Paper 284, 21–40.

Merschat, A.J., Hatcher Jr., R.D., 2007. The Cat Square terrane: Possible Siluro-Devonian remnant ocean basin in the Inner Piedmont, southern Appalachians, USA. In: Hatcher Jr., R.D., Carlson, M.P., McBride, J.H., Martínez Catalán, J.R. (Eds.), 4-D Framework of continental crustGeological Society of America Memoir 200, 553–565.

Murphy, J.B., Nance, R.D., 2002. Sm–Nd isotopic systematics as tectonic tracers: an example from West Avalonia in the Canadian Appalachians. Earth-Science Reviews 59, 77–100.

Murphy, J.B., Keppie, J.D., Nance, R.D., Dostal, J., 2010. Comparative evolution of the Iapetus and Rheic Oceans: A North America perspective. Gondwana Research 17, 189–192.

Nakamura, N., 1974. Determination of REE, Ba, Fe, Mg, Na and K in carbonaceous and ordinary chondrites. Geochimica et Cosmochimica Acta 38, 757–775.

Nance, R.D., Gutiérrez-Alonso, G., Keppie, J.D., Linnemann, U., Murphy, J.B., Quesada, C., Strachan, R.A., Woodcock, N.H., 2010. Evolution of the Rheic Ocean. Gondwana Research 17, 194–222.

Potrel, A., Peucat, J.J., Fanning, C.M., 1998. Archean crustal evolution of the West African Craton: example of the Amsaga Area (Reguibat Rise). U–Pb and Sm–Nd evidence for crustal growth and recycling. Precambrian Research 90, 107–117.

Rodríguez Aller, J., 2005. Recristalización y deformación de litologías supracorticales sometidas a metamorfismo de alta presión (Complejo de Malpica-Tuy, NO del Macizo Ibérico). Nova Terra 29 572 pp..

Rodríguez, J., Cosca, M.A., Gil Ibarguchi, J.I., Dallmeyer, R.D., 2003. Strain partitioning and preservation of $^{40}Ar/^{39}Ar$ ages during Variscan exhumation of a subducted crust (Malpica-Tui complex, NW Spain). Lithos 70, 111–139.

Rodríguez, J., Paquette, J.L., Gil Ibarguchi, J.I., 2007. U–Pb dating of Lower Ordovician alkaline magmatism in the Gondwana margin (Malpica-Tui Complex, Iberian Massif): Latest continental events before oceanic spreading. In: Arenas, R., Martínez Catalán, J.R., Abati, J., Sánchez Martínez, S. (Eds.), The rootless Variscan suture of NW Iberia (Galicia Spain). Field trip guide and conference abstracts. International Geological Correlation Programme 497. The Rheic Ocean: Its origin, evolution and correlatives. Publicaciones del Instituto Geológico y Minero de España, pp. 163–164.

Rodríguez-Alonso, M.D., Peinado, M., López-Plaza, M., Franco, P., Carnicero, A., Gonzálo, J.C., 2004. Neoproterozoic-Cambrian synsedimentary magmatism in the Central Iberian Zone (Spain): geology, petrology and geodynamic significance. International Journal of Earth Sciences 93, 897–920.

Roser, B.P., Korsch, R.J., 1986. Determination of tectonic setting of sansdtone-mudstone suites using SiO_2 content and K_2O/Na_2O ratio. Journal of Geology 94, 635–650.

Roser, B.P., Korsch, R.J., 1988. Provenance signatures of sandstone-mudstone suites determined using discriminant function analysis of major-element data. Chemical Geology 67, 119–139.

Sánchez Martínez, S., Arenas, R., Díaz García, S., Martínez Catalán, J.R., Gómez Barreiro, J., Pearce, J., 2007. The Careón Ophiolite, NW Spain: supra-subduction zone setting for the youngest Rheic Ocean floor. Geology 35, 53–56.

Searle, M.P., 2007. Diagnostic features and processes in the construction and evolution of Oman, Zagros, Himalayan, Karakoram and Tibetan-type orogenic belts. In: Hatcher Jr., R.D., Carlson, M.P., McBride, J.H., Martínez Catalán, J.R. (Eds.), 4-D Framework of continental crustGeological Society of America Memoir 200, 1–7.

Stampfli, G.M., Borel, G.D., 2002. A plate tectonic model for the Paleozoic and Mesozoic constrained by dynamic plate boundaries and restored synthetic oceanic isochrons. Earth and Planetary Science Letters 196, 17–33.

Stern, R.J., 2002. Crustal evolution in the East African Orogen: a neodymium isotopic perspective. Journal of African Earth Sciences 34, 109–117.

Strelow, F.W.E., 1960. An ion exchange selectivity scale of cations based on equilibrium distributions coefficients. Analytical Chemistry 32, 1185–1188.

Taylor, S.R., McLennan, S.M., 1985. The Continental Crust: Its Composition and Evolution. Blackwell, London. 312 pp.

Thompson, R.N., 1982. Magmatism in the British Tertiary Volcanic Province. Scottish Journal of Geology 19, 49–107.

Ugidos, J.M., Valladares, M.I., Barba, P., Ellam, R.M., 2003. The Upper Neoproterozoic-Lower Cambrian of the Central Iberian Zone, Spain: Chemical and isotopic (Sm–Nd) evidenc that the sedimentary succesion records an inverted stratigraphy of its source. Geochimica et Cosmochimica Acta 67, 2615–2629.

Winchester, J.W., 1963. Rare earth chromatography using bis-(2-ethylhexyl) (orthophosphoric acid). Journal of Chromatography 10, 502–506.

Winchester, J.A., Max, M.D., 1989. Tectonic setting discrimination in clastic sequence: an example from the late proterozoic Erris Group, NW Ireland. Precambrian Research 45, 191–201.

Capítulo 9

Geochemistry of the Ediacaran–Early Cambrian transition in Central Iberia: Tectonic setting and isotopic sources

9.1 Introducción

El estudio geoquímico (elementos mayores y trazas) e isotópico de las series siliciclásticas ediacarenses y cámbricas de las Unidades Superiores y de las Unidades Basales de los Complejos Alóctonos del NW del Macizo Ibérico, indica que existen diferencias importantes en relación a su origen, especialmente en la naturaleza de sus áreas fuentes (fuentes isotópicas Sm-Nd). Estas diferencias pueden explicarse en relación a una paleogeografía diferente de las respectivas cuencas sedimentarias en el margen de Gondwana, como ya se ha sugerido anteriormente (*Díez Fernández et al., 2010; Fernández Suárez et al., 2014; Albert et al., 2015a*), aunque nunca se habían puesto de manifiesto mediante el estudio de las características geoquímicas de los materiales paraderivados.

Para completar el estudio geoquímico de las series siliciclásticas de la transición Ediacarense – Cámbrico, es fundamental abordar el estudio de esta misma transición en alguno de los dominios que componen el Autóctono Ibérico. Los desplazamientos que cabe esperar en los terrenos alóctonos en relación a los dominios autóctonos son muy significativos (*Díez Fernández et al., 2016*). Por consiguiente, no será posible obtener un marco paleogeográfico completo de la transición Ediacarense – Cámbrico en el Macizo Ibérico si no se complementa el trabajo con el estudio de las series autóctonas. Para llevar a cabo este trabajo se ha elegido el sector meridional de la Zona Centroibérica, dado que es una región donde existe una estratigrafía muy completa de las series que definen el paso del Proterozoico al Paleozoico (*Álvarez Nava et al., 1988; San José et al., 1990; Vidal et al., 1994b; Pieren, 2000; Rodríguez Alonso et al., 2004*).

Las series metasedimentarias de bajo grado estudiadas corresponden al Alcudiense Inferior del Anticlinal Centro Extremeño (Ediacarense Superior), y a las denominadas Pizarras de Pusa del Anticlinal de Valdelacasa (Cámbrico Inferior). En total se han seleccionado 12 muestras de cada una de estas series para su estudio geoquímico e isotópico. Las composiciones de ambas series son sensiblemente distintas, lo que sugiere una variación en el ambiente geodinámico en el que se produjo su sedimentación.

9.2 Conclusiones parciales

Las rocas siliciclásticas ediacarenses del Alcudiense Inferior (Zona Centroibérica) presentan características geoquímicas propias de grauvacas. El valor bajo de la relación K_2O/Na_2O define estas metagrauvacas como cuarzo-intermedias, propiedad común en este tipo de litologías, y sugiere una proporción dominante de plagioclasa sobre el feldespato-K. Podemos descartar una alteración significativa en el origen de estas rocas, tanto en sus áreas fuente como en los procesos sedimentarios y post-deposicionales. Los valores de CIA apuntan a un bajo grado de meteorización en las rocas fuente, mientras que los bajos valores de las relaciones Rb/Sr, Th/U y Ti/Zr, similares a los que presenta la corteza continental superior, demuestran una muy limitada alteración durante los procesos típicamente sedimentarios (erosión, transporte y depósito), observada igualmente en los patrones de REE, similares al del PAAS y pone de manifiesto su afinidad con sedimentos terrígenos procedentes de rocas ígneas félsicas de la corteza continental superior.

En el caso de la segunda secuencia estudiada, es evidente la significativa homogeneidad química que presentan las pizarras cámbricas de la Formación Pusa, resultado de un mayor reciclaje sedimentario y una mayor madurez textural y mineralógica. A diferencia de las grauvacas ediacarenses, las pizarras muestran un carácter cuarzo-enriquecido, y diferentes abundancias de SiO_2, CaO, Al_2O_3, Th y Nb, que confirman su carácter más pelítico. Su mayor madurez sedimentaria no se traduce en una alteración química importante. Valores de CIA similares a los del PAAS sugieren una baja a moderada alteración en el área fuente, mientras que su similitud con los contenidos en determinados elementos mayores (Al_2O_3, CaO, Na_2O y K_2O), algunos de ellos altamente móviles durante los procesos sedimentarios, y una relación Th/U con valores análogos a la corteza continental superior, descartan un fuerte alteración post-deposicional. Las elevadas relaciones de Rb/Sr y Ti/Zr sugieren una posible removilización del Sr de las plagioclasas y unos mayores contenidos de Ti heredados de las rocas fuente. Esta ausencia de alteración se refleja nuevamente en unos patrones muy homogéneos de REE, similares a los del PAAS, confirmando su procedencia desde fuentes ígneas de afinidad continental. En este caso, las pizarras cámbricas muestran una procedencia intermedia, con un incremento de las fuentes máficas, aunque conservando un marcado carácter félsico.

Estos resultados sugieren que el contexto geodinámico más probable para la sedimentación de las grauvacas ediacarenses fue un margen activo. La cuenca sedimentaria estaría relacionada con el desarrollo de un arco evolucionado, construido sobre un margen continental adelgazado. Los patrones multielementales de ambas secuencias muestran diferencias apreciables, que implican claramente un cambio en el contexto tectónico en el que tuvo lugar la sedimentación durante la transición entre el Ediacarense Superior y el Cámbrico Inferior. En el caso de las metagrauvacas del Alcudiense Inferior, las características geoquímicas apuntan a una dinámica convergente, con una estrecha relación entre el relleno de la cuenca sedimentaria y la evolución del arco volcánico. En el caso de las pizarras cámbricas, el patrón multielemental muestra una mayor homogeneidad y reciclado, con características propias de un contexto de margen pasivo, según el modelo propuesto por *Winchester and Max (1989)*. De acuerdo con estas observaciones, los contenidos en Zr y Hf son menores de lo esperable, incluso menores que en el caso de las metagrauvacas ediacarenses, coherente con un mayor aporte de fuentes máficas, pero igualmente coherente con un contexto deposicional activo, como demuestra la relación La/Th muy superior al valor que *Bhatia y Crook (1986)* proponen para un margen pasivo.

Los resultados isotópicos (Sm-Nd) ofrecen una clara discriminación de las fuentes isotópicas en ambas litologías. Esta diferenciación se observa en: (i) los valores de la relación inicial $^{143}Nd/^{144}Nd$, con un valor medio de 0.511821 ± 0.000006 para las metagrauvacas ediacarenses (ca. 560 Ma) y un valor medio de 0.511716 ± 0.000005 para las pizarras cámbricas (ca. 530 Ma), valores claramente discriminantes entre ambos grupos; (ii) los valores de εNd inicial, con valores que oscilan entre -3.0 y -1.4 para las metagrauvacas precámbricas, claramente menos negativos que los observados en las pizarras cámbricas (-5.2 y -4.0); y por último, (iii) los valores de las edades modelo (T_{DM}), calculadas según *DePaolo (1981)*, que definen dos poblaciones bien diferenciadas, con valores para las metagrauvacas que varían entre 1256 y 1334 Ma, mientras que las edades modelo de las pizarras presentan edades más antiguas, que oscilan entre valores de 1444 y 1657 Ma. Ambos grupos de T_{DM} son coherentes con que el Cratón del Oeste de África (Cratón de Reguibad) resulte la fuente cratónica más probable de ambas secuencias.

Los resultados geoquímicos e isotópicos anteriormente expuestos son consistentes con un cambio progresivo en el contexto tectónico de sedimentación de las secuencias metasedimentarias de la Zona Centroibérica. Este cambio tuvo lugar en la transición entre el Neoproterozoico Superior y Cámbrico Inferior. El carácter discriminante de determinados elementos traza indica que el contexto geodinámico más probable para la sedimentación de las series ediacarenses fue un margen activo. Por el contrario, las pizarras cámbricas de la Formación Pusa se depositaron probablemente en relación con un contexto de margen pasivo. El relleno de las cuencas sedimentarias durante las últimas fases del Neoproterozoico se habría visto influenciado en mayor medida por la actividad magmática de un arco volcánico evolucionado. Una mayor proporción de material juvenil explica las T_{DM} más jóvenes, al igual que valores de εNd menos negativos. Con posterioridad, el cambio en el contexto tectónico afectó a los procesos sedimentarios que sufrieron los sedimentos paleozoicos depositados en el marco de un margen pasivo. Los resultados isotópicos obtenidos para estas series son coherentes con este cambio geodinámico, con valores más negativos de εNd y T_{DM} más antiguas. Todos estos resultados apoyan una sedimentación relacionada con el desarrollo de una amplia cuenca de tipo *back-arc* durante la mencionada transición temporal, anterior al desarrollo del margen pasivo registrado durante el Cambro-Ordovícico (*Murphy et al., 2006; Arenas et al., 2007; Nance et al., 2010*). Este tipo de cuenca explicaría las diferencias geoquímicas e isotópicas observadas en ambas secuencias y situaría las cuencas sedimentarias de las series estudiadas, teniendo en cuenta las diferentes proporciones de materiales juveniles y/o reciclados de origen cortical, en posiciones más o menos alejadas, respectivamente, del dominio continental del margen septentrional de Gondwana.

Tectonophysics 681 (2016) 15–30

Contents lists available at ScienceDirect

Tectonophysics

journal homepage: www.elsevier.com/locate/tecto

Geochemistry of the Ediacaran–Early Cambrian transition in Central Iberia: Tectonic setting and isotopic sources

José Manuel Fuenlabrada [a,*], Agustín P. Pieren [b], Rubén Díez Fernández [c], Sonia Sánchez Martínez [c], Ricardo Arenas [c]

[a] CAI de Geocronología y Geoquímica Isotópica, Universidad Complutense, 28040 Madrid, Spain
[b] Departamento de Estratigrafía, Universidad Complutense, 28040 Madrid, Spain
[c] Departamento de Petrología y Geoquímica e Instituto de Geociencias (UCM, CSIC), Universidad Complutense, 28040 Madrid, Spain

A R T I C L E   I N F O

Article history:
Received 4 August 2015
Received in revised form 12 November 2015
Accepted 18 November 2015
Available online 26 November 2015

Keywords:
Ediacaran-Cambrian transition
Whole-rock geochemistry
Sedimentary rocks
Sm-Nd isotope geochemistry
Iberian Massif

A B S T R A C T

A complete Ediacaran–Early Cambrian stratigraphic transition can be observed in the southern part of the Central Iberian Zone (Iberian Massif). Two different stratigraphic units, underlying Ordovician series, display geochemical and Sm–Nd isotopic features in agreement with an evolving geodynamic setting. Pusa Shales (Early Cambrian) rest unconformably on greywackes of the Lower Alcudian Formation (Late Ediacaran). Both sequences present minor compositional variations for major and trace element contents and similar REE patterns, close to those of PAAS (Post Archean Australian Shale). Trace element contents and element ratios suggest mixed sources, with intermediate to felsic igneous contributions for both units. Tectonic setting discrimination diagrams for the Ediacaran greywackes indicate that these turbiditic series were deposited in a sedimentary basin associated with a mature active margin (volcanic arc). However, the compositions of the Cambrian shales fit better with a more stable context, a back-arc or retro-arc setting. $\varepsilon Nd_{(T)}$ and TDM ages are compatible with dominance of a similar cratonic source for both sequences, probably the West Africa Craton. εNd_{565} values for the Ediacaran greywackes (-3.0 to -1.4) along with TDM ages (1256–1334 Ma) imply a significant contribution of juvenile material, probably derived from the erosion of the volcanic arc. However, εNd_{530} values in the Cambrian shales (-5.2 to -4.0) together with older TDM ages (1444–1657 Ma), suggest a higher contribution of cratonic isotopic sources, probably derived from erosion of the adjacent mainland. Coeval with the progressive cessation of arc volcanism along the peri-Gondwanan realm during the Cambrian, there was a period of more tectonic stability and increasing arrival of sediments from cratonic areas. The geochemistry of the Ediacaran–Cambrian transition in Central Iberia documents a tectonic switch in the periphery of Gondwana, from an active margin to a more stable context related to the onset of a passive margin.

1. Introduction

Geochemical composition and isotopic characteristics of fine-grained clastic rocks have proved to be a reliable record of continental crust evolution, and therefore are a useful indicator of the origin and tectonic setting in which sedimentation took place (Condie, 1993; McLennan et al., 1990; Taylor and McLennan, 1985). The relative absence of REE fractionation during depositional processes has allowed the use of Sm–Nd data to discriminate between sources, providing information about the paleogeography of sedimentary basins as indicated by the juvenile or more evolved character of their sediment infill (Murphy and Nance, 2002).

Over the last few years, we have focused our work on using whole-rock geochemistry and Sm–Nd isotopic features of metasedimentary series in the Iberian Massif as a potential mean of shedding light on the dynamic evolution of the peri-Gondwanan arc system and to reconstruct the paleogeography of this domain during Ediacaran–Early Paleozoic times. Geochemical features and Nd model ages of metasedimentary rocks from the allochthonous complexes of NW Iberia postulated an arc-derived provenance for the metagreywackes exposed in the Órdenes Complex (Upper Units) (Albert et al., 2015; Fuenlabrada et al., 2010), whereas older TDM ages obtained from metagreywackes and metapelites of the Basal Units pointed to a back-arc or retro-arc basin located in the interior of the continental domain (Díez Fernández et al., 2010, 2012; Fuenlabrada et al., 2012).

Ediacaran–Early Cambrian rocks crop out extensively in the Central Iberian Zone (Iberian Massif). These sequences are affected by low-grade metamorphism and exhibit a gradual and complete transition between both periods. The Central Iberian Zone (CIZ) has been a source of discussion on the provenance and tectonic settings of its Neoproterozoic

* Corresponding author at: CAI de Geocronología y Geoquímica Isotópica Facultad de Ciencias Geológicas Universidad Complutense de Madrid Calle José Antonio Novais, 12 28040, Madrid España.
E-mail address: jmfuenla@ucm.es (J.M. Fuenlabrada).

http://dx.doi.org/10.1016/j.tecto.2015.11.013
0040-1951/

and Cambrian sequences. Some studies considered a more stable and recycled deposition environment (passive margin model), with a significant homogeneity as one of the most important features shared among the complete sequence (Ugidos et al., 1997a, 1997b, 2003a; Valladares et al., 1998, 2000), suggesting that the West Africa Craton was the most likely source for the Late Precambrian rocks (Ugidos et al., 2003b). Geochemical and Sm–Nd data, along with U–Pb detrital zircon populations have allowed other authors to interpret the juvenile contribution to be linked to the waning activity of a long-lived peri-Gondwanan magmatic arc (Cadomian cycle) for the Ediacaran metasedimentary rocks of the CIZ and related peri-Gondwanan domains (Pastor-Galán et al., 2013; Fernández-Suárez et al., 2000, 2014; Gutiérrez-Alonso et al., 2003; Nägler et al., 1995; Orejana et al., 2015; Rodríguez Alonso et al., 2004b; Talavera et al., 2012; Villaseca et al., 2014), proposing a wide range of potential locations for these series along the northern margin of Gondwana during the Late Ediacaran and Early Paleozoic, and therefore different sources for the mantle-derived contributions. In recent years, attempts have been made to explain the evolution of the late stages of the Cadomian orogeny and the accumulation of thick siliciclastic sedimentary successions during the Precambrian–Cambrian transition (Rodríguez Alonso et al., 2004a). Some models propose a passive margin for its deposition (Valladares et al., 2000, 2002), whereas others favor the existence of asymmetric basins formed in a tectonically active setting (Rodríguez Alonso et al., 2004b; Villaseca et al., 2014). The latter models frame such tectonic activity within the evolution from a compressive (Cadomian orogeny) to an extensional regime along the northern margin of Gondwana (Nance et al., 2010).

In the present work, geochemical and Sm–Nd isotopic studies of representative fine-grained sedimentary rocks from the southern Central Iberian Zone have been carried out to discover the sedimentation environment of Late Neoproterozoic and Early Cambrian metasedimentary sequences. Slight differences in the compositions of relatively immobile trace elements as well as significant changes in Nd model ages suggest important differences in the contribution of juvenile or cratonic sources during Late Ediacaran–Early Cambrian times. These differences are used to explore the tectonic setting during this transition and further the knowledge of the geochemistry and sources of the sedimentary series of the peri-Gondwanan realm.

2. Geological setting

Stratigraphic, structural, magmatic and metamorphic criteria were used to define the geotectonic zones within the Iberian Massif section of the Variscan Belt (Arenas et al., 1988; Farias et al., 1987; Julivert et al., 1974; Lotze, 1945; Quesada, 1991) (Fig. 1). One of them is the Central Iberian Zone, an autochthonous section of the Iberian Massif that is bounded to the east and northeast by more external domains of the orogen, the West Asturian–Leonese Zone and the Cantabrian Zone (Fig. 1). The CIZ is thrust by the most internal domain of the orogen, which is represented by allochthonous complexes with high-P metamorphic belts and ophiolites featuring a Variscan suture (Fig. 1; Martínez Catalán et al., 2009). The domain located to the south of the CIZ, the Ossa–Morena Zone, has been recently identified as another allochthonous complex of the Iberian Massif, and is correlated with equivalent complexes of NW Iberia (Díez Fernández and Arenas, 2015).

The CIZ can be divided in two domains: the Ollo de Sapo Domain and the Schist–Greywacke Complex Domain. The Ollo de Sapo Domain, to the North, shows as an essential feature the presence of thick massifs of augen gneisses, abundant Variscan granitoids, and a high-grade regional metamorphism affecting thick Paleozoic series and minor Ediacaran rocks (Díez Montes et al., 2004). The domain to the South, received the name

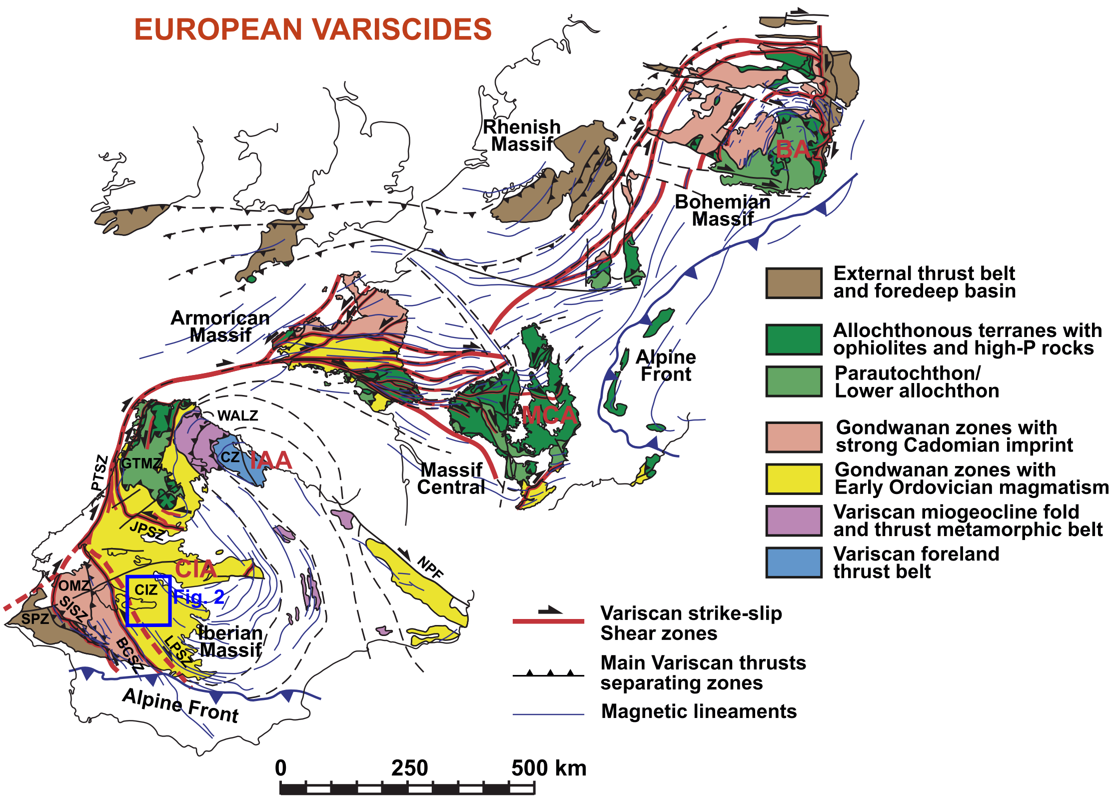

Fig. 1. Terranes and oroclines of the Variscan belt (Martínez Catalán, 2011). Arcs: BA, Bohemian; CIA, Central Iberian; IAA, Ibero-Armorican; MCA, Massif Central. Zones of the Iberian Massif: CIZ, Central Iberian; CZ, Cantabrian; GTMZ, Galicia–Trás-os-Montes; OMZ, Ossa–Morena; SPZ, South Portuguese; WALZ, West Asturian–Leonese. Shear zones and faults: BCSZ, Badajoz–Córdoba; JPSZ, Juzbado–Penalva; LPSZ, Los Pedroches; NPF, North Pyrenean; PTSZ, Porto–Tomar; SISZ, Southern Iberian. Location of the geological map and section presented in Fig. 2 is shown.

of Schist and Greywacke Complex (SGC) (Carrington da Costa, 1950) and it includes an extensive sequence of pre-Ordovician shales and sandstones, post-orogenic granitoids, and large areas with low to very low grade metamorphism. The boundary between these two domains of the CIZ is gradational, and consists of a transitional zone that combines characteristics of the Ollo de Sapo and the SGC.

The SGC has been divided into different lithostratigraphic units, mainly depending on the author and the area of study (Alvarez Nava et al., 1988; Díez Fernández et al., 2013; Pieren, 2000; San José et al., 1990; Vidal et al., 1994b). Yet, two clearly differentiated units can be distinguished: the Lower Unit and the Upper Unit (Rodríguez Alonso et al., 2004a). The Upper Unit can be further divided in Upper Alcudian and the Pusa Group. Upper Alcudian includes Late Ediacaran and Early Cambrian rocks, whereas the Pusa Group is Early Cambrian since its base.

The Lower Unit crops out extensively in the central and southern part of the CIZ (Alcudia Anticline and its extension to the NW, in

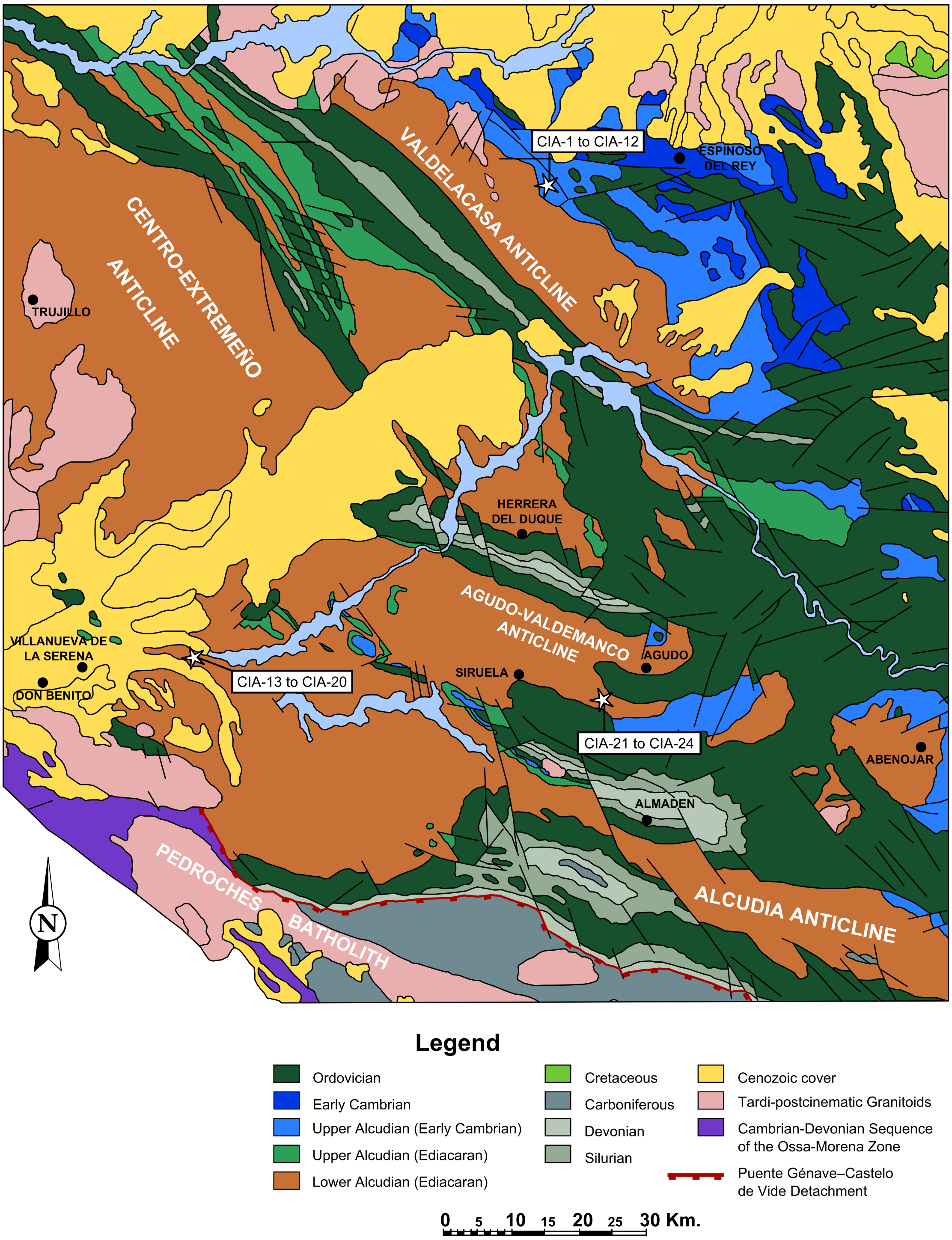

Fig. 2. Geological map of the southern part of the Central Iberian Zone (modified after IGME, 1994 and Pieren, 2000). Sampling locations of the Ediacaran and Cambrian samples are included. Puente Génave–Castelo de Vide Detachment is also included (Martín Parra et al., 2006).

the Centro-Extremeño Anticline or Río Zujar Dome) and has been previously referred to as Lower Alcudian (San José et al., 1990); Domo Extremeño Group in the Montes de Toledo, Extremadura and Alcudia (Alvarez Nava et al., 1988); Lower Series in the Western Central area of the CIZ (Ugidos et al., 1997b; Valladares et al., 2000, 2002); and Beiras Group in Portugal (Silva et al., 1988). The thickness of this unit is unknown since its lower boundary remains unexposed, but the sequences exceed 4000 m. The metasedimentary rock series consists of a monotonous succession of shales and sandstones with some interbedded conglomerates and volcanoclastic layers, mainly in its upper part. The sediments of the Lower Unit have been interpreted as laid down in submarine fans, slopes and channels (San José et al., 1990; Valladares et al., 2000), but evidence of shallower depositional environments have also been found (Rodríguez Alonso et al., 2004b). As a whole, this sedimentary sequence is considered as a set of turbidites deposited in a prograding synorogenic clastic wedge filling a back-arc basin (Rodríguez Alonso et al., 2004b). Based on the presence of Cloudina carinata (Late Ediacaran, Cortijo et al., 2010) and other types of microfossils (Jensen et al., 2007; Vidal et al., 1994a, 1994b), the Lower Unit is Neoproterozoic in age. In the area, where the samples CIA-13 to CIA-20 were collected (Figs. 2 and 3b), the Lower Alcudian starts with shales, silts and thin beds of sandstones, which become thicker and more abundant in the middle part; the upper part is characterized by the presence of polygenic conglomerates (with greywackes, vein quartz, and metamorphic and granodioritic cobbles) and pebbly mudstones alternating with shales and sandstones (García-Hidalgo et al., 1993). The whole sequence is interpreted as the progradation of a turbiditic fan, where the upper part was not deep, and thus it also shows outer shelf deposits. The samples were taken in the interval a of thick Bouma sequences within the middle part. In the Agudo–Valdemanco Anticline the absence of marker layers, such as the mentioned conglomerates, has not allowed the distinction of different parts within the Lower Alcudian turbidites, but the samples CIA-21 to CIA-24 were collected in the a interval of very well exposed thick Bouma sequences.

The Upper Unit has been given different names by different authors on different anticlines: Upper Alcudian or Ibor Group, Pusa Formation or Río Huso and Valdelacasa Groups (Alvarez Nava et al., 1988; San José et al., 1990; Vidal et al., 1994a) in the Centro-Extremeño and Alcudia anticlines, and the “Montes de Toledo” region; the Middle and Upper

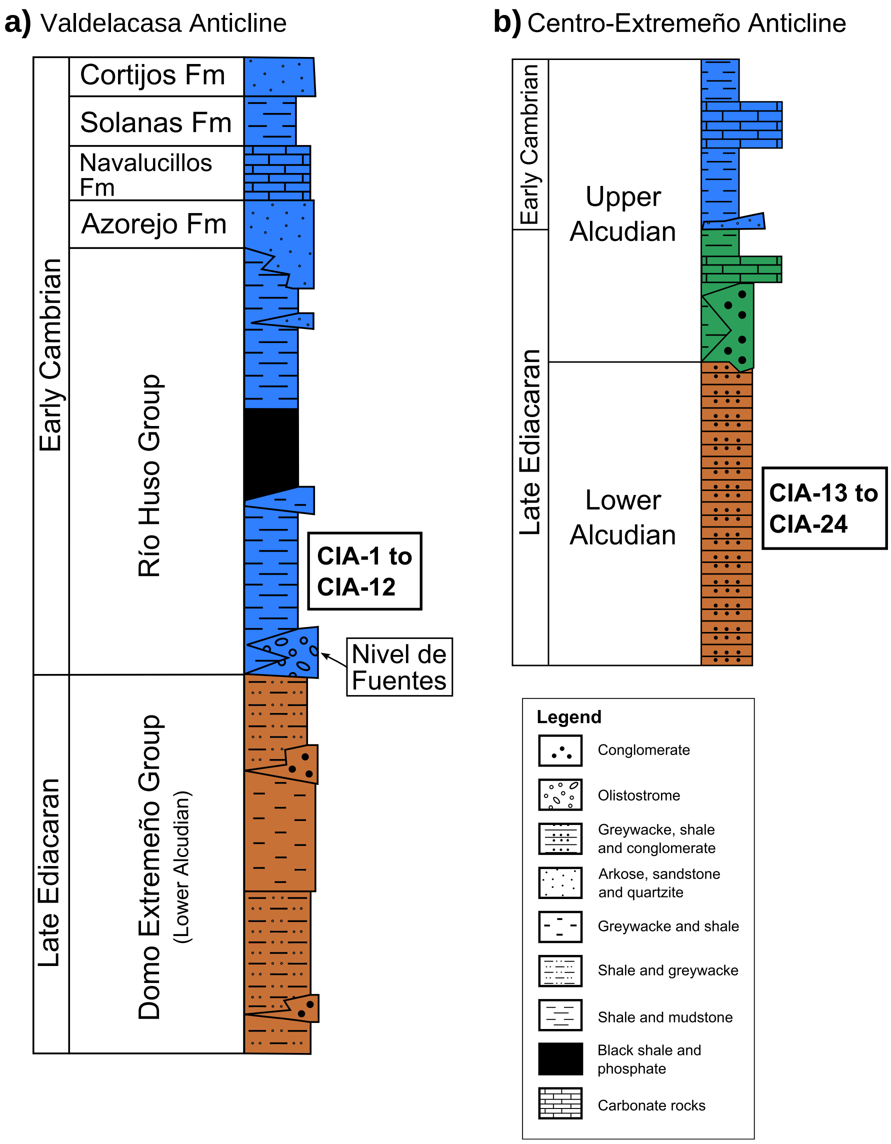

Fig. 3. Synthetic stratigraphic columns of the Valdelacasa and Alcudia Anticlines (modified after Vidal et al., 1999). The location of the analyzed samples is shown. Color legend as in Fig. 2.

J.M. Fuenlabrada et al. / Tectonophysics 681 (2016) 15–30

Series in the western central part of the CIZ (Ugidos et al., 1997b; Valladares et al., 2000), and Douro Group in Portugal (Sousa, 1982). The older units are more frequent towards SW and the younger Cambrian units towards NE. The local names and their distribution are summarized by Rodríguez Alonso et al. (2004b). The Upper Unit shows greater lithological variety than the Lower Unit although it is mainly pelitic. The basal part of the Upper Unit is separated from the deposits of the Lower Unit by an angular unconformity (Rodríguez Alonso et al., 2004b). The record of tectonic activity consists of discontinuous accumulations of megabreccias, olistostromes and chaotic deposits, which may be accompanied by some episodes of volcanism. Deposition took place in sedimentary environments ranging from turbiditic platform to offshore siliciclastic–carbonate turbiditic platform. This mixed platform is better developed towards Extremadura and Montes de Toledo. The rest of the Upper Unit includes gray, dark-gray and black shales, conglomerates and sandstones, together with discontinuous and minor interbedded layers of limestone, olistostromes, phosphates, and volcanic and volcanoclastic rocks. The sedimentary facies of the Upper Unit are more diverse and reflect a more complex evolution than those of the Lower Unit. Deposition took place on turbiditic slopes, mixed platform (carbonate–siliciclastic), siliciclastic platform, and even transitional marine-continental platform environments along the southern boundary of the CIZ (Pieren, 2000; Pieren et al., 1991). The fossil record found in this unit places the Proterozoic–Cambrian transition in the Upper Alcudian or Ibor Group below the Pusa Group (García Hidalgo, 1993; Liñán et al., 1984; San José et al., 1990), which is entirely Cambrian. Pusa Shales were mostly deposited in shallow waters, in a clear transition from a turbiditic environment to a continental platform (Simancas et al., 2004).

The Pusa Group is conformably covered by transgressing sandstones deposited during the middle stages of the Early Cambrian. These fossil rich sediments, well-exposed in upright synclines south of Toledo (Azorejo Sandstones) and south of Salamanca (Tamames Sandstones), were deposited on shallow marine platforms, and are followed by carbonates formed in a shallow shelf (Navalucillos Limestones in Montes de Toledo and Tamames Limestones in Salamanca) (Díez Balda, 1986;

Table 1
Whole rock major and trace element data of Lower Alcudian greywackes (Late Ediacaran).

	CIA-13	CIA-14	CIA-15	CIA-16	CIA-17	CIA-18	CIA-19	CIA-20	CIA-21	CIA-22	CIA-23	CIA-24
SiO_2	71.18	71.4	71.3	73.31	71.96	70.98	70.38	72.48	66.31	64.58	66.93	70
Al_2O_3	13.15	13.48	13.05	12.19	12.77	12.65	13.71	12.67	14.79	15.83	15.53	13.27
Fe_2O_3	4.92	5.03	4.99	5.08	5.01	4.92	5.28	5.05	5.47	6.26	5.19	4.53
MnO	0.035	0.047	0.046	0.066	0.047	0.036	0.044	0.057	0.066	0.064	0.051	0.065
MgO	1.91	1.86	1.97	1.74	1.77	1.49	1.73	1.58	2.02	2.36	1.93	1.5
CaO	0.27	0.59	0.48	0.27	0.28	0.29	0.38	0.76	1.29	0.74	0.47	1.45
Na_2O	2.89	3.25	2.97	2.84	2.81	2.79	2.99	3	2.96	2.81	3.08	3.44
K_2O	1.92	1.85	1.85	1.53	1.79	1.84	1.9	1.75	2.95	3.22	3.21	2.39
TiO_2	0.723	0.841	0.745	0.71	0.703	0.67	0.753	0.731	0.629	0.747	0.699	0.763
P_2O_5	0.17	0.2	0.18	0.13	0.13	0.16	0.14	0.14	0.15	0.17	0.16	0.15
LOI[a]	2.24	2.36	2.4	2.2	2.22	2.21	2.37	2.51	3.16	3.24	2.69	2.89
Total	99.42	100.9	99.99	100.1	99.49	98.02	99.68	100.7	99.79	100	99.93	100.5
CIA	66	63	64	65	65	65	65	62	60	64	63	56
Sc	12	13	12	12	12	12	13	12	11	14	12	10
Be	2	2	2	2	2	2	2	2	3	3	3	2
V	94	99	97	94	95	93	97	94	72	93	84	85
Cr	80	100	90	80	90	80	80	90	60	80	80	90
Co	11	16	18	14	15	15	14	15	13	16	17	16
Ni	40	40	40	30	40	40	40	40	30	40	40	20
Cu	40	40	50	10	30	40	30	30	30	30	30	20
Zn	80	230	90	100	90	110	80	80	100	110	100	70
Ga	17	19	17	15	17	17	18	16	19	24	22	17
Rb	73	73	71	59	76	69	76	66	103	129	127	81
Sr	91	122	100	102	98	108	106	106	211	152	187	226
Y	25.5	31.6	26	25.6	25.1	25.2	25.9	26.6	35.5	40.3	31.6	23.3
Zr	226	360	243	218	228	192	209	293	223	243	237	307
Nb	10.9	12.7	10.5	9.8	10.4	9.7	11	10.2	13.7	15.4	13.5	11.2
Cs	3	3.2	3.1	2.6	3.2	2.7	3.1	2.7	5.7	6.4	6.4	4.1
Ba	395	446	422	341	363	422	451	400	740	778	834	679
Hf	5.5	8.5	5.9	5.4	5.7	4.7	5.2	6.6	5.8	6.2	5.8	7.2
Ta	0.8	0.88	0.78	0.74	0.76	0.73	0.81	0.79	1.06	1.16	1	0.83
Pb	12	14	15	20	14	12	12	15	67	17	16	20
Th	8.62	9.7	8.13	7.97	8.47	7.77	8.79	8.6	10.9	12.8	11.1	11
U	2.39	2.87	2.59	2.12	2.46	2.32	2.55	2.57	3.45	3.89	3.26	2.82
Al_2O_3/Na_2O	4.6	4.1	4.4	4.3	4.5	4.5	4.6	4.2	5.0	5.6	5.0	3.9
Al_2O_3/TiO_2	18.2	16.0	17.5	17.2	18.2	18.9	18.2	17.3	23.5	21.2	22.2	17.4
SiO_2/Al_2O_3	5.4	5.3	5.5	6.0	5.6	5.6	5.1	5.7	4.5	4.1	4.3	5.3
K_2O/Na_2O	0.7	0.6	0.6	0.5	0.6	0.7	0.6	0.6	1.0	1.1	1.0	0.7
Rb/Sr	0.80	0.60	0.71	0.58	0.78	0.64	0.72	0.62	0.49	0.85	0.68	0.36
Ti/Zr	19.18	14.00	18.38	19.52	18.48	20.92	21.60	14.96	16.91	18.43	17.68	14.90
Ti/Nb	398	397	425	434	405	414	410	430	275	291	310	408
La/Sc	2.53	2.55	2.30	2.28	2.43	2.28	2.30	2.56	3.04	2.82	2.93	3.34
La/Th	3.52	3.41	3.39	3.43	3.44	3.53	3.40	3.57	3.06	3.09	3.17	3.04
Th/U	3.61	3.38	3.14	3.76	3.44	3.35	3.45	3.35	3.16	3.29	3.40	3.90
Th/Nb	0.79	0.76	0.77	0.81	0.81	0.80	0.80	0.84	0.80	0.83	0.82	0.98
Th/Sc	0.72	0.75	0.68	0.66	0.71	0.65	0.68	0.72	0.99	0.91	0.93	1.10
Zr/Sc	18.83	27.69	20.25	18.17	19.00	16.00	16.08	24.42	20.27	17.36	19.75	30.70
Co/Th	1.28	1.65	2.21	1.76	1.77	1.93	1.59	1.74	1.19	1.25	1.53	1.45

Oxides are in weight percent (wt.%).
Trace elements are in parts per million (ppm).
CIA: Chemical Index of Alteration (Nesbitt and Young, 1982). Oxides in molar proportions.
[a] Loss on ignition.

Díez Balda et al., 2004). These units of the Early Cambrian transgression were never found towards the S and SW of Guadarranque Syncline, therefore they do not crop out neither in the Centro-Extremeño anticline nor in Agudo-Valdemanco nor in the Alcudia anticline. These series accumulated following the Cadomian activity, prior to Cambro-Ordovician rifting. Finally, Ordovician quartz sands, that also constitute the Armorican Quartzite, rest discordantly over the Cambrian and Neoproterozoic sequence (Liñán et al., 2002; Rodríguez Alonso et al., 2004a).

3. Samples, analytical methods and geochemical tools

3.1. Samples

Samples of metasedimentary rocks were selected in low grade metamorphic areas located in the southern part of the Central Iberian Zone (Fig. 1). Twelve shale (slate) samples were collected in the Early Cambrian Pusa Shales Formation (Upper Unit), above the conglomerate layer referred to as “Nivel de Fuentes”, 70 km N of the Centro-Extremeño Dome, in the Valdelacasa Anticline (CIA-1 to CIA-12 (UTM30/325.295/4.392.922), Figs. 2 and 3a). These samples show a slaty cleavage defined by muscovite, chlorite, quartz, and plagioclase. Sampled rocks collected are shales because of the total lack of sandstones or greywackes in the unit.

Eight samples of greywackes (*a* and *b* layers of the Bouma sequence) were collected from the Lower Alcudian (Lower Unit), in the channel of Río Zujar, in the Alcudia Anticline, Centro-Extremeño Dome (CIA-13 to CIA-20 (UTM30/273.270/4.316.456), Late Ediacaran, Figs. 2 and 3b). Four additional greywacke samples of this Late Ediacaran unit were collected in the Agudo–Valdemanco Anticline of the Centro-Extremeño Dome (CIA-21 to CIA-24 (UTM30/327.349/4.315.193) Figs .2 and 3b). The sampled horizons correspond to full or truncated Bouma sequences in fine to medium grain sandy units. The quartz–micaceous matrix is oriented to define a slaty cleavage (chlorite–sericite) that wraps around clasts of quartz, chert, K-feldspar, plagioclase, muscovite, biotite and opaque minerals.

Table 2
Whole rock major and trace element data of Pusa Shales (Early Cambrian).

	CIA-1	CIA-2	CIA-3	CIA-4	CIA-5	CIA-6	CIA-7	CIA-8	CIA-9	CIA-10	CIA-11	CIA-12
SiO_2	61.36	59.95	58.99	58.59	59.64	60.06	59.97	59.37	58.72	60.47	60.64	61.03
Al_2O_3	18.89	18.65	19.04	19.39	19.19	18.4	18.78	19.03	19.12	18.89	18.83	18.8
Fe_2O_3	7.17	6.66	6.95	7.63	7.23	7.1	7	6.92	6.98	7.22	7.09	7.04
MnO	0.075	0.111	0.098	0.089	0.077	0.085	0.067	0.082	0.08	0.069	0.083	0.081
MgO	2.78	2.81	2.9	3	2.8	2.72	2.51	2.89	2.93	2.67	2.78	2.76
CaO	0.25	0.93	0.66	0.43	0.45	0.64	0.27	0.36	0.51	0.24	0.28	0.47
Na_2O	1.78	2.03	1.87	1.87	1.97	1.88	1.55	1.43	1.64	1.62	1.82	1.93
K_2O	3.4	3.42	3.56	3.5	3.52	3.38	3.57	3.66	3.43	3.48	3.39	3.34
TiO_2	0.765	0.749	0.757	0.744	0.763	0.736	0.743	0.76	0.722	0.745	0.786	0.785
P_2O_5	0.12	0.12	0.12	0.12	0.12	0.14	0.17	0.13	0.18	0.12	0.14	0.14
LOI[a]	3.77	4.5	4.2	4.06	3.98	4	3.97	4.28	4.35	4.04	3.8	3.94
Total	100.4	99.92	99.15	99.42	99.74	99.15	98.62	98.91	98.66	99.55	99.64	100.3
CIA	74	69	71	72	72	71	74	74	73	74	73	72
Sc	17	17	18	18	18	17	17	18	17	17	18	17
Be	3	4	4	4	4	4	4	4	3	4	4	4
V	115	115	117	118	118	113	115	118	115	118	116	116
Cr	90	100	100	100	100	100	100	100	90	90	100	100
Co	10	20	20	19	18	16	13	21	18	16	19	18
Ni	50	50	50	50	50	50	50	50	40	50	50	50
Cu	60	40	110	50	70	40	60	50	50	30	40	40
Zn	120	130	140	150	140	130	130	130	140	130	140	140
Ga	28	28	30	30	29	28	30	30	27	29	29	28
Rb	152	161	170	165	161	155	170	173	152	159	158	156
Sr	97	96	97	96	101	98	97	74	80	84	81	91
Y	30.9	34.9	34.1	31.8	34.1	32	34.2	34.1	32.2	31.6	34.1	32.9
Zr	156	163	155	149	155	153	158	158	144	147	167	161
Nb	16.3	15.7	15.6	15.4	15.7	15.5	15.4	15.7	13.2	14.5	14.9	15.2
Cs	7.4	8.2	8.8	8.4	8.2	7.8	7.9	9.3	7.9	8	7.9	8
Ba	595	604	630	619	630	609	644	645	610	614	606	594
Hf	4.1	4.2	4.1	3.8	4	3.9	4.2	4	3.7	4	4.3	4.1
Ta	1.08	1.04	1.07	1.1	1.34	1.09	1.15	1.12	1.05	1.04	1.09	1.1
Pb	16	19	15	11	14	16	11	10	24	12	19	10
Th	12.8	13.1	13.5	13.1	13.3	12.9	13.5	13.3	12.2	12.9	13.3	13.3
U	2.7	3.61	3.43	2.97	3.19	2.84	3.03	3.18	3.35	2.98	3.17	3.32
Al_2O_3/Na_2O	10.6	9.2	10.2	10.4	9.7	9.8	12.1	13.3	11.7	11.7	10.3	9.7
Al_2O_3/TiO_2	24.7	24.9	25.2	26.1	25.2	25.0	25.3	25.0	26.5	25.4	24.0	23.9
SiO_2/Al_2O_3	3.2	3.2	3.1	3.0	3.1	3.3	3.2	3.1	3.1	3.2	3.2	3.2
K_2O/Na_2O	1.9	1.7	1.9	1.9	1.8	1.8	2.3	2.6	2.1	2.1	1.9	1.7
Rb/Sr	1.57	1.68	1.75	1.72	1.59	1.58	1.75	2.34	1.90	1.89	1.95	1.71
Ti/Zr	29.40	27.55	29.28	29.93	29.51	28.84	28.19	28.84	30.06	30.38	28.22	29.23
Ti/Nb	281	286	291	290	291	285	289	290	328	308	316	310
La/Sc	2.45	2.52	2.34	2.34	2.39	2.36	2.57	2.34	2.27	2.45	2.28	2.38
La/Th	3.25	3.27	3.13	3.22	3.24	3.12	3.24	3.17	3.16	3.22	3.09	3.05
Th/U	4.74	3.63	3.94	4.41	4.17	4.54	4.46	4.18	3.64	4.33	4.20	4.01
Th/Nb	0.79	0.83	0.87	0.85	0.85	0.83	0.88	0.85	0.92	0.89	0.89	0.88
Th/Sc	0.75	0.77	0.75	0.73	0.74	0.76	0.79	0.74	0.72	0.76	0.74	0.78
Zr/Sc	9.18	9.59	8.61	8.28	8.61	9.00	9.29	8.78	8.47	8.65	9.28	9.47
Co/Th	0.78	1.53	1.48	1.45	1.35	1.24	0.96	1.58	1.48	1.24	1.43	1.35

Oxides are in weight percent (wt.%).
Trace elements are in parts per million (ppm).
CIA: Chemical Index of Alteration (Nesbitt and Young, 1982). Oxides in molar proportions.
[a] Loss on ignition.

Table 3
Whole rock rare earth element data of Lower Alcudian greywackes (Late Ediacaran).

	CIA-13	CIA-14	CIA-15	CIA-16	CIA-17	CIA-18	CIA-19	CIA-20	CIA-21	CIA-22	CIA-23	CIA-24
La	30.3	33.1	27.6	27.3	29.1	27.4	29.9	30.7	33.4	39.5	35.2	33.4
Ce	60.4	65.5	55.4	54.3	58.6	55	60.7	60	66.3	78.7	70.1	65.5
Pr	7.6	8.06	6.86	6.62	7.26	6.75	7.49	7.53	8.34	9.92	8.76	8
Nd	29.1	31	26.2	26	28.4	26.6	28.8	29.4	32.1	38.1	33.6	29.6
Sm	5.61	6.04	5.32	5.42	5.42	5.28	5.84	5.94	6.84	8.09	6.91	5.77
Eu	1.25	1.38	1.19	1.18	1.26	1.14	1.25	1.26	1.41	1.44	1.23	1.23
Gd	4.73	5.22	4.67	4.52	4.4	4.22	4.5	4.93	5.84	6.73	5.66	4.24
Tb	0.76	0.89	0.75	0.72	0.77	0.75	0.8	0.78	0.99	1.18	0.9	0.7
Dy	4.43	5.39	4.6	4.64	4.57	4.38	4.75	4.58	6.01	7.01	5.35	4.1
Ho	0.91	1.05	0.9	0.92	0.91	0.87	0.92	0.92	1.19	1.38	1.08	0.8
Er	2.5	3.01	2.59	2.5	2.55	2.47	2.72	2.56	3.43	3.87	3.15	2.26
Tm	0.382	0.459	0.389	0.384	0.406	0.368	0.413	0.4	0.505	0.584	0.498	0.349
Yb	2.62	3.00	2.59	2.62	2.66	2.55	2.63	2.67	3.26	3.79	3.20	2.28
Lu	0.367	0.434	0.388	0.39	0.406	0.372	0.405	0.385	0.459	0.541	0.439	0.345
Σ REE	151	165	139	138	147	138	151	152	170	201	176	159
Eu/Eu*	0.75	0.76	0.73	0.73	0.79	0.74	0.75	0.72	0.69	0.60	0.60	0.76
$(La/Sm)_N$	3.3	3.4	3.2	3.1	3.3	3.2	3.2	3.2	3.0	3.0	3.1	3.6
$(Gd/Yb)_N$	1.44	1.39	1.44	1.38	1.32	1.32	1.36	1.47	1.43	1.42	1.41	1.48
$(La/Yb)_N$	7.73	7.38	7.13	6.97	7.32	7.19	7.60	7.69	6.85	6.97	7.36	9.80

Rare earth element data in parts per million (ppm).

In this region, no samples were taken in the Upper Alcudian Unit, which unconformably lies on the Lower Alcudian turbidites, because the sedimentary environments correspond to transitional continental-fan-shallow marine deposits, which do not meet the purposes of the whole rock geochemistry of this paper, whereas the Pusa Shales are a better option to characterize the Upper Unit, but it does not crop out southwards of the Valdelacasa or Navalpino anticlines.

3.2. Analytical methods

Geochemical and isotopic analyses were performed on powdered rock samples milled at Universidad Complutense de Madrid. Whole rock major and trace elements analyses were performed at Activation Laboratories Ltd (Actlabs) in Canada, using fusion with lithium metaborate or tetraborate for sample digestion. The analytical techniques for major and trace element determination were ICP-OES and ICP-MS, respectively. The results are given in Tables 1 to 4.

Sm–Nd isotopic analyses were performed at the Geochronology and Isotope Geochemistry Service of Universidad Complutense de Madrid, using Isotope Dilution Thermal Ionization Mass Spectrometry (ID-TIMS). Samples were spiked with a mixed ^{149}Sm–^{150}Nd tracer and analyzed in an IsotopX-Phoenix spectrometer (TIMS), in single collection and dynamic multicollection mode for Sm and Nd, respectively. The ^{143}Nd/^{144}Nd ratios were corrected for ^{142}Ce and ^{144}Sm interferences and normalized to ^{146}Nd/^{144}Nd $= 07219$ value (O'Nions et al., 1979) in order to correct procedural and instrumental mass fractionation. Drifts from La Jolla reference value (Lugmair et al., 1983) were corrected by analyzing the standard along with the samples, yielding an average value of ^{143}Nd/^{144}Nd $= 0.511851$ for 6 replicas, with an internal precision of ± 0.00002 (2σ). Errors on the ^{147}Sm/^{144}Nd and ^{143}Nd/^{144}Nd ratios were estimated at less than 0.1% and 0.006%, respectively.

3.3. Geochemical tools

Metasedimentary rocks have been widely studied to unravel the composition of the upper continental crust (Condie and Wronkiewicz, 1990; Taylor and McLennan, 1985). Some authors have developed useful discrimination diagrams to constrain the tectonic setting and the provenance sources using major element compositions (Bhatia, 1983; Roser and Korsch, 1985, 1986, 1988), although major element diagrams should be used carefully (Armstrong-Altrin and Verma, 2005).

There is a general agreement about the relative absence of changes in the minor and trace element composition of sedimentary rocks after their deposition and during secondary processes; consequently

Table 4
Whole rock rare earth element data of Pusa Shales (Early Cambrian).

	CIA-1	CIA-2	CIA-3	CIA-4	CIA-5	CIA-6	CIA-7	CIA-8	CIA-9	CIA-10	CIA-11	CIA-12
La	41.6	42.8	42.2	42.2	43.1	40.2	43.7	42.2	38.6	41.6	41.1	40.5
Ce	78	80.9	78.9	77.2	80.6	75	81.9	77.2	71.7	76.7	76.8	74.9
Pr	9.75	10.1	9.85	9.96	10.2	9.51	10.3	9.92	9.14	9.72	9.9	9.48
Nd	36.9	38.7	37.6	37.6	38.6	35.5	39.1	37.1	36.5	36.4	37.7	35.3
Sm	7.13	7.52	7.68	7.21	7.71	7.04	7.74	7.6	7.41	7.19	7.58	7.12
Eu	1.42	1.52	1.5	1.41	1.5	1.4	1.47	1.53	1.49	1.42	1.51	1.39
Gd	5.53	6.37	6.23	5.55	6.3	5.54	6.5	6.35	7.01	5.61	6.32	5.7
Tb	0.9	1.05	1.02	0.92	1	0.91	1.03	0.99	1.02	0.94	1.01	0.93
Dy	5.42	6.05	5.77	5.45	5.85	5.63	6.1	6.06	5.5	5.55	5.94	5.48
Ho	1.1	1.14	1.16	1.08	1.15	1.08	1.17	1.17	1.11	1.05	1.13	1.09
Er	3.04	3.28	3.23	3.15	3.31	3.01	3.4	3.32	3.11	3.08	3.21	3.02
Tm	0.464	0.493	0.5	0.484	0.503	0.456	0.506	0.517	0.466	0.476	0.511	0.469
Yb	3.15	3.31	3.32	3.2	3.29	3.14	3.25	3.3	2.93	3.04	3.36	3.2
Lu	0.455	0.456	0.484	0.466	0.492	0.459	0.487	0.491	0.445	0.454	0.471	0.455
Σ REE	195	204	199	196	204	189	207	198	186	193	197	189
Eu/Eu*	0.70	0.68	0.67	0.69	0.66	0.69	0.64	0.68	0.64	0.69	0.67	0.67
$(La/Sm)_N$	3.60	3.51	3.39	3.61	3.45	3.52	3.48	3.43	3.21	3.57	3.35	3.51
$(Gd/Yb)_N$	1.40	1.53	1.50	1.38	1.53	1.41	1.59	1.53	1.91	1.47	1.50	1.42
$(La/Yb)_N$	8.83	8.65	8.50	8.82	8.76	8.56	8.99	8.55	8.81	9.15	8.18	8.46

Rare earth element data in parts per million (ppm).

their geochemical features mostly depend on the nature of the source areas. Trace elements such as REE, Hf, Ti, Cr, Co, Zr, Nb, Ta, Y, Th and Sc make excellent discriminating proxies for provenance and tectonic setting determination studies (Bhatia and Crook, 1986; McLennan et al., 1990; Taylor and McLennan, 1985), mainly because these elements, and particularly their ratios (e.g. Th/Sc, La/Sc, Ti/Zr, Zr/Sc and La/Th) are preserved during sedimentary processes due to their low mobility during weathering processes, transport, diagenesis or metamorphism (McLennan et al., 1983; Nesbitt et al., 1980; Taylor and McLennan, 1985; Wronkiewicz and Condie, 1987), and their very low residence time in oceanic waters (Henderson, 1982 and Holland, 1978). Similarly, incompatible and compatible elements and their mutual relationships allow distinguishing between areas with more felsic or mafic source components. Elements such as La and Th; and the Co, Cr or Sc are commonly used to discriminate between felsic and mafic contributions in different tectonic environments (Feng and Kerrich, 1990; Taylor and McLennan, 1985; Wronkiewicz and Condie, 1987, 1990). The effects of homogenization in sedimentary processes result in a relatively uniform distribution of REE in detrital rocks, that show the average composition of the source area, and whose pattern reflects the REE abundance in the upper crust, mainly because very limited or no REE fractionation takes place during deposition of fine-grained sediments (McLennan et al., 1980; Taylor and McLennan, 1985).

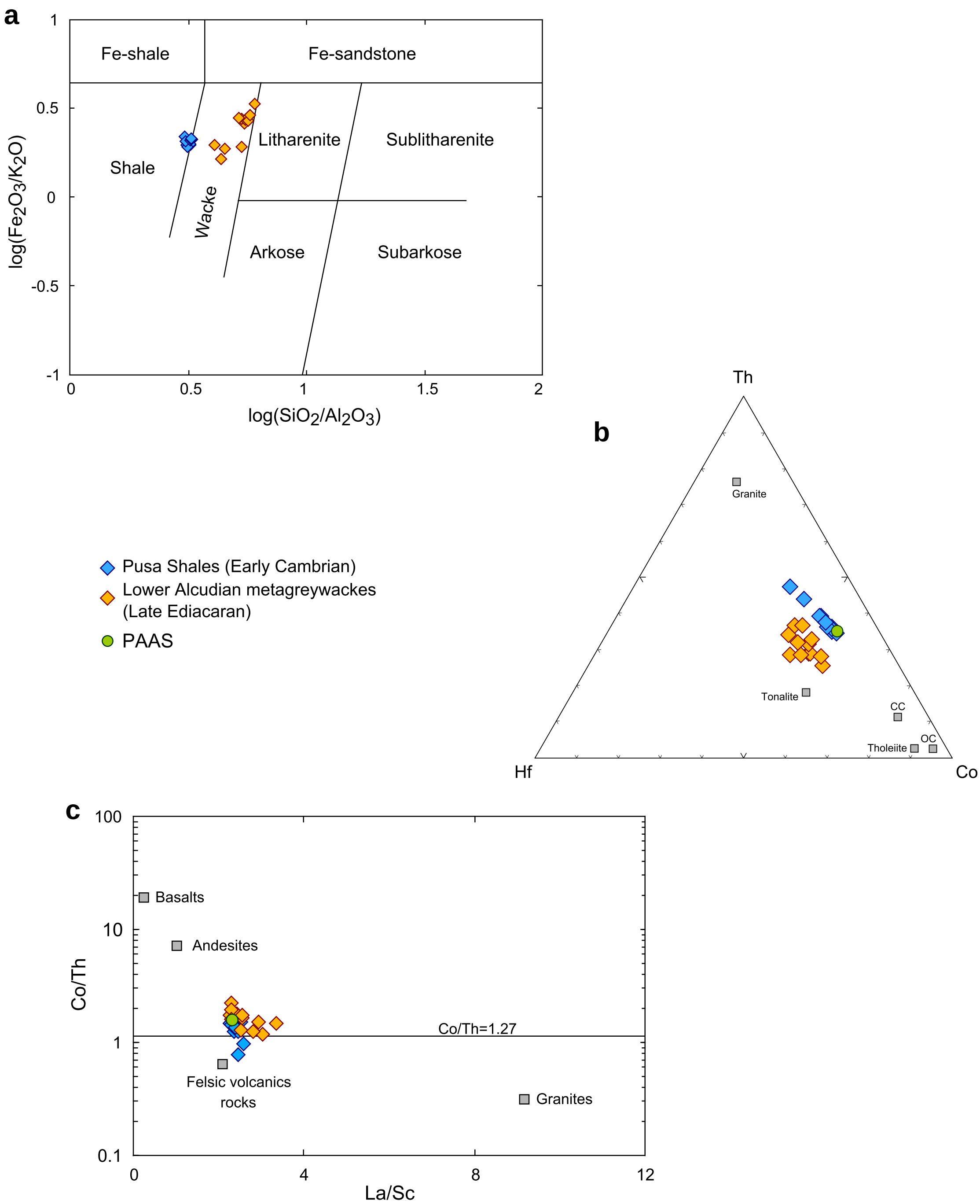

Fig. 4. Chemical diagrams for the metasedimentary rocks from the southern Central Iberian Zone (Iberian Massif). (a) Chemical classification scheme for siliciclastic sediments (Herron, 1988). (b) Th–Hf–Co ternary plot (Taylor and McLennan, 1985). CC, continental crust; OC, oceanic crust. (c) Co/Th vs La/Sc plot (average compositions of igneous rocks from Condie, 1993).

Like trace elements analysis, Sm–Nd systematics and U–Pb dating of detrital zircon have become suitable approaches to infer the evolution and the relative position of the paleo-basins, as well as the potential provenance of metasedimentary rocks (Linnemann and Romer, 2002; Linnemann et al., 2004). The Sm–Nd system has been widely used as a powerful tool to represent crustal and mantle evolution. Both elements are compatible and have low coefficients of partition in most petrogenetic processes, being rarely affected by intracrustal processes (anatexis, fractionation or metamorphism) and processes following sedimentation (diagenesis, weathering or hydrothermal processes). These processes cause minimal effects on the Sm/Nd ratio of a given sedimentary rock, being thus completely inherited from the depleted mantle (DePaolo, 1981; DePaolo and Wasserburg, 1976). Since Nd model ages (TDM) represent the average age of extraction from the depleted mantle of the constituents in a clastic rock, these ages have proved to be a reliable tool to constrain the provenance of sediments, as well as to reveal some of their pre-and post-depositional history (Allègre and Rousseau, 1984). Similarly, Nd model ages, along with detrital zircon ages have become crucial to infer the evolution of the continental crust, especially in orogenic belts (e.g., Linnemann and Romer, 2002; Linnemann et al., 2004).

4. Whole rock geochemistry

4.1. Composition and classification

4.1.1. Greywackes

Our greywacke samples show no significant chemical variations in major elements (Table 1), with SiO_2 contents (70.1 wt.%, on average) being higher than the shale samples, and lower contents of Al_2O_3, Fe_2O_3 and K_2O (13.59 wt.%, 5.14 wt.% and 2.18 wt.%, respectively). They show very low CaO content (0.61 wt.%, on average) compared to typical upper crust (4.2 wt.%). Following Crook (1974), all the greywacke samples are quartz-intermediate (K_2O/Na_2O: 0.54–1.15), and on the diagram proposed by Herron (1988) they plot into the greywacke field (Fig. 4a).

SiO_2/Al_2O_3 (4.1 to 6.0), and low K_2O/Na_2O (0.5 to 1.1) ratios reflect immature sediments, with a predominance of plagioclase over K-feldspar, and values close to those of the upper crust (4.3 and 0.9, respectively). Immaturity is also confirmed by the Al_2O_3/Na_2O (3.9–5.6) and Al_2O_3/TiO_2 (16.0–23.5) ratios, which lay within the typical range of the upper continental crust (3.9 and 30.4, respectively; Taylor and McLennan, 1985). The Rb/Sr ratio varies with weathering and diagenetic processes, being increased by the loss of Sr from plagioclase. McLennan et al. (1993) interpreted Rb/Sr values over 0.5 as related to post-depositional processes of alteration. Our greywacke samples display values between 0.4 and 0.8, very close to PAAS. A low degree of post-depositional alteration is also confirmed by relatively low CIA values (Chemical Index of Alteration, Nesbitt and Young, 1982), which range from 56 to 66 (Table 1).

The greywacke samples are characterized by $(La/Yb)_N$ (7.50, on average) and $(La/Sm)_N$ (3.22, on average) slightly lower than PAAS (9.08 and 4.02, respectively) (Table 3). Chondrite normalized (Nakamura, 1974) fractionation patterns for these samples exhibit enrichment in LREE relative to HREE, which display nearly flat patterns, with values of $(Gd/Yb)_N$ close to the unity (1.40, on average), and similar to those of the PAAS ($(Gd/Yb)_N$: 1.34). The greywacke samples, especially those collected in the Agudo–Valdemanco Anticline (CIA-21 to CIZ-24), show similar patterns to PAAS (Fig. 5a), with lower LREE values and higher dispersion of HREE abundances. All the samples show a negative Eu anomaly, whose values range from 0.60 to 0.79 (Eu/Eu*, calculated according to Taylor and McLennan, 1985).

Th/Nb ratios (between 0.8 and 1.0) obtained for the greywackes are similar to those of PAAS (0.77), while Ti/Zr (14.0–21.6) and Zr/Sc (16.0–30.7) ratios have lower and higher values than PAAS, respectively. These results point to a mixed source dominated by felsic material,

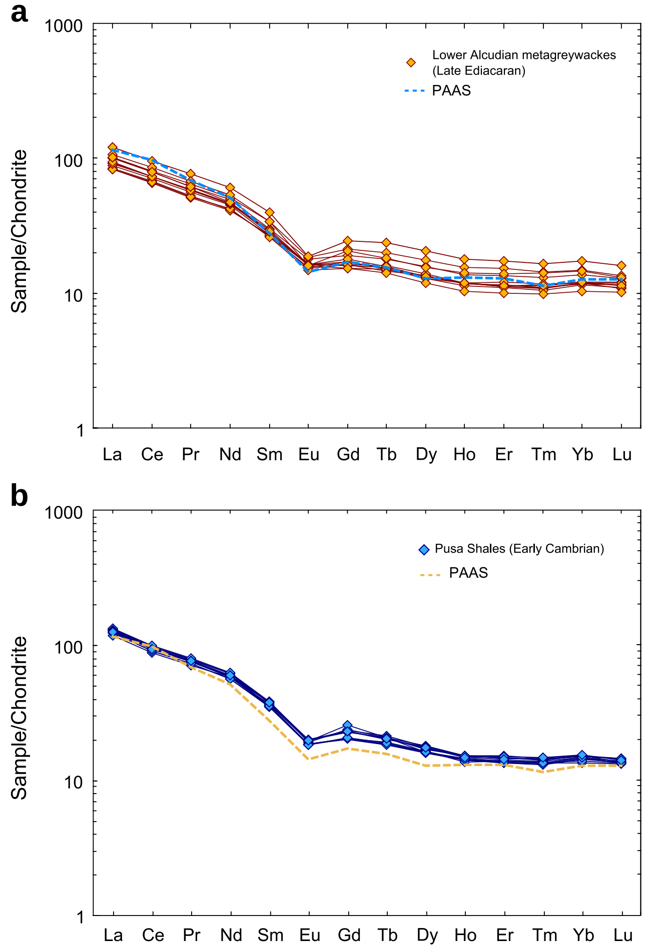

Fig. 5. Chondrite normalized rare earth element plots. (a) Late Ediacaran greywackes. (b) Early Cambrian shales. The dotted line corresponds to the PAAS (Post Archean Australian Shale; Taylor and McLennan, 1985). Normalizing values are from Nakamura (1974).

which is confirmed by lower Cr content (83 ppm, avg. value) and Ni content (37 ppm, avg. value); and by La/Th values (3.0–3.6) (Fig. 4b) higher than PAAS (2.6).

4.1.2. Shales

The most relevant geochemical feature of our shale samples is their compositional homogeneity (Table 2). They show SiO_2 values ranging between 58.59 and 61.36 wt.%, high values of Al_2O_3 (18.4–19.39 wt.%.) and low CaO (from 0.24 to 0.93 wt.%), Na_2O (1.43–2.03 wt.%.) and K_2O contents (3.34–3.66 wt.%). Fe_2O_3 (6.66–7.63 wt.%), MgO (2.51–3.00 et.%) and TiO_2 (0.72 to 0.79 wt.%) are similar to PAAS. SiO_2 and K_2O/Na_2O values (1.68–2.56) indicate that all samples are quartz-rich (Crook, 1974). According to the diagram by Herron (1988) to evaluate maturity in sedimentary rocks, all samples can be classified as shales, grouping close to the wacke field (Fig. 4a).

Al_2O_3, CaO, Na_2O and K_2O contents similar to those of PAAS make strong chemical alteration processes after sedimentation unlikely. Low values of Ti/Zr (Table 2) confirm this assertion. Alteration of plagioclase following deposition would explain the strong Sr anomaly compared to PAAS and hence the higher Rb/Sr ratio observed in these samples (average: 1.8), well above 0.5. The CIA values for shale samples vary from 69 to 74, falling within the typical values for average shales (70–75) and similar to those of PAAS (70), which is considered to represent a low to moderate degree of alteration. The Sr negative anomaly could be explained after weathering and decomposition of plagioclase during Early Cambrian times, confirmed by values of the $Al_2O_3/(CaO + Na_2O)$ ratio, ranging from 6.3 to 10.3. However, deep changes in composition are ruled out by the Th/U values (average 4.2), which are similar to the upper crust (3.8).

High MgO, Fe_2O_3 and Al_2O_3 along with lower SiO_2 content point to a mixture of sources. Very low values of CaO relative to PAAS (1.30 wt.%) on the other hand suggest a dominant pelitic contribution. Despite the high variability in the Al_2O_3 contents, positive correlations between this oxide and Fe_2O_3 and MgO indicate predominance of clay minerals and micas, confirmed by K_2O/Al_2O_3 values (0.18 average), between 0.0 and 0.3 (Cox et al., 1995).

The shale samples show very similar REE contents (Table 4), with REE values ranging from 186.4 to 206.6 ppm. They also display very similar chondrite-normalized (Nakamura, 1974) fractionation patterns (Fig. 5b), with $(La/Yb)_N$ values between 8.18 and 9.15. LREE (La–Sm) show moderate enrichment relative to HREE, with almost flat patterns, and $(Gd/Yb)_N$ values between 1.38 and 1.91. All samples present a slight negative Eu anomaly, with very homogeneous values between 0.64 and 0.70 (calculated following Taylor and McLennan, 1985), usually interpreted as an inheritance from an igneous source (Awwiller, 1994; Compton et al., 2003; McLennan and Taylor, 1991; McLennan et al., 1980). Despite some differences in abundance between samples, the REE patterns of the shales are similar to those of PAAS.

The content of trace elements is rather homogeneous and only shows very slight variations with respect to PAAS. Elements that are typically associated with heavy minerals, such as Zr, Nb, Th and U, have lower values compared to PAAS, except for Y, which is slightly higher. Co, Cu and Rb contents are similar to those of PAAS. The different Sr and Ba contents, related to PAAS, may be due to selective alteration of plagioclase relative to other feldspars. The high coefficient of correlation between Rb and K_2O ($r = 0.88$) favors the same behavior in the case of K-feldspar. Those two elements, together with Ba, seem to have remained unaffected after chemical alterations.

Shale samples show a Th/Sc ratio (Table 2) slightly lower than PAAS, indicating a mixture of sources. This statement is confirmed by values of La/Sc and Ti/Zr equal to PAAS (La/Sc = 2.4, Ti/Zr = 29.1; averages); and values of Zr/Sc slightly lower than PAAS. The concentrations of Cr (average 97.5 ppm) and Ni (average 49.2 ppm) are very similar to PAAS, but the values of Ti/Nb (297 on average) are low. Altogether these ratios confirm a contribution from different sources, although dominated by a felsic input and affected by recycling processes to some extent.

4.1.3. Th–Hf–Co diagram

A Th–Hf–Co ternary diagram (Fig. 4b) shows different patterns for both groups of rocks, with a greater scatter in the case of the greywackes, likely inherited from a more dynamic environment and fractionation effects by slight weathering and/or recycling. This diagram supports a mixed source for both the greywackes and shales, with a slight trend in the case of the shales to a more granitic average, clearly close to PAAS values. Co/Th vs. La/Sc diagram (Fig. 4c) reinforces the dominantly felsic provenance for the shales too (close to the Co/Th value of 1.27). The greywackes preserve the scatter observed in former diagrams, what together with significantly greater Eu anomalies than PAAS favor the idea of sediments eroded from an intermediate (andesite–diorite) and recycled sedimentary sources (Taylor and McLennan, 1985).

4.2. Tectonic setting

According to the results here exposed, we do not observe atypical deviations of the Ediacaran greywackes and Early Cambrian shales chemistry from reference compositions (PAAS), ruling out significant post-depositional alterations as a result of metamorphism. Likewise, the content in certain LILE (Rb, Cs) that are linked to micas and clay minerals is comparable to that of unaltered rocks, whereas low Na, Ca and Sr contents might indicate slight weathering, but with no significant consequences for using provenance and tectonic setting discrimination diagrams based on immobile trace elements (REE, Y, Zr, Ti, Nb, Th, Sc, Hf and Co).

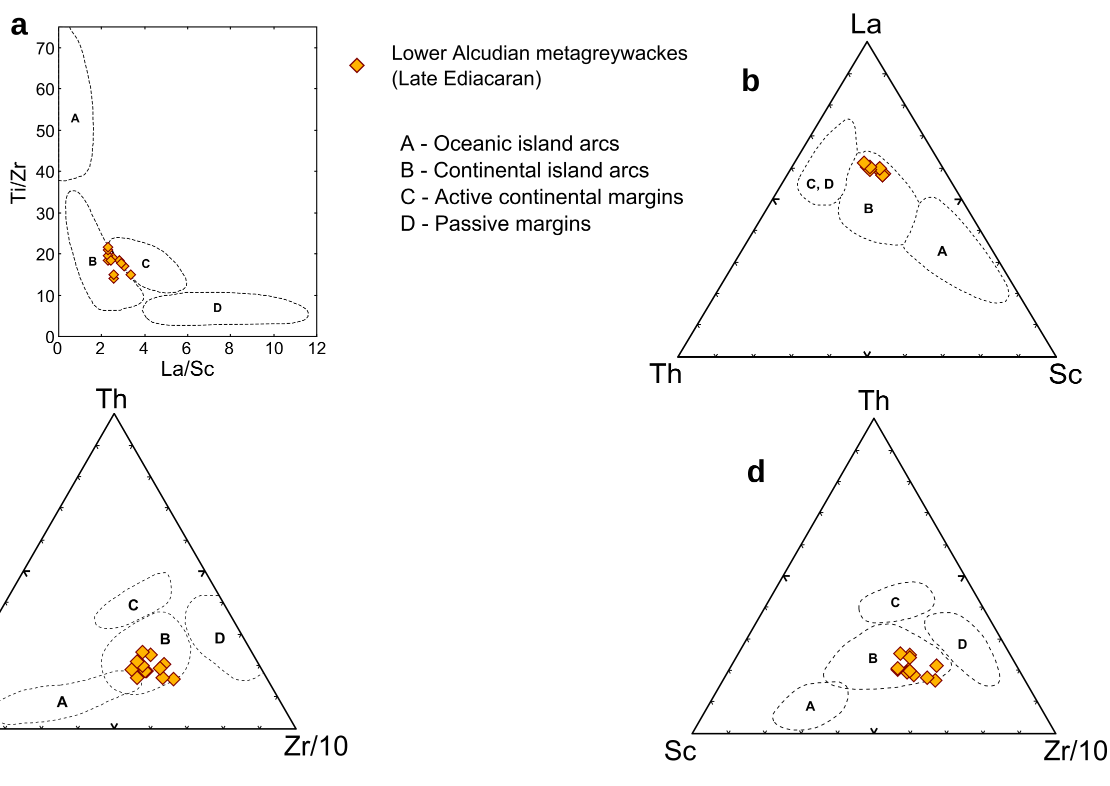

Fig. 6. Trace element diagrams with tectonic setting discrimination fields for Lower Alcudian greywackes (Bhatia and Crook, 1986).

Although tectonic setting discrimination diagrams should be used carefully, those developed by Bhatia and Crook (1986) have proved to be an invaluable tool to distinguish between four tectonic settings for sandstone deposition: (A) oceanic island arc, (B) continental island arc, (C) active continental margin, and (D) passive margin. A plot of Ti/Zr versus La/Sc clearly reveals the Late Ediacaran greywackes as deposited in an active margin (Fig. 6a). La/Sc ratios range from 2.3 to 3.3, whereas Ti/Zr ratios are all above 10 (14–21.6), fairly far from expected values of a passive geodynamic setting. Ternary diagrams (La–Th–Sc, Th–Co–Zr/10 and Th–Sc–Zr/10) suggest a similar environment of sedimentation for the greywackes, as they all plot well inside field B (active continental margin; Fig. 6b, c and d, respectively). Such results constrain the deposition of the Late Ediacaran greywackes to basins related to convergent dynamics, most likely in a continental volcanic arc built on a thinned continental margin (Bhatia and Crook, 1986).

A set of major and trace elements was normalized to PAAS following Thompson (1982) (Fig. 7). The pattern for the Ediacaran greywacke samples is consistent with the main features observed by Winchester and Max (1989) in sediments accumulated in active margins. The diagram shows a decrease in most LILE elements (Cs, Rb, Th, U, La, Ce and K_2O), generating a fractionation of positive slope, while values for HSFE elements (Zr, Hf, Sm, HREE and Sc) are close to unit (Fig. 7a). A negative TiO_2 anomaly can be observed. There is no significant positive Sr anomaly, possibly due to weak alteration in post-depositional processes, in agreement with low CIA values (63, on average) (Table 1). Significant lower Cr and Ni values suggest a mixed source, related to an evolved (felsic) volcanic arc.

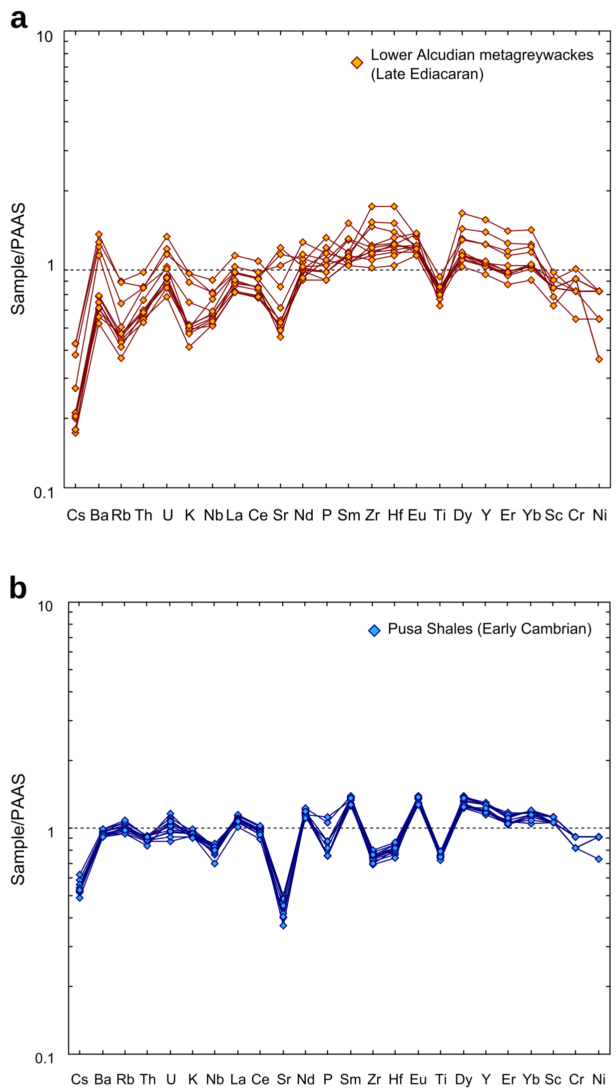

Fig. 7. PAAS-normalized trace elements diagrams. (a) Late Ediacaran greywackes. (b) Early Cambrian shales. PAAS after Taylor and McLennan (1985).

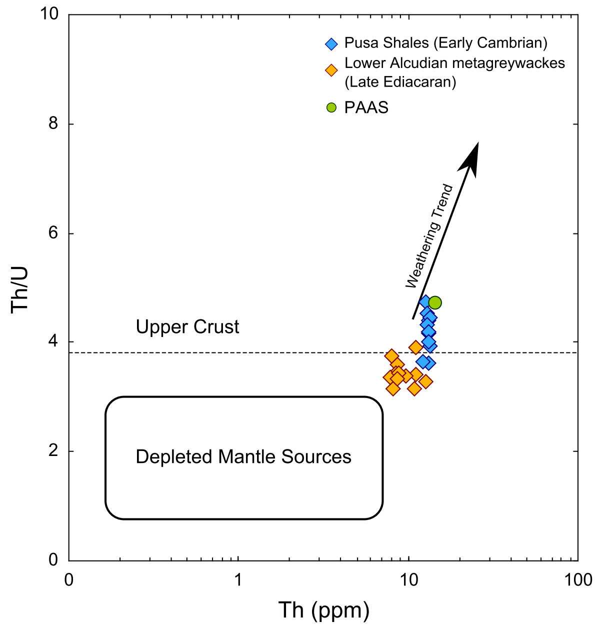

Fig. 8. Th/U versus Th plot after McLennan et al. (1993). See text for discussion.

In the shales, the patterns of major and trace elements contents normalized to PAAS are similar to those described by Winchester and Max (1989) for passive continental margins (Fig. 7b). This is typified by normalized values of Rb, Th, U, K, La, Ce and Y close to the unit, and by the existence of negative anomalies of variable intensity in the case of Sr, P and Ti. According to those patterns, the Cambrian shales may have been deposited away from an arc edifice, and thus relatively far from the areas of greatest magmatic activity and closer to emerged sections of a mainland.

In a plot of Th/U versus Th (McLennan et al., 1993), the two sedimentary sequences present clearly different trends (Fig. 8). The Cambrian shales display Th/U values above 3.5–4.0, typical for (i) igneous rocks emplaced at upper continental crust, (ii) cratonic provenance, and (iii) certain alteration and recycling. On the contrary, the Ediacaran greywackes show lower Th/U values, lower Th, and slightly lower U abundances (Table 1), all of which are probably inherited from the source rocks and associated with a depleted mantle (juvenile) contribution (Fig. 8).

4.3. Sm–Nd isotope geochemistry

Sm–Nd isotopic data obtained from the greywackes and shales are given in Table 5 and 6 and plotted in Fig. 9. Geochronological data for calculation of $\varepsilon Nd_{(T)}$ were estimated according to stratigraphic and structural features of the selected samples. The reference age considered for the sedimentation of the Ediacaran greywackes and Cambrian shales is 565 Ma and 530 Ma, respectively (see section Geological setting). The analyzed rocks show $^{147}Sm/^{144}Nd$ ratios varying from 0.1161 to 0.1315, which are normal values for clastic sediments (0.1 to 0.13; Zhao et al., 1992), and similar to those of continental crust (~0.12). These ratios are also lower than the upper limit ($^{147}Sm/^{144}Nd$ = 0.165) proposed by Stern (2002) as suitable to perform Nd TDM calculations.

The samples show relatively uniform $\varepsilon Nd_{(0)}$ values within each group (an average of −9.7 and −7.1 for the shales and greywackes, respectively). In the case of the Early Cambrian shales, $\varepsilon Nd_{(530)}$ values

Table 5
Whole rock Nd isotope data of Lower Alcudian greywackes (Late Ediacaran).

	Sm	Nd	$^{147}Sm/^{144}Nd$	$^{143}Nd/^{144}Nd$	$SErr*10^{-6}$	$\varepsilon Nd_{(0)}$	$\varepsilon Nd_{(565)}$[a]	T_{DM} (Ma)[b]
CIA-13	3.38	16.74	0.1220	0.512280	2	−7.0	−1.6	1269
CIA-14	3.78	18.81	0.1214	0.512269	2	−7.2	−1.8	1278
CIA-15	3.28	16.10	0.1230	0.512291	2	−6.8	−1.4	1263
CIA-16	3.18	15.57	0.1236	0.512293	2	−6.7	−1.5	1268
CIA-17	3.68	18.18	0.1223	0.512290	2	−6.8	−1.4	1256
CIA-18	3.24	15.79	0.1242	0.512293	1	−6.7	−1.5	1277
CIA-19	3.49	17.07	0.1236	0.512277	2	−7.0	−1.8	1295
CIA-20	3.40	16.77	0.1224	0.512266	1	−7.2	−1.9	1296
CIA-21	6.33	29.50	0.1298	0.512310	2	−6.4	−1.6	1329
CIA-22	6.69	31.95	0.1265	0.512305	2	−6.5	−1.4	1290
CIA-23	5.33	26.38	0.1221	0.512258	2	−7.4	−2.0	1305
CIA-24	4.86	25.32	0.1161	0.512188	2	−8.8	−3.0	1334

[a] εNd(t) calculated for 565 Ma.
[b] Nd model ages calculated according to DePaolo (1981).

range between −5.2 and −4.0 (Table 6), clearly lower than those of the Late Ediacaran greywackes, which vary between −3.0 and −1.4 (Table 5). Nd TDM model ages are Mesoproterozoic and vary between 1444 and 1657 Ma (Table 6) with an average value of 1516 Ma for the Pusa Shales; and between 1256 and 1334 Ma with an average value of 1288 Ma for the Ediacaran greywackes (Table 5).

5. Discussion

A series of magmatic arcs formed on the periphery of Gondwana during the Neoproterozoic (Cadomian–Pan-African cycle) and Cambrian (c 750–500 Ma) are considered one of the main sediment suppliers for the sedimentary sequences that make the pre-Silurian basement units of Western and Central Europe (Albert et al., 2015; Murphy and Nance, 2002; Murphy et al., 2006; Stampfli and Borel, 2002; Von Raumer and Stampfli, 2008; Von Raumer et al., 2015). The Iberian Massif represents a good example for the evolution of a Late Ediacaran active margin in the northern margin of West-Central Gondwana and its subsequent transition to a passive margin in Cambrian–Ordovician times (Murphy et al., 2006; Nance et al., 2008, 2010).

The late stages of the Cadomian orogeny have been identified in the CIZ as responsible for an intra-Alcudian unconformity of Precambrian–Cambrian age (Martínez Poyatos, 2002; Martínez Poyatos et al., 2014; Pieren and García Hidalgo, 1999; Pieren et al., 1987; Simancas et al., 2004; Talavera et al., 2015). This tectonic event could explain the different geochemical and isotopic records found in the two series studied in this work. In this regard, it has been proposed that the Neoproterozoic–Cambrian sequences of the CIZ record an evolving geodynamic setting (Pieren, 2000; Rodríguez Alonso et al., 2004b). Moreover, some authors have suggested a division of the CIZ into two different domains sharing a common depositional history (Orejana et al., 2015; Villaseca et al., 2014). Our results confirm the aforementioned difference between the northern and southern sequences on the basis of the presence of a juvenile contribution for the Late Ediacaran greywackes collected close to the southern margin of CIZ. But, more importantly, the data here presented provide compelling geochemical evidence about the contrasted paleogeographic scenarios for the deposition of sediments in the CIZ during the Ediacaran and then the Cambrian.

Our geochemical results point to an active margin setting as the most reasonable scenario for the deposition of the Ediacaran–Cambrian series of the CIZ. Trace element diagrams of the Ediacaran greywackes indicate a clear affinity to a continental island arc (Fig. 6). On the other hand, although Early Cambrian sequences here exposed are not represented by wacke-type samples, limiting a complete comparison of source composition and tectonic setting, an approach has been achieved by correlating major and trace geochemical values with those reported for the four main geodynamic settings (Fig. 7). Considering their composition, the Cambrian shales display typical patterns for a passive margin environment. Yet, according to Bhatia and Crook (1986), the lower content of Zr in shales, and therefore lower Zr/Nb and Zr/Th ratios, and relatively higher Ba, Rb, Sr, V and Sc abundances are more compatible with an active geodynamic environment, which is confirmed by La/Th ratios well above 2 (3.3 average value).

The Nd model ages of the Ediacaran greywackes (1256–1334 Ma) are clearly younger than those obtained for the Early Cambrian shales (1444–1657 Ma) (Fig. 9). Younger Nd model ages in greywackes can be explained by a larger supply of juvenile material, as also indicated by higher $\varepsilon Nd_{(T)}$ values (−3.0 to −1.5) than in the Cambrian shales (−5.2 to −4.1). In the latter, the older Nd model ages are compatible with the presence of more recycled crustal material. A larger juvenile (mantle-derived) contribution in the Neoproterozoic greywackes locates the basins relatively closer to the major axis of magmatic activity of the arc

Table 6
Whole rock Nd isotope data of Pusa Shales (Early Cambrian).

	Sm	Nd	$^{147}Sm/^{144}Nd$	$^{143}Nd/^{144}Nd$	$SErr*10^{-6}$	$\varepsilon Nd_{(0)}$	$\varepsilon Nd_{(530)}$[a]	T_{DM} (Ma)[b]
CIA-1	4.74	21.78	0.1315	0.512147	1	−9.6	−5.2	1657
CIA-2	4.64	21.71	0.1290	0.512162	2	−9.3	−4.7	1583
CIA-3	4.38	21.71	0.1219	0.512172	1	−9.1	−4.0	1444
CIA-4	4.36	22.13	0.1191	0.512115	1	−10.2	−5.0	1493
CIA-5	4.80	23.67	0.1224	0.512144	2	−9.6	−4.6	1498
CIA-6	4.46	22.03	0.1222	0.512125	2	−10.0	−5.0	1527
CIA-7	4.61	22.68	0.1228	0.512148	1	−9.6	−4.6	1499
CIA-8	4.31	21.49	0.1213	0.512134	1	−9.8	−4.7	1496
CIA-9	4.86	23.23	0.1265	0.512159	1	−9.3	−4.6	1542
CIA-10	4.52	22.43	0.1218	0.512136	2	−9.8	−4.7	1501
CIA-11	4.32	21.34	0.1224	0.512166	1	−9.2	−4.2	1462
CIA-12	3.94	19.86	0.1200	0.512129	2	−9.9	−4.8	1485

[a] $\varepsilon Nd_{(T)}$ calculated for 530 Ma.
[b] Nd model ages calculated according to DePaolo (1981).

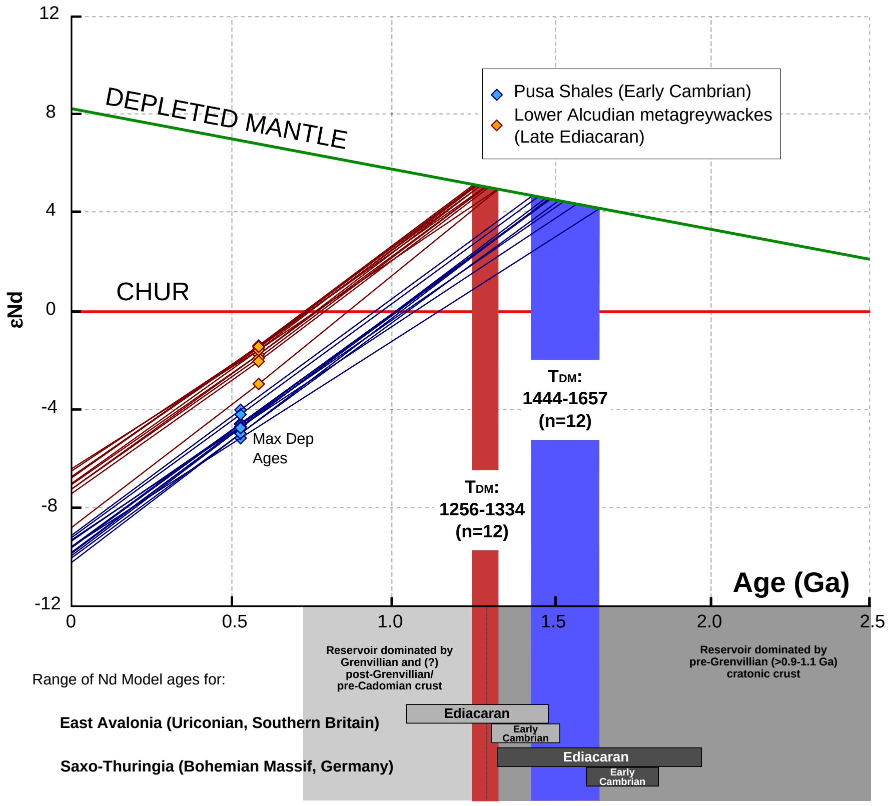

Fig. 9. TDM model ages (DePaolo, 1981) of the Late Ediacaran greywackes and the Early Cambrian shales of the southern CIZ (Iberian Massif). Diamonds show the εNd values at 565 Ma and 530 Ma, reference ages for the deposition of the Late Ediacaran greywackes and the Early Cambrian shales, respectively. Data source for comparative model ages from different regions taken from Linnemann and Romer (2002) and Thorogood (1990).

system. Rodríguez Alonso et al. (2004b) found clear evidence of magmatism coeval with Neoproterozoic–Cambrian sedimentation, strongly suggesting a tectonically and magmatically active environment as the direct contributor to the metasedimentary rocks of the CIZ. Our geochemical results accord well with this active environment. Whereas tectonic setting discrimination diagrams indicate a deposition environment linked to an active arc system, the lack of strong geochemical evidence of a mafic source for the Ediacaran greywackes suggests a mature active margin.

TDM ages are notably older than the deposition age. This is in agreement with a mixed source for the sediments that would consist of a juvenile (arc-derived) contribution and a much older (cratonic) input. Older TDM ages and lower $\varepsilon Nd_{(T)}$ values in the Paleozoic shales than in the Precambrian greywackes reveal that during the Early Cambrian the juvenile input either waned or was outpaced by more evolved and older crustal material, probably coming from the emergent Gondwana hinterland. Trace element discrimination diagrams (Fig. 7) suggest a passive margin-like environment for the Early Cambrian series. In order to reconcile all these observations, we support previous models that proposed a wide back-arc as the most likely setting for the autochthonous series of the CIZ during the Early Paleozoic (e.g. Orejana et al., 2015). Accordingly, the Cambrian series must have been laid down closer to the mainland than to the main axis of volcanic arc activity. Such a scenario explains the more homogeneous and recycled character of the sediments and the controversial trace element results that indicate an active geodynamic setting. A wide back-arc basin is in agreement with the accepted transition from a convergent regime (Cadomian arc) to an extensional regime (Nance et al., 2010). These arc-related basins along the northern margin of Gondwana would have been filled with different proportions of crustal recycled materials from different sources, more or less close to the areas of major magmatic activity.

Despite the relative scarcity of Nd model ages from comparable lithologies of the same age in the Variscan and East Avalonia terranes, our results do not disagree with those from other regions of Europe (Fig. 9). Other Variscan (Saxo-Thuringia, Bohemian Massif — Germany; Linnemann and Romer, 2002; Linnemann et al., 2004) and East Avalonian (Uriconian, southern Britain. Thorogood, 1990) tectonostratigraphic terranes show a relative increase in the Nd model ages in younger stratigraphic units, presumably as a result of a greater contribution from older sources. As in the case of the Ediacaran and Cambrian transition in the CIZ, εNd results show a relative drop in Ediacaran Saxo-Thuringia and Uriconian Ediacaran relative to Cambrian sedimentary units, probably linked with the supply of different proportion of juvenile arc-related material. Cambrian sediments show less positive values of εNd, probably inherited from reworking of older sediments and long-established continental crust. Nd model ages for the CIZ here presented are in agreement with a similar cratonic source to Saxo-Thuringia sedimentary units (Fig. 9), with a progressive westward decrease of the T_{DM} along the Avalonian–Cadomian arc, according to Linnemann and Romer (2002).

An extensive analysis of U–Pb detrital zircon populations in the Iberian Massif (Díez Fernández et al., 2010, 2012; Fernández Suárez et al., 2000, 2002, 2014; Orejana et al., 2015; Pereira et al., 2012; Ugidos et al., 2003b) has shown a wide range of potential provenance sources for the Late Ediacaran–Early Cambrian sandstones. The presence or absence of Stenian–Tonian zircon populations has provided an important clue in interpreting tentatively the paleogeographic positions of the different Iberian terranes. According to the Nd model ages here presented, the West Africa Craton is envisaged as the main cratonic source for the metasedimentary rock sequences of the CIZ. The geochemical and isotopic results here reported are in agreement with the development of paleo-basins along the northern margin of Gondwana associated with the activity of a mature and evolved magmatic arc during the Late Precambrian and Early Cambrian. The record of this transition in the CIZ depicts an evolving tectonic scenario from a convergent and active setting to an extensional context, prior to the development of a Cambro-Ordovician passive margin. This transition represents a drift of the major magmatic activity of the arc system to a more distal position from the Gondwana margin along the Late Neoproterozoic, while the basins towards the mainland remain very distant from the main axis of volcanic arc activity during Early Cambrian times.

Acknowledgments

Financial support has been provided by the Spanish projects CGL2012-34618 and CGL2013-48877 (Ministerio de Economía y Competitividad). Insightful reviews of the manuscript performed by anonymous referees are gratefully acknowledged, as well as the important editorial work of Brendan Murphy aimed at improving the final version of the present work.

References

Albert, R., Arenas, R., Gerdes, A., Sánchez Martínez, S., Fernández-Suárez, J., Fuenlabrada, J.M., 2015. Provenance of the Variscan Upper Allochthon (Cabo Ortegal Complex, NW Iberian Massif). Gondwana Res. 28, 1434–1448. http://dx.doi.org/10.1016/j.gr.2014.10.016.

Allègre, C.J., Rousseau, D., 1984. The growth of the continent through geological time studies by Nd isotope analysis of shales. Earth Planet. Sci. Lett. 67, 19–34.

Alvarez Nava, H., García Casquero, J.L., Gil Toja, A., Hernández Urroz, J., Lorenzo Alvarez, S., López Díaz, F., Mira López, M., Monteserín, V., Nozal, F., Pardo, M.V., Picart, J., Robles, R., Santamaría, J., Sole, F.J., 1988. Unidades litoestratigráficas de los materiales Precámbrico-Cámbricos en la mitad suroriental de la Zona 917 Centro-Ibérica. II Congreso Geológico de España, SGE, Granada 1, pp. 19–22.

Arenas, R., Farias, P., Gallastegui, G., Gil Ibarguchi, J.I., González Lodeiro, F., Klein, E., Marquínez, J., Martín Parra, L.M., Martínez Catalán, J.R., Ortega, E., Pablo Maciá, J.G., Peinado, M., Rodríguez Fernández, L.R., 1988. Características geológicas y significado de los dominios que componen la Zona de Galicia-Trás-os-Montes, II Congreso Geológico de España. Simposios. Temas Geol. Min. 9, 75–84.

Armstrong-Altrin, J.S., Verma, S.P., 2005. Critical evaluation of six tectonic setting discrimination diagrams using geochemical data of Neogene sediments from known tectonic settings. Sediment. Geol. 177 (1–2), 115–129.

Awwiller, D.N., 1994. Geochronology and mass transfer in gulf coast mudrocks (South-Central Texas, USA): Rb–Sr, Sm–Nd and REE systematics. Chem. Geol. 116, 61–84.

Bhatia, M.R., 1983. Plate tectonics and geochemical composition of sandstones. The Journal of Geology 91, 611–627.

Bhatia, M.R., Crook, K.A.W., 1986. Trace elements characteristics of greywackes and tectonic setting discrimination of sedimentary basins. Contrib. Mineral. Petrol. 92, 181–193.

Carrington da Costa, J., 1950. Noticia sobre uma carta geologica do Buçaco, de Nery Delgado. Publicación Especial de la Comision de Servicio Geológico de Portugal, Lisboapp. 1–27.

Compton, J.S., White, R.A., Smith, M., 2003. Rare earth element behavior in soils and salt pan sediments of a semi-arid granitic terrain in the Western Cape, South Africa. Chem. Geol. 20, 239–255.

Condie, K.C., 1993. Chemical composition and evolution of the upper continental crust: contrasting results from surface samples and shales. Chem. Geol. 104, 1–37.

Condie, K.C., Wronkiewicz, D.J., 1990. A new look at the Archean–Proterozoic boundary: sediments and the tectonic setting constraint. In: Naqvi, S.M. (Ed.), Precambrian Continental Crust and Its Economic Resources. Elsevier, Amsterdam, pp. 61–84.

Cortijo, I., Mus, M.M., Jensen, S., Palacios, T., 2010. A new species of Cloudina from the terminal Ediacaran of Spain. Precambrian Res. 176, 1–10.

Cox, R., Lowe, D.R., Cullers, R.L., 1995. The influence of sediment recycling and basement composition on evolution of mudrock chemistry in the southwestern, United States. Geochim. Cosmochim. Acta 59 (14), 2919–2940.

Crook, K.A.W., 1974. Lithogenesis and geotectonics: the significance of compositional variations in flysch arenites (greywackes). In: Doti, R.H., Shaver, R.H. (Eds.), Modern and Ancient Geosynclinal Sedimentation. Society of Economic Palaeontologists and Mineralogists Special Publication vol. 19, pp. 304–310.

DePaolo, D.J., 1981. Neodymium isotopes in the Colorado Front Range and crustal–mantle evolution in the Proterozoic. Nature 291, 193–196.

DePaolo, D.J., Wasserburg, G.J., 1976. Nd isotopic variations and petrogenetic models. Geophys. Res. Lett. 3, 249–252.

Díez Balda, M.A., 1986. El Complejo Esquisto-Grauváquico, las series paleozoicas y la estructura hercínica al Sur de Salamanca (Ph. D Thesis) Thesis Universidad de Salamanca, Salamanca (162 pp.).

Díez Balda, M.A., Rodríguez Alonso, M.D., Liñán, E., Gámez Vintaned, J.A., López Díaz, F., Moreno, F., Moreno-Eiris, E., Perejón, A., Pieren, A., Martínez Poyatos, D., Vegas, R., 2004. La transgresión cámbrica. In: Vera, J.A. (Ed.), Geología de España. SGE-IGME, Madrid, p. 81.

Díez Fernández, R., Arenas, R., 2015. The Late Devonian Variscan suture of the Iberian Massif: a correlation of high-pressure belts in NW and SW Iberia. Tectonophysics 654, 96–100.

Díez Fernández, R., Martínez Catalán, J.R., Gerdes, A., Abati, J., Arenas, R., Fernández-Suárez, J., 2010. U–Pb ages of detrital zircons from the Basal allochthonous units of NW Iberia: provenance and paleoposition on the northern margin of Gondwana during the Neoproterozoic and Paleozoic. Gondwana Res. 18, 385–399.

Díez Fernández, R., Martínez Catalán, J.R., Arenas, R., Abati, J., Gerdes, A., Fernández-Suárez, J., 2012. U–Pb detrital zircon analysis of the lower allochthon of NW Iberia: age constraints, provenance and links with the Variscan mobile belt and Gondwanan cratons. J. Geol. Soc. Lond. 169, 655–665.

Díez Fernández, R., Gómez Barreiro, J., Martínez Catalán, J.R., Ayarza, P., 2013. Crustal thickening and attenuation as revealed by regional fold interference patterns: Ciudad Rodrigo basement area (Salamanca, Spain). J. Struct. Geol. 46, 115–128.

Díez Montes, A., Navidad, M., González Lodeiro, F., Martínez Catalán, J.R., 2004. El Ollo de Sapo. In: Vera, J.A. (Ed.), Geología de España. SGE-IGME, Madrid, pp. 69–72.

Farias, P., Gallastegui, G., Gonzalez Lodeiro, F., Marquinez, J., Martin Parra, L.M., Martinez Catalan, J.R., Pablo Macia, J.G., Rodriguez Fernandez, L.R., 1987. Aportaciones al conocimiento de la litoestratigrafia y estructura de Galicia Central. Memorias del Museo e Laboratorios Mineros y Geologicos, Univeridade Porto 1 pp. 411–431.

Feng, R., Kerrich, R., 1990. Geochemistry of fine-grained clastic sediments in the Archean Abitibi greenstones belt, Canada: implications for provenance and tectonic setting. Geochim. Cosmochim. Acta 54, 1061–1081.

Fernández-Suárez, J., Gutiérrez-Alonso, G., Jenner, G.A., Tubrett, M.N., 2000. New ideas on the Proterozoic–Early Palaeozoic evolution of NW Iberia: insights from U–Pb detrital zircon ages. Precambrian Res. 102, 185–206.

Fernández-Suárez, J., Gutiérrez-Alonso, G., Pastor-Galán, D., Hofmann, M., Murphy, J.B., Linnemanm, U., 2014. The Ediacaran–Early Cambrian detrital zircon record of NW Iberia: possible sources and paleogeographic constraints. Int. J. Earth Sci. 103 (5), 1335–1357.

Fernández-Suárez, J., Gutiérrez-Alonso, G., Jeffries, T.E., 2002. The importance of along-margin terrane transport in northern Gondwana: insights from detrital zircon parentage in Neoproterozoic rocks from Iberia and Brittany. Earth Planet. Sci. Lett. 204, 75–88.

Fuenlabrada, J.M., Arenas, R., Sánchez Martínez, S., Díaz García, F., Castiñeiras, P., 2010. A peri-Gondwanan arc in NW Iberia. I: isotopic and geochemical constraints on the origin of the arc—a sedimentary approach. Gondwana Res. 17, 338–351.

Fuenlabrada, J.M., Arenas, R., Díez Fernández, R., Sánchez Martínez, S., Abati, J., López Carmona, A., 2012. Sm–Nd isotope geochemistry and tectonic setting of the metasedimentary rocks from the basal allochthonous units of NW Iberia (Variscan suture, Galicia). Lithos 148, 196–208.

García Hidalgo, J.F., 1993. Las pistas fósiles de los anticlinales de Alcudia y Abenójar (Zona Centroibérica). Edad de las series. Geogaceta 14, 57–59.

García-Hidalgo, J.F., Pieren Pidal, A.P., Olivé Davó, A., Carbajal Menéndez, A., 1993. Geologic map and memory no 779 "Villanueva de La Serena". Geologic Map of Spain 1: 50.000 (M.A.G.N.A. Serie)IGME, Madrid.

Gutiérrez-Alonso, G., Fernández-Suárez, J., Jeffries, T.E., Jenner, G.A., Tubrett, M.N., Cox, R., Jackson, S.E., 2003. Terrane accretion and dispersal in the northern Gondwana margin. An early Paleozoic analogue of a long-lived active margin. Tectonophysics 365, 221–232.

Henderson, P., 1982. Inorganic Geochemistry. Pergamon Press, Oxford.

Herron, M.M., 1988. Geochemical classification of terrigenous sands and shales from core or log data. J. Sediment. Petrol. 58, 820–829.

Holland, H.D., 1978. The Chemistry of the Atmosphere and Oceans. Wiley, New York (351 pp.).

Jensen, S., Palacios, T., Martí Mus, M., 2007. A brief review of the fossil record of the Ediacaran–Cambrian transition in the area of Montes de Toledo-Guadalupe, Spain. In: Komarover, P., Vickers-Rich (Eds.), The Rise and Fall of the Ediacaran Biota. Geological Society of London, London, UK, pp. 223–235.

Julivert, M., Fontboté, J.M., Ribeiro, A., Conde, L., 1974. Mapa tectónico de la Península Ibérica y Baleares a escala 1:1.000.000 y memoria explicativa. IGME, Madrid.

Liñán, E., Palacios, T., Perejón, A., 1984. Precambrian–Cambrian boundary and correlation from southwestern and central part of Spain. Geol. Mag. 131, 221–228.

Liñán, E., Gonzalo, R., Palacios, T., Gómez Vintaned, J.A., Ugidos, J.M., Mayoral, E., 2002. Cambrian. In: Gibbons, W., Moreno, T. (Eds.), The Geology of Spain. The Geological Society, London, pp. 17–29.

Linnemann, U., Romer, Rolf L., 2002. The Cadomian Orogeny in Saxo-Thuringia, Germany: geochemical and Nd–Sr–Pb isotopic characterization of marginal basins with constraints to geotectonic setting and provenance. Tectonophysics 352 (1–2), 33–64.

Linnemann, U., Neal, J., McNaughton, Rolf L., Romer, Michael Gehmlich, Drost, Kerstin, Tonk, Christian, 2004. West African provenance for Saxo-Thuringia (Bohemian Massif): did Armorica ever leave pre-Pangean Gondwana? — U/Pb-SHRIMP zircon evidence and the Nd-isotopic record. Int. J. Earth Sci. 93 (5), 683–705.

Lotze, F., 1945. Zur Gliederung der Vadziden der Iberischen Meseta. Geotekt. Forsch. 6, 78–92.

Lugmair, G.W., Shimamura, T., Lewis, R.S., Anders, E., 1983. Sm-146 in the early solar-system — evidence from neodymium in the Allende meteorite. Science 222, 1015–1018.

Martín Parra, L.M., González Lodeiro, F., Martínez Poyatos, D., Matas, J., 2006. The Puente Génave–Castelo de Vide Shear Zone (southern Central Iberian Zone, Iberian Massif): geometry, kinematics and regional implications. Bull. Soc. Geol. Fr. 177, 191–202.

Martínez Catalán, J.R., 2011. Are the oroclines of the Variscan belt related to late Variscan strike-slip tectonics? Terra Nova 23, 241–247.

Martínez Catalán, J.R., Arenas, R., Abati, J., Sánchez Martínez, S., Díaz García, F., Fernández-Suárez, J., González Cuadra, P., Castineiras, P., Gómez Barreiro, J., Díez Montes, A., González Clavijo, E., Rubio Pascual, F.J., Andonaegui, P., Jeffries, T.E., Alcock, J.E., Díez Fernández, R., López Carmona, A., 2009. A rootless suture and the loss of the roots of a mountain chain: the Variscan belt of NW Iberia. Compt. Rendus Geosci. 341, 114–126.
Martínez Poyatos, D.J., 2002. Estructura del borde meridional de la Zona Centroibérica, y su relación con el contacto entre las zonas Centroibérica y de Ossa Morena. Laboratorio Xeolóxico de Laxe, serie Nova Terra 18 (295 pp.).
Martínez Poyatos, D., Talavera, C., Montero, P., González Lodeiro, F., 2014. The intra-Alcudian (Cadomian) angular unconformity in Central Iberia: constraints from U–Pb detrital zircon ages. Gondwana 15 Abstracts Book, p. 108.
McLennan, S.M., Taylor, S.R., 1991. Sedimentary rocks and crustal evolution: tectonic setting and secular trends. The Journal of Geology 99, 1–21.
McLennan, S.M., Nance, W.B., Taylor, S.R., 1980. Rare earth element-thorium correlations in sedimentary rocks and the composition of the continental crust. Geochim. Cosmochim. Acta 44, 1833–1839.
McLennan, S.M., Taylor, S.R., Eriksson, K.A., 1983. Geochemistry of Archaean shales from the Pilbara Supergroup, Western Australia. Geochim. Cosmochim. Acta 47 (7), 1211–1222.
McLennan, S.M., Taylor, S.R., McCulloch, M.T., Maynard, J.B., 1990. Geochemical and Nd–Sr isotopic composition of deep-sea turbidites: crustal evolution and plate tectonic associations. Geochim. Cosmochim. Acta 54, 2015–2050.
McLennan, S.M., Hemming, S.R., McDaniel, D.K., Hanson, G.N., 1993. Geochemical approaches to sedimentation, provenance and tectonics. In: Johnssons, M.J., Basu, A. (Eds.), processes controlling the composition of clastic sediments. Geol. Soc. Am. Spec. Pap. 284, 21–40.
Murphy, J.B., Nance, R.D., 2002. Sm–Nd isotopic systematics as tectonic tracers: an example from West Avalonia in the Canadian Appalachians. Earth Sci. Rev. 59 (1–4), 77–100.
Murphy, J.B., Gutiérrez-Alonso, G., Nance, R.D., Fernández-Suárez, J., Keppie, J.D., Quesada, C., Strachan, R.A., Dostal, J., 2006. Origin of the Rheic Ocean: rifting along a Neoproterozoic suture? Geology 34, 325–328.
Nägler, T.F., Schiller, H.J., Gebauer, D., 1995. Evolution of the Western European continental crust: implications from Nd and Pb isotopes in Iberian sediments. Chem. Geol. 121, 345–357.
Nakamura, N., 1974. Determination of REE, Ba, Fe, Mg, Na and K in carbonaceous and ordinary chondrites. Geochim. Cosmochim. Acta 38, 757–775.
Nance, R.D., Murphy, J.B., Strachan, R.A., Keppie, J.D., Gutierrez-Alonso, G., Fernandez-Suarez, J., Quesada, C., Linnemann, U., D'Lemos, R., Pisarevsky, S.A., 2008. Neoproterozoic–early Palaeozoic tectonostratigraphy and palaeogeography of the peri-Gondwanan terranes: Amazonian vs West African connections. Geol. Soc. Lond., Spec. Publ. 297 (1), 345–383.
Nance, R.D., Gabriel Gutiérrez-Alonso, J.D., Keppie, J.D., Linneman, U., Murphy, J.B., Quesada, C., Strachan, R.A., Woodcock, N.H., 2010. Evolution of the Rheic Ocean. Gondwana Res. 17, 194–222.
Nesbitt, H.W., Young, G.M., 1982. Early Proterozoic climates and plate motions inferred from major element chemistry of lutites. Nature 299, 715–717.
Nesbitt, H.W., Markovics, G., Price, R.C., 1980. Chemical processes affecting alkalis and alkali earths during continental weathering. Geochim. Cosmochim. Acta 44, 1659–1666.
O'Nions, R.K., Carter, S.R., Evensen, N.M., Hamilton, P.J., 1979. Geochemical and cosmochemical applications of Nd isotope analysis. Annu. Rev. Earth Planet. Sci. 7, 11–38.
Orejana, D., Merino Martínez, E., Villaseca, C., Andersen, T., 2015. Ediacaran–Cambrian paleogeography and geodynamic setting of the Central Iberian Zone: constraints from coupled U–Pb–Hf isotopes of detrital zircons. Precambrian Res. 261, 234–251.
Pastor-Galán, D., Gutiérrez-Alonso, G., Fernández-Suárez, J., Murphy, J.B., Nieto, F., 2013. Tectonic evolution of NW Iberia during the Paleozoic inferred from the geochemical record of detrital rocks in the Cantabrian Zone. Lithos 182–183, 211–228.
Pereira, M.F., Linnemann, U., Hofmann, M., Chichorro, M., Solá, A.R., Medina, J., Silva, J.B., 2012. The provenance of Late Ediacaran and Early Ordovician siliciclastic rocks in the Southwest Central Iberian Zone: constraints from detrital zircon data on northern Gondwana margin evolution during the late Neoproterozoic. Precambrian Res. 192–195, 166–189.
Pieren Pidal, A.P., 2000. Las sucesiones anteordovícicas de la región oriental de la provincial de Badajoz y área contigua de la de Ciudad Real. Thesis Universidad Complutense Madrid, Ph. D (379 pp.).
Pieren, A.P., García Hidalgo, J.F., 1999. El Alcudiense Superior del anticlinal de Alcudia revisitado (Ciudad Real, España Central). XV Reunión de Geología del Oeste Peninsular (International Meeting on Cadomian Orogens). Annual Meeting of IGCP Project 376 (Laurentia–Gondwana Connections Before Pangea), Extended Abstracts, pp. 205–214.
Pieren, A.P., Pineda, A., Herranz, P., 1987. Discordancia intra-Alcudiense en el anticlinal de Agudo. Geogaceta 2, 26–29.
Pieren, A.P., Herranz Araujo, P., García Gil, S., 1991. Evolución de los depósitos continentales del Proteorozoico superior en "La Serena", Badajoz (ZCI). Cuadernos do Laboratorio Xeolóxico de Laxe 16 pp. 179–191.
Quesada, C., 1991. Geological constraints on the Paleozoic tectonic evolution of tectonostratigraphic terranes in the Iberian Massif. Tectonophysics 185, 225–245.
Rodríguez Alonso, M.D., Díez Balda, M.A., Perejón, A., Pieren, A., Liñán, E., López Díaz, F., Moreno, F., Gámez Vintaned, J.A., González Lodeiro, F., Martínez Poyatos, D., Vegas, R., 2004a. Dominio del Complejo esquisto-grauváquico. Estratigrafía. La secuencia litoestratigráfica del Neoproterozoico–Cámbrico inferior. In: Vera, J.A. (Ed.), Geología de España. Sociedad Geológica de España — Instituto Geológico y Minero de España, Madrid, pp. 78–81.
Rodríguez Alonso, M.D., Peinado, M., López-Plaza, M., Franco, P., Carnicero, A., Gonzalo, J.C., 2004b. Neoproterozoic–Cambrian synsedimentary magmatism in the Central Iberian Zone (Spain): geology, petrology and geodynamic significance. Int. J. Earth Sci. 93, 897–920.
Roser, B.P., Korsch, R.J., 1985. Plate tectonics and geochemical composition of sandstones: a discussion. J. Geol. 93, 81–84.
Roser, B.P., Korsch, R.J., 1986. Determination of tectonic setting of sandstones–mudstone suites using SiO_2 content and K_2O/Na_2O ratio. J. Geol. 94, 635–650.
Roser, B.P., Korsch, R.J., 1988. Provenance signatures of sandstone–mudstone suites determined using discriminate function analysis of major-element data. Chem. Geol. 67, 119–139.
San José, M.A., Pieren, A.P., García Hidalgo, F.J., Vilas, L., Herranz, P., Peláez, J.R., Perejón, A., 1990. Central Iberian Zone: ante-Ordovician stratigraphy. In: Dallmeyer, R.D., Martínez García, E. (Eds.), Pre-Mesozoic Geology of Iberia. Springer, Berlin Heidelberg New York, pp. 147–159.
Silva, A.F., Romão, J.M., Sequeira, A.J.D., Ribeiro, M.L., 1988. Geotransversal no Grupo das Beiras (Complexo Xisto-Grauváquico) entre os sinclinórios de Mação e Penha Garcia (Centro-Oeste de Portugal). X Reunião de Geologia do Oeste Peninsular (poster), Bragança.
Simancas, F., Expósito, I., Azor, A., Martínez Poyatos, D., González Lodeiro, F., 2004. From the Cadomian orogenesis to the Early Palaeozoic Variscan rifting in Southwest Iberia. J. Iber. Geol. 30, 53–71.
Sousa, M.B., 1982. Litoestratigrafia e estrutura do "Complexo Xisto-Grauváquico" ante-ordovícico-Grupo do Douro (NE de Portugal). Univ Coimbra, Coimbra (Tese de Doutoramento, 223 pp.).
Stampfli, G.M., Borel, G.D., 2002. A plate tectonic model for the Paleozoic and Mesozoic constrained by dynamic plate boundaries and restored synthetic oceanic isochrons. Earth Planet. Sci. Lett. 196, 17–33.
Stern, Robert J., 2002. Crustal evolution in the East African Orogen: a neodymium isotopic perspective. J. Afr. Earth Sci. 34 (3–4), 109–117.
Talavera, C., Montero, P., Martínez Poyatos, D., Williams, I.S., 2012. Ediacaran to Lower Ordovician age for rocks ascribed to the Schist–Graywacke Complex (Iberian Massif, Spain): evidence from detrital zircon SHRIMP U–Pb geochronology. Gondwana Res. 22, 928–942.
Talavera, C., Martínez Poyatos, D., González Lodeiro, F., 2015. SHRIMP U–Pb geochronological constraints on the timing of the intra-Alcudian (Cadomian) angular unconformity in the Central Iberian Zone (Iberian Massif, Spain). Int. J. Earth Sci. 104 (7), 1739–1757. http://dx.doi.org/10.1007/s00531-015-1171-5.
Taylor, S.R., McLennan, S.M., 1985. The Continental Crust: Its Composition and Evolution. Blackwell, Oxford, p. 312 (ISBN-13: 978–0632011483).
Thompson, R.N., 1982. Magmatism of the British Tertiary province. Scott. J. Geol. 18, 49–107.
Thorogood, E.J., 1990. Provenance of the pre-Devonian sediments of England and Wales: Sm–Nd isotopic evidence. J. Geol. Soc. Lond. 147, 591–594.
Ugidos, J.M., Valladares, M.I., Recio, C., Rogers, G., Fallick, A.E., Stephens, W.E., 1997a. Provenance of Upper Precambrian/Lower Cambrian shales in the Central Iberian Zone. Spain: evidence from a chemical and isotopic study. Chem. Geol. 136 (55), 70.
Ugidos, J.M., Armenteros, I., Barba, P., Valladares, M.I., Colmenero, J.R., 1997b. Geochemistry and petrology of recycled orogen-derived sediments: a case study from Upper Precambrian siliciclastic rocks of the Central Iberian Zone, Iberian Massif, Spain. Precambrian Res. 84, 163–180.
Ugidos, J.M., Valladares, M.I., Barba, P., Ellam, R.M., 2003a. The Upper Neoproterozoic–Lower Cambrian of the Central Iberian Zone, Spain: chemical and isotopic (Sm–Nd) evidence that the sedimentary succession records an inverted stratigraphy of its source. Geochim. Cosmochim. Acta 67, 2615–2629.
Ugidos, J.M., Bilström, K., Valladares, M.I., Barba, P., 2003b. Geochemistry of the Upper Neoproterozoic and Lower Cambrian siliciclastic rocks and U–Pb dating on detrital zircons in the Central Iberian Zone, Spain. Int. J. Earth Sci. 92, 661–676.
Valladares, M.I., Barba, P., Colmenero, J.R., Armenteros, I., Ugidos, J.M., 1998. La sucesión sedimentaria del Precámbrico Superior–Cámbrico Inferior en el sector central de la Zona Centro Ibérica: litoestratigrafía, geoquímica y facies sedimentarias. Rev. Soc. Geol. Esp. 11, 271–283.
Valladares, M.I., Barba, P., Ugidos, J.M., Colmenero, J.R., Armenteros, I., 2000. Upper Neoproterozoic–Lower Cambrian sedimentary successions in the Central Iberian Zone (Spain): sequence stratigraphy, petrology and chemostratigraphy. Implications for other European zones. Int. J. Earth Sci. 89, 2–20.
Valladares, M.I., Barba, P., Ugidos, J.M., 2002. Precambrian. In: Gibbons, W., Moreno, T. (Eds.), The Geology of Spain. The Geological Society, London, pp. 7–16.
Vidal, G., Palacios, T., Gámed-Vintaned, J.A., Díez Balda, M.A., Grant, S.W., 1994a. Neoproterozoic–early Cambrian geology and paleontology of Iberia. Geol. Mag. 131, 729–765.
Vidal, G., Jensen, S., Palacios, T., 1994b. Neoproterozoic (Vendian) ichnofossils from Lower Alcudian strata in central Spain. Geol. Mag. 131, 169–179.
Vidal, G., Palacios, T., Moczydlowska, M., Gubanov, A.P., 1999. Age constraint from small shelly fossils on the early Cambrian terminal Cadomian Phase in Iberia. GFF 121, 137–143.
Villaseca, C., Merino, E., Oyarzun, R., Orejana, D., Pérez-Soba, C., Chicharro, E., 2014. Contrasting chemical and isotopic signatures from Neoproterozoic metasedimentary rocks in the Central Iberian Zone (Spain) of pre-Variscan Europe: implications for terrane analysis and Early Ordovician magmatic belts. Precambrian Res. 245, 131–145.
Von Raumer, J.F., Stampfli, G.M., 2008. The birth of the Rheic Ocean: Early Palaeozoic subsidence patterns and subsequent tectonic plate scenarios. Tectonophysics 461, 9–20.
Von Raumer, J.F., Stampfli, G.M., Arenas, R., Sánchez Martínez, S., 2015. Ediacaran to Cambrian oceanic rocks of the Gondwana margin and their tectonic interpretation. Int. J. Earth Sci. 104, 1107–1121. http://dx.doi.org/10.1007/s00531-015-1142-x.

Winchester, J.A., Max, M.D., 1989. Tectonic setting discrimination in clastic sequences: an example from the late proterozoic Erris Group, NW Ireland. Precambrian Res. 45, 191–201.
Wronkiewicz, D.J., Condie, K.C., 1987. Geochemistry of archean shales from the Witwatersrand supergroup, south Africa: Source-area weathering and provenance. Geochim. Cosmochim. Acta 51, 2401–2416.
Wronkiewicz, D.J., Condie, K.C., 1990. Geochemistry and mineralogy of sediments from the Ventersdorp and Transvaal Supergroups, South Africa: cratonic evolution during the early Proterozoic. Geochim. Cosmochim. Acta 54 (2), 343–354.
Zhao, J.X., McCulloch, M.T., Bennett, V.C., 1992. Sm–Nd and U–Pb zircon isotopic constraints on the provenance of sediments from the Amadeus Basin, central Australia: evidence for REE fractionation. Geochim. Cosmochim. Acta 56 (3), 921–940.

Capítulo 10

Geochemistry and tectonostratigraphy of the basal allochthonous units of SW Iberia (Évora Massif, Portugal): Keys to the reconstruction of pre-Pangean paleogeography in southern Europe

10.1 Introducción

Como se ha descrito en el primero de los trabajos publicados que se incluyen en esta Tesis Doctoral, recientemente ha sido propuesto un modelo de correlación de los terrenos alóctonos del NW y SW del Macizo Ibérico. La propuesta de correlación se justificó en un principio por la gran similitud litológica, metamórfica y geocronológica que existe entre las Unidades Alóctonas Basales del NW y ciertas unidades de alta-P del SW, como las denominadas Unidad Central, Unidad de Cubito-Moura y Unidad de Escoural (*Díez Fernández y Arenas, 2015*). Estas similitudes ya fueron reconocidas bastante tiempo atrás (*Castro, 1987*), aunque el marco geológico general que se consideraba entonces para el Macizo Ibérico era muy diferente. Por otra parte, la sección geológica que se ha presentado para el sector occidental del Macizo Ibérico también apoya la correlación propuesta (*Díez Fernández y Arenas, 2015*).

La posible existencia de un Terreno Alóctono Basal con recorrido desde el NW hasta el SW del Macizo Ibérico, también puede investigarse tomando en consideración las características geoquímicas de las litologías implicadas. Por ello, siguiendo la línea de investigación que se desarrolla en esta Tesis Doctoral, hemos investigado la composición de la serie siliciclástica metasedimentaria de la Unidad de Escoural, que forma parte del Macizo de Évora, en Portugal. El estudio planteado pretende investigar las posibles similitudes composicionales con las Unidades Basales del NW. Los metasedimentos de la Unidad de Escoural tienen una edad que se considera Ediacarense y resultan afines a la Serie Negra, el conjunto litológico más antiguo en el SW del Macizo Ibérico (*Alía, 1963; Pereira et al., 2008*). Por lo tanto, su edad es similar a la que presentan los niveles siliciclásticos más antiguos que se han estudiado en el desarrollo de esta Tesis en otros sectores del Macizo Ibérico. Están afectados por un metamorfismo Varisco de alta-P, con intercalaciones de eclogitas de edad estimada en ca. 370 Ma (*Moita et al., 2005*). Las características composicionales de estos metasedimentos se han investigado en 11 muestras de metagrauvacas distribuidas en todos los niveles de la Unidad de Escoural. La metodología seguida en este caso es igual a la expuesta en capítulos anteriores: un estudio geoquímico (elementos mayores y trazas) e isotópico (Sm-Nd), estableciendo, finalmente, una comparación con las litologías de las Unidades Basales del NW.

La investigación que se presenta en este trabajo tiene un doble interés; por una parte, aportar argumentos importantes que ayuden a corroborar la correlación planteada entre el NW y SW del Macizo Ibérico; y por otra parte, responder al objetivo general de esta Tesis, que plantea un estudio geoquímico de los metasedimentos de la transición Ediacarense – Cámbrico en el Macizo Ibérico. Si los datos geoquímicos pudiesen confirmar la correlación planteada, apoyaría la existencia de una sección prácticamente continua de unos 1000 km de longitud del paleomargen Ediacarense de Gondwana. Esta sección ofrecería una importante oportunidad para avanzar en la reconstrucción de dicho margen, en la distinción del contexto geodinámico implicado y en la paleogeografía del Ediacarense en el entorno peri-Gondwánico.

10.2 Conclusiones parciales

Las series metasedimentarias de la Unidad de Escoural (Mázico de Évora - Portugal) muestran composiciones químicas características de grauvacas. No existen indicios que apunten hacia una fuerte alteración química, como indican: los valores medios de CIA y PIA alejados de los del PAAS; un marcado carácter inmaduro, con un bajo fraccionamiento del Al frente al Si; unos patrones de REE similares a los del PAAS, característicos de fuentes ígneas félsicas de procedencia cortical; y por último, unos valores medios de las relaciones Ti/Zr y Th/U similares a los de la corteza continental superior. Por su parte, los análisis isotópicos reflejan unos valores de εNd inicial, calculados para una edad máxima de sedimentación de ca. 560 Ma (*Pereira et al., 2008*), que varían entre -10.2 y -4, mientras que las edades modelo (T_{DM}) presentan un rango de edades mesoproterozoicas - paleoproterozoicas, que oscilan entre 1499 y 1853 Ma.

Las grauvacas ediacarenses del Macizo de Évora muestran características geoquímicas compatibles con un margen continental convergente. A pesar de que algunas concentraciones elementales (U, Zr, Nb y LREE) apuntan a la implicación de una corteza continental engrosada, estos elementos muestran una capacidad discriminante limitada, debido a la gran influencia que ejercen determinadas fases minerales en sus concentraciones, por lo que resulta más fiable el uso de sus relaciones. Los valores de las relaciones Th/U, La/Th, La/Sc, Th/Sc, Ti/Zr, y Zr/Hf son compatibles con una sedimentación relacionada con la actividad de un arco volcánico desarrollado sobre una corteza continental adelgazada. Los patrones multielementales confirman la anterior afirmación y muestran una tendencia general hacia valores cercanos a la unidad, con una ligera pendiente positiva desde los contenidos de los elementos LILE hasta los de los elementos HFSE. No se observa una anomalía negativa significativamente acusada del Sr, lo que es coherente con un bajo grado de reciclado sedimentario y de alteración química. Los contenidos en REE, Sc, Zr, Hf y Th muestran valores muy similares a los del PAAS, común en rocas metasedimentarias corticales de procedencia félsica, que se ve confirmado por una anomalía negativa del TiO_2.

Los resultados anteriormente expuestos son coherentes con la sedimentación de las metagrauvacas de la Unidad de Escoural en relación con un ambiente geodinámico convergente. Esta sedimentación se produjo en una extensa cuenca marginal *back-arc* o *retro-arc*, en relación con el desarrollo de un sistema de arco evolucionado Cadomiense. Los valores negativos de εNd y las edades T_{DM} relativamente antiguas sugieren que la cuenca sedimentaria estaba localizada en una posición alejada del foco magmático principal. Por consiguiente, estos contenidos isotópicos indican la participación mayoritaria de material cortical antiguo procedente del área cratónica asociada al margen septentrional de Gondwana (Cratón del Oeste de África).

Desde un punto de vista geoquímico e isotópico, son muchas las similitudes entre las series inferiores de las Unidades Basales del NW del Macizo Ibérico y las series equivalentes del Macizo de Évora. Estas similitudes les confieren un carácter discriminante con respecto a otras series cercanas. Ambas secuencias están dominadas por series grauváquicas con un bajo grado de alteración y que muestran una evidente inmadurez, tanto química como textural. Este hecho, junto con una apreciable conservación de estructuras turbidíticas en los niveles menos deformados, apoya una sedimentación altamente influenciada por el contexto tectónico y dentro de cuencas sedimentarias localizadas en las proximidades del área fuente. Estas características sugieren que la sedimentación de ambas series tuvo lugar en un mismo tipo de contexto geodinámico, que estaría relacionado con la actividad de un arco volcánico Cadomiense y la apertura de una amplia cuenca *back-arc* a lo largo del margen peri-Gondwánico septentrional. A pesar de que las T_{DM} de las series del NW de Iberia son ligeramente más antiguas que las observadas en las Unidades Alóctonas Basales del SW (Unidad de Escoural y Unidad Central), los valores conjuntos de las tres series muestran una clara diferencia con los valores, significativamente más jóvenes, observados en las series neoproterozoicas subyacentes del dominio autóctono (Zona Centroibérica). Estas diferencias implican probablemente una ubicación de las cuencas diferente en el margen peri-Gondwánico durante el Ediacarense Superior y representan también un nuevo factor de discriminación de las Unidades Basales del Macizo Ibérico.

Lithos 268–271 (2017) 285–301

Contents lists available at ScienceDirect

Lithos

journal homepage: www.elsevier.com/locate/lithos

Geochemistry and tectonostratigraphy of the basal allochthonous units of SW Iberia (Évora Massif, Portugal): Keys to the reconstruction of pre-Pangean paleogeography in southern Europe

Rubén Díez Fernández [a,b,*], José Manuel Fuenlabrada [c], Martim Chichorro [d], M. Francisco Pereira [b], Sonia Sánchez-Martínez [a], José B. Silva [e], Ricardo Arenas [a]

[a] Departamento de Petrología y Geoquímica e Instituto de Geociencias (UCM, CSIC), Universidad Complutense de Madrid, 28040 Madrid, Spain
[b] IDL/Departamento de Geociências, ECT, Universidade de Évora, Évora, Portugal
[c] CAI de Geocronología y Geoquímica Isotópica, Universidad Complutense, 28040 Madrid, Spain
[d] CiCEGE/Departamento de Ciências da Terra, Universidade Nova de Lisboa, Lisbon, Portugal
[e] IDL/Departamento de Geologia, Faculdade de Ciências, Universidade de Lisboa, Lisbon, Portugal

ARTICLE INFO

Article history:
Received 20 July 2016
Accepted 21 October 2016
Available online 16 November 2016

Keywords:
Whole-rock geochemistry
Sm–Nd systematics
Allochthonous terranes
Gondwana
Suture zone
Variscan orogen

ABSTRACT

The basal allochthonous units of NW and SW Iberia are members of an intra-Gondwana suture zone that spreads across the Iberian Massif and was formed during the collision of Gondwana and Laurussia in the late Paleozoic. This suture zone is made of allochthonous terranes and is currently preserved as a tectonically dismembered ensemble. A multi-proxy analysis is applied to the basal allochthonous units of Iberia to test their affinity and potential usage for tracing a suture zone. A comparison of the lithostratigraphy, tectonometamorphic evolution, geochronology, and geochemical characteristics of the Ediacaran series of these units reveals striking affinities. They derive from rather similar immature sedimentary successions, deposited along the same continental margin, and in relation to a Cadomian magmatic arc. Sm–Nd systematics indicates that the isotopic sources are among the oldest of the Iberian Massif (ca. 2.15–1.5 Ga), suggesting a very strong contribution from the West African Craton. These Ediacaran series were affected by high-P and low- to medium-T metamorphism (blueschist to eclogite facies) during the Late Devonian (ca. 370 Ma). They occur below allochthonous ophiolitic sequences, and on top of autochthonous or parautochthonous domains lacking of high-P and low- to medium-T Devonian metamorphism, i.e., tectonically sandwiched between lithosphere-scale thrusts. The combination of all these characteristics makes these particular Ediacaran series different from the rest of the terranes of the Iberian Massif. Such singularity could be useful for tracing more occurrences of the same suture zone along the Variscan orogen, particularly in cases where its preservation and recognition may be cryptic. It also contributes to improve the paleogeographic reconstruction of the margin of Gondwana during the Ediacaran.

1. Introduction

Among the Iberian basement areas, today part of the European Variscan basement, several allochthonous terranes are assembled in a huge pile of Variscan nappes (Arenas et al., 1986; Díez Fernández and Arenas, 2015; Martínez Catalán et al., 2007; Ribeiro et al., 1990; Ries and Shackleton, 1971). At the base of these nappes, a set of high-P units has been identified, meaning that the upper nappes were formerly separated from their relative autochthons by a continental subduction zone.

The various exhumation mechanisms of such high-P assemblages imply contrasted structural relationships and severe internal structural distortion after exhumation (e.g., Beaumont et al., 2009; Chemenda et al., 1996; Faure et al., 2003). The quantity of crustal material returning from mantle depths or being eroded/obliterated during its return to shallower depths (e.g., Beaumont et al., 2009; Gerya et al., 2008) remain a source of uncertainty for paleogeographic reconstructions. The assessment of a pre-orogenic position and the paleogeography of subducted continental crust, consequently, cannot only be based on classical stratigraphy and metamorphic-structural criteria, but would need also restoration of tectonic events, using proxies able to resist severe deformation and recrystallization.

If considering highly deformed basement areas, the chemical bulk composition of metasedimentary rocks does not change considerably, besides loss of water and carbon dioxide or in the case of metasomatism. The ratios of trace-elements are best preserved due to their low mobility

* Corresponding author at: Departamento de Petrología y Geoquímica e Instituto de Geociencias (UCM, CSIC), Universidad Complutense de Madrid, 28040 Madrid, Spain.
E-mail addresses: rudiez@ucm.es (R.D. Fernández), jmfuenla@pdi.ucm.es (J.M. Fuenlabrada), ma.chichorro@fct.unl.pt (M. Chichorro), mpereira@uevora.pt (M.F. Pereira), s.sanchez@geo.ucm.es (S. Sánchez-Martínez), jbsilva@fc.ul.pt (J.B. Silva), arenas@geo.ucm.es (R. Arenas).

http://dx.doi.org/10.1016/j.lithos.2016.10.031
0024-4937/

during weathering, transport, diagenesis or metamorphism (McLennan et al., 1983; Nesbitt et al., 1980; Taylor and McLennan, 1985; Wronkiewicz and Condie, 1987), thus offering a robust approach for provenance studies and geodynamic setting discrimination (Bhatia and Crook, 1986; McLennan et al., 1990; Taylor and McLennan, 1985; Thorogood, 1990). This way a combination of structural, metamorphic, stratigraphic, and geochemical data seems adequate to overcome the uncertainties derived from paleogeographic studies dealing with high-P terranes (e.g., Albert et al., 2015b; Fuenlabrada et al., 2012; Mahlen et al., 2005).

Following the closure of various oceanic basins, the collision between Gondwana and Laurussia formed the Variscan orogen during the Devonian and Carboniferous (Franke, 1989; Matte, 1991). This orogen occupied the core of Pangea (Bambach et al., 1980), which formed by a stepwise process of collision affecting terranes dispersed along the Gondwana margin (e.g., Stampfli et al., 2013; von Raumer et al., 2015). A complex internal zone separates the two main landmasses, and contains terranes with continental and oceanic affinity (Arenas et al., 2007a; Ballèvre et al., 2009; Díaz García et al., 1999; Faure et al., 2009; Kroner and Romer, 2013; Quesada et al., 1994; Rossi et al., 2009; Schulmann et al., 2009), many of which are suspected to define a rootless suture zone that may be extended across the orogen (Arenas et al., 2016a; Díez Fernández and Arenas, 2015).

The southern part of the Variscan orogen, the so-called Iberian Massif, has been divided into allochthonous and autochthonous terranes according to structural and tectonometamorphic criteria (Fig. 1a; Arenas et al., 1986; Díez Fernández and Arenas, 2015; Martínez Catalán et al., 2007; Ribeiro et al., 1990). Separated by lithosphere-scale thrusts, a nappe stack of peri-Gondwanan continental and oceanic (ophiolitic) terranes was progressively juxtaposed to mainland Gondwana during the Variscan collision (e.g., Díez Fernández et al., 2016). Located at the base of the allochthonous tectonic pile, the so-called basal allochthonous units (commonly referred to as basal units) have been proposed as a coherent continental terrane that experienced high-P metamorphism. This basal allochthonous terrane spreads under different ophiolitic units across the Iberian Massif and over sections of the Variscan orogen characterized by medium- to low-P metamorphism (Fig. 1b). The structural position of this terrane across Iberia was presented by Díez Fernández and Arenas (2015) (see also extended discussion by Díez Fernández and Arenas, 2016 as well as previous contributions by Arenas et al., 1986; Azor et al., 1994; Castro, 1987; Fonseca et al., 1999; Martínez Catalán et al., 1996; Pereira et al., 2009; Ribeiro et al., 1990; Ries and Shackleton, 1971). Díez Fernández and Arenas (2015) followed the trace of the tectonic pair made by this particular set of high-P units together with the allochthonous ophiolitic units through NW and SW Iberia, describing what they believe would represent an intra-Gondwanan suture zone related to the closure of a short-lived oceanic basin. According to Díez Fernández and Arenas (2015), the basal allochthonous units of SW Iberia crop out in two domains (Fig. 1): (i) a northern domain, referred to as the Central Unit (Azor et al., 1994) and included in the Coimbra-Cordoba shear zone (Burg et al., 1981; Pereira et al., 2010), and (ii) a southern domain including the Évora Massif (Pereira et al., 2009).

A first quantitative approach to the internal coherence of the basal allochthonous terrane can be obtained by means of the equivalent timing of the high-P metamorphism that characterizes its initial Variscan orogenic record in NW and SW Iberia (e.g., Abalos et al., 1991; Abati et al., 2010; Booth-Rea et al., 2006; Moita et al., 2005; Ordóñez Casado, 1998; Rodríguez et al., 2003; Rosas et al., 2008; Rubio Pascual et al., 2013). However, this aspect does not provide information about whether the basal allochthonous terrane is a composite set of different continental units experiencing a similar Variscan evolution, or a large, yet single piece of continental crust involved in a complex subduction-exhumation system and then incorporated to the base of an allochthonous tectonic stack.

In this contribution, new geochemical data (whole-rock and Sm–Nd) from the basal allochthonous units of SW Iberia (Évora Massif) are faced against data from equivalent tectonometamorphic units located in the allochthonous complexes of NW Iberia. Their comparison should prove if these particular allochthonous units define a single or a composite terrane, the answer having considerable implications for the amalgamation of Pangea.

2. Geological setting

2.1. The Évora Massif

2.1.1. Regional structure

The Évora Massif (after Carvalhosa, 1983) is defined by a two-layer crustal structure consisting of an underlying high-grade domain mantled by a low- to medium-grade domain (Fig. 2). Both layers are exposed in an open, dome-like mega-structure that is transected by strike-slip shear zones and reworked by upright folds trending NW-SE (Pereira et al., 2003, 2007, 2009). The low- to medium-grade domain occupies the cores of upright synforms and includes gneisses, schists, and amphibolites formed during the Variscan evolution (Chichorro, 2006; Pereira et al., 2007, 2008). Coring upright antiforms, the exposures of the high-grade domain are made of gneisses and migmatites that are closely associated with Variscan syn-kinematic granitic rocks and gabbro-diorites dated at Carboniferous (Lima et al., 2013; Moita et al., 2009, 2015; Pereira and Silva, 2002; Pereira et al., 2009; Pin et al., 2008), some of which may also reach the structural levels of the low- to medium-grade domain. Those two domains are separated by extensional shear zones, which are responsible for regional telescoping of Variscan metamorphic isograds and the development of syn-orogenic sedimentary basins (Pereira et al., 2009, 2012b).

In the central western part of the Évora Massif (Fig. 2a), the upright geometry of the Cabrela-Carvalhal synform reveals the structural stack of all the distinctive tectonostratigraphic units of this region (Fig. 3a and b; Chichorro, 2006). At the bottom of the tectonic pile, the high-grade domain does not contain evidence of a high-P metamorphic event, rather it shows a not well-preserved Variscan Barrovian evolution (garnet/staurolite isograd) followed by pervasive shearing at low-P/high-T conditions (Chichorro et al., 2003; Pereira and Silva, 2002). On top of it, the lower part of the low- to medium-grade domain is occupied by a dominantly terrigenous sequence associated with orthogneisses and minor amphibolites and marbles (Carvalhosa, 1965; Chichorro, 2006). This sequence contains lenses of metabasites transformed into eclogites in the Late Devonian (ca. 371 Ma, ca. 1.8 GPa; Leal, 2001; Moita et al., 2005; Pedro, 1996). Although the nature of the current tectonic contact between this sequence and the underlying high-grade domain is extensional (Chichorro et al., 2003; Pereira et al., 2009), the juxtaposition of such a high-P domain on top of another domain that has only experienced medium- to low-P conditions (high-grade domain) requires a preexisting major thrust (Díez Fernández and Arenas, 2015).

The upper contact of the high-P sequence is also an extensional fault that separates it from an overlying mafic series (Pereira et al., 2007). The whole sequence resting on top of this fault lacks of high-P metamorphism (medium- to low-P Variscan evolution; Chichorro, 2006; Pereira et al., 2007), what points again to the existence of another major thrust, which would separate the overlying sequence from the underlying high-P sequence in the first place. This preexisting fault would probably represent an accretionary thrust formed during the continental subduction process that affected the eclogite-bearing sequence.

2.1.2. Tectonostratigraphy of the allochthonous units

The basal allochthonous unit with high-P rocks exposed in the Cabrela-Carvalhal synform comprises albite-bearing schists and paragneisses, banded metagreywackes, mica schists, and interbedded layers of black quartzites, amphibolites, orthogneisses and minor marbles (Fig. 3c). The age of the sedimentary protoliths of this sequence, particularly those occupying the lower parts, has been estimated as

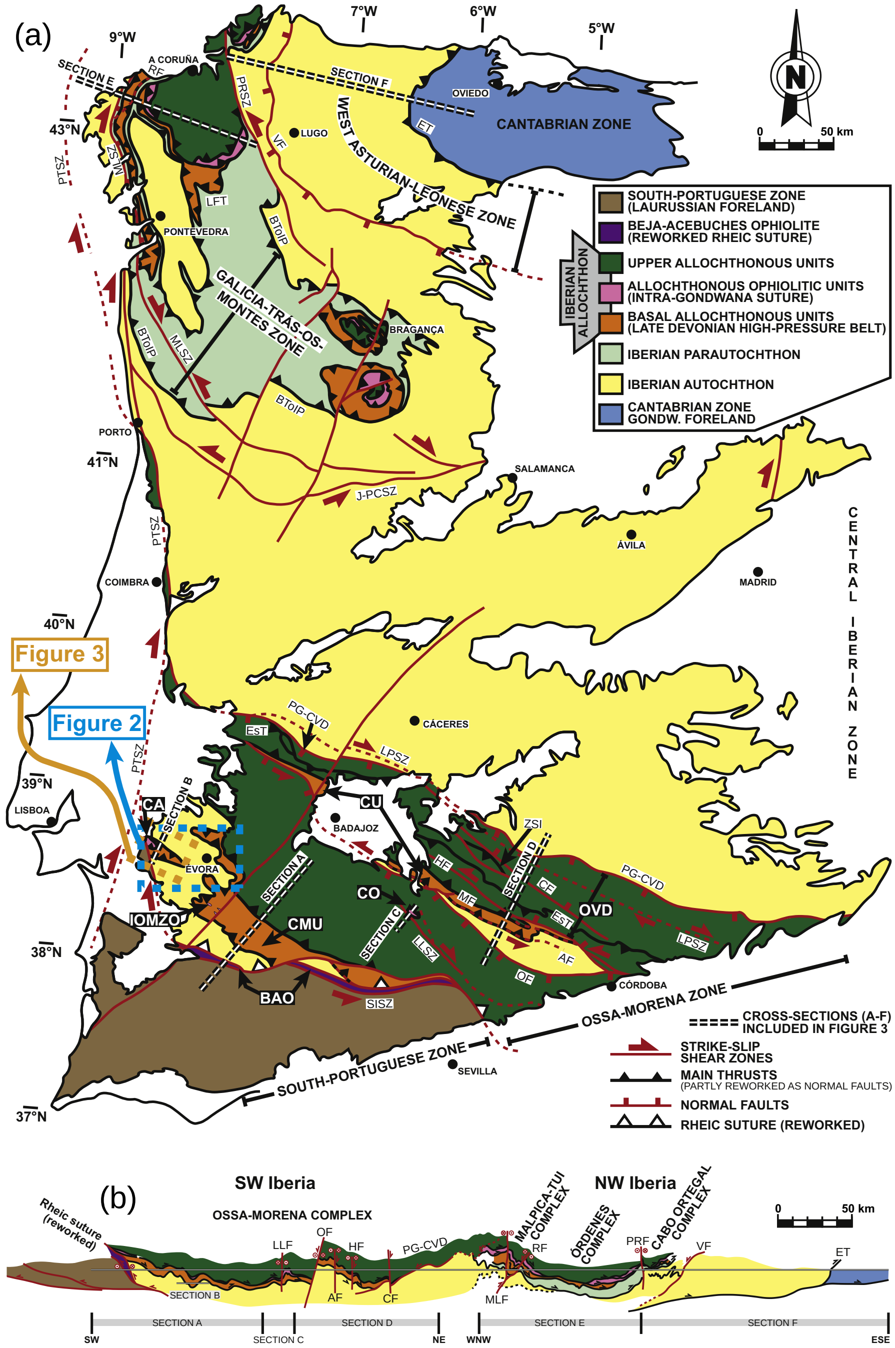

Fig. 1. (a) Geological map showing the distribution of autochthonous and allochthonous terranes of the Iberian Massif (Díez Fernández and Arenas, 2015). Locations of the Évora Massif (Fig. 2) and Cabrela-Carvalhal synform (Fig. 3) are indicated. (b) Composite cross-section. Abbreviations: AF — Azuaga Fault; BToIP — Basal Thrust of the Iberian Parautochthon; BAO — Beja–Acebuches Ophiolite; CA — Carvalhal Amphibolites; CF — Canaleja Fault; CMU — Cubito–Moura Unit; CO — Calzadilla Ophiolite; CU — Central Unit; EsT — Espiel Thrust; ET—Espina Thrust; HF— Hornachos Fault; IOMZO —Internal Ossa-Morena Zone Ophiolites; J-PCSZ — Juzbado-Penalva do Castelo Shear Zone; LFT — Lalín-Forcarei Thrust; LPSZ — Los Pedroches Shear Zone; LLSZ — Llanos Shear Zone; MLSZ — Malpica–Lamego Shear Zone; MF — Matachel Fault; OF — Onza Fault; OVD — Obejo–Valsequillo Domain; PG-CVD — Puente Génave–Castelo de Vide Detachment; PRSZ— Palas de Rei Shear Zone; PTSZ — Porto–Tomar Shear Zone; RF — Riás Fault; SISZ —South Iberian Shear Zone; VF — Viveiro Fault; and ZSI — Zalamea de la Serena Imbricates.

late Ediacaran (ca. 560–550 Ma; Pereira et al., 2008), whereas some of the metaigneous felsic rocks have been dated at Cambrian (ca. 530–505 Ma; Chichorro et al., 2008). This sequence has been divided in two members (e.g., Carvalhosa and Zbyszewski, 1994; Chichorro, 2006), a lower one referred to as Escoural Unit and equivalent to the Ediacaran Serie Negra Formation proposed by Carvalhosa (1965), and an upper member referred to as Monfurado Unit, which is regionally considered as an Early Cambrian succession (Fig. 3c).

Above the high-P sequence succeeds a thick pile (>1 km thick) of metabasites alternating with minor metasedimentary rocks (Fig. 3d). This upper sequence is named Carvalhal Unit, and has been divided in two members (Carvalhosa and Zbyszewski, 1994; Chichorro, 2006). The lower one has relatively higher metamorphic degree (mylonitic amphibolites and mica schists) and the metabasites show E-MORB affinity (Pereira et al., 2007). The upper member has lower metamorphic degree (greenschists and phyllites) and the metabasites show N-MORB affinity

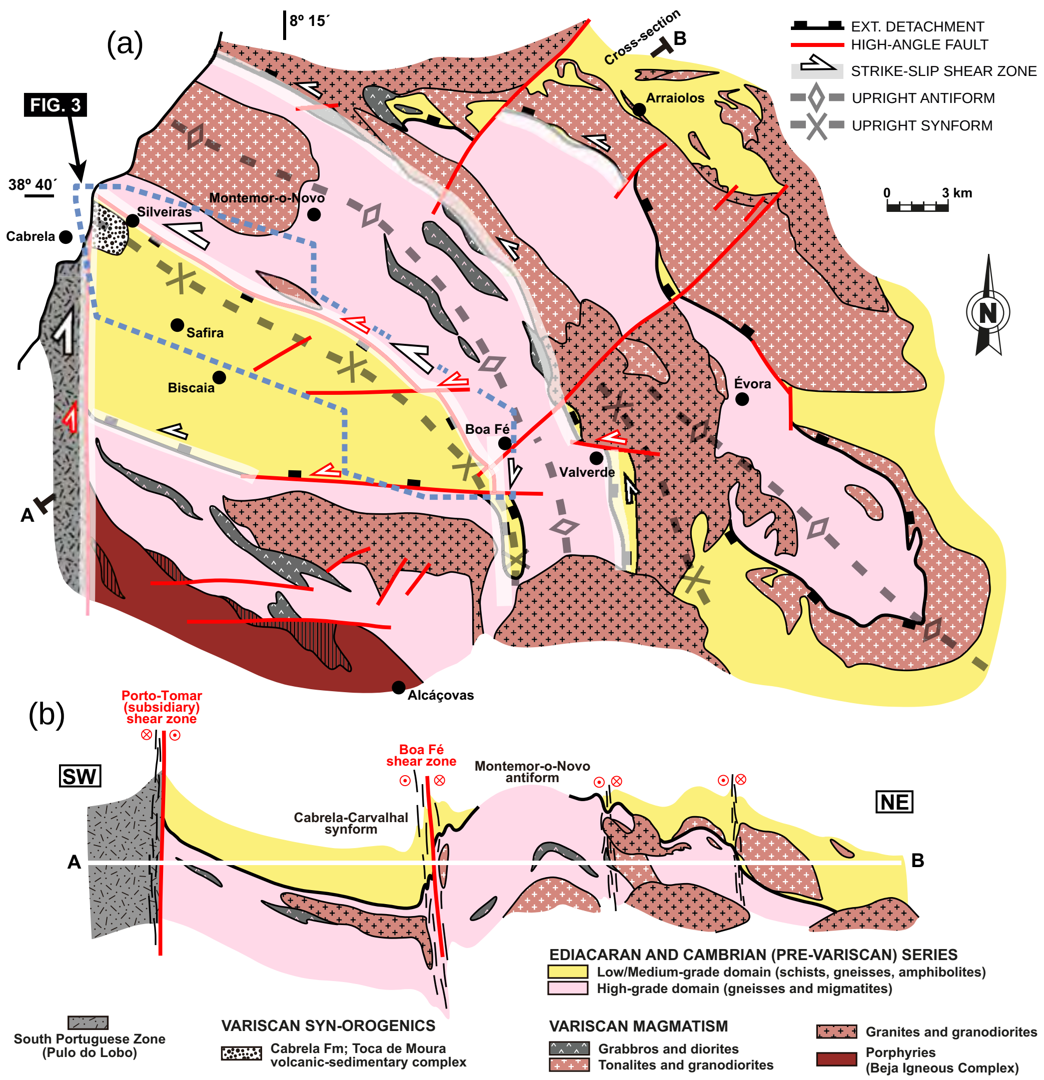

Fig. 2. (a) Simplified geological map and (b) NE–SW cross-section of the Évora Massif showing the two-layer crustal architecture and the main regional structures (after Carvalhosa et al., 1969, 1987; Carvalhosa and Zbyszewski, 1994; Carvalhosa, 1999; Pereira and Silva, 2002; Pereira et al., 2003, 2007, 2009). Location of Fig. 3 is indicated with a blue dashed line. (For interpretation of the references to colour in this figure legend, the reader is referred to the web version of this article.)

(Carvalhosa, 1999; Carvalhosa and Zbyszewski, 1994; Chichorro, 2006; Pereira et al., 2007). There are no isotopic age constrains for this upper sequence. However, a broad Cambrian-Ordovician age is considered the most probable age according to the regional setting (Chichorro, 2006), although younger ages should not be discarded. Early Cambrian magmatism in this region is typically felsic, whereas Middle Cambrian–Ordovician magmatism is more mafic and with larger mantle contributions (Chichorro et al., 2008; Díez Fernández et al., 2015; Pereira et al., 2007; Sánchez-García et al., 2010).

Culminating the regional structure, the Cabrela Unit consists of metasedimentary and metavolcanic rocks (mostly low-grade metamorphism) that rest discordantly over the crystalline basement described above (Carvalhal Unit), and account for a Lower Carboniferous syn-orogenic marine basin (Pereira and Oliveira, 2001, 2003; Z. Pereira et al., 2006; Pereira et al., 2012a, 2012b; Ribeiro, 1983).

2.2. NW Iberian massif

2.2.1. Regional structure

The Variscan regional structure of NW Iberia is defined by an autochthonous/parautochthonous domain overridden by a set of allochthonous terranes preserved as klippen (Fig. 1; Martínez Catalán et al., 2007). Schists, gneisses and migmatites of the autochthon/parautochthon are exposed along contiguous upright antiforms and domes separating the klippen (Fig. 1b). Initial Variscan deformation in the autochthonous/parautochthonous domain developed mostly at medium-P conditions and was followed by low-P and high-T metamorphism and extensive Carboniferous magmatism (Alcock et al., 2015; Arenas and Martínez Catalán, 2003; Escuder Viruete et al., 1997; Fernández-Suárez et al., 2000). The allochthonous terranes can be divided in three main counterparts, from bottom to top: the basal, ophiolitic, and upper allochthonous units (Arenas et al., 1986, 2016b; Martínez Catalán et al., 2009). The basal contacts of all these units are, originally, major thrusts, but many of them were reactivated and reworked as either secondary thrusts and/or later extensional shear zones (Díez Fernández et al., 2013; Gómez Barreiro et al., 2010; Martínez Catalán et al., 2002, 2007).

The basal allochthonous units consist of two dominantly terrigenous sequences (Díez Fernández et al., 2010) affected by a high-P metamorphic event (eclogite and blueschist facies conditions) dated at ca. 370 Ma (ca. 1.4–2.5 GPa; Abati et al., 2010; Arenas et al., 1995; Gil Ibarguchi and Ortega Gironés, 1985; López-Carmona et al., 2013, 2014; Rodríguez et al., 2003). The ophiolitic units are tectonic slices made of thick (from 300 m up to 4000 m) sequences of mafic rocks that may alternate with some metasedimentary rocks, layers of

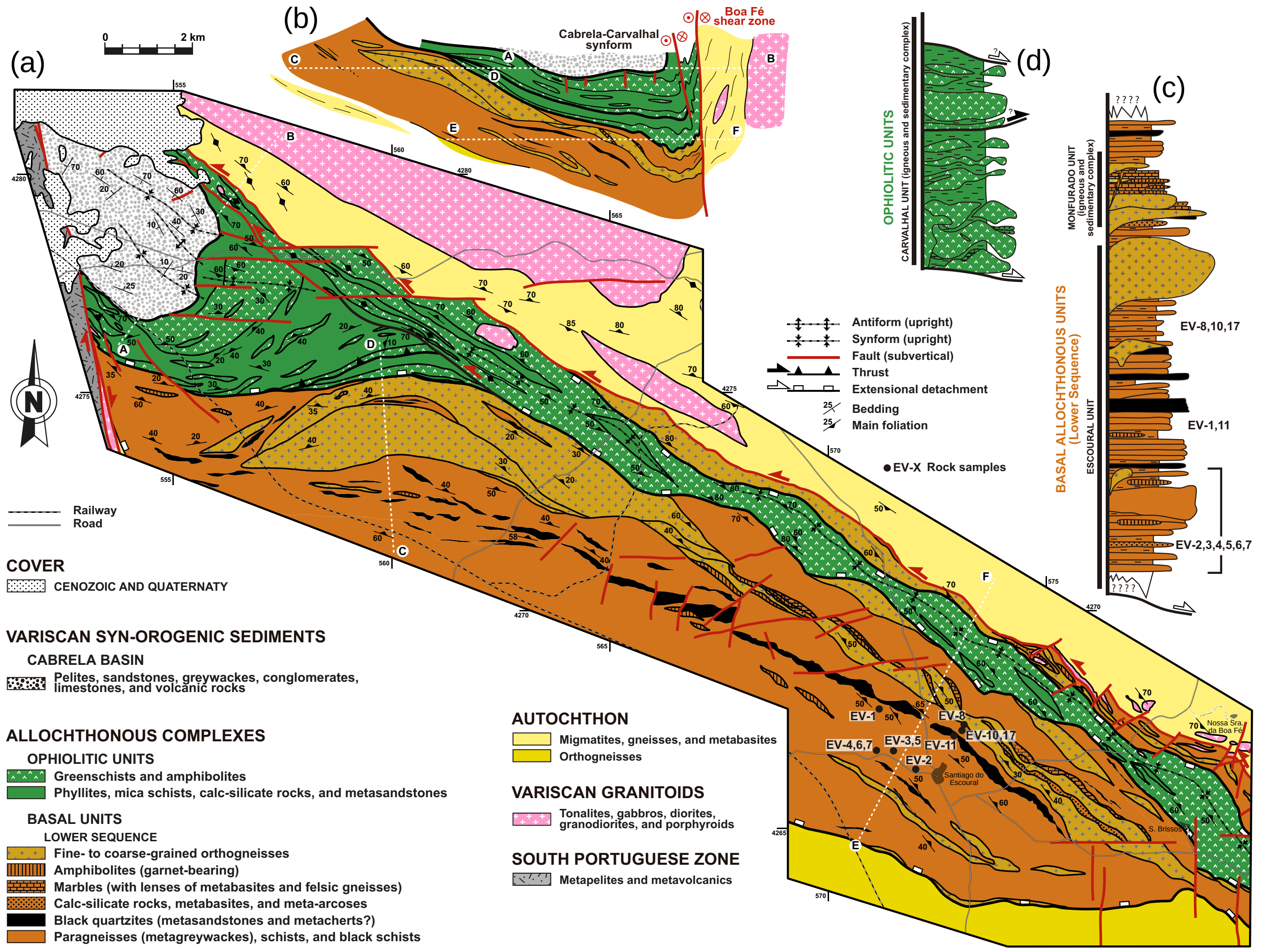

Fig. 3. (a) Geological map, (b) composite cross-section and (c and d) idealized tectonostratigraphic columns of the Cabrela-Carvalhal synform (after Chichorro, 2006). The white dashed lines show the trace of individual cross-sections, which are referred to as A–B, C–D, and E–F. Location of samples analyzed for whole-rock geochemistry and Sm–Nd isotopes is indicated in the map and columns.

ultramafics, and minor granitoids (Arenas et al., 2007a; Díaz García et al., 1999; Sánchez Martínez et al., 2009). These sequences were strongly deformed and metamorphosed under low- to medium-P greenschist and amphibolite facies conditions during the Variscan orogeny (Arenas and Sánchez Martínez, 2015, and references therein).

The upper allochthonous units are constituted by metasedimentary rocks, large massifs of granitic orthogneisses and gabbros, some ultramafic massifs, and minor lenses of mafic rocks (e.g., Albert et al., 2012; Andonaegui et al., 2012; Fuenlabrada et al., 2010; Girardeau and Ibarguchi, 1991; Gómez Barreiro et al., 2007). These tectonic units show a two-layer structure regarding their metamorphic imprint. The uppermost section recorded intermediate-P metamorphism, whereas the lower section attained high-P and high-T conditions during the initial stages of the Variscan orogeny (ca. 400 Ma; Fernández-Suárez et al., 2007; Gil Ibarguchi et al., 1990; Ordóñez Casado et al., 2001).

2.2.2. Lithostratigraphy of the basal and ophiolitic allochthonous units

The lower sequence of the basal allochthonous units of NW Iberia includes albite-bearing schists and paragneisses and banded metagreywackes (Bouma cycles), some quartzites, amphibolites, orthogneisses, and minor calc-silicate layers, whereas the uppermost sequence is dominated by mica schists, with minor graphite-bearing schists, metabasites, calc-silicate layers, and metacherts. The maximum age of deposition (as constrained from detrital zircon) of the sedimentary protoliths of these series is late Ediacaran (ca. 560–550 Ma) and Middle-Late Cambrian (ca. 512–480 Ma), respectively (Díez Fernández et al., 2010, 2013). The crystallization age of the igneous rocks intruding the series (orthogneisses and amphibolites) ranges between Middle-Late Cambrian and Ordovician (Abati et al., 2010; Díez Fernández et al., 2012a; Montero et al., 2009).

The ophiolitic units can be grouped according to their age and relative structural position. The lower ophiolitic units consist of either a thick sequence of metabasites (greenschists) intercalated with some metasedimentary rocks (mica schists and phyllites) and rare tonalitic orthogneisses (ca. 500 Ma, Vila de Cruces Ophiolite; Arenas et al., 2007b), or a ca. 4000 m thick sequence of metagabbros and minor ultramafic rocks (ca. 495 Ma, Bazar Ophiolite; Sánchez Martínez et al., 2012). The upper ophiolitic units are Middle Devonian (ca. 395 Ma) in age and represent amphibolites after gabbroic rocks (Purrido Ophiolite; Sánchez Martínez et al., 2006, 2011), or peridotites and deformed gabbros intruded by stocks of pegmatoids, gabbros, and doleritic dykes (Careón Ophiolite; Díaz García et al., 1999; Sánchez Martínez et al., 2007b), or a sequence of greenschists with few lenses of metagabbroic rocks, and some alternations of phyllites and rare serpentinite pods (Moeche Ophiolite; Arenas et al., 2014b; Sánchez Martínez et al., 2007a).

3. Geochemistry

3.1. Analytical methods

Geochemical and isotopic analyses were performed on powdered rock samples milled at Universidad Complutense de Madrid and then analyzed for major and trace elements at Activation Laboratories Ltd. (ActLabs) in Canada. Procedural method for the analysis comprises fusion sample digestion (lithium metaborate or tetraborate) and ICP-OES or ICP-MS analytical techniques for major and trace elements, respectively. Resulting data from the geochemical analysis are given in Table 1 (major and trace elements) and Table 2 (REE; Rare Earth Elements). Additional whole-rock geochemical data obtained from M.F. Pereira et al. (2006), who sampled equivalent layers, have been also incorporated to the geochemical plots and considered in the discussion.

Sm–Nd isotope analyses (Table 3) were performed at the Geochronology and Isotope Geochemistry Service of Universidad Complutense de Madrid (https://www.ucm.es/isotope), using Isotope Dilution Mass Spectrometry (ID-TIMS). Samples were spiked with appropriate amounts of a mixed ^{149}Sm–^{150}Nd tracer before performing HF-HNO_3-HCl sample digestion and a double-step chromatography separation process. Purified samples were loaded on a pre-conditioned Re triple-filament disposition and analyzed on an IsotopX-Phoenix mass spectrometer (TIMS), following a single collection and dynamic multicollection mode for Sm and Nd, respectively. All Nd isotope ratios were normalized to $^{146}Nd/^{144}Nd = 0.7219$ (O'Nions et al., 1979), and possible ^{142}Ce and ^{144}Sm interferences were corrected. La Jolla reference standard

Table 1
Whole rock major and trace element composition of the Ediacaran metagreywackes of the Escoural Unit (basal allochthonous units of SW Iberia).

	EV-1	EV-2	EV-3	EV-4	EV-5	EV-6	EV-7	EV-8	EV-10	EV-11	EV-17
SiO_2	56.33	69.68	61.34	55.81	67.09	59.1	60.19	61.71	60.69	54.75	64.13
Al_2O_3	18.18	14.92	18.19	19.28	16.18	18.31	18.23	15.8	17.64	18.6	16.82
Fe_2O_3	8.39	3.8	5.91	7.99	4.12	7.37	7.13	4.29	5.22	8.61	5
MnO	0.098	0.052	0.075	0.106	0.1	0.103	0.079	0.097	0.038	0.103	0.045
MgO	4.14	1.16	3.09	3.8	1.84	3.65	3.59	3.07	3.57	4.97	2.4
CaO	1.39	0.5	0.37	1.05	0.78	0.65	0.5	1.82	0.79	1.47	1.06
Na_2O	3	4.58	2.3	2.98	4.68	2.75	2.55	4.18	5.47	3.85	4.6
K_2O	4.04	2.47	5.67	4.82	3.06	4.53	4.69	2.55	1.36	3.89	1.74
TiO_2	0.802	0.358	0.675	0.893	0.532	0.793	0.801	0.75	0.86	0.79	0.791
P_2O_5	0.22	0.09	0.19	0.2	0.14	0.19	0.18	0.2	0.2	0.17	0.19
LOI[a]	2.35	2.01	2.34	2.53	1.59	2.72	2.41	4.33	4.17	2.29	3.22
Total	98.9	99.6	100.2	99.5	100.1	100.2	100.4	98.8	100.0	99.5	100.0
CIA	62	58	64	63	57	64	65	56	61	59	61
PIA	67	60	75	69	59	72	74	57	62	63	62
Sc	23	7	12	19	10	16	16	18	22	26	18
Be	3	3	5	5	3	4	5	2	2	3	2
V	178	35	84	150	56	129	124	179	208	179	132
Cr	120	30	60	100	50	90	80	110	130	130	100
Co	22	13	17	25	12	21	20	22	5	25	6
Ni	50	<20	30	50	<20	40	40	40	<20	40	<20
Cu	40	30	<10	50	10	40	30	40	20	50	20
Zn	40	60	50	90	40	100	70	90	<30	30	40
Ga	23	18	23	29	21	27	25	21	23	20	20
Rb	141	88	218	213	124	196	194	87	41	111	60
Sr	115	70	114	122	184	128	99	167	196	118	222
Y	26.9	34.9	37.1	39.9	38.9	31.9	33.7	28.9	31.1	28.0	25.1
Zr	185	241	221	190	268	170	174	169	197	189	198
Nb	11.9	13.9	19.5	18.7	17.0	19.1	19.8	11.1	11.8	9.4	10.9
Cs	4.7	2.1	5.1	5.9	2.6	5.5	5.5	2.8	1.8	4.2	2.3
Ba	784	689	1011	715	703	698	704	1798	769	973	743
Hf	4.1	5.8	5.6	4.9	6.6	5.1	4.8	4.5	5.2	4.5	5.5
Ta	0.9	1.3	1.6	1.3	1.4	1.4	1.4	0.8	0.9	0.7	0.8
Pb	8.0	11.0	7.0	10.0	7.0	10.0	7.0	< 5	< 5	7.0	< 5
Th	9.4	18.4	20.1	15.5	18.7	18.7	15.4	8.5	10.7	7.4	8.8
U	2.6	4.8	5.3	4.0	4.8	4.6	3.9	4.4	5.0	2.7	2.7
Al_2O_3/Na_2O	6.1	3.3	7.9	6.5	3.5	6.7	7.1	3.8	3.2	4.8	3.7
Al_2O_3/TiO_2	22.7	41.7	26.9	21.6	30.4	23.1	22.8	21.1	20.5	23.5	21.3
SiO_2/Al_2O_3	3.1	4.7	3.4	2.9	4.1	3.2	3.3	3.9	3.4	2.9	3.8
K_2O/Na_2O	1.3	0.5	2.5	1.6	0.7	1.6	1.8	0.6	0.2	1.0	0.4
Ba/Sr	6.8	9.8	8.9	5.9	3.8	5.5	7.1	10.8	3.9	8.2	3.3
Ti/Zr	26.0	8.9	18.3	28.2	11.9	28.0	27.6	26.6	26.2	25.1	23.9
La/Th	4.2	3.3	2.9	3.3	3.3	2.9	3.2	4.1	4.1	4.2	4.8
Th/Sc	0.4	2.6	1.7	0.8	1.9	1.2	1.0	0.5	0.5	0.3	0.5
Zr/Sc	8.0	34.4	18.4	10.0	26.8	10.6	10.9	9.4	9.0	7.3	11.0
Zr/Th	19.6	13.1	11.0	12.3	14.3	9.1	11.3	19.9	18.4	25.5	22.5
Zr/Hf	45.1	41.6	39.5	38.8	40.6	33.3	36.3	37.6	37.9	42.0	36.0
Cr/Th	12.7	1.6	3.0	6.5	2.7	4.8	5.2	13.0	12.1	17.5	11.4
Cr/Ni	2.4		2.0	2.0		2.3	2.0	2.8		3.3	
Th/Cr	0.08	0.61	0.34	0.16	0.37	0.21	0.19	0.08	0.08	0.06	0.09
Th/Co	0.43	1.42	1.18	0.62	1.56	0.89	0.77	0.39	2.14	0.30	1.47

Oxides are in weight percent (wt%).
Trace elements are in parts per million (ppm).
CIA: Chemical Index of Alteration (Nesbitt and Young, 1982).
PIA: Plagioclase Index of Alteration (Fedo et al., 1995).
[a] Loss on ignition.

Table 2
Whole rock Rare Earth Element data of the Ediacaran metagreywackes of the Escoural Unit (basal allochthonous units of SW Iberia).

	EV-1	EV-2	EV-3	EV-4	EV-5	EV-6	EV-7	EV-8	EV-10	EV-11	EV-17
La	39.10	61.00	58.40	51.10	62.00	53.50	49.90	34.80	44.10	31.50	42.40
Ce	76.50	117.00	114.00	100.00	121.00	104.00	97.40	69.00	86.50	63.30	80.60
Pr	8.62	12.60	12.30	11.20	13.20	11.20	10.90	7.72	9.66	7.20	9.03
Nd	32.20	46.60	45.00	41.20	47.80	39.50	40.40	29.30	37.80	28.30	33.00
Sm	6.58	8.79	8.74	8.36	9.30	7.97	7.97	6.17	7.14	5.89	6.22
Eu	1.50	1.08	1.46	1.62	1.17	1.32	1.45	1.22	1.11	1.19	1.19
Gd	5.57	6.37	6.44	6.77	7.24	6.11	6.33	4.77	5.30	5.07	4.77
Tb	0.82	1.01	1.00	1.09	1.13	0.91	0.99	0.75	0.84	0.83	0.73
Dy	4.85	5.72	6.07	6.54	6.62	5.34	5.71	4.64	5.11	4.81	4.13
Ho	0.93	1.10	1.23	1.27	1.31	1.09	1.14	0.95	1.05	1.01	0.83
Er	2.67	3.42	3.75	3.89	3.92	3.28	3.34	2.76	3.06	3.02	2.46
Tm	0.41	0.52	0.57	0.58	0.59	0.52	0.52	0.44	0.49	0.45	0.38
Yb	2.91	3.59	3.69	3.85	3.65	3.53	3.60	2.82	3.34	3.06	2.62
Lu	0.446	0.555	0.623	0.612	0.591	0.545	0.542	0.476	0.555	0.472	0.417
Σ REE	183	269	263	238	280	239	230	166	206	156	189
Eu/Eu*	0.76	0.44	0.60	0.66	0.44	0.58	0.63	0.69	0.55	0.67	0.67
$(La/Sm)_N$	3.67	4.28	4.12	3.77	4.11	4.14	3.86	3.48	3.81	3.30	4.21
$(Gd/Yb)_N$	1.53	1.41	1.39	1.40	1.58	1.38	1.40	1.35	1.26	1.32	1.45
$(La/Yb)_N$	8.98	11.36	10.58	8.88	11.36	10.13	9.27	8.25	8.83	6.88	10.82

Rare earth elements data in parts per million (ppm).

($^{143}Nd/^{144}Nd = 0.511858$; Lugmair et al., 1983) was run along with the samples yielding an average value of $^{143}Nd/^{144}Nd = 0.511847$ for 7 replicas, with and internal precision of ± 0.000006 (2σ). Analytical errors on $^{147}Sm/^{144}Sm$ and $^{143}Nd/^{144}Nd$ ratios were estimated at less than 0.1% and 0.006%, respectively, and the total procedural blanks using this procedure were always under 0.1 ng.

3.2. Rock sampling and petrography

Eleven samples of metasandstones were collected from the late Ediacaran Escoural Unit of the Évora Massif (Fig. 3a and c). These samples correspond to single layers of rock taken from sections of the succession richer in metasandstone beds, but yet showing a layered appearance made of grey metasandstones and metapelites (Fig. 4a). Monfurado and Carvalhal units were considered as not suitable for establishing correlations with the basal allochthonous units of NW Iberia (see discussion in Sections 5.1 and 5.2), and thus they were not sampled for geochemical analyses.

All of the rock samples are albite-bearing schists with a main foliation (S_e) marked by quartz + biotite + white mica + plagioclase (albite-oligoclase) ± opaque minerals ± tourmaline (Fig. 4b). The albite porphyroblasts include an internal schistosity (S_i) that is usually oblique to the main foliation (Fig. 4c), and is defined by quartz + white mica + chlorite + opaque minerals (ilmenite) ± garnet (Fig. 4d). Biotite, when trapped within albite, may either overprint the internal fabric or constitute a foliation defined by quartz + white mica + biotite ± opaque minerals that occupies a more external position within the porphyroblasts (Fig. 4b–d). Occasionally, the second internal fabric continues out of the albite porphyroblasts and into the main foliation (Fig. 4e). In the matrix, it is also possible to observe relicts of a previous fabric made of quartz + white mica + biotite, either in the form of disrupted and crenulated microlithons surrounded by the main foliation, or as polygonal arcs in the quartz-rich bands of the gneissic banding (Fig. 4e). A similar folded fabric can be also observed within albite porphyroblasts (Fig. 4c). The orientation of albite crystals ranges between subparallel and oblique to the main foliation. In fact, these minerals are sometimes flanked by asymmetric pressure shadows consisting of plagioclase, quartz, and mica, all of which are subconcordant with the main foliation of the surrounding matrix. The amount of opaque minerals varies from sample to sample, although it is usually moderate (samples EV-8 and EV-10) to low (rest of the samples). Opaque minerals may occur in association with any of the fabrics described in these metasedimentary rocks, but in some cases they occur preferentially as part of the internal fabric preserved in porphyroblasts. Scattered porphyroblasts of cordierite are also found parallel to the main foliation. Some calcite is found filling late fractures that cut across the main foliation.

3.3. Results

3.3.1. Whole-rock geochemistry

The normally applied geochemical discrimination diagrams characterize the analyzed rocks as described below.

Most of the rocks plot in the greywacke field (Herron, 1988), and only four samples fall close to the shale field (Fig. 5a).

Table 3
Whole rock Nd isotope data of the Ediacaran metagreywackes of the Escoural Unit (basal allochthonous units of SW Iberia).

Sample	Sm	Nd	$^{147}Sm/^{144}Nd$	$^{143}Nd/^{144}Nd$	$\pm SErr * 10^{-6}$	$\varepsilon Nd_{(0)}$	$\varepsilon Nd_{(560)}$[a]	T_{DM} (Ma)[b]
EV-1	6.29	31.57	0.1204	0.512065	2	−11.2	−5.7	1596
EV-2	11.20	60.53	0.1119	0.511804	1	−16.3	−10.2	1853
EV-3	6.69	35.50	0.1139	0.511909	2	−14.2	−8.3	1731
EV-4	9.13	46.14	0.1196	0.511958	2	−13.3	−7.8	1755
EV-5	7.84	41.77	0.1135	0.511874	1	−14.9	−9.0	1776
EV-6	7.11	38.50	0.1117	0.511850	1	−15.4	−9.3	1781
EV-7	7.45	38.24	0.1177	0.511967	2	−13.1	−7.5	1707
EV-8	5.35	27.07	0.1195	0.512075	1	−11.0	−5.5	1564
EV-10	5.23	26.20	0.1206	0.512051	1	−11.4	−6.0	1620
EV-11	5.78	28.07	0.1244	0.512168	1	−9.2	−4.0	1499
EV-17	5.79	31.23	0.1121	0.511890	2	−14.6	−8.5	1727

[a] εNd(t) calculated for 560 Ma.
[b] Nd model ages calculated according to DePaolo (1981).

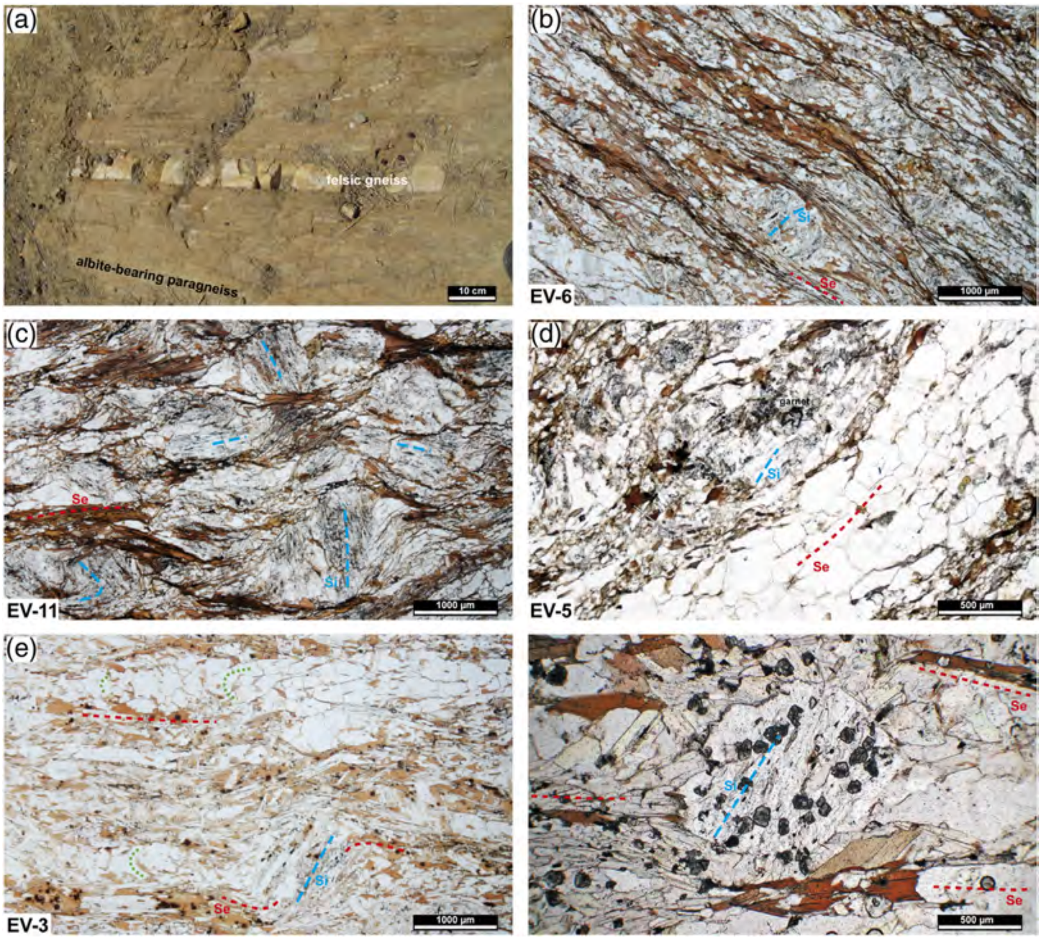

Fig. 4. (a) Banded appearance (sedimentary layering) of the paragneisses of the Lower Sequence. Lighter bands are richer in albite. Note the lens of felsic orthogneiss in the central part. (b) Main (external) foliation (S_e, short-dashed line) of the albite-bearing paragneisses of the Lower Sequence (EV-6; quartz + biotite + white mica + plagioclase ± opaque minerals ± tourmaline). Note the oblique character of the internal foliation (S_i, long-dashed line) in the albite porphyroblasts. (c) Paragneiss of the Lower Sequence (EV-1) with albite porphyroblasts oriented to the main foliation and including an internal straight fabric that ranges from parallel to normal to the main foliation, or a folded internal fabric. (d) Internal foliation (quartz + white mica + chlorite + opaque minerals ± garnet) of an albite porphyroblast in the paragneisses of the Lower Sequence. Note the growth of biotite over this fabric. (e) Continuity between the internal and external foliation in an albite porphyroblast (EV-3) of the paragneisses of the Lower Sequence. Note the polygonal arcs (pointed line) that occur in the quartz-rich bands of the paragneiss. (f) Albite-bearing paragneisses of the Ediacaran series included in the basal allochthonous units of NW Iberia (from Díez Fernández, 2011).

There is neither a large variation in major element contents, nor significant differences relative to PAAS (Post Archean Australian Shale; Taylor and McLennan, 1985). Sample average values fit accurately those displayed by the average shale, with homogenous SiO_2, Al_2O_3, Fe_2O_5, CaO, K_2O, Ti_2O and P_2O_5 contents (61, 17.5, 6.2, 0.9, 3.5, 0.7 and 0.2 avg. wt%, respectively). Higher Na_2O contents (3.7 wt%) diverge from those of PAAS (1.2 wt%), as expected for albite-rich rocks such as the ones analyzed here.

Chemical Index of Alteration (CIA; Nesbitt and Young, 1982) show values that correspond to low weathered rocks, ranging from 56 to 65, and with an average value of 61, far from those typical for average shale (70–75; McLennan et al., 1993) (Table 1).

No important alteration at the source area is deduced from PIA values (Plagioclase Index of Alteration; Fedo et al., 1995), which vary between 57 and 75, with an average value of 65, the latter revealing to be lower than PAAS (79), thus indicating no significant transformation from plagioclase/K-feldspar to clay minerals. This is also suggested by Na_2O and K_2O contents (average values of 3.7 and 3.5 wt%, respectively), very close to those of the upper continental crust (UCC: 3.35 and 3.10 wt%, respectively; Condie, 1993). Negative correlation between CIA values and Ba/Sr ratios (−0.22) confirms their low weathering character.

A general immature character can be inferred from the SiO_2/Al_2O_3 ratio (3.5 on average), which is lower than that of the UCC (4.5 on average) and indicative of a low fractionation of Al_2O_3 from SiO_2. In addition, Al_2O_3/Na_2O (5.1 on average), Al_2O_3/TiO_2 (25 on average) and Ti/Zr (22.8 on average) ratios are similar to those of the UCC (4.5, 24.0 and 21.4, respectively), thus confirming the general immature character for these clastic sediments. Some of the samples (EV-2 to EV-7), however, show differentiated Zr/Sc and Th/Sc ratios, which indicate that those particular sedimentary beds could have undergone slight recycling processes (McLennan et al., 1993).

The REE-abundances of the Ediacaran metasedimentary rocks from the Évora Massif (Table 2) show slight variability (bulk content ranging from 156 to 280 ppm). Their chondrite-normalized patterns are very similar to those of PAAS (Fig. 5b), characteristic of felsic igneous sources and upper crustal provenance. REE distribution patterns display a significant LREE enrichment featuring a REE fractionation with high $(La/Yb)_N$ (6.9–11.4), almost flat HREE with $(Gd/Yb)_N$ close to unity (1.3–1.6), and negative Eu anomalies ($Eu/Eu^* = 0.44–0.76$, average of 0.61).

The analyzed Ediacaran metagreywackes vary in the Al_2O_3/TiO_2 ratio from 20.5 to 41.7, which fit with an intermediate-felsic source (e.g., Roser and Korsch, 1986), with some of the values well above the limit of a felsic provenance (Table 1). This dominant felsic character is confirmed by Cr/Th ratios, with an average value of 8.2 (1.6–17.5); and the Eu/Eu* ratio, with an average value of 0.58 (0.44–0.61). These numbers meet the values proposed by Cullers (1994) for sedimentary rocks with a dominant felsic provenance (Cr/Th = 2.5–17.5 and

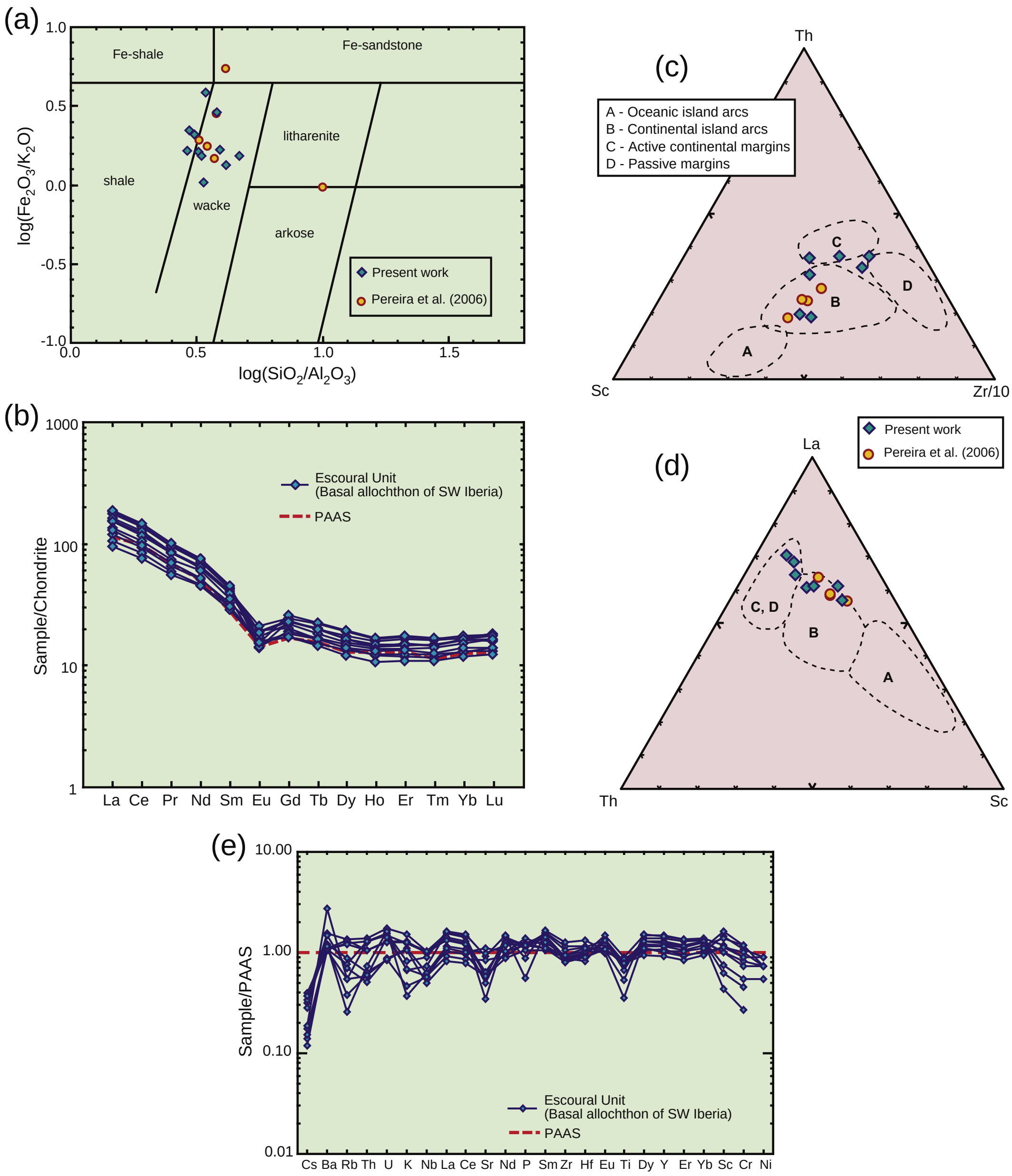

Fig. 5. Chemical diagrams for the Ediacaran siliciclastic metasedimentary rocks from the Escoural Unit (basal allochthonous units of SW Iberian Massif). Previous data obtained by M.F. Pereira et al. (2006) are indicated. (a) Chemical classification (after Herron, 1988). (b) Chondrite normalized REE plot. The dotted line corresponds to the PAAS (Post Archean Australian Shale; Taylor and McLennan, 1985). Normalizing values are from Nakamura (1974). (c) and (d) are trace element diagrams with tectonic setting discrimination fields (after Bhatia and Crook, 1986). (e) PAAS-normalized trace elements diagrams (PAAS after Taylor and McLennan, 1985).

Eu/Eu* = 0.48–0.78). Cr and Ni, common elements in sediments derived from ultramafic rocks, show abundances in some cases below the determination limit, and Cr/Ni ratios are very low (2.4 on average) and similar to PAAS (2.0), what along with a Th/Cr ratio higher than PAAS are good indicators of a felsic provenance. La/Th (3.7), Th/Sc (1) and Th/Co (1) average values are in agreement with the felsic character of the sources too (Cullers, 2002). The samples have La/Th, Th/Sc and Th/Co ratios similar or even higher than PAAS (2.6, 0.9 and 0.6 respectively; Taylor and McLennan, 1985) and UCC (2.7, 0.7 and 0.7, respectively; Condie, 1993), what means higher content in La and Th, elements preferentially accumulated in felsic rocks.

3.3.2. Tectonic setting

No significant deviations in the geochemical composition relative to PAAS have been observed in the Ediacaran metasedimentary rocks of the Évora Massif. Moreover, the lower CIA values of the samples, compared to those of PAAS, rule out a strong weathering and alteration during post-deposition processes. Consequently, the samples are suitable for the use of provenance and tectonic setting discrimination diagrams based on immobile trace elements.

Following Bhatia and Crook (1986), the chemical discrimination of the Ediacaran greywackes shows a clear affinity to active continental margin settings (Fig. 5c and d). Most of our samples plot into or very close to field B, suggesting deposition on the realm of a continental arc. This result is also supported by average values of La/Th, Ti/Zr, Zr/Th and Zr/Hf ratios (3.7, 22.8, 16.1 and 39.0, respectively), which are close to the values proposed by Bhatia and Crook (1986) for greywackes deposited in a continental arc setting, in contrast with the typical values displayed by sediments deposited over a thick continental margin.

If compared to PAAS in a multivariation diagram (Fig. 5e), the patterns obtained are consistent with those exhibited by sediments deposited on an active margin setting (Winchester and Max, 1989). REE patterns show a relatively positive slope from a slight depletion displayed by most LILE elements (Cs, Th, Rb, Sr and K) to HSFE elements contents (Ti, Zr, Hf, Sc, Sm and HREE), very close to those of PAAS, with a characteristic negative Ti anomaly (Fig. 5e). Unlike Winchester and Max conclusions, no significant P_2O_5 depletion is observed, probably because of the presence of some apatite and monazite, which exert a high influence on P_2O_5 concentration.

3.3.3. Sm–Nd isotope geochemistry

The Nd model ages of the high-P metasedimentary rocks of the Ediacaran series of the Évora Massif are shown in a εNd vs Age diagram (Fig. 6). $^{147}Sm/^{144}Nd$ values range from 0.1117 to 0.1244 (average of 0.1168), and are similar to those of the continental crust (ca. 0.12). All the ratios are under 0.165, which is considered the upper limit applicable for T_{DM} calculations (Stern, 2002). The ratios are also coherent with those proposed as normal values for clastic sediments (0.1–0.13; Zhao et al., 1992).

The samples have an $\varepsilon Nd_{(0)}$ average value of −13.1, while $\varepsilon Nd_{(560)}$ values vary from −10.2 to −4 (maximum depositional age of ca. 560–550 Ma; Pereira et al., 2008). Nd T_{DM} model ages (DePaolo, 1981) are early Mesoproterozoic–Paleoproterozoic (1499–1853 Ma), with an average value of 1692 Ma.

4. Correlation of major tectonic units from NW Iberia and the Évora massif

A reinterpretation of lithostratigraphy and structure in the Évora Massif leads to the conclusion that it can be correlated with equivalent units in NW Iberia (Díez Fernández and Arenas, 2015). In both areas, high-grade domains lacking an initial high-P overprint occur under a strongly deformed sequence of Ediacaran and Cambrian schists, paragneisses and orthogneisses that experienced high-P metamorphism in Late Devonian times. These gneisses are overlain by a sequence lacking high-P metamorphism and dominated by metabasites with MORB-affinity that may alternate with some layers of metasedimentary rocks. Such piling of tectonometamorphic units seems to mimic the nappe stack defined by the basal and ophiolitic allochthonous units in NW Iberia, and is, consequently, considered here yet another klippe of the allochthonous complexes of the Iberian Massif (Fig. 1). Correlatives of the upper allochthonous units that are located on top of the ophiolitic units do not occur in the Carvalhal-Cabrela synform. The erosional nature of the basal contact of the overlying Cabrela Unit (Carboniferous syn-orogenics) may well explain such absence.

Following this interpretation for the Évora Massif, the Escoural and Monfurado units together would be a correlative to the lower sequence of the basal allochthonous units of NW Iberia. The upper sequence of the basal units seems to be absent in the Cabrela-Carvalhal synform, since a series dominated by mica schists, containing minor metabasites, and affected by conspicuous high-P metamorphism, is yet to be found in this area. A plausible reason for its lack in this particular section of SW Iberia is that the basal contact of the Carvalhal Unit is an extensional detachment. Note how its basal contact cuts the underlying gneisses in the Cabrela-Carvalhal synform, thus removing the underlying crust located along its trace (Fig. 3a and b).

The Carvalhal Unit, dominated by metabasites with MORB-affinity, represents a good candidate for an ophiolitic sequence in the Évora Massif as it has almost the same lithological constitution, structural position, and probable age than the Vila de Cruces ophiolite, one of the lower ophiolitic units of NW Iberia. Mafic units like these represent tectonic slices of transitional oceanic crust (oceanic supracrust) that usually account for a broad transition from a continental-oceanic crust (e.g., upper sequence of the basal allochthonous units; Díez Fernández et al., 2010, 2013) to an oceanic-continental crust (e.g., Vila de Cruces and Carvalhal ophiolites; Arenas et al., 2007b). In this regard, a group of Cambrian-Ordovician dismembered ophiolitic sequences has been described southeast of the Évora Massif, the so-called Internal Ossa-Morena Zone Ophiolite Sequences (Fonseca et al., 1999; Pedro et al., 2010). Those ophiolitic sequences have been interpreted as a complete (but dismembered) section of oceanic lithosphere, including dunites

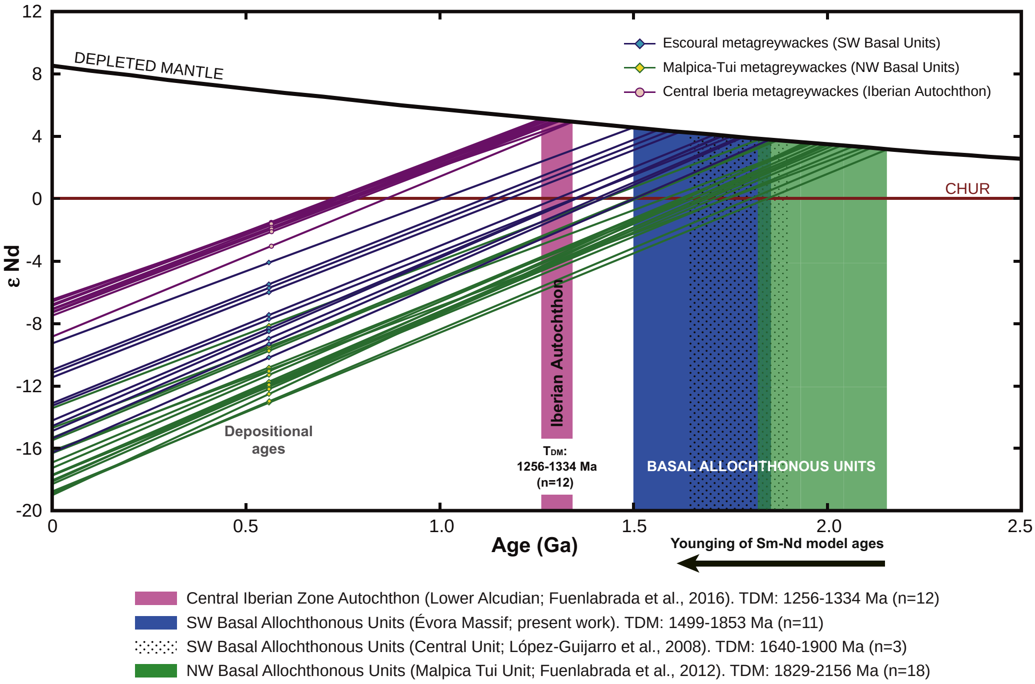

Fig. 6. TDM model ages (DePaolo, 1981) of the late Ediacaran metagreywackes of the basal allochthonous units of SW Iberia (Iberian Massif). Diamonds show the εNd values at ca. 560 Ma. Model ages from late Ediacaran metasedimentary rocks of the basal allochthonous units of NW Iberia (Malpica-Tui Unit; Fuenlabrada et al., 2012), the basal allochthonous units of Central Iberia (Central Unit; López-Guijarro et al., 2008), and the Autochthon of the Central Iberian Zone (Fuenlabrada et al., 2016), are included for correlation and comparison.

and wehrlites, pyroxenite cumulates, metagabbros and flasergabbros, metadoleritic dikes, metabasalts, and metacherts (Pedro, 2004). They occur on top of a sequence of mica schists and minor metabasites and marbles (Cubito-Moura Unit; Araújo et al., 2005; Pedro et al., 2005) affected by high-P metamorphism during the Late Devonian (Booth-Rea et al., 2006; Rosas et al., 2008; Rubio Pascual et al., 2013). This high-P unit meets the main features to be a tectonostratigraphic correlative of the upper sequence of the basal allochthonous units of NW Iberia (Díez Fernández and Arenas, 2015).

Striking similarities between units are not only found at a large scale. All the microstructural characteristics observed during the thin-section analysis of our samples of Ediacaran metasedimentary rocks (see Section 3.2, and further details in Chichorro, 2006) are rather similar to those described for the basal allochthonous units of NW Iberia in previous works. The existence of aligned microinclusions (quartz + white mica + garnet ± chlorite ± rutile) within albite porphyroblasts is a distinctive feature of the metasedimentary rocks of the basal allochthonous units in NW Iberia (Fig. 4f). This ensemble formed under high-P conditions and represents the first Variscan metamorphic imprint that can be recognized in the metasedimentary rocks (Arenas et al., 1995). Subsequent exhumation favored a progressive retrogression of the high-P fabric, which is now preserved as an either non-retrogressed high-P foliation inside albite porphyroblasts, or as a variably retrogressed and crenulated foliation, preserved either within or outside albite porphyroblasts (e.g., Arenas et al., 1995; Díez Fernández, 2011; Díez Fernández and Martínez Catalán, 2012; Díez Fernández et al., 2011). A comparable mineral assemblage with identical microstructural relationships exists in the basal allochthonous units of SW Iberia (Fig. 4b, c, and d), although in this region it has been tentatively proposed as a vestige of Cadomian deformation (Chichorro, 2006).

Retrogression affecting the internal fabrics is more intense in the Évora Massif (e.g., Escoural Unit) if compared to NW Iberia. For instance, biotite growth largely overprints the internal fabric and rutile is usually transformed into ilmenite. Isotopic dating of these fabrics is lacking. However, the non-Precambrian age is clear for the basal allochthonous units of NW Iberia, as such internal fabrics are also found in metasedimentary rock series with Middle Cambrian maximum depositional ages (Arenas et al., 1995; Díez Fernández et al., 2010). Given that the basal allochthonous units of NW and SW Iberia experienced equivalent tectonometamorphic evolution during the Variscan orogeny, we propose that the internal fabrics they preserve account for a Variscan high-P event, at least the associations bearing quartz + white mica + garnet ± chlorite ± rutile. Yet, an imprint of Precambrian shearing cannot be fully discarded, since other exposures of Ediacaran metasedimentary rocks in SW Iberia were affected by Precambrian deformation (e.g., Quesada, 1990). Finally, even though other para-derived units of the Iberian Massif experienced high-P metamorphic conditions, fast exhumation, and severe retrogression during the Variscan orogeny, none of them exhibits such a microstructural record like the basal allochthonous units. This record seems somehow distinctive for the metasedimentary rocks of the latter units in response to Late Devonian high-P metamorphism.

5. Comparative lithostratigraphy and geochemistry

The lower series of the basal allochthonous units of NW Iberia and the Évora Massif share two fundamental features that make them different from other series in their respective regions. (i) They are dominated by late Neoproterozoic metagreywackes, and (ii) they contain various Cambrian-Ordovician metagranitic and mafic rocks, the latter occurring in the metasedimentary rocks and within the metagranitoids (most likely basic dikes).

From a chemical point of view (compare with Fuenlabrada et al., 2012), besides some shales, the majority of the sequence consists of wackes, both in NW Iberia and SW Iberia (Fig. 5a). Sediments are generally immature and derive from source areas subjected to low weathering. This is not only suggested by their chemical composition (see Section 3.3.1), but also by the fact that micas and feldspar can be still observed as detrital grains in the less deformed sections of the series (e.g., Díez Fernández, 2011). Source areas are dominated by felsic igneous upper crustal rocks in both cases. The variation in REE contents is limited and follows PAAS (Fig. 7a). Finally, trace elements show rather similar trends in both regions (Fig. 7b).

A minor regional difference is the occurrence of black quartzites in the Évora Massif. Black metasedimentary rocks intercalated between Ediacaran metagreywackes have been also identified in the lower sequence of the basal allochthonous units of NW Iberia (Díez Fernández et al., 2010). The latter are essentially siliciclastic, as they have plenty

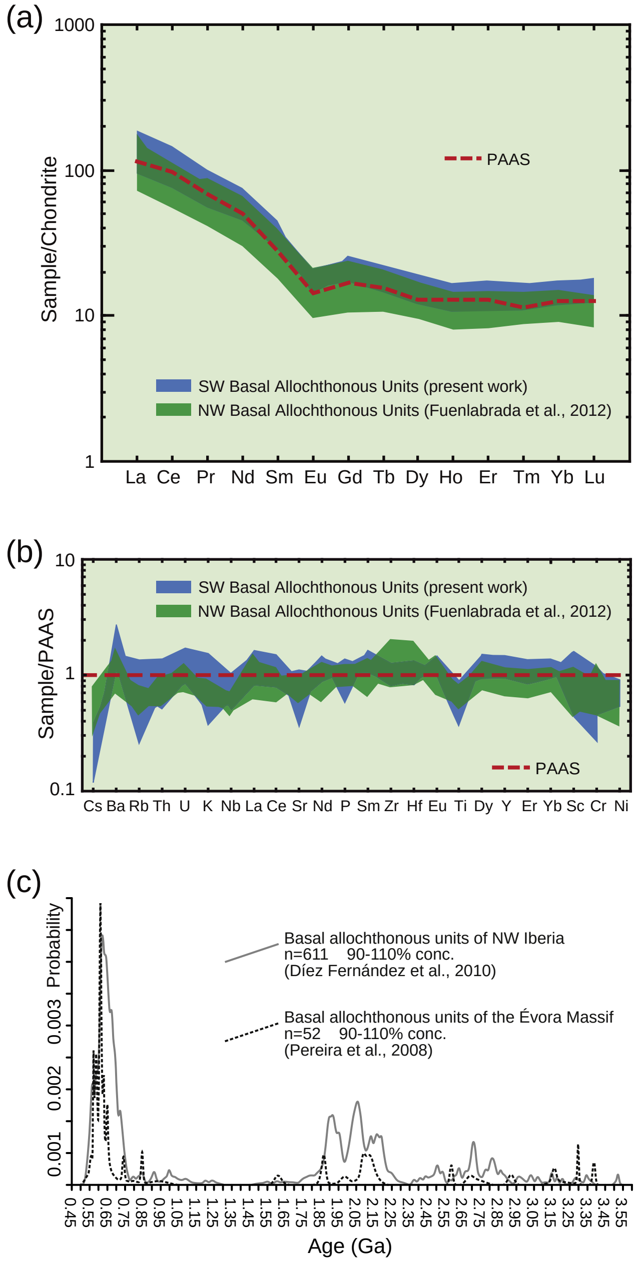

Fig. 7. Diagrams for comparing the content in (a) REE and (b) trace elements of the Ediacaran series of the basal allochthonous units of NW and SW Iberia. (c) Composite probability density plot of detrital zircon ages from the basal allochthonous units of NW Iberia (grey line) and from the Évora Massif (black dashed line). Data have been extracted from Fig. 5b and e, and from Pereira et al. (2008), Díez Fernández et al. (2010), and Fuenlabrada et al. (2012).

of detrital grains, but they never define quartz-rich competent layers like in the Cabrela-Carvalhal synform. The siliciclastic nature of the primary protoliths of the black quartzites of SW Iberia seems well established (De Oliveira et al., 2003). But the origin of the silica-rich matrix characterizing some of those layers is yet under discussion, since a post-depositional derivation (diagenetic silicification of dominantly terrigenous sediments) is a rather likely option for the case of late Neoproterozoic successions deposited in the periphery of Gondwana (Dabard, 2000; Dabard and Loi, 1998). Following this line of evidence, the previous authors indicated that such silicification is episodic, not uniform, and largely controlled by local conditions in the environment, thus calling "*into question the use of graphitic cherts as markers for lithostratigraphic correlation*". Their conclusions seem well suited for the case of the Iberian Massif, and particularly for the lower part of the basal allochthonous units discussed here, where, from a lithostratigraphical point of view, they only differ from each other in the presence or absence of quartz-rich black layers. Besides, most of the grey color dominating these series comes from the moderate to high content in carbonaceous material and heavy minerals, particularly high in the blackish terms (e.g., De Oliveira et al., 2003). This adds to the dominantly immature character of the protoliths and common sedimentary facies (Bouma cycles) observed in both NW and SW Iberian basal allochthonous units. Apparently, there seems to exist a common petrological origin for most of the sedimentary successions, despite some of the less abundant lithologies are exclusive to some regions. Quartzites, however, are also found in the Ediacaran series of the basal allochthon of NW Iberia (Díez Fernández et al., 2010), although they contain much less carbonaceous material and heavy minerals and thus have no blackish appearance.

Another lithostratigraphic difference is the lack of marbles in the basal allochthonous units of NW Iberia. Although carbonate-richer horizons are frequent in NW Iberia, they occur only as thin calc-silicate layers in the whole series, never thicker than 20 cm. Marbles of the basal allochthonous units of the Évora Massif occur in a metasedimentary and metavolcanic rock series dated at Early Cambrian (Monfurado Unit; Chichorro et al., 2008). Metasedimentary rocks of that particular age have not been found in the basal allochthonous units of NW Iberia. There, the set of Ediacaran metagreywackes rests right below a volcano-sedimentary succession with Middle Cambrian maximum depositional age (Díez Fernández et al., 2010). In NW Iberia, the two latter sequences are separated by a major extensional fault (Bembibre-Ceán detachment; Díez Fernández et al., 2012c; Gómez Barreiro et al., 2010), which must have removed any potential lithostratigraphic unit correlative to the Early Cambrian metasedimentary rocks of the Évora Massif. Therefore, the lack of Early Cambrian series in the basal allochthonous units of NW Iberia precludes any correlation based on geochemical proxies applied to successions of that age.

5.1. Comparison of tectonic setting and isotopic contributions during the Ediacaran

The Ediacaran series of the basal allochthonous units of NW Iberia were deposited in a back-arc or retro-arc basin related to a Cadomian peri-Gondwanan arc system built on a thinned continental margin. This is typified by (i) the association of sedimentary facies (identified in the less deformed protoliths), (ii) major and trace element geochemistry, and (iii) by the dominant input of Cadomian detrital zircons derived from present northern Africa (Díez Fernández et al., 2010; Fuenlabrada et al., 2012). These same proxies point to a similar geodynamic setting for the late Neoproterozoic rocks that constitute the basal allochthonous units of the Évora Massif. (i) Their immature character (Fig. 5a and Tables 1 and 2) along with their primary structure, formed after successive turbidity currents, suggest a tectonically controlled deposition close to the source area. (ii) Tectonic discrimination diagrams support an active margin setting for deposition (Fig. 5c and d, see also M.F. Pereira et al., 2006, 2007). (iii) The detrital input of this succession, as constrained from zircon analysis, is dominated by Neoproterozoic (Cadomian) grains (ca. 0.75–0.55 Ga), followed by Paleoproterozoic grains (ca. 2.15–1.8 Ga), and then several Archean and Tonian clusters (Pereira et al., 2008). These age populations match those of the basal allochthonous units of NW Iberia (Díez Fernández et al., 2010), both in age range and relative abundance (Fig. 7c).

Sm–Nd model ages of the Ediacaran metasedimentary rock sequences of the basal allochthonous units of the Évora Massif (1.50–1.85 Ga) are nearly similar to those of the metasedimentary rocks of the Central Unit (1.64–1.90 Ga; López-Guijarro et al., 2008), which is another basal allochthonous unit of SW Iberia (Díez Fernández and Arenas, 2015). A direct comparison of Sm–Nd model ages of the Ediacaran successions of the basal allochthonous units of Iberia reveals slightly older model ages for the NW Iberian rocks, which still partly overlap with the rest of the values obtained from correlative units located in SW Iberia, i.e. Escoural Unit and Central Unit (Fig. 6). The three main exposures of basal allochthonous units considered here define a clear rejuvenating trend from NW to SW. In absolute terms, differences between model ages are limited. However, if the range of Sm–Nd model ages of the basal allochthonous units is compared with that of the Ediacaran autochthonous series of the Central Iberian Zone (1.25–1.33 Ga; Fuenlabrada et al., 2016), located structurally underneath and geographically in between (Fig. 1), a sharp contrast emerges. The range of ages for the Ediacaran autochthonous series is clearly younger, does not overlap with that of the basal allochthon, and suggests a significant contribution from more juvenile isotopic sources (Fig. 6). Consequently, the basal allochthonous units were deposited in a rather different location across the continental margin relative to the autochthonous series, as it can also be deduced from the contrasting structural position they acquired during the Variscan collision (lower structural position in the Variscan tectonic pile implies inner paleogeographic location across Gondwana; Martínez Catalán et al., 2009).

Detrital zircon ages and geochemical data alike indicate that the West African Craton was one of the fundamental sources for the metasedimentary rocks of the Iberian Massif during the Neoproterozoic and Paleozoic (e.g., Albert et al., 2015a; Díez Fernández et al., 2012b; Fernández-Suárez et al., 2002, 2013; Martínez Catalán et al., 2004; Pereira, 2015). Accordingly, the contribution of juvenile material seems minor in any of the sets of basal allochthonous units of the Iberian Massif, as their Sm–Nd model ages approach or even match the range of protolith ages found in the aforementioned cratonic area (e.g., Ennih and Liégeois, 2008; Nance and Murphy, 1994).

A potential isotopic rejuvenation effect, expected for a magmatic arc system on its adjacent basins, is missing or weak in the Ediacaran series of the basal allochthonous units. This cannot be explained by a lack of material derived from erosion of igneous rocks formed in the context of a Neoproterozoic (Cadomian) magmatic arc. Populations of detrital zircon grains in the Ediacaran series peak consistently at ca. 0.65–0.55 Ma (Cadomian ages), and are in fact the dominant group of igneous-derived grains (Fig. 7c). It is the particular nature of the source area, probably made of a cratonic block (ca. 2.2–1.8 Ga old) and/or by recycled material derived from Eburnean crust (e.g., Abati et al., 2012), and then intruded by abundant, not-juvenile Neoproterozoic material, that confers a rather distinctive signature to the Ediacaran metasedimentary rocks of the basal allochthonous units of the Iberian Massif. Such signature makes them genetically correlatives by means of isotopic and geochemical composition and detrital zircon input. Accordingly, a fragment of the West African Craton intruded by Neoproterozoic felsic magmas, mostly sourced from the same craton in the context of a continental volcanic arc, is the most likely source for the Ediacaran metasedimentary rocks.

The lithostratigraphical, geochronological, and geochemical characteristics of the Ediacaran series studied in this work are, in general terms, equivalent to those exposed in the Saxo-Thuringian Zone of the Bohemian Massif. Similarities in the sedimentary record include (1) major and trace-elements signatures reflecting an active margin setting during deposition, (2) REE-patterns pointing to the continental crust as the dominant source for sediment (continental arc), (3) minor contrast among the location of source areas (indicated by Pb and Nd systematics), and (4) derivation from an old craton inferred from Nd isotopic data and U–Pb detrital zircon age populations (Linnemann and Romer, 2002; Linnemann et al., 2004, 2008).

Previous correlations established between Ediacaran series of the Bohemian Massif and SW Iberian Massif suggested a diachronic evolution along the northern margin of Gondwana during the late Neoproterozoic, including the development of a continental magmatic arc system and the opening of back-arc basins at the periphery of the West African Craton (Linnemann et al., 2008; M.F. Pereira et al., 2006). Given the correlation of Ediacaran rocks from NW Iberia and SW Iberia suggested in this work, similar subduction-related geotectonic processes may have also affected the metasedimentary rock series exposed in NW Iberia during the Neoproterozoic (e.g., Díez Fernández et al., 2010). The similarities shown by the Ediacaran series involved in the Variscan orogeny, both in SW Iberia, NW Iberia, and Central Europe, strengthen the idea of a rather continuous peripheral orogen that developed along the margin of Gondwana in Ediacaran times (Linnemann et al., 2007; Nance and Murphy, 1994). Some authors believe that this orogen and the terranes that derived from it can be followed up to basement rocks in China (in the so-called Asian or Chinese terranes; Stampfli et al., 2013; von Raumer et al., 2015), meaning that comparable units might be found along thousands of kilometers along the paleomargin of Gondwana.

5.2. A single Precambrian terrane?

The multi-proxy evaluation of the Ediacaran series of the basal allochthonous units of the Iberian Massif reveals striking similarities in their tectonostratigraphy, metamorphic and microstructural evolution, geochronology of main tectonic events, protolith ages, provenance of their metasedimentary rocks, and whole-rock and isotope geochemistry. They reinforce recently proposed structural correlations between high-P allochthonous terranes of the Iberian Massif (Fig. 1; Díez Fernández and Arenas, 2015), and put forward the existence of a rather distinctive Ediacaran series as the base to a far-traveled tectonic pile made of continental and ophiolitic terranes with Gondwanan derivation. These particular series, the Ediacaran basal allochthonous units, would consist of metagreywackes and albite-bearing schists and paragneisses (showing clear Bouma cycles in the less-deformed terms), layers of black (organic- and heavy minerals-rich) metasedimentary rocks, lenses of mafic rocks (eclogites, variably retrogressed eclogites, and amphibolites), and bodies of orthogneisses of Cambrian-Ordovician age. Sm–Nd model ages of its metasedimentary rocks would approach significantly a Paleoproterozoic range (Fig. 6; 2.15–1.5 Ga), and their deposition would be connected to a peri-Gondwanan arc system built close to, and probably at the expense of the West African Craton.

Some differences in the lithostratigraphy of the previously described basal allochthonous units, such as the absence of an Early Cambrian sequence containing marbles in NW Iberia, or the presence of black quartzites in the Évora Massif instead of black metapelites like in NW Iberia, may be explained by tectonic removal via Variscan faults and/or by lateral variations within a single paleogeographic domain, respectively. The latter hypothesis could also provide an explanation for the slight variation observed in the isotopic contributions of the metasedimentary series in NW and SW Iberia. Note that we are dealing with a quite large piece of continental crust, which according to present-day structures extends for at least 400 km in both, cross-section and along strike (Fig. 1), and is still rather homogeneous regarding most of its distinctive features. Building on this thought, the basal allochthonous units exposed in the Central Unit, located in between NW Iberia and the Évora Massif (Fig. 1), show an intermediate composition in terms of isotopic sources (Fig. 6). Thus, there is a regional trend suggesting more (yet limited) contributions of juvenile material towards the occurrences located to the SW. The absence of sharp changes within the basal allochthon, such as that between the autochthon and the whole basal allochthon, suggests that the different Ediacaran series making the basal allochthon belonged to the same paleogeographic domain, a section of a continental margin with little, though progressive variations in its sources.

The age of post-Precambrian and pre-Variscan magmatism that affected the series of the basal allochthonous units is also slightly different. Its age range is Cambrian to Ordovician in NW Iberia (e.g., Díez Fernández et al., 2012a) and in the Central Unit (e.g., Ordóñez Casado, 1998), whereas it is essentially Cambrian in SW Iberia (e.g., Chichorro et al., 2008). Such small variations in the age of early Paleozoic magmatic events may be due to slightly different positions of these series along the margin of Gondwana in Cambrian-Ordovician times. However, the synchrony of high-P Variscan metamorphism affecting those same series suggests that they were spread laterally along the same continental margin in Late Devonian times, when they all were simultaneously incorporated to a continental subduction system.

The Ediacaran series of the basal allochthonous units of the Iberian Massif are overlain by pieces of transitional and oceanic crust representing a Variscan intra-Gondwana suture zone (Díez Fernández and Arenas, 2015). This suture zone probably resulted from the closure of a Devonian peri-Gondwanan basin opened in the course of the multi-stage collision between Gondwana and Laurussia in late Paleozoic times (Arenas et al., 2014a, 2014b). This suture zone is traceable at a regional scale by means of the Late Devonian high-P metamorphism that affects the upper part of its lower plate, i.e., the basal allochthonous units themselves. The lithological and geochemical data of these high-P units, along with the regional tectonostratigraphic frame, provide solid grounds on which future research could identify more occurrences of that suture zone throughout the Variscan orogen.

We are aware that the geological features here suggested to be used as an additional guide for tracing a suture zone might not be applicable to other sections of the Variscan orogen. Changes in the Precambrian paleogeography along-strike of the Gondwana margin are likely, although pending proper description. However, these proxies seem to work quite well for the case of the Iberian Massif and thence, they should be considered as a new approach to understand, evaluate, and acknowledge the fundamental role of the Precambrian geology in the reconstruction of Paleozoic geodynamics at a much larger scale.

The correlation and geochemical affinity between the Ediacaran series of the basal allochthonous units of the Iberian Massif pointed out here leads to the question whether various Precambrian continental terranes participated in the Late Devonian subduction system formed during the collision of Gondwana and Laurussia. We rather suggest that it was a single, yet slightly heterogeneous continental margin whose lower section consisted of Ediacaran immature sedimentary series deposited in relation to a Cadomian magmatic arc.

6. Conclusions

We conclude that the lithostratigraphical, tectonometamorphic, geochronological, and geochemical affinities between the basal allochthonous units of NW and SW Iberia suggest that their high-P rocks define the base of an intra-Gondwana suture zone of the Iberian Massif, derived from a rather similar Ediacaran immature sedimentary series, formerly deposited along the same continental active margin related to a Cadomian magmatic arc. The isotopic sources of these series, as constrained by Sm–Nd systematics, are among the oldest of the Iberian Massif (2.15–1.5 Ga), indicating a very strong contribution of sources located in the West African Craton. The age of the first deformation and metamorphism recorded in these series is Late Devonian (ca. 370 Ma) and is related to continental subduction (blueschist to eclogite facies metamorphism). Remnants of the basal allochthonous units are overlain by allochthonous ophiolitic units of different age and nature, and are found on top of sections of continental crust lacking of pervasive high-P and low- to medium-T Devonian metamorphism, i.e., separated by crustal-scale thrusts. All these characteristics combined make these particular Ediacaran series genuinely different from the rest of the Iberian terranes, what it also makes them an excellent candidate to trace cryptic occurrences of a dismembered intra-Gondwana suture zone along the Variscan orogen, even in the absence of actual ophiolitic rocks.

By establishing a correlation between the basal allochthonous units of Iberia, it has been reduced the number of individual terranes located at the core of Pangea during its amalgamation. Separate exposures of Ediacaran series may well correspond to a single, yet tectonically dismembered terrane. Besides, the basal allochthonous units constitute the base of one of the fundamental suture zones occurring in the Variscan orogen, what makes their characterization a primary goal for future tectonic studies concerned with tracing such major tectonic boundary along this late Paleozoic mountain belt.

Acknowledgments

Insightful comments provided by Jürgen von Raumer and an anonymous reviewer are kindly acknowledged. Financial support has been provided by Fundação para a Ciência e Tecnologia (Portugal) through research project “GOLD” (PTDC/GEO-GEO/2446/2012: COMPETE: FCOMP-01-0124-FEDER-029192), and by Ministerio de Economía y Competitividad (Spain) through research project CGL2012-34618. Rubén Díez Fernández appreciates financial support from Fundação para a Ciência e Tecnologia (Portugal) through its postdoctoral program (SFRH/BPD/85209/2012). This work is a contribution to IGCP project 648 (Supercontinent Cycle and Global Geodynamics).

References

Abalos, B., Gil Ibarguchi, J.I., Eguiluz, L., 1991. Cadomian subduction, collision and Variscan transpression in the Badajoz-Cordoba Shear Belt, Southwest Spain. Tectonophysics 199, 51–72.

Abati, J., Gerdes, A., Fernández-Suárez, J., Arenas, R., Whitehouse, M.J., Díez Fernández, R., 2010. Magmatism and early-Variscan continental subduction in the northern Gondwana margin recorded in zircons from the basal units of Galicia, NW Spain. Geological Society of America Bulletin 122, 219–235.

Abati, J., Aghzer, A.M., Gerdes, A., Ennih, N., 2012. Insights on the crustal evolution of the West African Craton from Hf isotopes in detrital zircons from the Anti-Atlas belt. Precambrian Research 212–213, 263–274.

Albert, R., Arenas, R., Sánchez-Martínez, S., Gerdes, A., 2012. The eclogite facies gneisses of the Cabo Ortegal Complex (NW Iberian Massif): tectonothermal evolution and exhumation model. Journal of Iberian Geology 38, 389–406.

Albert, R., Arenas, R., Gerdes, A., Sánchez Martínez, S., Fernández-Suárez, J., Fuenlabrada, J.M., 2015a. Provenance of the Variscan Upper Allochthon (Cabo Ortegal Complex, NW Iberian Massif). Gondwana Research 28, 1434–1448.

Albert, R., Arenas, R., Gerdes, A., Sánchez Martínez, S., Marko, L., 2015b. Provenance of the high-P and high-T unit of the Cabo Ortegal Complex (NW Iberian Massif). Journal of Metamorphic Geology 33, 959–979.

Alcock, J.E., Martínez Catalán, J.R., Rubio Pascual, F.J., Montes, A.D., Díez Fernández, R., Gómez Barreiro, J., Arenas, R., Dias da Silva, Í., González Clavijo, E., 2015. 2-D thermal modeling of HT-LP metamorphism in NW and Central Iberia: Implications for Variscan magmatism, rheology of the lithosphere and orogenic evolution. Tectonophysics 657, 21–37.

Andonaegui, P., Castiñeiras, P., González Cuadra, P., Arenas, R., Sánchez Martínez, S., Abati, J., Díaz García, F., Martínez Catalán, J.R., 2012. The Corredoiras orthogneiss (NW Iberian Massif): Geochemistry and geochronology of the Paleozoic magmatic suite developed in a peri-Gondwanan arc. Lithos 128–131, 84–99.

Araújo, A., Fonseca, P.E., Munhá, J.M., Moita, P., Pedro, J., Ribeiro, A., 2005. The Moura Phyllonitic Complex: an accretionary complex related with obduction in the Southern Iberia Variscan Suture. Geodinamica Acta 18, 375–388.

Arenas, R., Martínez Catalán, J.R., 2003. Low-P metamorphism following a Barrovian-type evolution. Complex tectonic controls for a common transition, as deduced in the Mondoñedo thrust sheet (NW Iberian-Massif). Tectonophysics 365, 143–164.

Arenas, R., Sánchez Martínez, S., 2015. Variscan ophiolites in NW Iberia: Tracking lost Paleozoic oceans and the assembly of Pangea. Episodes 38, 315–333.

Arenas, R., Gil Ibarguchi, J.I., González Lodeiro, F., Klein, E., Martínez Catalán, J.R., Ortega Gironés, E., Pablo Maciá, J.G.d., Peinado, M., 1986. Tectonostratigraphic units in the complexes with mafic and related rocks of the NW of the Iberian Massif. Hercynica 2, 87–110.

Arenas, R., Rubio Pascual, F.J., Díaz García, F., Martínez Catalán, J.R., 1995. High-pressure micro-inclusions and development of an inverted metamorphic gradient in the Santiago-schists (Órdenes-Complex, NW Iberian Massif, Spain) - evidence of subduction and syncollisional decompression. Journal of Metamorphic Geology 13, 141–164.

Arenas, R., Martínez Catalán, J.R., Sánchez Martínez, S., Díaz García, F., Abati, J., Fernández-Suárez, J., Andonaegui, P., Gómez Barreiro, J., 2007a. Paleozoic ophiolites in the Variscan suture of Galicia (northwest Spain): distribution, characteristics and meaning. In: Hatcher, R.D., Carlson, M.P., Mcbride, J.H., Martínez Catalán, J.R. (Eds.), 4-D Framework of Continental Crust. Geological Society of America Memoir, Boulder, Colorado, pp. 425–444.

Arenas, R., Martínez Catalán, J.R., Sánchez Martínez, S., Fernández-Suárez, J., Andonaegui, P., Pearce, J.A., Corfú, F., 2007b. The Vila de Cruces ophiolite: A remnant of the early Rheic Ocean in the Variscan suture of Galicia (northwest Iberian Massif). The Journal of Geology 115, 129–148.

Arenas, R., Díez Fernández, R., Sánchez Martínez, S., Gerdes, A., Fernández-Suárez, J., Albert, R., 2014a. Two-stage collision: Exploring the birth of Pangea in the Variscan terranes. Gondwana Research 25, 756–763.

Arenas, R., Sánchez Martínez, S., Gerdes, A., Albert, R., Díez Fernández, R., Andonaegui, P., 2014b. Re-interpreting the Devonian ophiolites involved in the Variscan suture: U–Pb and Lu–Hf zircon data of the Moeche Ophiolite (Cabo Ortegal Complex, NW Iberia). International Journal of Earth Sciences 103, 1385–1402.

Arenas, R., Díez Fernández, R., Rubio Pascual, F.J., Sánchez Martínez, S., Martín Parra, L.M., Matas, J., González del Tánago, J., Jiménez-Díaz, A., Fuenlabrada, J.M., Andonaegui, P., García-Casco, A., 2016a. The Galicia–Ossa-Morena Zone: Proposal for a new zone of the Iberian Massif. Variscan implications. Tectonophysics 681, 135–143.

Arenas, R., Sánchez Martínez, S., Díez Fernández, R., Gerdes, A., Abati, J., Fernández-Suárez, J., Andonaegui, P., González Cuadra, P., López Carmona, A., Albert, R., Fuenlabrada, J.M., Rubio Pascual, F.J., 2016b. Allochthonous terranes involved in the Variscan suture of NW Iberia: A review of their origin and tectonothermal evolution. Earth-Science Reviews 161, 140–178.

Azor, A., Lodeiro, F.G., Simancas, J.F., 1994. Tectonic evolution of the boundary between the Central Iberian and Ossa-Morena zones (Variscan belt, southwest Spain). Tectonics 13, 45–61.

Ballèvre, M., Bosse, V., Ducassou, C., Pitra, P., 2009. Palaeozoic history of the Armorican Massif: Models for the tectonic evolution of the suture zones. Comptes Rendus Geoscience 341, 174–201.

Bambach, R.K., Scotese, C.R., Ziegler, A.M., 1980. Before Pangea: The Geographies of the Paleozoic World. American Scientist 68, 26–38.

Beaumont, C., Jamieson, R.A., Butler, J.P., Warren, C.J., 2009. Crustal structure: A key constraint on the mechanism of ultra-high-pressure rock exhumation. Earth and Planetary Science Letters 287, 116–129.

Bhatia, M.R., Crook, K.A.W., 1986. Trace elements characteristics of greywackes and tectonic setting discrimination of sedimentary basins. Contributions to Mineralogy and Petrology 92, 181–193.

Booth-Rea, G., Simancas, J.F., Azor, A., Azañón, J.M., González-Lodeiro, F., Fonseca, P., 2006. HP-LT Variscan metamorphism in the Cubito-Moura schists (Ossa-Morena Zone, southern Iberia). Comptes Rendus Geoscience 338, 1260–1267.

Burg, J.P., Iglesias, M., Laurent, P., Matte, P., Ribeiro, A., 1981. Variscan intracontinental deformation: the Coimbra-Cordoba shear zone (SW Iberian Peninsula). Tectonophysics 78, 161–177.

Carvalhosa, A., 1965. Contribuição para o conhecimento geológico da região entre Portel e Ficalho (Alentejo). Memorias dos Serviços Geológicos de Portugal 11, 1–130.

Carvalhosa, A., 1983. Esquema geológico do Maciço de Évora. Comunicações dos Serviços Geológicos de Portugal 69, 201–208.

Carvalhosa, A., 1999. Carta Geológica de Portugal, Noticia Explicativa da Folha 36-C (Arraiolos), scale 1:50,000. Instituto Geológico e Mineiro.

Carvalhosa, A., Zbyszewski, G., 1994. Carta Geológica de Portugal, Noticia Explicativa da Folha 35-D (Montemor-o-Novo), scale 1:50,000. Instituto Geológico e Mineiro.

Carvalhosa, A., Galopim de Carvalho, A.M., Matos Alves, C.A., Pina, H.L., 1969. Carta Geológica de Portugal, Noticia Explicativa da Folha 40-A (Évora), scale 1:50,000. Serviços Geológicos de Portugal.

Carvalhosa, A., Gonçalves, F., Oliveira, V., 1987. Carta Geológica de Portugal, Noticia Explicativa da Folha 36-D (Redondo), scale 1:50,000. Instituto Geológico e Mineiro.

Castro, A., 1987. Implicaciones de la zona Ossa-Morena y dominios equivalentes en el modelo geodinámico de la Cadena Hercinica europea. Estudios Geológicos 43, 249–260.

Chemenda, A.I., Mattauer, M., Bokun, A.N., 1996. Continental subduction and a mechanism for exhumation of high-pressure metamorphic rocks: new modelling and field data from Oman. Earth and Planetary Science Letters 143, 173–182.

Chichorro, M., 2006. Tectonic evolution of Montemor-o-Novo Shear Zone (SW Ossa Morena Zone - Santiago do Escoural - Cabrela Área). Universidade de Évora, Évora, Portugal, p. 569.

Chichorro, M., Pereira, M.F., Apraiz, A., Silva, J.B., 2003. High temperature-Low pressure tectonites from the Boa Fé Fault Zone (Évora Massif, Ossa-Morena Zone, Portugal): Evidences for transtensional tectonics. Geogaceta 34, 43–46.

Chichorro, M., Pereira, M.F., Díaz-Azpiroz, M., Williams, I.S., Fernández, C., Pin, C., Silva, J.B., 2008. Cambrian ensialic rift-related magmatism in the Ossa-Morena Zone (Évora-Aracena metamorphic belt, SW Iberian Massif): Sm–Nd isotopes and SHRIMP zircon U–Th–Pb geochronology. Tectonophysics 461, 91–113.

Condie, K.C., 1993. Chemical composition and evolution of the upper continental crust: contrasting results from surface samples and shales. Chemical Geology 104, 1–37.

Cullers, R.L., 1994. The controls on the major and trace element variation of shales, siltstones and sandstones of Pennsylvanian–Permian age from uplifted continental blocks in Colorado to platform sediment in Kansas, USA. Geochimica et Cosmochimica Acta 58, 4955–4972.

Cullers, R.L., 2002. Implications of elemental concentrations for provenance, redox conditions, and metamorphic studies of shales and limestones near Pueblo, CO, USA. Chemical Geology 191, 305–327.

Dabard, M.-P., 2000. Petrogenesis of graphitic cherts in the Armorican segment of the Cadomian orogenic belt (NW France). Sedimentology 47, 787–800.

Dabard, M.-P., Loi, A., 1998. Environnement de dépôt des formations à phtanites interstratifiés du Protérozoïque supérieur armoricain (France): conséquences sur la genèse des phtanites. Comptes Rendus de l'Académie des Sciences - Series IIA - Earth and Planetary Science 326, 763–769.

De Oliveira, D.P.S., Reed, R.M., Milliken, K.L., Robb, L.J., Inverno, C.M.C., D'Orey, F.L.C., 2003. Série Negra black quartzites - Tomar Cordoba Shear Zone, E Portugal: mineralogy and cathodoluminescence studies. Cuadernos do Laboratorio Xeolóxico de Laxe 28, 193–211.

DePaolo, D.J., 1981. Neodymium isotopes in the Colorado Front Range and crustal-mantle evolution in the Proterozoic. Nature 291, 193–196.

Díaz García, F., Arenas, R., Martínez Catalán, J.R., del Tanago, J.G., Dunning, G.R., 1999. Tectonic evolution of the Careon ophiolite (northwest Spain). A remnant of oceanic lithosphere in the Variscan belt. The Journal of Geology 107, 587–605.

Díez Fernández, R., 2011. Evolución estructural y cinemática de una corteza continental subducida: la Unidad de Malpica-Tui (NO del Macizo Ibérico). Nova Terra 40, 1–228.

Díez Fernández, R., Arenas, R., 2015. The Late Devonian Variscan suture of the Iberian Massif: A correlation of high-pressure belts in NW and SW Iberia. Tectonophysics 654, 96–100.

Díez Fernández, R., Arenas, R., 2016. Reply to Comment on "The Late Devonian Variscan suture of the Iberian Massif: A correlation of high-pressure belts in NW and SW Iberia". Tectonophysics 670, 155–160.

Díez Fernández, R., Martínez Catalán, J.R., 2012. Stretching lineations in high-pressure belts: the fingerprint of subduction and subsequent events (Malpica–Tui complex, NW Iberia). Journal of the Geological Society 169, 531–543.

Díez Fernández, R., Martínez Catalán, J.R., Gerdes, A., Abati, J., Arenas, R., Fernández-Suárez, J., 2010. U–Pb ages of detrital zircons from the Basal allochthonous units of NW Iberia: Provenance and paleoposition on the northern margin of Gondwana during the Neoproterozoic and Paleozoic. Gondwana Research 18, 385–399.

Díez Fernández, R., Martínez Catalán, J.R., Arenas, R., Abati, J., 2011. Tectonic evolution of a continental subduction-exhumation channel: Variscan structure of the basal allochthonous units in NW Spain. Tectonics 30, TC3009.

Díez Fernández, R., Castiñeiras, P., Gómez Barreiro, J., 2012a. Age constraints on Lower Paleozoic convection system: magmatic events in the NW Iberian Gondwana margin. Gondwana Research 21, 1066–1079.

Díez Fernández, R., Martínez Catalán, J.R., Arenas, R., Abati, J., Gerdes, A., Fernández-Suárez, J., 2012b. U–Pb detrital zircon analysis of the lower allochthon of NW Iberia: age constraints, provenance and links with the Variscan mobile belt and Gondwanan cratons. Journal of the Geological Society 169, 655–665.

Díez Fernández, R., Martínez Catalán, J.R., Gómez Barreiro, J., Arenas, R., 2012c. Extensional flow during gravitational collapse: a tool for setting plate convergence (Padrón migmatitic dome, Variscan belt, NW Iberia). The Journal of Geology 120, 83–103.

Díez Fernández, R., Foster, D.A., Gómez Barreiro, J., Alonso-García, M., 2013. Rheological control on the tectonic evolution of a continental suture zone: the Variscan example from NW Iberia (Spain). International Journal of Earth Sciences 102, 1305–1319.

Díez Fernández, R., Pereira, M.F., Foster, D.A., 2015. Peralkaline and alkaline magmatism of the Ossa-Morena zone (SW Iberia): Age, source, and implications for the Paleozoic evolution of Gondwanan lithosphere. Lithosphere 7, 73–90.

Díez Fernández, R., Arenas, R., Pereira, M.F., Sánchez Martínez, S., Albert, R., Martín Parra, L.M., Rubio Pascual, F.J., Matas, J., 2016. Tectonic evolution of Variscan Iberia: Gondwana - Laurussia collision revisited. Earth-Science Reviews 162, 269–292.

Ennih, N., Liégeois, J.P., 2008. The boundaries of the West African craton, with special reference to the basement of the Moroccan metacratonic Anti-Atlas belt. In: Ennih, N., Liégeois, J.P. (Eds.), The Boundaries of the West African Craton. Geological Society, London, Special Publications:pp. 1–17. http://dx.doi.org/10.1144/SP1297.1141.

Escuder Viruete, J.E., Indares, A., Arenas, R., 1997. P–T path determinations in the Tormes Gneissic Dome, NW Iberian Massif, Spain. Journal of Metamorphic Geology 15, 645–663.

Faure, M., Lin, W., Schärer, U., Shu, L., Sun, Y., Arnaud, N., 2003. Continental subduction and exhumation of UHP rocks. Structural and geochronological insights from the Dabieshan (East China). Lithos 70, 213–241.

Faure, M., Lardeaux, J.-M., Ledru, P., 2009. A review of the pre-Permian geology of the Variscan French Massif Central. Comptes Rendus Geoscience 341, 202–213.

Fedo, C.M., Nesbitt, H.W., Young, G.M., 1995. Unravelling the effects of potassium metasomatism in sedimentary rocks and paleosols, with implications for paleoweathering conditions and provenance. Geology 23, 921–924.

Fernández-Suárez, J., Dunning, G.R., Jenner, G.A., Gutiérrez-Alonso, G., 2000. Variscan collisional magmatism and deformation in NW Iberia: constraints from U–Pb geochronology of granitoids. Journal of the Geological Society 157, 565–576.

Fernández-Suárez, J., Gutiérrez-Alonso, G., Jeffries, T.E., 2002. The importance of along-margin terrane transport in northern Gondwana: insights from detrital zircon parentage in Neoproterozoic rocks from Iberia and Brittany. Earth and Planetary Science Letters 204, 75–88.

Fernández-Suárez, J., Arenas, R., Abati, J., Martínez Catalán, J.R., Whitehouse, M.J., Jeffries, T.E., 2007. U–Pb chronometry of polymetamorphic high-pressure granulites: An example from the allochthonous terranes of the NW Iberian Variscan belt. Geological Society of America Memoirs 200, 469–488.

Fernández-Suárez, J., Gutiérrez-Alonso, G., Pastor-Galán, D., Hofmann, M., Murphy, J.B., Linnemann, U., 2013. The Ediacaran–Early Cambrian detrital zircon record of NW Iberia: possible sources and paleogeographic constraints. International Journal of Earth Sciences 1–23.

Fonseca, P., Munhá, J., Pedro, J., Rosas, F., Moita, P., Araújo, A., Leal, N., 1999. Variscan ophiolites and high-pressure metamorphism in southern Iberia. Ofioliti 24, 259–268.

Franke, W., 1989. Variscan plate-tectonics in Central-Europe — current ideas and open questions. Tectonophysics 169, 221–228.

Fuenlabrada, J.M., Arenas, R., Sánchez Martínez, S., Díaz García, F., Castiñeiras, P., 2010. A peri-Gondwanan arc in NW Iberia: I: Isotopic and geochemical constraints on the origin of the arc — A sedimentary approach. Gondwana Research 17, 338–351.

Fuenlabrada, J.M., Arenas, R., Díez Fernández, R., Sánchez Martínez, S., Abati, J., López Carmona, A., 2012. Sm–Nd isotope geochemistry and tectonic setting of the metasedimentary rocks from the basal allochthonous units of NW Iberia (Variscan suture, Galicia). Lithos 148, 196–208.

Fuenlabrada, J.M., Pieren, A.P., Díez Fernández, R., Sánchez Martínez, S., Arenas, R., 2016. Geochemistry of the Ediacaran-Early Cambrian transition in Central Iberia: Tectonic setting and isotopic sources. Tectonophysics 681, 15–30.

Gerya, T.V., Perchuk, L.L., Burg, J.-P., 2008. Transient hot channels: Perpetrating and regurgitating ultrahigh-pressure, high-temperature crust–mantle associations in collision belts. Lithos 103, 236–256.

Gil Ibarguchi, J.I., Ortega Gironés, E., 1985. Petrology, structure and geotectonic implications of glaucophane-bearing eclogites and related rocks from the Malpica–Tuy (MT) Unit, Galicia, Northwest Spain. Chemical Geology 50, 145–162.

Gil Ibarguchi, J.I., Mendia, M., Girardeau, J., Peucat, J.J., 1990. Petrology of eclogites and clinopyroxene garnet metabasites from the Cabo-Ortegal complex (Northwestern Spain). Lithos 25, 133–162.

Girardeau, J., Ibarguchi, J.I.G., 1991. Pyroxenite-Rich Peridotites of the Cabo Ortegal Complex (Northwestern Spain): Evidence for Large-Scale Upper-Mantle Heterogeneity. Journal of Petrology Special Volume 135–154.

Gómez Barreiro, J., Martínez Catalán, J.R., Arenas, R., Castiñeiras, P., Abati, J., Díaz García, F., Wijbrans, J.R., 2007. Tectonic evolution of the upper allochthon of the Órdenes complex (northwestern Iberian Massif): Structural constraints to a polyorogenic peri-Gondwanan terrane. In: Linnemann, U., Nance, R.D., Kraft, P., Zulauf, G. (Eds.), The evolution of the Rheic Ocean: From Avalonian-Cadomian active margin to Alleghenian-Variscan collision. Geological Society of America Special Paper, pp. 315–332 (doi: 310.1130/2007.2423(1115)).

Gómez Barreiro, J., Martínez Catalán, J.R., Díez Fernández, R., Arenas, R., Díaz García, F., 2010. Upper crust reworking during gravitational collapse: the Bembibre-Pico Sacro detachment system (NW Iberia). Journal of the Geological Society 167, 769–784.

Herron, M.M., 1988. Geochemical classification of terrigenous sands and shales from core or log data. Journal of Sedimentary Petrology 58, 820–829.

Kroner, U., Romer, R.L., 2013. Two plates — Many subduction zones: The Variscan orogeny reconsidered. Gondwana Research 24, 298–329.

Leal, N., 2001. Estudo petrológico e geoquímico de rochas metamórficas maficas de alta pressão das regiões do Alvito-Viana do Alentejo e de Safira (Zona de Ossa-Morena, Maciço Ibérico). Unpublished. Universidade de Lisboa, Lisboa, p. 401.

Lima, S.M., Neiva, A.M.R., Ramos, J.M.F., 2013. Adakitic-like magmatism in western Ossa-Morena Zone (Portugal): Geochemical and isotopic constraints of the Pavia pluton. Lithos 160-161, 98–116.

Linnemann, U., Romer, R.L., 2002. The Cadomian Orogeny in Saxo-Thuringia, Germany: geochemical and Nd–Sr–Pb isotopic characterization of marginal basins with constraints to geotectonic setting and provenance. Tectonophysics 352, 33–64.

Linnemann, U., McNaughton, N.J., Romer, R.L., Gehmlich, M., Drost, K., Tonk, C., 2004. West African provenance for Saxo-Thuringia (Bohemian Massif): Did Armorica ever leave pre-Pangean Gondwana? U/Pb-SHRIMP zircon evidence and the Nd-isotopic record. International Journal of Earth Sciences 93, 683–705.

Linnemann, U., Gerdes, A., Drost, K., Buschmann, B., 2007. The continuum between Cadomian orogenesis and opening of the Rheic Ocean: Constraints from LA-ICP-MS U–Pb zircon dating and analysis of plate-tectonic setting (Saxo-Thuringian zone, northeastern Bohemian Massif, Germany). In: Linnemann, U., Nance, R.D., Kraft, P., Zulauf, G. (Eds.), The evolution of the Rheic Ocean: From Avalonian-Cadomian active margin to Alleghenian-Variscan collision. Geological Society of America Special Paper 423, pp. 61–96.

Linnemann, U., Pereira, F., Jeffries, T.E., Drost, K., Gerdes, A., 2008. The Cadomian Orogeny and the opening of the Rheic Ocean: The diacrony of geotectonic processes constrained by LA-ICP-MS U–Pb zircon dating (Ossa-Morena and Saxo-Thuringian Zones, Iberian and Bohemian Massifs). Tectonophysics 461, 21–43.

López-Carmona, A., Pitra, P., Abati, J., 2013. Blueschist-facies metapelites from the Malpica–Tui Unit (NW Iberian Massif): phase equilibria modelling and H_2O and Fe_2O_3 influence in high-pressure assemblages. Journal of Metamorphic Geology 31, 263–280.

López-Carmona, A., Abati, J., Pitra, P., Lee, J.W., 2014. Retrogressed lawsonite blueschists from the NW Iberian Massif: P–T–t constraints from thermodynamic modelling and $^{40}Ar/^{39}Ar$ geochronology. Contributions to Mineralogy and Petrology 167, 1–20.

López-Guijarro, R., Armendariz, M., Quesada, C., Fernández-Suárez, J., Murphy, J.B., Pin, C., Bellido, F., 2008. Ediacaran-Palaeozoic tectonic evolution of the Ossa Morena and Central Iberian zones (SW Iberia) as revealed by Sm–Nd isotope systematics. Tectonophysics 461, 202–214.

Lugmair, G.W., Shimamura, T., Lewis, R.S., Anders, E., 1983. Sm-146 in the early solarsystem — evidence from neodymium in the Allende meteorite. Science 222, 1015–1018.

Mahlen, N.J., Johnson, C.M., Baumgartner, L.P., Beard, B.L., 2005. Provenance of Jurassic Tethyan sediments in the HP/UHP Zermatt-Saas ophiolite, western Alps. Geological Society of America Bulletin 117, 530–544.

Martínez Catalán, J.R., Arenas, R., Díaz García, F., Rubio Pascual, F.J., Abati, J., Marquínez García, J., 1996. Variscan exhumation of a subducted paleozoic continental margin: The basal units of the Ordenes Complex, Galicia, NW Spain. Tectonics 15, 106–121.

Martínez Catalán, J.R., Díaz García, F., Arenas, R., Abati, J., Castineiras, P., González Cuadra, P., Gómez Barreiro, J., Rubio Pascual, F.J., 2002. Thrust and detachment systems in the Ordenes complex (northwestern Spain): implications for the Variscan-Appalachian geodynamics. In: Martínez Catalán, J.R., Hatcher, R.D., Arenas, R., Díaz García, F. (Eds.), Variscan-Appalachian Dynamics: the Building of the Late Paleozoic Basement. Geological Society of America Special Paper, pp. 163–182 (doi: 110.1130/1130–8137–2364-1137.1163).

Martínez Catalán, J.R., Fernández-Suárez, J., Jenner, G.A., Belousova, E., Díez Montes, A., 2004. Provenance constraints from detrital zircon U–Pb ages in the NW Iberian Massif: implications for Palaeozoic plate configuration and Variscan evolution. Journal of the Geological Society 161, 463–476.

Martínez Catalán, J.R., Arenas, R., Díaz García, F., Gómez Barreiro, J., González Cuadra, P., Abati, J., Castiñeiras, P., Fernández-Suárez, J., Sánchez Martínez, S., Andonaegui, P., González Clavijo, E., Díez Montes, A., Rubio Pascual, F.J., Valle Aguado, B., 2007. Space and time in the tectonic evolution of the northwestern Iberian Massif. Implications for the Variscan belt. In: Hatcher, R.D., Carlson, M.P., Mcbride, J.H., Martínez Catalán, J.R. (Eds.), 4-D Framework of Continental Crust. Geological Society of America Memoir, Boulder, Colorado, pp. 403–423.

Martínez Catalán, J.R., Arenas, R., Abati, J., Sánchez Martínez, S., Díaz García, F., Fernández-Suárez, J., González Cuadra, P., Castineiras, P., Gómez Barreiro, J., Díez Montes, A., González Clavijo, E., Rubio Pascual, F.J., Andonaegui, P., Jeffries, T.E., Alcock, J.E., Díez Fernández, R., López Carmona, A., 2009. A rootless suture and the loss of the roots of a mountain chain: The Variscan belt of NW Iberia. Comptes Rendus Geoscience 341, 114–126.

Matte, P., 1991. Accretionary history and crustal evolution of the Variscan belt in Western Europe. Tectonophysics 196, 309–337.

McLennan, S.M., Taylor, S.R., Eriksson, K.A., 1983. Geochemistry of Archaean shales from the Pilbara Supergroup, Western Australia. Geochimica et Cosmochimica Acta 47, 1211–1222.

McLennan, S.M., Taylor, S.R., McCulloch, M.T., Maynard, J.B., 1990. Geochemical and Nd–Sr isotopic composition of deep-sea turbidites: crustal evolution and plate tectonic associations. Geochimica et Cosmochimica Acta 54, 2015–2050.

McLennan, S.M., Hemming, S.R., McDaniel, D.K., Hanson, G.N., 1993. Geochemical approaches to sedimentation, provenance and tectonics. In: Johnssons, M.J., Basu, A. (Eds.), Processes controlling the composition of clastic sediments. Geological Society of America, Special Paper vol. 284, pp. 21–40.

Moita, P., Munhá, J., Fonseca, P.E., Pedro, J., Tassinari, C.C.G., Araújo, A., Palacios, T., 2005. Phase equilibria and geochronology of Ossa-Morena eclogites. XIV Semana de Geoquímica, VIII Congresso de Geoquímica dos Paises de Lingua Portuguese, pp. 463–466.

Moita, P., Santos, J.F., Pereira, M.F., 2009. Layered granitoids: interaction between continental crust recycling processes and mantle-derived magmatism. Examples from the Évora Massif (Ossa–Morena Zone, southwest Iberia, Portugal). Lithos 111, 125–141.

Moita, P., Santos, J.F., Pereira, M.F., Costa, M.M., Corfu, F., 2015. The quartz-dioritic Hospitais intrusion (SW Iberian Massif) and its mafic microgranular enclaves — Evidence for mineral clustering. Lithos 224-225, 78–100.

Montero, P., Bea, F., Corretge, L.G., Floor, P., Whitehouse, M.J., 2009. U–Pb ion microprobe dating and Sr and Nd isotope geology of the Galiñeiro Igneous Complex: A model for the peraluminous/peralkaline duality of the Cambro-Ordovician magmatism of Iberia. Lithos 107, 227–238.

Nakamura, N., 1974. Determination of REE, Ba, Fe, Mg, Na and K in carbonaceous and ordinary chondrites. Geochimica et Cosmochimica Acta 38, 757–775.

Nance, R.D., Murphy, J.B., 1994. Contrasting basement isotopic signatures and the palinspastic restoration of peripheral orogens: Example from the Neoproterozoic Avalonian-Cadomian belt. Geology 22, 617–620.

Nesbitt, H.W., Young, G.M., 1982. Early Proterozoic climates and plate motions inferred from major element chemistry of lutites. Nature 299, 715–717.

Nesbitt, H.W., Markovics, G., Price, R.C., 1980. Chemical processes affecting alkalis and alkali earths during continental weathering. Geochimica et Cosmochimica Acta 44, 1659–1666.

O'Nions, R.K., Carter, S.R., Evensen, N.M., Hamilton, P.J., 1979. Geochemical and cosmochemical applications of Nd isotope analysis. Annual Review of Earth and Planetary Sciences 7, 11–38.

Ordóñez Casado, B., 1998. Geochronological studies of the Pre-Mesozoic basement of the Iberian Massif: the Ossa Morena zone and the Allochthonous Complexes within the Central Iberian zone. Swiss Federal Institute of Technology, Zürich, Switzerland, p. 235.

Ordóñez Casado, B., Gebauer, D., Schafer, H.J., Gil Ibarguchi, J.I., Peucat, J.J., 2001. A single Devonian subduction event for the HP/HT metamorphism of the Cabo Ortegal complex within the Iberian Massif. Tectonophysics 332, 359–385.

Pedro, J., 1996. Estudo do metamorfismo de alta pressão na área de Safira (Montemor-o-Novo) Zona de Ossa Morena. GeoFCUL, Universidade de Lisboa, Lisboa, p. 69.

Pedro, J.C., 2004. Estudo Geológico e Geoquímico das Sequencias Ofiolíticas Internas da Zona de Ossa-Morena (Portugal). Universidade de Évora, Évora, Portugal, p. 225.

Pedro, J.C., Araújo, A., Fonseca, P.E., Munhá, J.M., 2005. Sequências ofiolíticas internas da zona de Ossa-Morena: implicações geodinâmicas na evolução da Cadeia Varisca Ibérica. Cuadernos do Laboratorio Xeolóxico de Laxe 30, 235–258.

Pedro, J., Araújo, A., Fonseca, P., Tassinari, C., Ribeiro, A., 2010. Geochemistry and U–Pb zircon age of the internal Ossa-Morena zone ophiolite sequences: a remnant of Rheic ocean in SW Iberia. Ofioliti 35, 117–130.

Pereira, M.F., 2015. Potential sources of Ediacaran strata of Iberia: a review. Geodinamica Acta 27, 1–14.

Pereira, Z., Oliveira, J.T., 2001. The Cabrela syncline stratigraphic sequence, Ossa-Morena zone, Portugal: a palynostratigraphic review. 15th International Senckenberg Conference and Joint Meeting IGCP 421/SDS, Frankfurt. Abstracts book 76.

Pereira, Z., Oliveira, J.T., 2003. Estudo palinostratigráfico do sinclinal da Estação de Cabrela. Implicações tectonostratigráficas. Ciências da Terra (UNL), Lisboa Num. Esp. V, CD-ROM, A118-A119.

Pereira, M.F., Silva, J.B., 2002. The geometry and kinematics of enclaves in sheared migmatites from the Évora Massif, Ossa-Morena Zone (Portugal). Geogaceta 31, 193–196.

Pereira, M.F., Silva, J.B., Chichorro, M., 2003. Internal Structure of the Évora Massif: The Évora High-grade Terrains and the Montemor-o-Novo Shear Zone (Ossa-Morena Zone, Portugal). Geogaceta 33, 71–74.

Pereira, M.F., Chichorro, M., Linnemann, U., Eguiluz, L., Silva, J.B., 2006a. Inherited arc signature in Ediacaran and Early Cambrian basins of the Ossa-Morena Zone (Iberian Massif, Portugal): paleogeographic link with European and North African Cadomian correlatives. Precambrian Research 144, 297–315.

Pereira, Z., Oliveira, V., Oliveira, J.T., 2006b. Palynostratigraphy of the Toca da Moura and Cabrela Complexes, Ossa–Morena Zone, Portugal. Geodynamic implications. Review of Palaeobotany & Palynology 139, 227–240.

Pereira, M.F., Silva, J.B., Chichorro, M., Moita, P., Santos, J.F., Apraiz, A., Ribeiro, C., 2007. Crustal growth and deformational processes in the northern Gondwana margin: constraints from the Évora Massif (Ossa-Morena Zone, southwest Iberia, Portugal). In: Linnemann, U., Nance, R.D., Kraft, P., Zulauf, G. (Eds.), The evolution of the Rheic Ocean: From Avalonian-Cadomian active margin to Alleghenian-Variscan collision. Geological Society of America Special Paper, pp. 333–358 (doi: 310.1130/2007.2423(1116)).

Pereira, M.F., Chichorro, M., Williams, I.S., Silva, J.B., 2008. Zircon U–Pb geochronology of paragneisses and biotite granites from the SW Iberian Massif (Portugal): evidence for a palaeogeographical link between the Ossa–Morena Ediacaran basins and the West African craton. Geological Society, London, Special Publications 297, 385–408.

Pereira, M.F., Chichorro, M., Williams, I.S., Silva, J.B., Fernández, C., Díaz-Azpíroz, M., Apraiz, A., Castro, A., 2009. Variscan intra-orogenic extensional tectonics in the Ossa-Morena Zone (Évora-Aracena-Lora del Río metamorphic belt, SW Iberian Massif): SHRIMP zircon U–Th–Pb geochronology. Geological Society, London, Special Publications 327, 215–237.

Pereira, M.F., Apraiz, A., Chichorro, M., Silva, J.B., Armstrong, R.A., 2010. Exhumation of high-pressure rocks in northern Gondwana during the Early Carboniferours (Coimbra-Cordoba shear zone, SW Iberian Massif): tectonothermal analysis and U–Th–Pb SHRIMP in-situ zircon geochronology. Gondwana Research 17, 440–460.

Pereira, M.F., Chichorro, M., Johnston, S.T., Gutiérrez-Alonso, G., Silva, J.B., Linnemann, U., Hofmann, M., Drost, K., 2012a. The missing Rheic Ocean magmatic arcs: Provenance analysis of Late Paleozoic sedimentary clastic rocks of SW Iberia. Gondwana Research 22, 882–891.

Pereira, M.F., Chichorro, M., Silva, J.B., Ordóñez-Casado, B., Lee, J.K.W., Williams, I.S., 2012b. Early carboniferous wrenching, exhumation of high-grade metamorphic rocks and basin instability in SW Iberia: Constraints derived from structural geology and U–Pb and ^{40}Ar–^{39}Ar geochronology. Tectonophysics 558-559, 28–44.

Pin, C., Fonseca, P.E., Paquette, J.-L., Castro, P., Matte, P., 2008. The ca. 350 Ma Beja Igneous Complex: A record of transcurrent slab break-off in the Southern Iberia Variscan Belt? Tectonophysics 461, 356–377.

Quesada, C., 1990. Precambrian successions in SW Iberia: their relationship to 'Cadomian' orogenic events. In: Lemos, D.R., Strachan, R.A., Topley, C.G. (Eds.), The Cadomian Orogeny, pp. 353–362.

Quesada, C., Fonseca, P.E., Munhá, J.M., Oliveira, J.T., Ribeiro, A., 1994. The Beja-Acebuches Ophiolite (southern Ibéria Variscan fold belt): geological characterization and geodynamic significance. Boletín Geologico y Minero 105, 3–49.

Ribeiro, A., 1983. Guia das excursões no bordo SW da ZOM. Relações entre formações do Devónico superior e o Maciço de Évora na região de Cabrela (Vendas Novas). Comunicaçoes dos Serviços Geológicos de Portugal 69, 267–269.

Ribeiro, A., Pereira, E., Dias, R., 1990. Structure in the northwest of the Iberian Peninsula. In: Dallmeyer, R.D., Martínez García, E. (Eds.), Pre-Mesozoic Geology of Iberia. Springer-Verlag, Berlin, Germany, pp. 220–236.

Ries, A.C., Shackleton, R.M., 1971. Catazonal Complexes of North-West Spain and North Portugal, Remnants of a Hercynian Thrust Plate. Nature Physical Science 234, 65–79.

Rodríguez, J., Cosca, M.A., Gil Ibarguchi, J.I., Dallmeyer, R.D., 2003. Strain partitioning and preservation of $^{40}Ar/^{39}Ar$ ages during Variscan exhumation of a subducted crust (Malpica-Tui complex, NW Spain). Lithos 70, 111–139.

Rosas, F.M., Marques, F.O., Ballèvre, M., Tassinari, C., 2008. Geodynamic evolution of the SW Variscides: Orogenic collapse shown by new tectonometamorphic and isotopic data from western Ossa-Morena Zone, SW Iberia. Tectonics 27. http://dx.doi.org/10.1029/2008TC002333.

Roser, B.P., Korsch, R.J., 1986. Determination of Tectonic Setting of Sandstone-Mudstone Suites Using SiO_2 Content and K_2O/Na_2O Ratio. The Journal of Geology 94, 635–650.

Rossi, P., Oggiano, G., Cocherie, A., 2009. A restored section of the "southern Variscan realm" across the Corsica–Sardinia microcontinent. Comptes Rendus Geoscience 341, 224–238.

Rubio Pascual, F.J., Matas, J., Martín Parra, L.M., 2013. High-pressure metamorphism in the Early Variscan subduction complex of the SW Iberian Massif. Tectonophysics 592, 187–199.

Sánchez Martínez, S., Jeffries, T.E., Arenas, R., Fernández-Suárez, J., García-Sánchez, R., 2006. A pre-Rodinian ophiolite involved in the Variscan suture of Galicia (Cabo ortegal complex, NW Spain). Journal of the Geological Society 163, 737–740.

Sánchez Martínez, S., Arenas, R., Andonaegui, P., Martínez Catalán, J.R., Pearce, J.A., 2007a. Geochemistry of two associated ophiolites from the Cabo Ortegal Complex (Variscan belt of NW Spain). Geological Society of America Memoirs 200, 445–467.

Sánchez Martínez, S., Arenas, R., Díaz García, F., Martínez Catalán, J.R., Gómez Barreiro, J., Pearce, J.A., 2007b. Careon ophiolite, NW Spain: suprasubduction zone setting for the youngest Rheic Ocean floor. Geology 35, 53–56.

Sánchez Martínez, S., Arenas, R., Fernández-Suárez, J., Jeffries, T.E., 2009. From Rodinia to Pangaea: ophiolites from NW Iberia as witness for a long-lived continental margin. In: Murphy, J.B., Keppie, J.D., Hynes, A.J. (Eds.), Ancient Orogens and Modern Analogues. Geological Society, London, Special Publications, pp. 317–341 (doi: 310.1144/SP1327.1114).

Sánchez Martínez, S., Arenas, R., Gerdes, A., Castiñeiras, P., Potrel, A., Fernández-Suárez, J., 2011. Isotope geochemistry and revised geochronology of the Purrido Ophiolite (Cabo Ortegal Complex, NW Iberian Massif): Devonian magmatism with mixed sources and involved Mesoproterozoic basement. Journal of the Geological Society 168, 733–750.

Sánchez Martínez, S., Gerdes, A., Arenas, R., Abati, J., 2012. The Bazar Ophiolite of NW Iberia: a relic of the Iapetus–Tornquist Ocean in the Variscan suture. Terra Nova 24, 283–294.

Sánchez-García, T., Bellido, F., Pereira, M.F., Chichorro, M., Quesada, C., Pin, C., Silva, J.B., 2010. Rift-related volcanism predating the birth of the Rheic Ocean (Ossa-Morena zone, SW Iberia). Gondwana Research 17, 392–407.

Schulmann, K., Konopasek, J., Janousek, V., Lexa, O., Lardeaux, J.M., Edel, J.B., Stipska, P., Ulrich, S., 2009. An Andean type Palaeozoic convergence in the Bohemian Massif. Comptes Rendus Geoscience 341, 266–286.

Stampfli, G.M., Hochard, C., Vérard, C., Wilhem, C., vonRaumer, J., 2013. The formation of Pangea. Tectonophysics 593, 1–19.

Stern, R.J., 2002. Crustal evolution in the East African Orogen: a neodymium isotopic perspective. Journal of African Earth Sciences 34, 109–117.

Taylor, S.R., McLennan, S.M., 1985. The Continental Crust: Its Composition and Evolution. Blackwell, Oxford.

Thorogood, E.J., 1990. Provenance of the pre-Devonian sediments of England and Wales: Sm–Nd evidence. Journal of the Geological Society 147, 591–594.

von Raumer, J.F., Stampfli, G.M., Arenas, R., Sánchez Martínez, S., 2015. Ediacaran to Cambrian oceanic rocks of the Gondwana margin and their tectonic interpretation. International Journal of Earth Sciences 104, 1107–1121.

Winchester, J.A., Max, M.D., 1989. Tectonic setting discrimination in clastic sequences: an example from the late proterozoic Erris Group, NW Ireland. Precambrian Research 45, 191–201.

Wronkiewicz, D.J., Condie, K.C., 1987. Geochemistry of archean shales from the Witwatersrand supergroup, south Africa: Source-area weathering and provenance. Geochimica et Cosmochimica Acta 51, 2401–2416.

Zhao, J.X., McCulloch, M.T., Bennett, V.C., 1992. Sm–Nd and U–Pb zircon isotopic constraints on the provenance of sediments from the Amadeus Basin, central Australia: Evidence for REE fractionation. Geochimica et Cosmochimica Acta 56, 921–940.

Capítulo 11

Discusión y conclusiones

11.1 Características geoquímicas y contexto geodinámico

El Macizo Ibérico contiene un amplio registro sedimentario de la actividad orogénica Cadomiense, la cual tuvo lugar durante el Neoproterozoico y el Cámbrico (*Murphy y Nance, 1987; Murphy et al., 2004; Pereira et al., 2006; Linnemann et al., 2007 y 2014; Nance et al., 2008*). Estas secuencias sedimentarias, en gran medida siliciclásticas, representan secciones preservadas del margen de Gondwana, que se vieron afectadas posteriormente de manera variable, durante el ensamblaje de Pangea, por la colisión Varisca que tuvo lugar entre el Devónico y el Pérmico Inferior (*Matte, 1991; Martínez Catalán et al., 2007; Arenas et al., 2016*). La sedimentación de estas series estuvo aparentemente ligada al desarrollo y evolución de un sistema de arco magmático peri-Gondwánico y a la aparición de cuencas asimétricas unidas a este contexto activo (*Fernández-Suárez, 2003; Rodríguez Alonso et al., 2004; Pereira et al., 2006; Díez Fernández et al., 2010*). El estudio de las rocas sedimentarias depositadas en un contexto convergente proporciona una herramienta muy útil para avanzar en el conocimiento de la evolución cortical del margen peri-Gondwánico durante la transición Neoproterozoico - Cámbrico. El estudio que aquí se presenta se basa en la caracterización geoquímica e isotópica de series sedimentarias seleccionadas. Los trabajos que se han desarrollado para la preparación de esta memoria han tenido como objetivo principal complementar la información tectonoestratigráfica ya existente, y aportar nuevas claves para una reconstrucción paleogeográfica de los terrenos peri-Gondwánicos durante las etapas finales del Neoproterozoico y el Cámbrico Medio.

Numerosos trabajos han descrito las características sedimentológicas, geocronológicas y tectonoestratigráficas de las secuencias sedimentarias representadas en el Macizo Ibérico, pero en pocos casos estos estudios han dirigido su atención hacia la caracterización geoquímica de estos materiales o a la investigación isotópica de sus fuentes. Como se ha comentado a lo largo de esta Tesis Doctoral, el marco geodinámico en el que tuvo lugar la sedimentación determinó la naturaleza de las áreas fuente, los procesos erosivos y mecanismos de transporte sedimentario, y la propia formación y estructura de las cuencas sedimentarias sinorogénicas. El contexto tectónico condicionó la mineralogía que observamos en los sedimentos terrígenos estudiados, y a su vez la composición química de las rocas sedimentarias resultantes. El análisis de las composiciones químicas e isotópicas ha permitido realizar una correlación con composiciones análogas observadas en contextos tectónicos conocidos, aportando nuevas claves paleogeográficas. La selección de rocas metasedimentarias de los sectores menos deformados en las series, con estructuras estratigráficas y características petrológicas reconocibles, asegura la relativa ausencia de modificación sobre la composición química e isotópica original de las rocas detríticas (Fig. 11.1), facilitando una caracterización consistente de sus áreas fuente y del contexto geodinámico durante su sedimentación.

De una manera general, las series siliciclásticas ediacarenses estudiadas en el Macizo Ibérico (Unidades Basales del NW y SW de Iberia, secuencia del Alcudiense Inferior del Complejo Esquisto-Grauváquico) son turbiditas inmaduras, con un marcado carácter grauváquico y que en su mayor parte muestran secuencias de tipo Bouma preservadas. Este tipo de litologías se asocian a una sedimentación relacionada con ambientes mari-

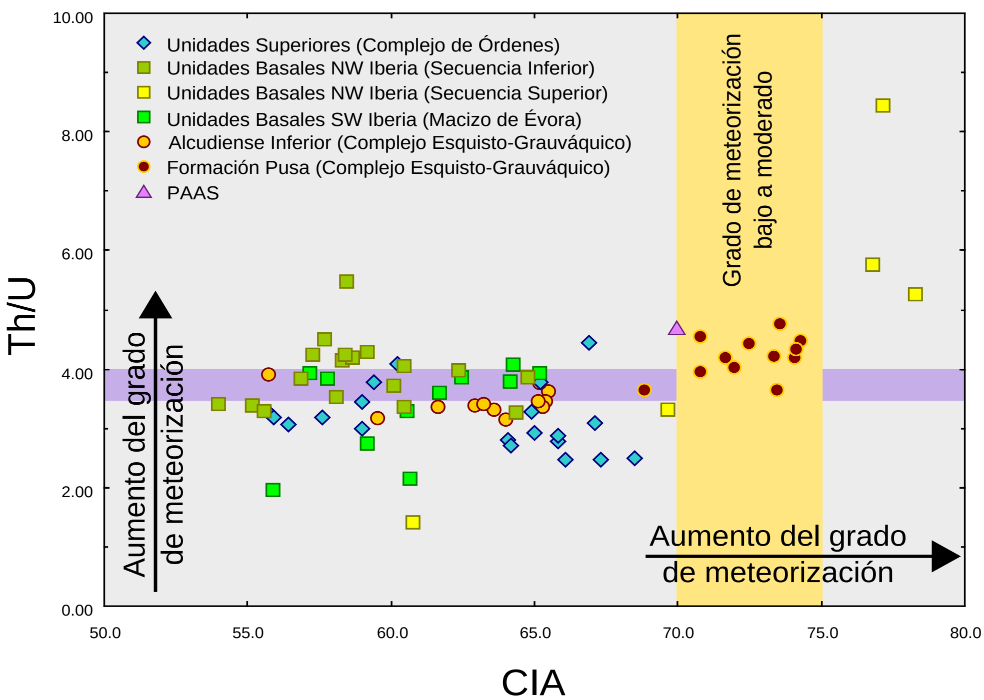

Fig. 11.1- Diagrama Th/U vs CIA. Se muestran los valores de CIA (*Chemical Index of Alteration*) para la totalidad de las muestras estudiadas (calculados según *Nesbitt y Young, 1982)*. Se incluye el campo con los valores de CIA típicos para pizarras (*shales*), que según *McLennan et al. (1993)* reflejan un grado bajo a moderado de alteración química por meteorización. Igualmente, se muestra el campo con los valores de la relación Th/U más comunes encontrados en rocas ígneas de la corteza superior (3.5 - 4.0; según *McLennan et al., 1993*).

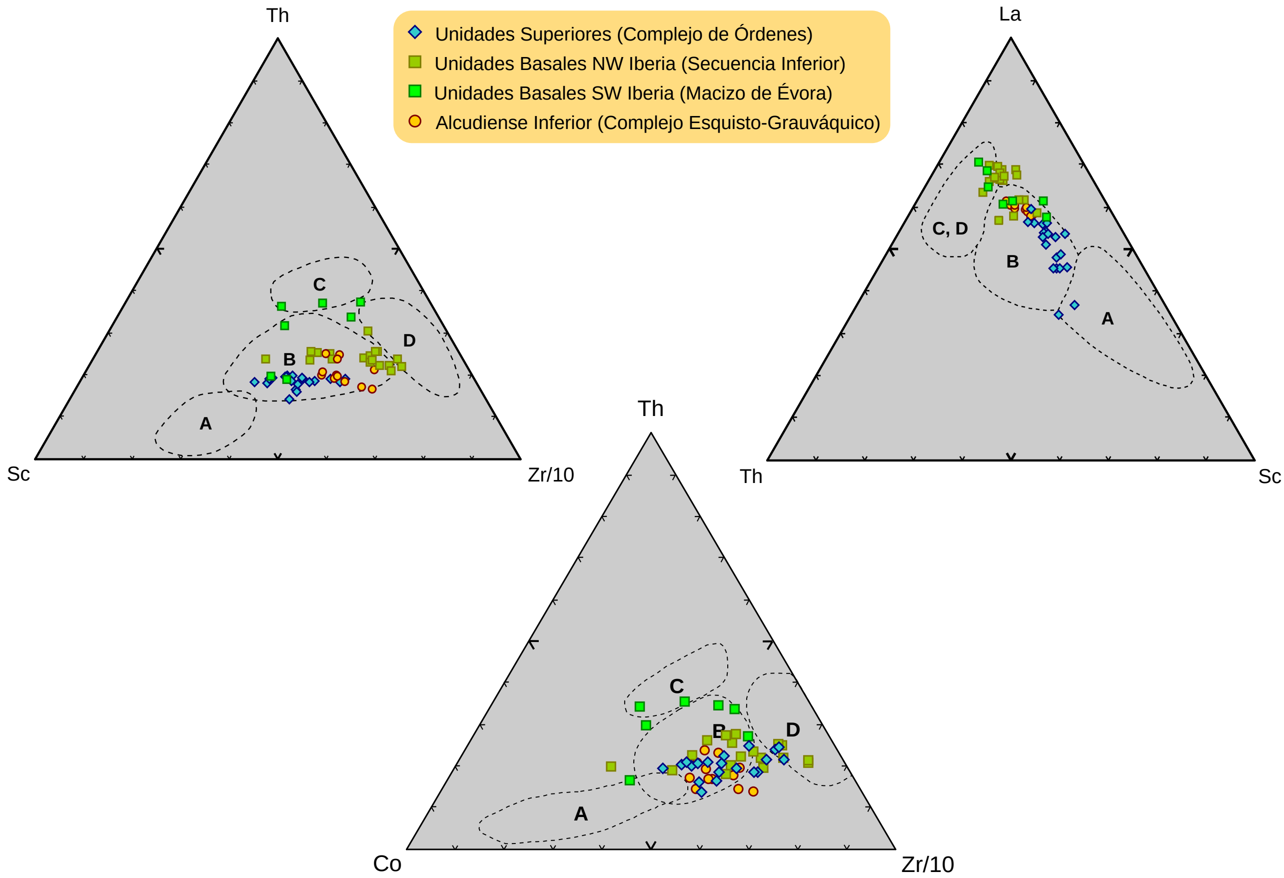

Fig. 11.2- Diagramas de elementos traza con campos para la discriminación del ambiente tectónico de sedimentación de las metagrauvacas estudiadas. Campos según *Bhatia y Crook (1986)*: A — Arco de islas oceánico; B — Arco de islas continental; C — Margen continental activo; D — Margen pasivo.

nos profundos ligados a contextos tectónicos activos (*Bouma, 2004*). Dichos contextos han conferido a los sedimentos unas características texturales reconocibles, resultado de una influencia limitada de los procesos de transporte y un menor grado de reciclaje sedimentario, en gran medida debido a una relativa cercanía entre las áreas fuente y las cuencas sedimentarias. Según lo observado en los diagramas de discriminación (Fig. 11.2), las series sedimentarias ediacarenses se depositaron en un margen activo, en relación con el desarrollo de un arco volcánico edificado sobre una corteza continental adelgazada. La composición intermedia-félsica de las grauvacas, afín a rocas ígneas características de la corteza continental superior (Fig. 11.3), apunta a un arco volcánico evolucionado cuyo desarrollo avala la continuidad de la actividad magmática Cadomiense durante el Ediacarense más tardío. Los patrones de multivariación elemental apoyan igualmente la implicación de un contexto geodinámico convergente (Fig. 11.4). Como se ha comentado en cada uno de los casos estudiados y a pesar de una clara afinidad por la implicación en el sistema de arcos de una corteza continental adelgazada, se observan también ciertos aspectos composicionales determinantes, que sugieren la posible implicación de una corteza continental más gruesa en el desarrollo y relleno de estas cuencas sedimentarias durante el Neoproterozoico. Esta controversia apunta a una ubicación de las cuencas sedimentarias en relación con una extensa cuenca *back-arc*, desarrollada en el margen de Gondwana durante las fases finales en la evolución del margen convergente Cadomiense (*Linnemann et al., 2008; Perei-*

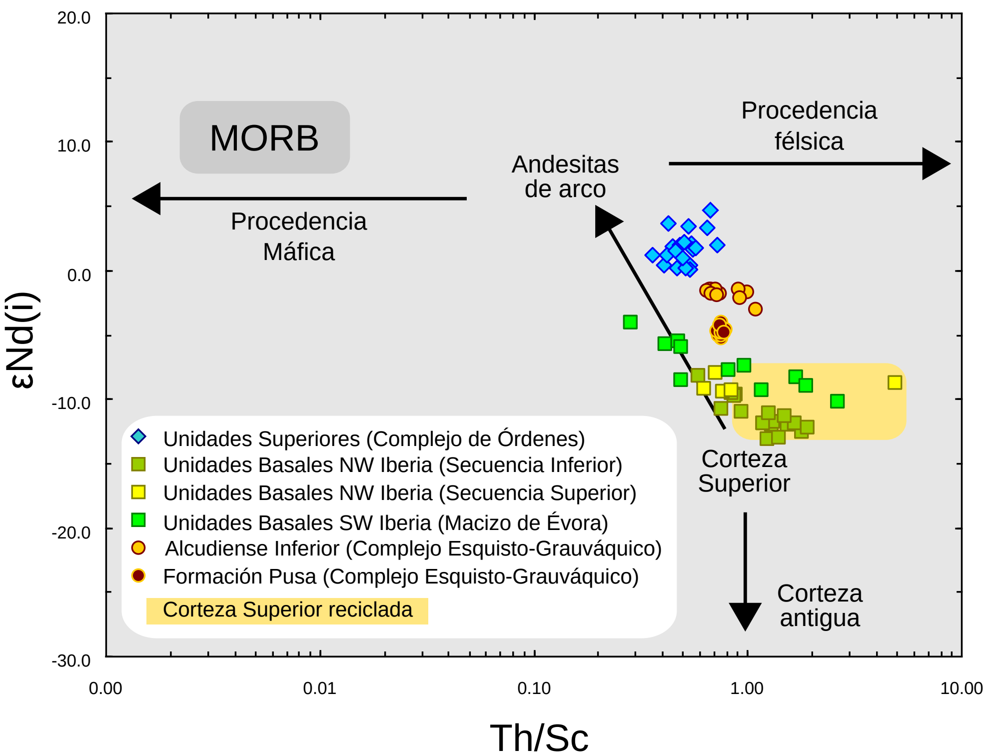

Fig. 11.3- Diagrama εNdi vs Th/Sc, donde se muestran los valores de ambos parámetros para la totalidad de las muestras estudiadas. Procedencias y campos reflejados según *McLennan et al. (1993)*.

ra et al., 2012). Este tipo de cuenca explicaría las características geoquímicas observadas en estas series, siendo coherente su existencia tanto con la influencia del arco volcánico Cadomiense sobre los procesos sedimentarios que tuvieron lugar durante el Ediacarense, como con la existencia de parámetros geoquímicos que indican paleogeografías más próximas al dominio continental.

Por su parte, las series sedimentarias cámbricas seleccionadas para este estudio muestran características claramente diferenciadas. Por una parte, las series metagrauváquicas que afloran en posiciones culminantes de las Unidades Superiores del Complejo de Órdenes muestran afinidad con contextos geodinámicos análogos a los observados en las series ediacarenses (Fig. 11.2). Tanto los diagramas de discriminación como los patrones de multivariación elemental (Fig. 11.5) muestran aspectos inequívocos de la implicación de un arco volcánico construido sobre una corteza continental adelgazada, asociado al desarrollo de un margen convergente. Una vez más la procedencia félsica confirma el carácter evolucionado del arco, sin la presencia de ninguna característica típicamente oceánica (Fig. 11.3). A pesar de la analogía mencionada, es clara la diferencia de los patrones observados en estas series cámbricas con respecto a las series ediacarenses. Estos patrones vienen caracterizados por: (i) una mayor variabilidad en sus concentraciones; (ii) una tendencia positiva, más evidente que en el caso de las rocas metasedimentarias ediacarenses estudiadas, desde unos bajos valores de los LILE, hasta unos contenidos de los HFSE cercanos a la unidad; y (iii) una anomalía claramente positiva del Sr (Fig. 11.4 y 11.5). Todos estos factores apoyan una mayor cercanía de las cuencas sedimentarias a unas áreas fuente localizadas en las partes más activas del arco volcánico y limitan la influencia de los procesos típicamente sedimentarios sobre su composición química (*Winchester y Max, 1989*). De igual manera, el estudio estructural y geocronológico de los diques de diabasa que intruyen

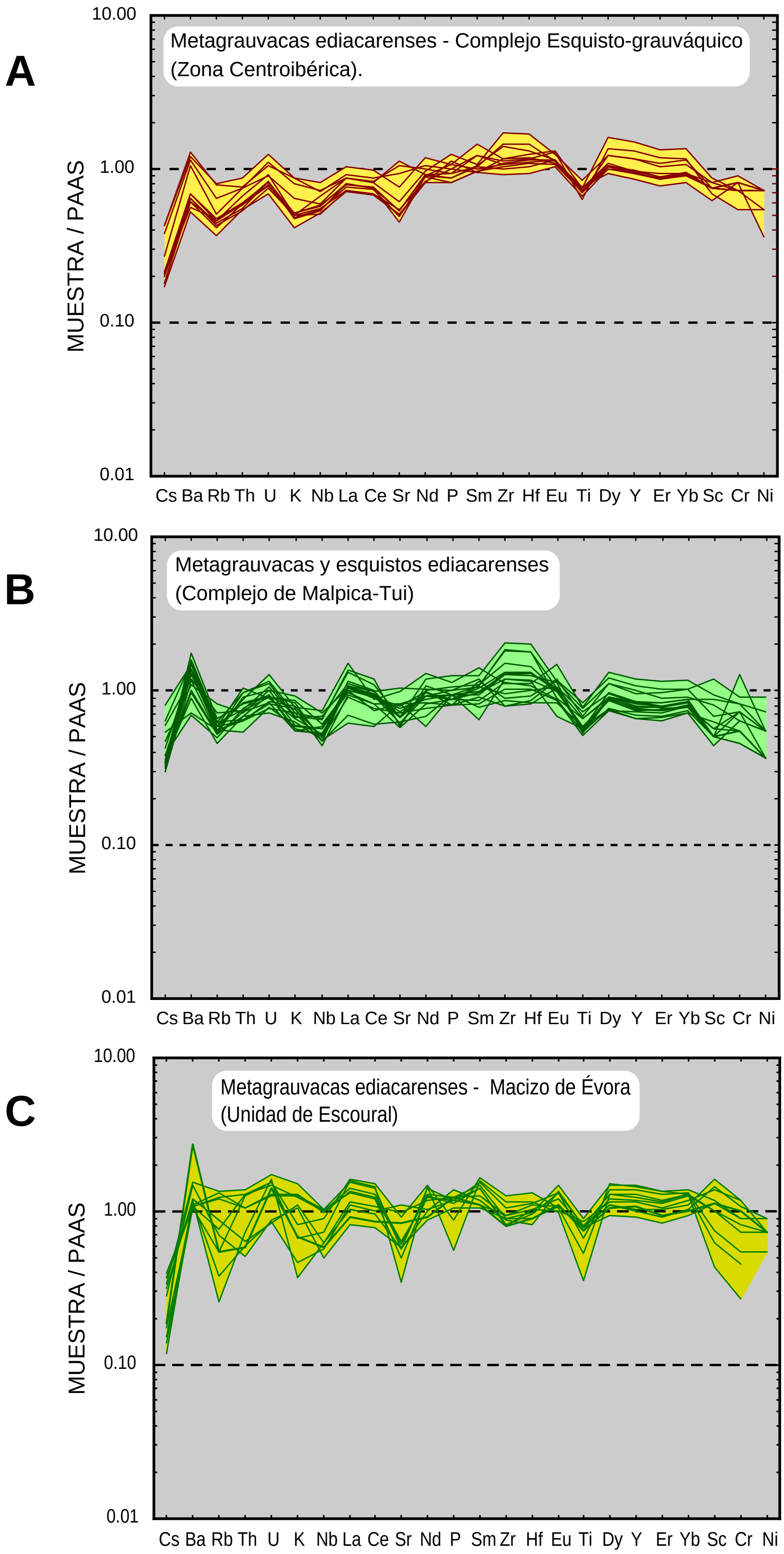

Fig. 11.4- Diagramas de multivariación elemental (según *Winchester y Max, 1989)*, con elementos mayores y traza normalizados al PAAS. A — Metagrauvacas ediacarenses de la Zona Centroibérica, B — Metagrauvacas y esquistos ediacarenses de la secuencia inferior de las Unidades Alóctonas Basales del NW de Iberia y C — Metagrauvacas ediacarenses de las Unidades Alóctonas Basales del SW de Iberia. PAAS según *Taylor y McLennan (1985*).

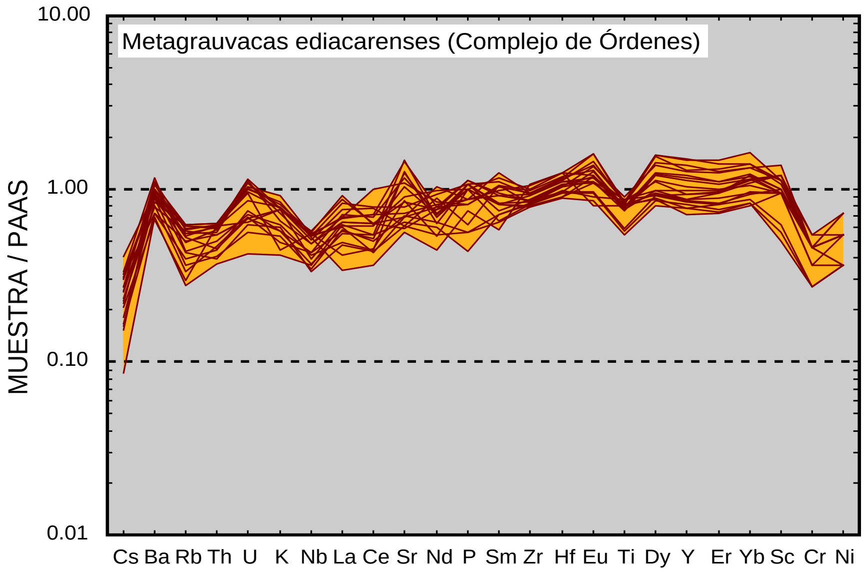

Fig. 11.5- Diagrama de multivariación elemental (según *Winchester y Max, 1989)*, con elementos mayores y traza, normalizados al PAAS, de las metagrauvacas ediacarenses de las Unidades Alóctonas Superiores del NW de Iberia. PAAS según *Taylor y McLennan (1985*).

estas series metasedimentarias culminantes avalan la existencia de un ambiente muy dinámico en el contexto de un margen activo. Las evidencias de diferentes fases de deformación en estas unidades apoyan una subducción inicial bajo el margen externo adelgazado de Gondwana, seguido de un evento extensional, probablemente asociado al desmantelamiento del edifico volcánico.

Por el contrario, las series metasedimentarias cámbricas estudiadas en las Unidades Basales del NW y en la Formación Pizarras de Pusa de la Zona Centroibérica presentan un marcado carácter pelítico, con un grado de madurez textural y mineralógico mayor que el observado en las grauvacas ediacarenses, lo que se refleja en composiciones químicas mucho más homogéneas (Fig. 11.6). Como se ha comentado en los trabajos publicados relativos a estas litologías, no ha sido posible el estudio de rocas grauváquicas en estas secuencias sedimentarias. En cualquier caso, es patente la diferencia de los patrones multielementales con los observados en las series precámbricas (Fig. 11.4). A diferencias de estos últimos, en los primeros se observa una clara homogeneidad de las abundancias elementales, muy similares a las del PAAS y por tanto, a la corteza continental superior. Esta característica es muy común en los sedimentos maduros con un elevado reciclaje sedimentario (Fig. 11.3). Un aspecto importante es la gran similitud observada entre los patrones de las pizarras de la Formación Pusa (Zona Centroibérica - Dominio Autóctono) y los micaesquistos de la secuencia superior de las Unidades Basales del NW de Iberia (Complejo Alóctono de Malpica-Tui) (Fig. 11.6). Esta similitud en los patrones multielementales en series que representan dominios tectonoestratigráficos diferentes confirma una influencia coherente del contexto tectónico de sedimentación sobre la composición química de los sedimentos siliciclásticos. Las características composicionales comunes indican paleogeografías comparables en relación al paleomargen de Gondwana. Teniendo en cuenta estos datos, tal como se ha comentado con anterioridad, los patrones químicos observados en estas series cámbricas resultan compatibles con el ensanchamiento de una extensa cuenca *back-arc* y quizás con un incipiente desarrollo de un margen pasivo. Se produce por tanto durante

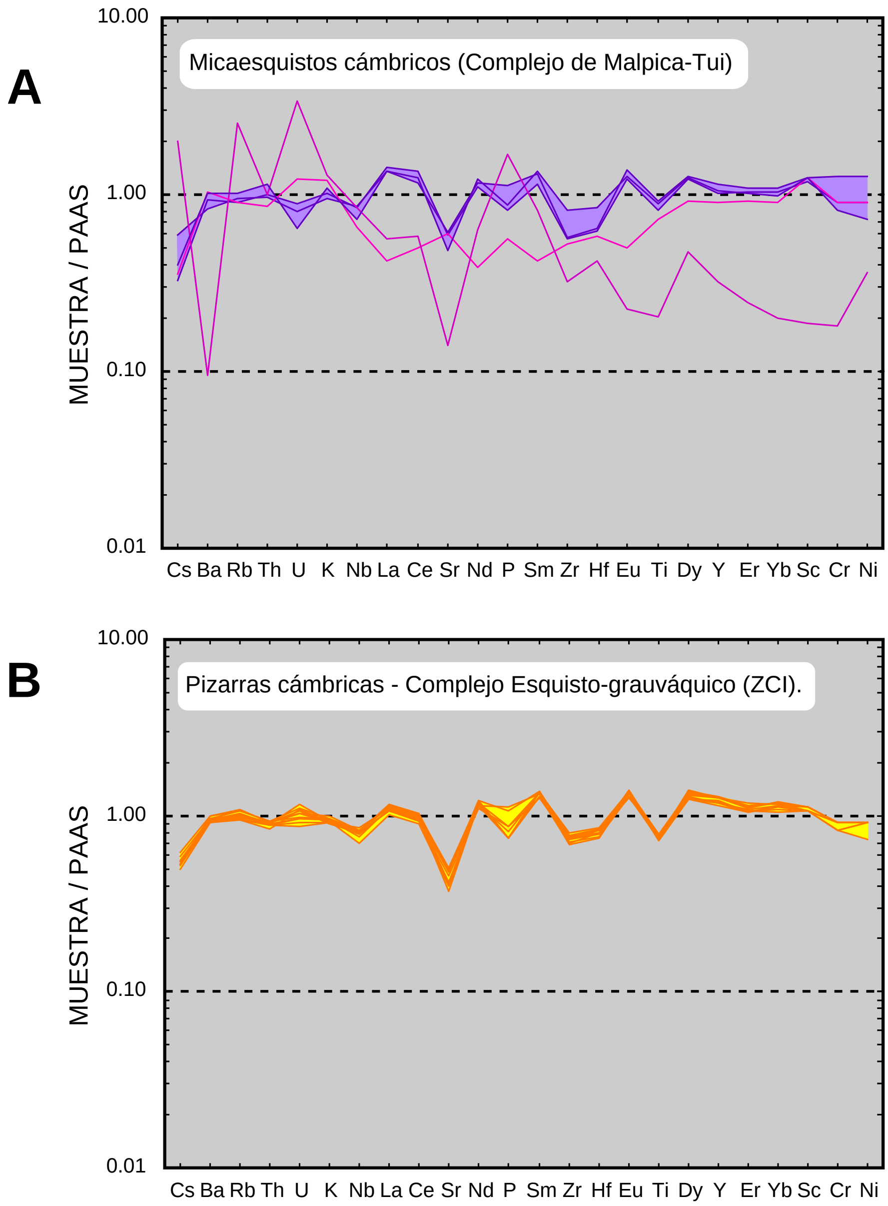

Fig. 11.6- Diagramas de multivariación elemental (según *Winchester y Max, 1989)*, con elementos mayores y traza normalizados al PAAS. A — Micaesquistos cámbricos de la secuencia superior de las Unidades Alóctonas Basales del NW de Iberia y B — Pizarras cámbricas de la Formación Pusa (Zona Centroibérica). PAAS según *Taylor y McLennan (1985)*.

el Cámbrico una transición en el ambiente deposicional, que refleja una influencia menor del sistema de arcos volcánicos y una transición hacia un margen pasivo (*Pieren, 2000; Díez Fernández et al., 2010*). Es importante incidir en el aspecto, ya comentado en capítulos previos, de la presencia de contenidos en Zr y Hf menores de los esperados en sedimentos reciclados. Estos contenidos relativamente bajos apoyan un cambio en la procedencia, con mayores aportes de composiciones máficas, lo que resulta evidente dada la mayor presencia de rocas máficas en la base de algunas de estas secuencias (*Rodríguez Alonso et al., 2004; Díez Fernández et al., 2010*).

11.2 Composición isotópica (Sm-Nd) y procedencia

El estudio de la sistemática Sm-Nd se ha realizado en las mismas series metasedimentarias y en concreto en las mismas muestras analizadas para elementos mayores y trazas, y permite un análisis de la proceden-

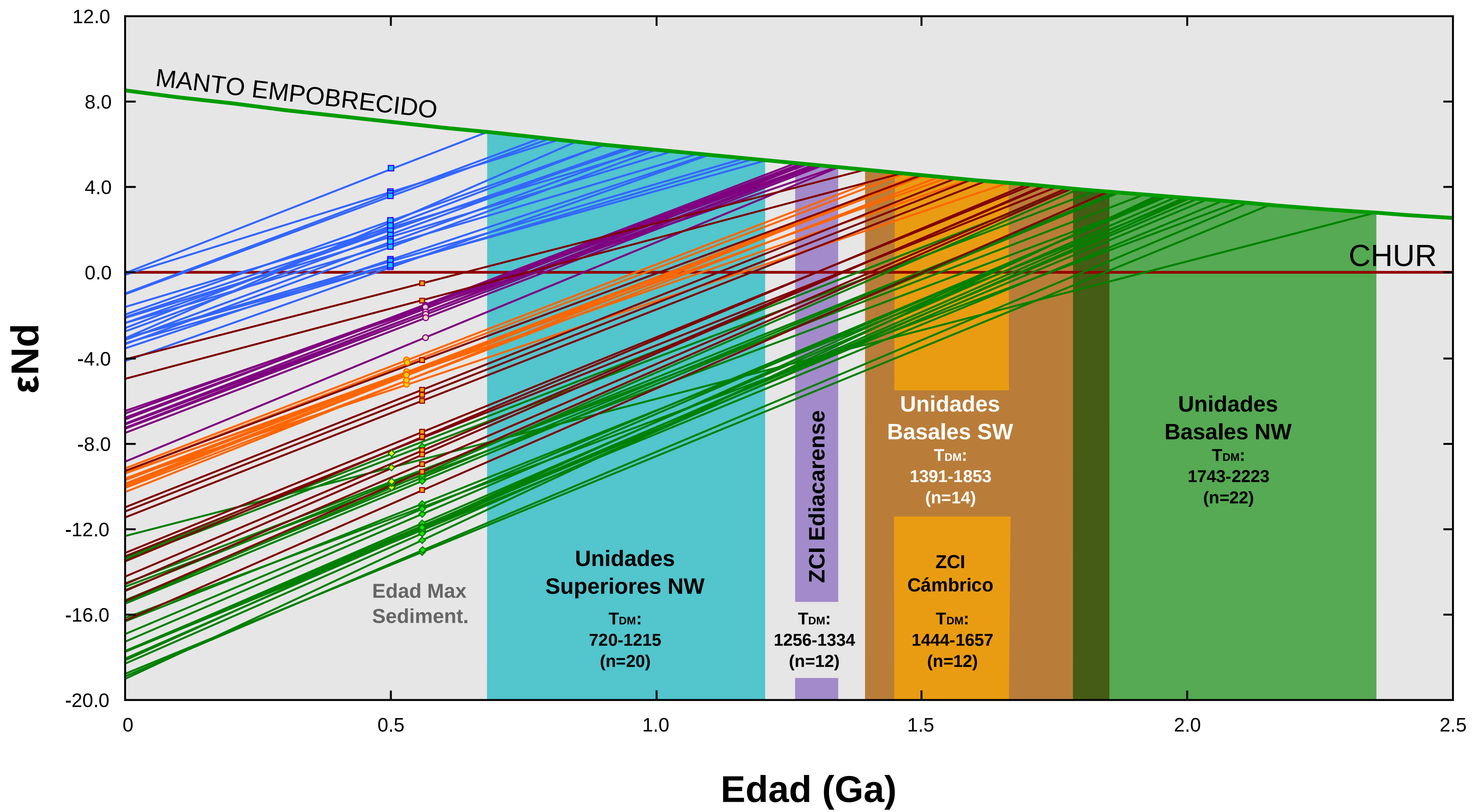

Fig. 11.7- Diagrama εNdi vs Edad, donde se muestran las líneas de evolución del Nd y las TDM (calculadas según *DePaolo, 1981*) de todas las rocas metasedimentarias estudiadas. Los puntos muestran los valores de εNd calculados para las respectivas edades máximas de sedimentación de cada una de las secuencias sedimentarias: metagrauvacas cámbricas de las Unidades Alóctonas Superiores del NW de Iberia, metagrauvacas ediacarenses del Alcudiense Inferior de la Zona Centroibérica, las pizarras cámbricas de la Fm Pusa de la Zona Centroibérica, las metagrauvacas y esquistos ediacarenses y micaesquistos cámbricos de las Unidades Alóctonas Basales del NW de Iberia, y las metagrauvacas ediacarenses de las Unidades Alóctonas Basales del SW del Macizo Ibérico.

cia de las fuentes isotópicas y una aproximación a la paleogeografía original de las unidades tectonoestratigráficas del Macizo Ibérico. Los datos isotópicos Sm-Nd proporcionan una buena estimación de la participación relativa de material juvenil y de material cortical antiguo desde las áreas fuente, lo que permite inferir la posible ubicación de las paleocuencas sedimentarias generadas durante la transición Ediacarense-Cámbrico.

De manera general, las series ediacarenses estudiadas presentan valores de εNdi muy negativos y valores muy antiguos de T_{DM}, lo que indica que estas rocas siliciclásticas contienen una proporción mayoritaria de materiales corticales procedentes de una zona cratónica continental adyacente (Fig. 11.3 y 11.7). Sin embargo, de acuerdo con su composición química se deduce que estas series estuvieron influenciadas también por el margen convergente Cadomiense y el arco volcánico peri-Gondwánico construido sobre el margen continental más externo. No obstante, las fuentes isotópicas dominantes son de origen continental antiguo y avalan la localización de las cuencas en posiciones más proximales al dominio puramente continental (Fig. 11.8). Los valores observados de las edades modelo para las series ediacarenses, siempre teniendo en cuenta que representan la mezcla de diferentes aportes sedimentarios y por tanto de diferentes momentos de extracción de sistema Sm-Nd de un manto empobrecido, son coherentes con una procedencia durante el Neoproterozoico desde las zonas cratónicas existentes en el actual margen N de África. Las T_{DM} son compatibles con la información proporcionada por la geocronología U-Pb de poblaciones de circones detríticos (*Fernández-Suárez et al., 2003; Ugidos et al., 2003; Díez Fernández et al., 2010; y 2014; Pereira et al., 2012; Albert et al., 2015a; Orejana et al., 2015*). En conjunto, estos datos parecen indicar que las cuencas ediacarenses se generaron en dominios próximos al Cratón del Oeste de África, ocupando posiciones laterales relativas a lo largo del margen de Gondwana. Esta interpretación viene a confirmar algunos modelos paleogeográficos presentados recientemente (*Díez Fernández et al., 2010; Albert et al., 2015a*).

Por el contrario, las fuentes isotópicas de las secuencias metagrauváquicas culminantes de las Unidades Superiores del Complejo de Órdenes, depositadas durante el Cámbrico Medio, confirman la fuerte implicación del arco volcánico Cadomiense en sus aportes detríticos. La Fig. 11.9 indica que estas grauvacas se proyectan dentro de los campos correspondientes a las rocas de arco asociadas a márgenes activos (*McLennan et al., 1993*). Estos aportes, eminentemente juveniles, confieren a estas grauvacas unos valores de εNdi positivos y edades modelo T_{DM} jóvenes, lo que sugiere que la cuenca sedimentaria original tuvo una localización muy próxima al foco principal de actividad volcánica (Fig. 11.7 y 11.8). No puede descartarse incluso que esta cuenca ocupase una posición intra-arco. Esta cercanía ya se había deducido a partir de las características geoquímicas de las metagrauvacas, y tomando en consideración la coincidencia, dentro del margen de error, entre la edad máxima de sedimentación de esta serie (*Fernández-Suárez et al., 2003*) y la edad del magmatismo (*Abati et al., 1999; Fernández-Suárez et al., 2007*). También resulta coetáneo el emplazamiento de una red de diques doleríticos. La erosión activa en el arco volcánico, probablemente ya en una etapa final de actividad, proporcionaría una fuente de materiales mayoritariamente juveniles, que junto con los aportes menores de otros materiales con fuentes isotópicas más antiguas darían lugar a los valores de T_{DM} mesoproterozoicos y neoproterozoicos (720-1215 Ma) obtenidos en estas metagrauvacas. Para interpretar el anterior rango de T_{DM}, hay que tener en cuen-

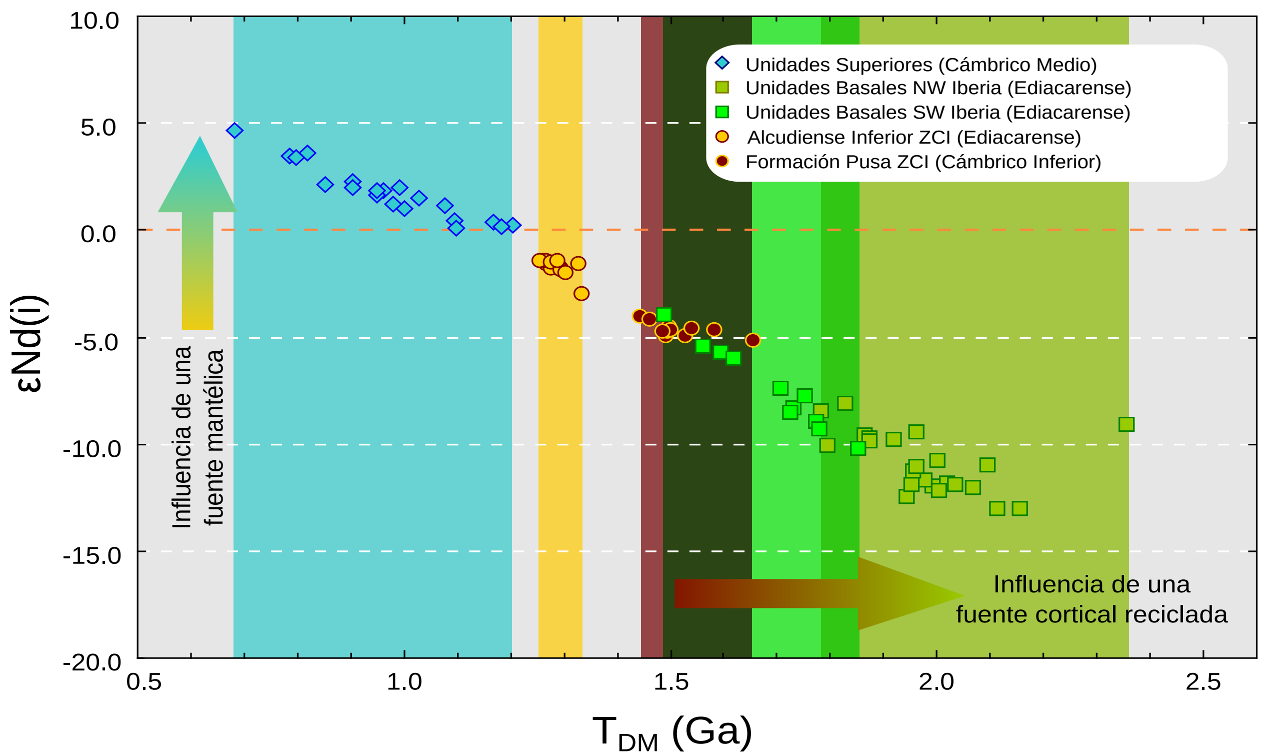

Fig. 11.8- Diagrama εNdi vs T_{DM}. Se muestran los rangos de valores de T_{DM} (calculadas según *DePaolo, 1981*) de todas las secuencias sedimentarias estudiadas, así como las direcciones de aumento de la influencia de una fuente isotópica más juvenil (mantélica) o más antigua (cortical). Los valores de εNdi presentados se han calculado teniendo en cuenta las edades máximas de sedimentación de cada una de las secuencias estudiadas.

ta la ausencia de circones detríticos de edad mesoproterozoica (*Fernández-Suarez et al., 2003*), lo que sugiere que las edades modelo reflejan más bien una mezcla de fuentes detríticas paleoproterozoicas y ediacarenses. Estas procedencias serían coherentes con una posición de la cuenca sedimentaria en la sección del margen que ocupó una posición exterior frente al Cratón del Oeste de África. Esta misma interpretación se ha propuesto para la procedencia de las series análogas localizadas en el Complejo de Cabo Ortegal (Gneises de Cariño; *Albert et al., 2015a*), aunque en ese caso los valores de T_{DM} son más antiguos (1.58 - 1.82 Ga) y parecen indicar una mayor influencia de los aportes continentales y por consiguiente una posición de la paleocuenca más próxima al dominio más continental.

El cambio en el contexto tectónico de sedimentación que se detecta por las diferencias composicionales entre las series metasedimentarias cámbricas y las series ediacarenses, se apoya también en los resultados obtenidos para las composiciones isotópicas de Nd (Fig. 11.7 y 11.9). Las pizarras cámbricas de la Formación Pusa (Complejo Esquisto-Grauváquico) muestran valores de εNdi claramente más negativos (entre -4.0 y -5.2) y unos valores de T_{DM} (1444 - 1657 Ma), más antiguos que los observados en las metagrauvacas ediacarenses del mismo dominio (1256 - 1334 Ma), lo que sugiere una mayor proporción de materiales corticales antiguos procedentes del área continental cercana (Fig. 11.8). Estas diferencias están, por tanto, relacionadas con una evolución geodinámica hacia una menor influencia del arco volcánico y un tránsito hacia un margen pasivo. En este escenario, las paleocuencas cámbricas del Complejo Esquisto-Grauváquico ocuparían posiciones más proximales al dominio continental, recibiendo mayor aporte de materiales pelíticos (Fig. 11.7 y 11.8). Esta transición se detecta también en la composición química de los micaesquistos cámbricos de la secuencia superior de las Unidades Basales del NW del Macizo Ibérico, pero no es tan evidente cuando se tienen en cuenta las composiciones isotópicas, aunque en este caso el número de muestras es muy limitado. En cualquier caso, los valores de εNdi muy negativos (entre -8.5 y -10.1) y las T_{DM} muy antiguas (1743 - 2223 Ma), similares a las observadas en la secuencia inferior de las mismas unidades (1756 - 2078 Ma), confirman que ambas secuencias comparten las mismas fuentes isotópicas (Fig. 11.7 y 11.8). Por lo tanto, las series sedimentarias de las Unidades Basales del NW de Iberia se depositaron durante la transición Ediacarense - Cámbrico Medio en un contexto cercano a la plataforma continental de Gondwana, que aportaría el material clástico de origen cortical antiguo. Las fuentes isotópicas continuaron siendo las mismas, pero las características químicas reflejan cambios asociados a una evolución geodinámica general, quizás ligada al ensanchamiento de la cuenca marginal y a la progresiva disminución de la actividad magmática en el arco volcánico. Las T_{DM} registradas en la secuencias metasedimentarias de las Unidades Basales del NW del Macizo Ibérico son compatibles con áreas fuente Paleoproterozoicas y Arcaicas, que situarían las cuencas en posiciones muy cercanas al Cratón del Oeste de África durante esta transición temporal.

11.3 Correlación entre terrenos alóctonos del Macizo Ibérico

Uno de los objetivos de esta Tesis Doctoral se ha centrado en la posible correlación entre algunos de los terrenos alóctonos del NW y SW del Macizo Ibérico. La similitud entre la secuencia inferior de las Unidades Basales del NW de Iberia y las unidades de Escoural y Monfurado (Macizo de Évora - Portugal), es reconocible desde un punto de vista litoestratigráfico, metamórfico, microestructural y geocronológico. En todas estas unidades son mayoritarias las litologías con características grauvacáquicas de edad Neoproterozoico Superior, siendo también abundantes los metagranitoides y rocas máficas de edad cambro-ordovícica. Las semejanzas son igualmente destacables cuando se consideran sus características geoquímicas. Las series grauváquicas ediacarenses de estas unidades presentan un claro carácter inmaduro con una bajo grado de meteorización (Fig. 11.1). Todas ellas muestran composiciones químicas similares que sugieren áreas fuente intermedio-félsicas, análogas a rocas ígneas de la corteza superior (Fig. 11.4), depositadas en un régimen geodinámico convergente ligado al desarrollo del arco Cadomiense. Las cuencas sedimentarias originarias que cabe deducir para ambos sectores, NW y SW de Iberia, estuvieron probablemente localizadas en posiciones cercanas al dominio continental de una gran cuenca *back-arc* peri-Gondwánica. Por otra parte, las poblaciones de edades U-Pb de circones detríticos en todas estas secuencias sedimentarias son igualmente muy similares y coherentes con una ubicación de las paleocuencas en la periferia del Cratón del Oeste de África (*Pereira et al., 2008; Díez Fernández et al., 2010*). Esta ubicación se confirma también con los valores de las edades modelo Sm-Nd, que se aproximan o coinciden con las edades de los protolitos presentes en esta área cratónica. Las T_{DM} de las unidades basales del Ma-

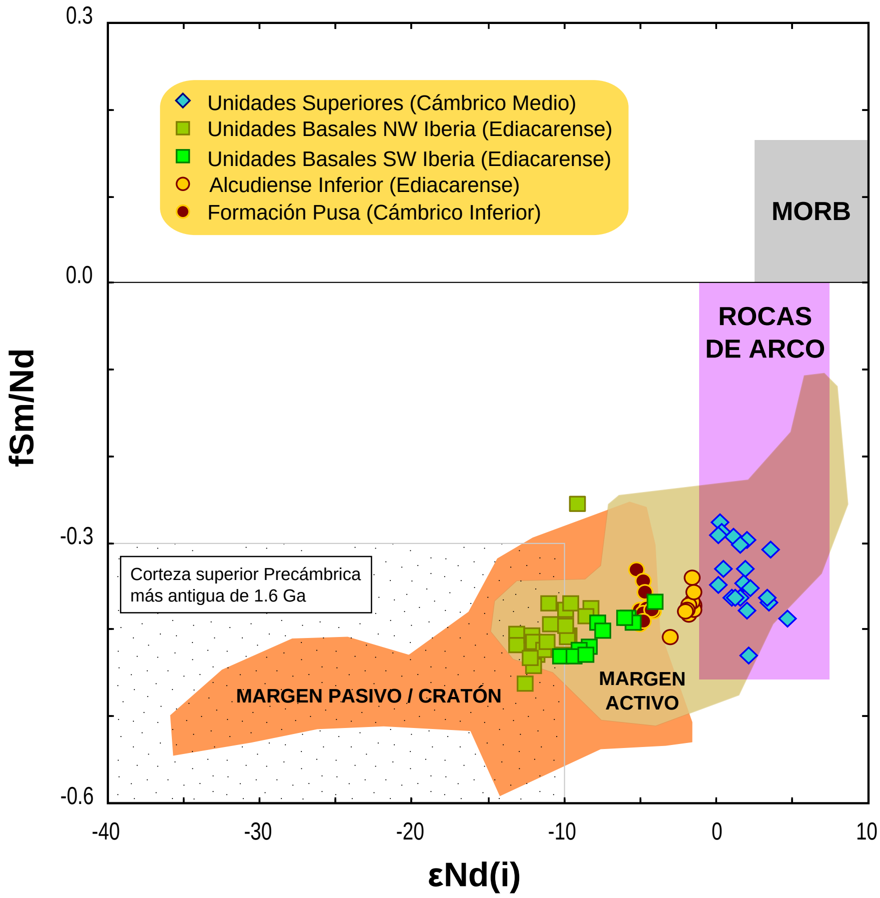

Fig. 11.9- Diagrama $f^{Sm/Nd}$ vs εNdi para las rocas metasedimentarias estudiadas. Campos incluidos en el diagrama según *McLennan y Hemming (1992)*.

cizo Ibérico presentan valores similares (Fig. 11.7 y 11.8), siendo ligeramente más jóvenes en el caso del Macizo de Évora (1499 - 1853 Ma). A pesar de que las Unidades Basales del NW de Iberia muestran edades más antiguas (1829 - 2156 Ma), resulta evidente el solapamiento entre éstas y las que se han obtenido en el Macizo de Évora y también en la denominada Unidad Central (1640 - 1900 Ma; *López-Guijarro et al., 2008*).

Las T_{DM} de las Unidades Basales exhiben una tendencia de rejuvenecimiento progresivo desde el NW hasta el SW del Macizo Ibérico, que se produce sin un cambio significativo en las fuentes isotópicas. Esta evolución implica algún grado de cambio en la naturaleza de los aportes detríticos y conlleva un mayor aporte de material juvenil hacia el SW. Este tipo de variaciones dentro de unidades equivalentes tiene su explicación en una posiblemente considerable extensión de las cuencas sedimentarias de referencia, por su distribución paralela a lo largo del margen peri-Gondwánico, que condicionaría la diferente proporción de materiales mantélicos y corticales dependiendo de su localización con respecto al arco volcánico; y por su probable alternancia lateral a lo largo del mencionado margen. Un aspecto muy revelador es la gran diferencia existente entre los valores de las edades modelo de las Unidades Alóctonas Basales y los que se han obtenido en las series sedimentarias ediacarenses del dominio autóctono subyacente (Fig. 11.7). Mientras que el grupo de Unidades Alóctonas Basales presenta un rango de valores de T_{DM} comprendido entre 1.50 y 2.16 Ga, las series neoproterozoicas del dominio autóctono (Zona Centroibérica) muestran valores que varían entre 1.26 y 1.33 Ga. No existe ningún solapamiento entre estas edades, que indican una mayor contribución de fuentes algo más jóvenes en la Zona Centroibérica (Fig. 11.8 y 11.9). La diferenciación paleogeográfica entre ambos dominios del Macizo Ibérico se puso de manifiesto mediante la utilización de geocronología U-Pb en circones detríticos, y ha sido clásicamente explicada acudiendo a una posible localización algo más oriental de la Zona Centroibérica en el paleo-margen de Gondwana (*Díez Fernández et al., 2010; Ábalos et al., 2012; Albert et al., 2015a*). Estos argumentos avalan una localización diferenciada de las cuencas sedimentarias ediacarenses en el paleo-margen de Gondwana. Las diferentes Unidades Alóctonas Basales del Macizo Ibérico pueden considerarse conjuntos equivalentes, que parecen representar un mismo dominio paleogeográfico. Proceden de cuencas sedimentarias originales distintas de las que se reconocen para el dominio autóctono relativo que representa la Zona Centroibérica, ocupando ambos dominios posiciones paleogeográficas diferenciadas.

11.4 Paleogeografía de las cuencas sedimentarias en la transición Ediacarense-Cámbrico

Los resultados que se han presentado en esta Tesis Doctoral permiten complementar el conocimiento previo sobre la paleogeografía de las cuencas sedimentarias peri-Gondwánicas, y por tanto de los terrenos del Macizo Ibérico, durante las etapas finales del Neoproterozoico y el Cámbrico Medio. Los numerosos intentos llevados a cabo para reconocer la paleogeografía original que ocuparon estos terrenos se han basado esencialmente en datos geoquímicos y geocronológicos, estos últimos utilizando, sobre todo, las poblaciones de edades U-Pb determinadas en circones detríticos (*Fernández Suárez et al., 2000, 2002 y 2014; Ugidos et al., 2003; Díez Fernández et al., 2010 y 2012b; Pereira et al., 2012; Orejana et al., 2015; Cambeses et al., 2017*). Un aspecto importante en la interpretación de la edad de los circones detríticos es la presencia o ausencia de circones de edad mesoproterozoica. A pesar de que la proporción de circones con estas edades es relativamente escasa o está virtualmente ausente en las rocas ediacarenses que actualmente afloran en los dominios continentales del N de África (*Morag et al., 2012; Linnemann et al., 2014*), la presencia de circones con edades Steniense - Toniense se considera un aspecto muy revelador a la hora de interpretar las diferentes procedencias de los sedimentos terrígenos neoproterozoicos. La determinación de las edades modelo Sm-Nd presentadas en esta Tesis Doctoral puede contribuir a un mejor conocimiento de la ubicación de las cuencas sedimentarias, ya que estos datos permiten una comparación directa con las edades de los diferentes dominios peri-Gondwánicos actuales.

Los valores de T_{DM} (720 - 2223 Ma)obtenidos en las series metasedimentarias estudiadas son equivalentes a las edades publicadas para el margen N de África (*Avigad et al., 2003 y 2012; Abati et al., 2010b; Díez Fernández et al., 2010; Albert et al., 2015a; Orejana et al., 2015; y referencias ahí incluidas*), apoyando su afinidad isotópica con dominios típicamente Gondwánicos. Las T_{DM} obtenidas son en su mayoría valores paleoproterozoicos y mesoproterozoicos; teniendo en cuenta que estos valores representan una mezcla ponderada de los diferentes aportes terrígenos de las áreas fuentes adyacentes (*Murphy y Nance, 2002*), los valores muy antiguos de T_{DM} encontrados en las secuencias sedimentarias ediacarenses de las Unidades Alóctonas Basales, indican que estas unidades ocuparon durante el Neoproterozoico Superior posiciones laterales dentro de una amplia cuenca *back-arc* situada en las proximidades del Cratón del Oeste de África (Fig. 11.10). Las edades U-Pb de circones detríticos son también coherentes con esta conclusión (*Díez Fernández, et al., 2010; Pereira et al., 2012; Orejana et al., 2015*). Únicamente este área cratónica presenta edades lo suficientemente antiguas (Arcaicas - Paleoproterozoicas), como para que la mezcla resultante con áreas fuente isotópicas más jóvenes proporcione edades modelo tan antiguas. Sus características geoquímicas e isotópicas, sin descartar la influencia del arco magmático peri-Gondwánico, sitúan a estas series en los dominios de la plataforma continental más interna, donde accedían aportes terrígenos derivados de sectores muy antiguos de la corteza del N de África.

La evolución que se detecta durante el Cámbrico es compatible con la disminución de la actividad magmática del arco o el alejamiento del mismo hacia posiciones más distales del margen, como se deduce a partir de las características geoquímicas de la secuencia superior de las Unidades Basales del NW de Iberia. Esta transición se hace aun más notoria en las secuencias Cámbricas de la Zona Centroibérica (Formación Pusa). Sus valores de T_{DM} menores que los de las Unidades Basales (Fig. 11.8) sugieren una posición inicial más oriental en el margen de Gondwana (Fig. 11.10). En ambas unidades se observa una tendencia geoquímica e isotópica compatible con un ensanchamiento de la cuenca *back-arc*, y por tanto con un alejamiento de las mismas de la actividad magmática más intensa del arco volcánico. La evolución geodinámica es compatible con el comienzo de un proceso de rifting que acabará estableciendo un margen pasivo Cambro - Ordovícico, coincidente con las etapas iniciales de la apertura del Océano Reico (*Stampfli y Borel, 2002; Murphy et al., 2006; Nance et al., 2008 y 2010*).

La posición lateral relativa propuesta para las paleocuencas sedimentarias en el margen de Gondwana durante el Ediacarense y el Cámbrico Medio (Fig. 11.10), así como el contexto geodinámico en el que tuvo lugar la sedimentación, son congruentes con la distribución actual de los dominios alóctonos y autóctonos en el Macizo Ibérico. Estos dominios alóctonos presentan en el NW y SW de Iberia un apilamiento tectónico de mantos de cabalgamiento sobre un dominio parautóctono y autóctono. Este cabalgamiento tuvo lugar durante la Orogenia Varisca e implica una doble colisión oblicua, con un claro componente dextral, entre Laurussia y Gondwana (*Arenas et al., 2014; Arenas y Sánchez Martínez, 2015*). Las Unidades Superiores de los complejos alóctonos del NW de Iberia constituían la parte más externa de una amplia plataforma continental en el margen N de Gondwana. Los protolitos de estas unidades se originaron durante el Cámbrico Medio en posiciones frontales en relación al Cratón del Oeste de África, pero asentadas junto a la parte más activa de un arco volcánico. En este contexto, las Unidades Basales ocuparían una posición adyacente al dominio más continental (Fig. 11.10).

Durante un primer episodio de la colisión oblicua Varisca, las Unidades Superiores experimentaron subducción bajo Laurussia (*Arenas et al., 2014; Albert et al., 2015c; Arenas et al., 2016*), acompañada por un primer evento de HP-UHP que se registra en la sección inferior de estas unidades (ca. 400-390 Ma; *Ordóñez Casado et al., 2001; Fernández Suárez et al., 2007*). La continuación de la convergencia dextra facilitó la apertura de una amplia cuenca de tipo *pull-apart* durante el Devónico Inferior, cuyo cierre posterior dio lugar a una zona de sutura compleja caracterizada por la presencia de dos cinturones ofiolíticos de diferente origen y edad (*Arenas et al., 2014; Arenas y Sánchez Martínez, 2015*). La apertura y posterior cierre de esta cuenca *pull-apart* permitió la aproximación de secciones de la plataforma de Gondwana situadas más hacia el E. Durante una nueva colisión se desarrolló un nuevo episodio metamórfico de HP (ca. 370

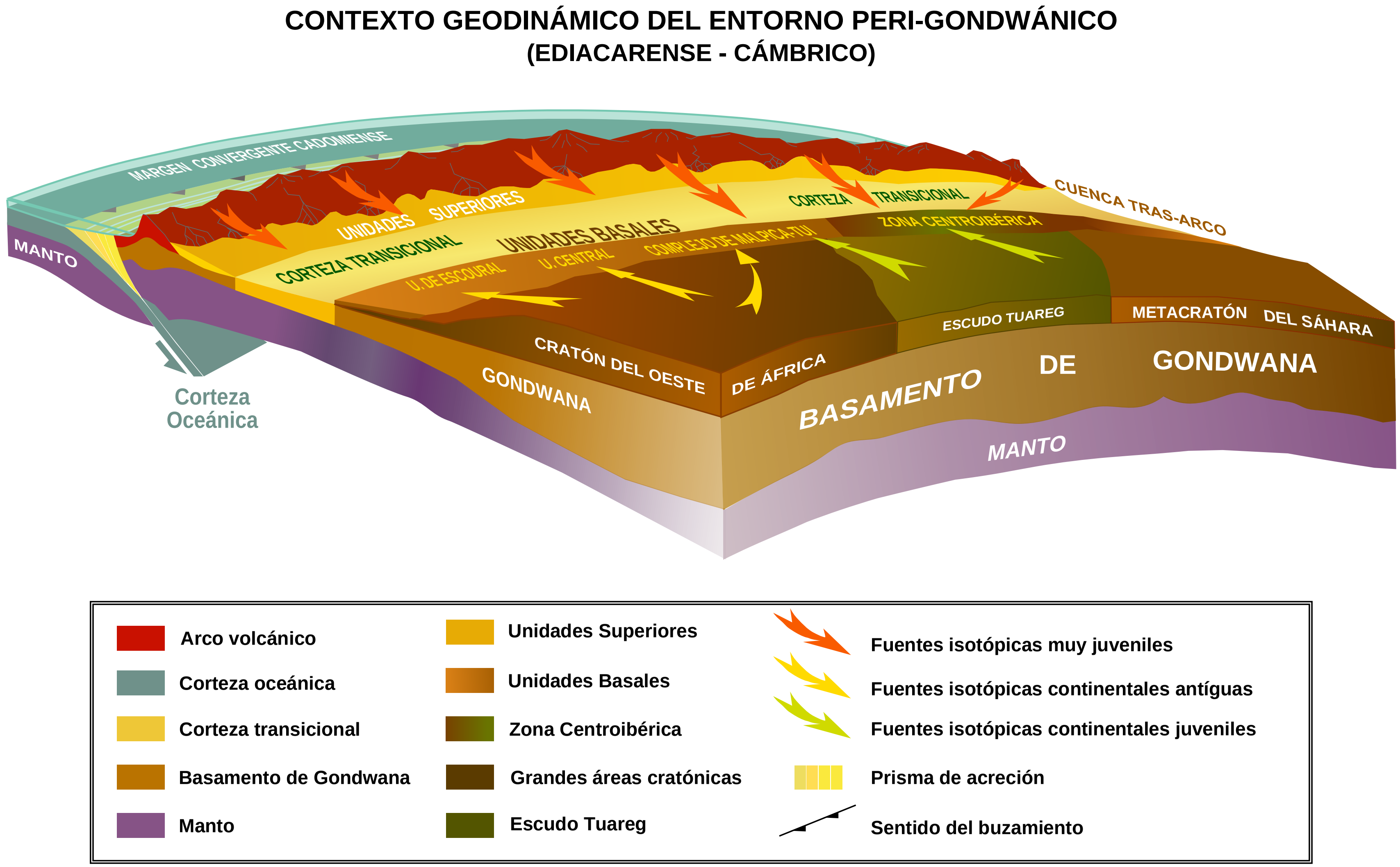

Fig. 11.10- Modelo esquemático (no a escala) de una sección del paleomargen de Gondwana durante la transición Ediacarense - Cámbrico. Se muestra la posición relativa de los terrenos peri-Gondwánicos en relación a un arco volcánico y a una amplia cuenca *back-arc* desarrollada en el marco de un margen activo Cadomiense. Las flechas incluidas muestran las probables procedencias de los materiales detríticos suministrados a cada una de las cuencas sedimentarias estudiadas. Ver el texto para una explicación más extensa.

Ma; *Abati et al., 2010a; Díez Fernández et al., 2012*), originado por la subducción profunda de una parte del margen adelgazado de Gondwana representado por las Unidades Basales Alóctonas del Macizo Ibérico (*Díez Fernández at al., 2010; Díez Fernández y Arenas, 2015*). Las secuencias sedimentarias representadas en las Unidades Basales se depositaron en la parte más interna de la cuenca marginal, junto al dominio puramente continental y en la proximidad del Cratón del Oeste de África (*Díez Fernández et al., 2010*) (Fig. 11.10). La continuación de la convergencia dextral entre ambas grandes masas continentales facilitó el acercamiento de los dominios sedimentarios representados por la Zona Centroibérica. Sus valores de T_{DM} son más jóvenes que los observados en las Unidades Basales y resultan compatibles con una posición más oriental durante el Ediacarense, en las proximidades de un dominio Gondwánico caracterizado por áreas fuente más jóvenes. Éstas estarían ubicadas en posiciones intermedias hacia el Metacratón del Sáhara (*Díez Fernández et al., 2010 y 2012; Ábalos et al., 2012; Talavera et al., 2012*), o quizás incluso en regiones todavía más hacia el E (*Bea et al., 2010; Fernández-Suárez et al., 2014*). Estos dominios autóctonos ocuparían la posición estructural inferior en el cinturón de cabalgamiento generado durante la colisión Varisca en el Macizo Ibérico. Por todo ello, la paleogeografía presentada para los terrenos peri-Gondwánicos estudiados resulta coherente tanto con una alineación de los mismos en el margen Africano de Gondwana, como con su posición estructural actual resultante de la colisión Varisca que dio lugar al ensamblado de Pangea.

El presente trabajo ha permitido comprobar que el uso de las herramientas geoquímicas e isotópicas en series sedimentarias antiguas permite conocer la influencia de contextos tectónicos concretos sobre los procesos sedimentarios y las áreas fuente asociadas a una cuenca sedimentaria particular. Estos contextos geodinámicos tuvieron un efecto importante, tanto en las procedencia de los sedimentos terrígenos, como en los procesos sedimentarios durante el relleno de las paleocuencas estudiadas, como se desprende de la observada variabilidad en los contenidos de elementos mayores y trazas registrados en las diferentes secuencias estudiadas. La posibilidad de obtener información acerca del ambiente deposicional y de la procedencia de series metasedimentarias deformadas y probablemente alteradas en eventos tectonometamórficos posteriores a su formación, supone un valor añadido a estas técnicas, que complementan los estudios llevados a cabo por métodos más tradicionales.

Capítulo 12

Referencias

12.1 Referencias

ÁBALOS, B., GIL IBARGUCHI, J.I., SÁNCHEZ-LORDA, M.E., PAQUETTE, J.L. (2012). African/Amazonian Proterozoic correlations of Iberia: A detrital zircon U-Pb study of early Cambrian conglomerates from the Sierra de la Demanda (northern Spain). Tectonics, 31, TC3003.

ABATI, J., DUNNING, G.R., ARENAS, R., DÍAZ GARCÍA, F., GONZÁLEZ CUADRA, P., MARTÍNEZ CATALÁN, J.R., ANDONAEGUI, P. (1999). Early Ordovician orogenic event in Galicia (NW Spain): evidences from U–Pb ages in the uppermost unit of the Órdenes Complex. Earth and Planetary Science Letters, 165, 213–228.

ABATI, J. (2002). Petrología Metamórfica y Geocronología de la unidad culminante del Complejo de Órdenes en la región de Carballo (Galicia, NW del Macizo Ibérico). Nova Terra, 20, 269 pp.

ABATI, J., GERDES, A., FERNÁNDEZ-SUÁREZ, J., ARENAS, R., WHITEHOUSE, M.J., DÍEZ FERNÁNDEZ, R. (2010a). Magmatism and early-Variscan continental subduction in the northern Gondwana margin recorded in zircons from the basal units of Galicia, NW Spain. Geological Society of America Bulletin, 122, 219–235.

ABATI, J., AGHZER, A.M., GERDES, A., ENNIH, N. (2010b). Detrital zircon ages of Neoproterozoic sequences of the Moroccan Anti-Atlas belt. Precambrian Research, 181, 115–128.

ALBERT, R., ARENAS, R., GERDES, A., SÁNCHEZ MARTÍNEZ, S., FERNÁNDEZ-SUÁREZ, J., FUENLABRADA, J.M. (2015a). Provenance of the Variscan Upper Allochthon (Cabo Ortegal Complex, NW Iberian Massif). Gondwana Research, 28, 1434–1448.

ALBERT, R. (2015b). The Eclogitic Gneisses of the Cabo Ortegal Complex: provenance and tectonothermal evolution (zircon U-Pb/ Lu-Hf methods). Tesis de la Universidad Complutense de Madrid, 336 pp.

ALBERT, R., ARENAS, R., GERDES, A., SÁNCHEZ MARTÍNEZ, S., MARKO, L. (2015c). Provenance of the HP-HT subducted margin in the Variscan belt (Cabo Ortegal Complex, NW Iberian Massif). Journal of Metamorphic Geology, 33, 959–979.

ALÍA MEDINA, M. (1963). Rasgos estructurales de la Baja Extermadura. Boletín de la Real Sociedad Española de Historia Natural. Sección Geológica, 61(2), 247-262.

ALVAREZ NAVA, H., GARCÍA CASQUERO, J.L., GIL TOJA, A., HERNÁNDEZ URROZ, J., LORENZO ALVAREZ, S., LÓPEZ DÍAZ, F., MIRA LÓPEZ, M., MONTESERÍN, V., NOZAL, F., PARDO, M.V., PICART, J., ROBLES, R., SANTAMARÍA, J., SOLE, F.J. (1988). Unidades litoestratigráficas de los materiales Precámbrico-Cámbricos en la mitad suroriental de la Zona Centro-Ibérica. II Congreso Geológico de España, SGE, Granada 1, 19–22.

ANDONAEGUI, P., ARENAS, R., ALBERT, A., SÁNCHEZ MARTÍNEZ, S., DÍEZ FERNÁNDEZ, R., GERDES, A. (2016). The last stages of the Avalonian–Cadomian arc in NW Iberian Massif: isotopic and igneous record for a long-lived peri-Gondwanan magmatic arc. Tectonophysics, 681, 6–14.

ARENAS, R., MARTÍNEZ CATALÁN, J.R., SÁNCHEZ MARTÍNEZ, S., FERNÁNDEZ-SUÁREZ, J., ANDONAEGUI, P., PEARCE, J.A., CORFU, F. (2007). The Vila de Cruces Ophiolite: a remnant of the early Rheic Ocean in the Variscan suture of Galicia (NW Iberian Massif). Journal of Geology, 115, 129–148.

ARENAS, R., SÁNCHEZ MARTÍNEZ, S., CASTIÑEIRAS, P., JEFFRIES, T.E., DÍEZ FERNÁNDEZ, R., ANDONAEGUI, P. (2009). The basal tectonic mélange of the Cabo Ortegal Complex (NW Iberian Massif): a key unit in the suture of Pangea. Journal of Iberian Geology, 35, 85–125.

ARENAS, R., DÍEZ FERNÁNDEZ, R., SÁNCHEZ MARTÍNEZ, S., GERDES, A., FERNÁNDEZ-SUÁREZ, J. AND ALBERT, R. (2014). Two-stage collision: Exploring the birth of Pangea in the Variscan terranes. Gondwana Research, 25, 756- 763.

ARENAS, R. AND SÁNCHEZ MARTÍNEZ, S. (2015). Variscan ophiolites in NW Iberia: Tracking lost Paleozoic oceans and the assembly of Pangea. Episodes, 38, 315-333.

ARENAS, R., DÍEZ FERNÁNDEZ, R., RUBIO PASCUAL, F.J., SÁNCHEZ MARTÍNEZ, S., MARTÍN PARRA, L.M., MATAS, J., GONZÁLEZ DEL TÁNAGO, J., JIMÉNEZ-DÍAZ, A., FUENLABRADA, J.M., ANDONAEGUI, P., GARCÍA-CASCO, A. (2016a). The Galicia – Ossa-Morena zone: proposal for a new zone of the Iberian Massif. Variscan implications. Tectonophysics, 681, 135–143.

ARENAS, R., SÁNCHEZ MARTÍNEZ, S., DÍEZ FERNÁNDEZ, R., GERDES, A., ABATI, J., FERNÁNDEZ-SUÁREZ, J., ANDONAEGUI P., GONZÁLEZ CUADRA, P., LÓPEZ CARMONA, A., ALBERT, R., FUENLABRADA, J. M., RUBIO PASCUAL, F.J. (2016b). Allochthonous terranes involved in the Variscan suture of NW Iberia: A review of their origin and tectonothermal evolution. Earth-Science Reviews, 161, 140–178.

ARMSTRONG-ALTRIN, J.S., VERMA, S.P. (2005). Critical evaluation of six tectonic setting discrimination diagrams using geochemical data of Neogene sediments fromknown tectonic settings. Sedimentary Geology, 177 (1–2), 115–129.

ARNDT N.T., GOLDSTEIN S.L. (1987). Use and abuse of crust-formation ages. Geology, 15, 893-895.

AVIGAD, D., KOLODNER, K., McWILLIAMS, M., PERSING, H., WEISSBROD, T. (2003). Origin of northern Gondwana Cambrian sandstone revealed by detrital zircon SHRIMP dating. Geology, 31, 227–230.

AVIGAD, D., GERDES, A., MORAG, N., BECHSTÄDT, T. (2012). Coupled U–Pb-Hf of detrital zircons of Cambrian sandstones from Morocco and Sardinia: Implications for provenance and Precambrian crustal evolution of North Africa. Gondwana Research, 21, 690–703.

AZCÁRRAGA, J. (2000). Evolución tectónica y metamórfica de los mantos inferiores de grado alto y alta presión del complejo de Cabo Ortegal. Nova Terra, 17, 346 pp.

BEA, F., MONTERO, P., TALAVERA, C., ABU ANBAR,M., SCARROW, J., MOLINA, J.F.,MORENO, J.A. (2010). The palaeogeographic position of Central Iberia in Gondwana during the Ordovician: evidence from zircon geochronology and Nd isotopes. Terra Nova, 22, 341–346.

BHATIA, M.R. (1983). Plate tectonics and geochemical composition of sandstones. Journal of Geology, 91, 611–627.

BHATIA, M.R. (1985). Rare earth element geochemistry of Australian Paleozoic graywackes and mudrocks: provenance and tectonic controls. Sedimentary Geology, 45, 97-113.

BHATIA, M.R., AND CROOK, K.A.W. (1986). Trace element characteristics of graywackes and tectonic setting discrimination of sedimenatry basins. Contributions to Mineralogy and Petrology, 92, 181-193.

BOUMA, A.H. (1962). Sedimentology of some Flysch Deposits; a Graphic Approach to Facies Interpretation. Elsevier Pub. Co., 168 pp.

BOUMA, A.H. (2004). Key controls on the characteristics of turbidite systems. Geological Society, London, Special Publications, 222, 9-22.

CAMBESES, A., SCARROW, J.H., MONTERO, P., LÁZARO, C., BEA, F. (2017). Palaeogeography and crustal evolution of the Ossa–Morena Zone, Southwest Iberia, and the North Gondwana margin during the Cambro-Ordovician: a review of isotopic evidence. International Geology Review, 59(1), 94–130.

CASTIÑEIRAS, P. (2005). Origen y evolución tectonotermal de las unidades de O Pino y Cariño (Complejos Alóctonos de Galicia). Nova Terra, 28, 279 pp.

CASTRO, A. (1987). Implicaciones de la Zona Ossa-Morena y dominios equivalentes en el modelo geodinámico de la Cadena Hercínica Europea. Estudios Geológicos, 43, 249–260.

CHICHORRO, M. (2006). Tectonic evolution of Montemor-o-Novo Shear Zone (SW Ossa Morena Zone - Santiago do Escoural - Cabrela Área). Universidade de Évora, Évora, Portugal, 569 pp.

COX, R., LOWE, D.R., CULLERS, R.L. (1995). The influence of sediment recycling and basement composition on evolution of mudrock chemistry in the southwestern, United States. Geochimica et Cosmochimica Acta, 59(14), 2919–2940.

CROOK, K.A.W. (1974). Lithogenesis and geotectonics: the significance of compositional variation in flysch arenites (greywackes). Society of Economical, Paleontological and Mineralogical Special Publications, 19, 304–310.

CONDIE, K.C., NOLL, P.D., CONWAY, C.M. (1992). Geochemical and detrital mode evidence for two sources of Early Proterozoic sedimentary rocks from the Tonto Basin Supergroup, central Arizona. Sedimentary Geology, 77, 51–76.

CONDIE, K.C. (1993). Chemical composition and evolution of the upper continental crust: contrasting results from surface samples and shales. Chemical Geology, 104, 1–37.

CULLERS, R.L. (1994). The controls on the major and trace element variation of shales, siltstones, and sandstones of Pennsylvanian-Permian age from uplifted continental blocks in Colorado to platform sediment in Kansas, USA. Geochimica et Cosmochimica Acta, 58, 4955-4972.

CULLERS, R.L. (1995): The controls on the major- and trace-element evolution of shales, siltstones and sandstones of Ordovician to Tertiary age in the Wet Mountains region, Colorado, U. S. A. Chemical Geology, 123, 107-131.

CULLERS, R.L., BOCK, B., GUIDOTTI, C. (1997). Elemental distributions and neodymium isotopic compositions of Silurian metasediments, western Maine, USA: redistribution of the rare earth elements. Geochimica et Cosmochimica Acta, 61, 1847–1861.

DEPAOLO, D.J., WASSERBURG, G. J. (1976a). Nd isotopic variations and petrogenic models. Geophysical Research Letters, 3, 249–252.

DEPAOLO, D.J., WASSERBURG, G.J. (1976b). Inferences about magma sources and mantle structure from variations of $^{143}Nd/^{144}Nd$. Geophysical Research Letters, 3, 743-746.

DEPAOLO, D.J. (1981). Neodymium isotopes in the Colorado Front Range and crust – mantle evolution in the Proterozoic. Nature, 291, 193–197.

DEPAOLO, D.J. (1988). Neodymium Isotope Geochemistry, an Introduction. Berlin, Springer-Verlag, 187 pp.

DICKIN, A. (1995). Radiogenic Isotope Geochemistry. Cambridge University Press, Cambridge, 492 pp.

DUNAI, T.J. (2010). Cosmogenic nuclides: principles, concepts, and applications in the earth surface sciences. Cambridge University Press, Cambridge, 198 pp.

DICKINSON, W.R. (1982). Compositions of Sandstones in Circum-Pacific Subduction Complexes and Fore-Arc Basins. American Association of Petroleum Geologists Bulletin, 66 (2), 121-137.

DICKINSON, W.R., BEARD, L.S., BRAKENRIDGE, G.R., ERJAVEE, J.R., FERGUSON, R.C., INMAN, K.F. (1983). Provenance of North American Phanerozoic Sandstones in Relation to Plate Tectonic Setting. Geological Society of American Bulletin, 94 (2), 222-235.

DICKINSON, W.R. (1985). Interpreting provenance relations from detrital modes of sandstones. In Zuffa, G.G., ed. Provenance of arenites. Dordrecht, Reidel, NATO ASI Series, 148, 333-361.

DICKINSON, W.R. (1988). Provenance and sediment dispersal in relation to paleotectonics and paleogeography of sedimentary basins. In Kleinspehn, K.L., and Paola, C., eds. New perspectives in basin analysis. Berlin, Springer, 3-25.

DICKINSON, W.R., AND SUCZEK, C.A. (1979). Plate tectonics and sandstone composition. American Association of Petroleum Geologists Bulletin, 63 (12), 2164-2172.

DÍAZ GARCÍA, F. (1990). La geología del sector occidental del Complejo de Órdenes (Cordillera Hercínica, NW de España). Nova Terra, 3, 230 pp.

DÍEZ FERNÁNDEZ, R., MARTÍNEZ CATALÁN, J.R., GERDES, A., ABATI, J., ARENAS, R., FERNÁNDEZ-SUÁREZ, J. (2010). U–Pb ages of detrital zircons from the Basal allochthonous units of NW Iberia: provenance and paleoposition on the northern margin of Gondwana during the Neoproterozoic and Paleozoic. Gondwana Research, 18, 385–399.

DÍEZ FERNÁNDEZ, R. (2011). Evolución estructural y cinemática de una corteza continental subducida: la Unidad de Malpica-Tui (NO del Macizo Ibérico). Nova Terra, 40, 228 pp.

DÍEZ FERNÁNDEZ, R., MARTÍNEZ CATALÁN, J.R., ARENAS, R., ABATI, J. (2012a). The onset of the assembly of Pangaea in NW Iberia: constraints on the kinematics of continental subduction. Gondwana Research, 22, 20–25.

DÍEZ FERNÁNDEZ, R., MARTÍNEZ CATALÁN, J.R., ARENAS, R., ABATI, J., GERDES, A., FERNÁNDEZ-SUÁREZ, J. (2012b). U–Pb detrital zircon analysis of the lower allochthon of NW Iberia: age constraints, provenance and links with the Variscan mobile belt and Gondwanan cratons. Journal of Geological Society. London, 169, 655–665.

DÍEZ FERNÁNDEZ, R., ARENAS, R. (2015). The Late Devonian Variscan suture of the Iberian Massif: A correlation of high-pressure belts in NW and SW Iberia. Tectonophysics, 654, 96–100.

DÍEZ FERNÁNDEZ, R., ARENAS, R., FRANCISCO PEREIRA, M., SÁNCHEZ MARTÍNEZ, S., ALBERT ROPER, R., MARTÍN PARRA, L. M., RUBIO PASCUAL, F. J., MATAS, J. (2016). Tectonic evolution of Variscan Iberia: Gondwana–Laurussia collision revisited. Earth-Science Reviews, 162, 269–292.

DÍEZ FERNÁNDEZ, R., FUENLABRADA, J.M., CHICHORRO, M., PEREIRA, M.F., SÁNCHEZ-MARTÍNEZ, S., SILVA, J.B., ARENAS, R. (2017). Geochemistry and tectonostratigraphy of the basal allochthonous units of SW Iberia (Évora Massif, Portugal): Keys to the reconstruction of pre-Pangean paleogeography in southern Europe. Lithos, 268-271, 285–301

DÍEZ MONTES, A. (2007). La geología del Dominio Ollo de Sapo en las comarcas de Sanabria y Terra do Bolo. Nova Terra, 34, 494 pp.

FARIAS, P. (1990). La geología de la región del Sinforme de Verín (Cordillera Herciniana, NW de España). Nova Terra, 2, 201 pp.

FAURE, G. (1986). Principles of Isotope Geology. Wiley, New York, 606 pp.

FAURE, G., AND MENSING, T.M. (2005). Isotopes: Principles and Applications. 3rd ed. Hoboken, New Jersey: John Wiley & Sons, 928 pp.

FEDO, C.M., NESBITT, H.W., YOUNG, G.M. (1995). Unraveling the effects of potassium metasomatism in sedimentary rocks and paleosols, with implications for paleoweathering conditions and provenance. Geology, 23, 921–924.

FERNÁNDEZ RODRÍGUEZ, F.J. (1997). Estructuras desarrolladas en gneises bajo condiciones de alta P y T (Gneises de Chimparra, Cabo Ortegal, A Coruña, Galicia, España). Nova Terra, 13, 250 pp.

FERNÁNDEZ-SUÁREZ, J., GUTIÉRREZ-ALONSO, G., JENNER, G.A., TUBRETT, M.N. (2000). New ideas on the Proterozoic–Early Palaeozoic evolution of NW Iberia: insights from U–Pb detrital zircon ages. Precambrian Research, 102, 185–206.

FERNÁNDEZ-SUÁREZ, J., GUTIÉRREZ-ALONSO, G., JEFFRIES, T.E. (2002). The importance of along-margin terrane transport in northern Gondwana: insights from detrital zircon parentage in Neoproterozoic rocks from Iberia and Brittany. Earth and Planetary Science Letters, 204, 75–88.

FERNÁNDEZ-SUÁREZ, J., DÍAZ GARCÍA, F., JEFFRIES, T.E., ARENAS, R., ABATI, J. (2003). Constraints on the provenance of the uppermost allochthonous terrane of the NW Iberian Massif: Inferences from detrital zircon U-Pb ages. Terra Nova, 15, 138–144.

FERNÁNDEZ-SUÁREZ, J., ARENAS, R., ABATI, J., MARTÍNEZ CATALÁN, J.R., WHITEHOUSE, M.J., JEFFRIES, T.E. (2007). U–Pb chronometry of polymetamorphic high-pressure granulites: an example from the allochthonous terranes of the NW Iberian Variscan belt. In: Hatcher Jr., R.D., Carlson, M.P., McBride, J.H., Martínez Catalán, J.R. (Eds.), 4-D Framework of Continental Crust: Geological Society of America Memoir, 200, 469–488.

FERNÁNDEZ-SUÁREZ, J., GUTIÉRREZ-ALONSO, G., PASTOR-GALÁN, D., HOFMANN, M., MURPHY, J.B., LINNEMANM, U. (2014). The Ediacaran–Early Cambrian detrital zircon record of NW Iberia: possible sources and paleogeographic constraints. International Journal of Earth Sciences, 103 (5), 1335–1357.

FLOYD, P.A., LEVERIDGE, B.E. (1987). Tectonic environment of the Devonian Gramscatho Basin, South Cornwall: Framework mode and geochemical evidence from turbiditic sandstones. Journal of Geological Society. London, 144, 531-542.

FLOYD, P.A., SHAIL, R., LEVERIDGE. B.E., FRANKE, W. (1991). Geochemistry and provenance of Rhenohercynian synorogenic sandstones: implications for tectonic environment discrimination. In: Morton, A.C., Todd, S.P., Haughton, P.D.W. (Eds.), Developments in sedimentary provenance studies. Geol. Soc. London, Spec. Publ. 57, 173-188.

GARCÍA IZQUIERDO, B., CAPOTE DEL VILLAR, R., LUNAR HERNÁNDEZ, R., MONTERRUBIO, S. (2011). Evolución geodinámica y procesos mantélicos en el Macizo de Herbeira, Complejo de Cabo Ortegal (NO de la Península Ibérica). Nova Terra, 39, 246p.

GLEASON, J.D., PATCHETT, P.J., RUIZ, W.R.D. (1994). Nd isotopes link Ouachita turbidites to Appalachian sources. Geology, 22, 347–350.

GOLDSTEIN, S.L., O'NIONS, R.K., HAMILTON, P.J. (1984). A Sm–Nd isotopic study of atmospheric dusts and particulates from major river systems. Earth and Planetary Science Letters, 70, 221–236

GÓMEZ BARREIRO, J. (2007). La Unidad de Fornás: Evolución tectonometamórfica del SO del Complejo de Órdenes. Nova Terra, 32, 291 pp.

GONZÁLEZ CUADRA, P. (2007). La Unidad de Corredoiras (Complejo de Órdenes, Galicia): Evolución estructural y metamórfica. Nova Terra, 33, 254 pp.

GUTIÉRREZ ALONSO, G., FERNÁNDE SUÁREZ, J., JEFFRIES, T.E., JENNER, G.A., TUBRETT, M.N., COX, R., JACKSON, S.E. (2003). Terrane accretion and dispersal in the northern Gondwana margin. An Early Paleozoic analogue of a long-lived active margin. Tectonophysics, 365, 221–232.

HAWKESWORTH C.J., DHUIME, B., PIETRANIK, A.B., CAWOOD, P.A., KEMP, A.I.S., STOREY, C.D. (2010). The generation and evolution of the continental crust. Journal of the Geological Society. London, 167, 229–248

HENDERSON, P. (1982). Inorganic Geochemistry. Pergamon Press, Oxford, 364 pp.

HENDERSON, P. (1984). Rare Earth Element Geochemistry. Developments in Geochemistry 2. Elsevier, Amsterdam. 510 pp.

HELLER, P.L., PETERMAN, Z.E., O'NEAL, J.R., SHAFIQULLAH, M. (1985). Isotopic provenance of sandstones from the Eocene Tyee Formation, Oregon Coast Range. Geological Society of America Bulletin, 96, 770-780.

HEUMANN, K.G. (1986). Isotope-dilution mass spectrometry of inorganic and organic substances. Fresenius' Zeitschrift fuer Analytische Chemie, 325, 661-666.

JACOBSEN, S.B. Y WASSERBURG, G.J. (1980). Sm-Nd isotopic evolution of chondrites. Earth and Planetary Science Letters, 50 (1), 139-155.

JACOBSEN, S.B. Y WASSERBURG, G.J. (1984). Sm-Nd isotopic evolution of chondrites and achondrites, II. Earth and Planetary Science Letters, 67, 137-150.

JENSEN, S., PALACIOS, T., MARTÍ MUS, M. (2007). A brief review of the fossil record of the Ediacaran–Cambrian transition in the area of Montes de Toledo-Guadalupe, Spain. In: Komarover, P., Vickers-Rich (Eds.), The Rise and Fall of the Ediacaran Biota. Geological Society of London, London, UK, 223–235.

JOHNSSON, M.J. (1993). The system controlling the composition of clastic sediments. Geological Society of America, Special Papers, 284, 1-20,

JULIVERT, M., FONTBOTÉ, J.M., RIBEIRO, A., CONDE, L. (1972). Mapa Tectónico de la Península Ibérica y Baleares E. 1:1.000.000. Instituto Geológico y Minero de España, Madrid.

LINNEMANN, U., ROMER, R.L. (2002). The Cadomian Orogeny in Saxo-Thuringia, Germany: geochemical and Nd–Sr–Pb isotopic characterization of marginal basins with constraints to geotectonic setting and provenance. Tectonophysics, 352, 33–64.

LINNEMANN, U., MCNAUGHTON, N.J., ROMER, R.L., GEHMLICH, M., DROST, K., TONK, C. (2004). West African provenance for Saxo-Thuringia (Bohemian Massif): did Armorica ever leave pre-Pangean Gondwana?—U/Pb-SHRIMP zircon evidence and the Nd isotopic record. International Journal of Earth Sciences, 93, 683–705.

LINNEMANN, U., GERDES, A., DROST, K., BUSCHMANN, B. (2007). The continuum between Cadomian orogenesis and opening of the Rheic Ocean: constraints from LA-ICP-MS U–Pb zircon dating and analysis of plate-tectonic setting (Saxo-Thuringian zone, northeastern Bohemian Massif, Germany). In: Linnemann, U., Nance, R.D., Kraft, P., Zulauf, G. (Eds.), The evolution of the Rheic Ocean: From Avalonian–Cadomian Active Margin to Alleghenian–Variscan collision: Geological Society of America, Special Paper, 423, 61–96.

LINNEMANN, U., PEREIRA, M.F., JEFFRIES, T., DROST, K., GERDES, A. (2008). Cadomian Orogeny and the opening of the Rheic Ocean: new insights in the diacrony of geotectonic processes constrained by LA–ICP–MS U-Pb zircon dating (Ossa–Morena and Saxo-Thuringian Zones, Iberian and Bohemian Massifs). Tectonophysics, 461, 21–43.

LINNEMANN, U., GERDES, A., HOFMANN, M., MARKO, L. (2014). The Cadomian Orogen: Neoproterozoic to Early Cambrian crustal growth and orogenic zoning along the periphery of the West African Craton — Constraints from U–Pb zircon ages and Hf isotopes (Schwarzburg Antiform, Germany). Precambrian Research, 244, 236–278.

LLANA-FUÑEZ, S. (2001). La estructura de la Unidad de Malpica-Tui (Cordillera Varisca en Iberia). Serie Tesis Doctorales, 1, IGME, Madrid, 295 pp.

LÓPEZ CARMONA, A. (2015). Blueschist-facies rocks from the Malpica-Tui Complex (NW Iberian Massif). Nova Terra, 47, 299 pp.

LÓPEZ-GUIJARRO, R., ARMENDARIZ, M., QUESADA, C., FERNÁNDEZ-SUÁREZ, J., MURPHY, J.B., PIN, C., BELLIDO, F. (2008). Ediacaran-Palaeozoic tectonic evolution of the Ossa Morena and Central Iberian zones (SW Iberia) as revealed by Sm–Nd isotope systematics. Tectonophysics, 461, 202–214.

LOTZE, F. (1945). Zur gliederung der varisziden der Iberischen Meseta. Geotektonische Forschungen, 6, 78-92.

LUGMAIR, G.W., CARLSON, R.W. (1978). The Sm-Nd History of KREEP. Lunar and Planetary Science Conference, 9th. Houston, Tex. Proceedings. Vol. 1. New York, Pergamon Press, Inc., 689-704.

LUGMAIR, G.W., MARTI, K. (1978). Lunar Initial $^{143}Nd/^{144}Nd$: Differential evolution of the lunar crust and mantle. Earth and Planetary Science Letters, 39, 349-357.

MAAS, R., MCCULLOCH, M.T. (1991). The provenance of Archean clastic metasediments in the Narryer Geniss Complex, Western Australia: trace element geochemistry, Nd isotopes, and U-Pb ages for detrital zircons. Geochimica et Cosmochimica Acta, 55, 1915-1932.

MAKISHIMA, A. (2016). Thermal Ionization Mass Spectrometry (TIMS): Silicate Digestion, Separation, Measurement. Wiley-VCH, 376 pp.

MARTÍNEZ CATALÁN, J.R., ARENAS, R., DÍAZ GARCÍA, F., GÓMEZ BARREIRO, J., GONZÁLEZ CUADRA, P., ABATI, J., CASTIÑEIRAS, P., FERNÁNDEZ-SUÁREZ, J., SÁNCHEZ MARTÍNEZ, S., ANDONAEGUI, P., GONZÁLEZ CLAVIJO, E., DÍEZ MONTES, A., RUBIO PASCUAL, F.J., VALLE AGUADO, B. (2007). Space and time in the tectonic evolution of the northwestern Iberian Massif. Implications for the Variscan belt. In: Hatcher, R.D., Carlson, M.P., Mcbride, J.H., Martínez Catalán, J.R. (Eds.), 4-D Framework of Continental Crust. Geological Society of America Memoir, Boulder, Colorado, 403–423.

MARTÍNEZ CATALÁN, J.R., ARENAS, R., ABATI, J., SÁNCHEZ MARTÍNEZ, S., DÍAZ GARCÍA, F., FERNÁNDEZ-SUÁREZ, J., GONZÁLEZ CUADRA, P., CASTINEIRAS, P., GÓMEZ BARREIRO, J., DÍEZ MONTES, A., GONZÁLEZ CLAVIJO, E., RUBIO PASCUAL, F.J., ANDONAEGUI, P., JEFFRIES, T.E., ALCOCK, J.E., DÍEZ FERNÁNDEZ, R., LÓPEZ CARMONA, A. (2009). A rootless suture and the loss of the roots of a mountain chain: the Variscan belt of NW Iberia. Comptes Rendus Geoscience, 341 (2–3), 114–126.

MATTE, P. (1986). Tectonics and plate tectonics model for the Variscan belt of Europe. Tectonophysics, 126 (2–4), 329–374.

MATTE, P. (1991). Accretionary history and crustal evolution of the Variscan belt in Western Europe. Tectonophysics, 196, 309–337.

McCULLOCH, M.T. AND WASSERBURG, G.J. (1978). Sm-Nd and Rb-Sr chronology of continental crust formation. Science, 200, 1003-1011.

McLENNAN, S.M. (1989). Rare earth elements in sedimentary rocks: Influence of provenance and sedimentary processes: Mineralogy Society of America. Reviews in Mineralogy, 21, 169-200.

McLENNAN, S.M, McCULLOCH, M.T., TAYLOR, S.R., MAYNARD, J.B. (1989). Effects of sedimentary sorting on neodymium isotopes in deep-sea turbidites. Nature, 337, 547-549.

McLENNAN, S.M., TAYLOR, S.R., McCULLOCH, M.T., MAYNARD, J.B. (1990). Geochemical and Nd-Sr isotopic composition of deep-sea turbidites: crustal evolution and plate tectonic associations. Geochimica et Cosmochimica Acta, 54, 2015-2050.

McLENNAN, S.M., TAYLOR, S.R. (1991). Sedimentary rocks and crustal evolution: tectonic setting and secular trends. Journal of Geology, 99, 1–21.

McLENNAN, S.M., HEMMING, S. (1992). Samarium/neodymium elemental and isotopic systematics in sedimentary rocks. Geochimica et Cosmochimica Acta, 56 (3), 887-898.

McLENNAN, S.M., HEMMING, S., McDANIEL, D.K., HANSON, G.N. (1993). Geochemical approaches to sedimentation, provenance, and tectonics. In M. J. Johnsson, & A. Basu (Eds.), Processes Controlling the Composition of Clastic Sediments (pp. 21–40). Boulder, CO, USA: Geological Society of America, Special Paper.

McLENNAN, S.M., HEMMING, S.R., TAYLOR, S.R., ERIKSSON, K.A. (1995). Early Proterozoic crustal evolution: Geochemical and Nd-Pb isotopic evidence from metasedimentary rocks, southwestern North America. Geochimica et Cosmochimica Acta, 59, 1153-1177.

McLENNAN, S.M. (2001). Relationships between the trace element composition of sedimentary rocks and upper continental crust. Geochemistry, Geophysics, Geosystems, 2, 1021.

MENDIA, M. (2000). Petrología de la Unidad Eclogítica del Complejo de Cabo Ortegal (NW de España). Nova Terra, 16, 424 pp.

MILLER, R.G., O'NIONS, R.K. (1984). The provenance and crustal residence ages of British sediments in relation to palaeogeographic reconstructions. Earth and Planetary Science Letters, 68, 459–470.

MILLER, R.G., O'NIONS, R.K., HAMILTON, P.J., WELIN, E. (1986). Crustal residence ages of clastic sediments, orogeny and continental evolution. Chemical Geology, 57, 87-99.

MOITA, P., MUNHÁ, J., FONSECA, P.E., PEDRO, J., TASSINARI, C.C.G., ARAÚJO, A., PALACIOS, T. (2005). Phase equilibria and geochronology of Ossa-Morena eclogites. Presented at the XIV Semana de Geoquímica, VIII Congresso de Geoquímica dos Paises de Lingua Portuguese, Aveiro, Portugal, 463–466.

MORAG, N., AVIGAD, D., GERDES, A., HARLAVAN, Y. (2012). 1000–580 Ma crustal evolution in the northern Arabian–Nubian Shield revealed by U–Pb–Hf of detrital zircons from late Neoproterozoic sediments (Elat area, Israel). Precambrian Research, 208–211, 197–212.

MURPHY, J.B., NANCE, R.D. (1987). Model for the evolution of the Avalonian–Cadomian belt. Geology, 17, 735–738.

MURPHY, J.B., NANCE, R.D. (1991). Supercontinent model for the contrasting character of Late Proterozoic Orogenic belts. Geology, 19, 469–472.

MURPHY, J.B., NANCE, R.D. (2002). Sm–Nd isotopic systematics as tectonic tracers: an example from West Avalonia in the Canadian Appalachians. Earth Science Reviews, 59 (1–4), 77–100.

MURPHY, J.B., PISAREVSKY, S.A., NANCE, R.D., KEPPIE, J.D. (2004). Neoproterozoic Early Paleozoic evolution of peri-Gondwanan terranes: implications for Laurentia–Gondwana connections. International Journal of Earth Sciences, 93, 659–682.

MURPHY, J.B., GUTIÉRREZ-ALONSO, G., NANCE, R.D., FERNÁNDEZ-SUÁREZ, J., KEPPIE, J.D., QUESADA, C., STRACHAN, R.A., DOSTAL, J. (2006). Origin of the Rheic Ocean: Rifting along a Neoproterozoic suture? Geology, 34, 325–328.

NANCE, R.D., MURPHY, J.B., STRACHAN, R.A., D'LEMOS, R.S., TAYLOR, G.K. (1991). Late Proterozoic tectonostratigraphic evolution of the Avalonian and Cadomian terranes. Precambrian Research, 53, 41–78.

NANCE, R.D., MURPHY, J.B., STRACHAN, R.A., KEPPIE, J.D., GUTIERREZ-ALONSO, G., FERNANDEZ-SUAREZ, J., QUESADA, C., LINNEMANN, U., D'LEMOS, R., PISARE-

VSKY, S.A. (2008). Neoproterozoic–early Palaeozoic tectonostratigraphy and palaeogeography of the peri-Gondwanan terranes: Amazonian vs West African connections. Geological Society, London, Special Publications, 297 (1), 345–383.

NANCE, R.D., GUTIÉRREZ-ALONSO, G., KEPPIE, J.D., LINNEMANN, U., MURPHY, J.B., QUESADA, C., STRACHAN, R.A., WOODCOCK, N.H. (2010). Evolution of the Rheic Ocean. Gondwana Research, 17, 194–222.

NELSON, B.K., DEPAOLO, D.J. (1988a). Application of Sm–Nd and Rb–Sr isotope systematics to studies of provenance and basin analysis. Journal of Sedimentary Petrology, 58, 348–357.

NELSON, B.K., DEPAOLO, D.J. (1988b). Comparison of isotopic and petrographic provenance indicators in sediments from Tertiary continental basins of New Mexico. Journal of Sedimentary Petrology, 58, 348– 357.

NESBITT, H.W., MARKOVICS, G., PRICE, R.C. (1980). Chemical processes affecting alkali and alkaline earth during continental weathering. Geochimica et Cosmochimica Acta, 44, 1659-1666.

NESBITT, H.W., YOUNG, G.M. (1982). Early Proterozoic climates and plate motions inferred from major element chemistry of lutites. Nature, 299, 715-717.

NESBITT, H.W., YOUNG, G.M. (1996). Petrogenesis of sediments in the absence of chemical weathering: effects of abrasion and sorting on bulk composition and mineralogy. Sedimentology, 43, 341-358.

NESBITT, H.W., YOUNG, G.M., McLENNAN, S.M., KEAYS, R.R. (1996). Effects of chemical weathering and sorting on the petrogenesis of siliciclastic sediments, with implications for provenance studies. Journal of Geology, 104, 525-542.

O'NIONS, R.K., CARTER, S.R., EVENSEN, N.M., HAMILTON, P.J. (1979). Geochemical and Cosmochemical Applications of Nd Isotope Analysis. Annual Review of Earth and Planetary Sciences, 7, 11-38

O'NIONS, R.K., HAMILTON, P.J., HOOKER, P.J. (1983). A Nd isotope investigation of sediments related to crustal development in the British Isles. Earth and Planetary Science Letters, 63, 229–240.

ORDÓÑEZ CASADO, B., GEBAUER, D., SCHÄFER, H.J., GIL IBARGUCHI, J.I., PEUCAT, J.J. (2001). A single Devonian subduction event for the HP/HT metamorphism of the Cabo Ortegal complex within the Iberian Massif. Tectonophysics, 332, 359-385.

OREJANA, D., MERINO MARTÍNEZ, E., VILLASECA, C., ANDERSEN, T. (2015). Ediacaran–Cambrian paleogeography and geodynamic setting of the Central Iberian Zone: constraints from coupled U–Pb–Hf isotopes of detrital zircons. Precambrian Research, 261, 234–251.

PEREIRA, M.F., CHICHORRO, M., LINNEMANN, U., EGUILUZ, L., SILVA, J.B. (2006). Inherited arc signature in Ediacaran and Early Cambrian basins of the Ossa-Morena Zone (Iberian Massif, Portugal): paleogeographic link with European and North African Cadomian correlatives. Precambrian Research, 144, 297–315.

PEREIRA, M.F., SILVA, J.B., CHICHORRO, M., MOITA, P., SANTOS, J.F., APRAIZ, A., RI-

BEIRO, C. (2007). Crustal growth and deformational processes in the northern Gondwana margin: constraints from the Évora Massif (Ossa-Morena Zone, southwest Iberia, Portugal). In: Linnemann, U., Nance, R.D., Kraft, P., Zulauf, G. (Eds.), The evolution of the Rheic Ocean: From Avalonian-Cadomian active margin to Alleghenian-Variscan collision. Geological Society of America, Special Paper 423, 333–358.

PEREIRA, M.F., CHICHORRO, M., WILLIAMS, I.S., SILVA, J.B. (2008). Zircon U–Pb geochronology of paragneisses and biotite granites from the SW Iberian Massif (Portugal): evidence for a palaeogeographical link between the Ossa–Morena Ediacaran basins and the West African Craton. Geological Society. London, Special Publications 297, 385–408.

PEREIRA, M.F., LINNEMANN, U., HOFMANN, M., CHICHORRO, M., SOLÁ, A.R., MEDINA, J., SILVA, J.B. (2012). The provenance of Late Ediacaran and Early Ordovician siliciclastic rocks in the Southwest Central Iberian Zone: constraints from detrital zircon data on northern Gondwana margin evolution during late Neoproterozoic. Precambrian Research, 192–195, 166–189.

PETTIJOHN, F.J., POTTER, P.E., SIEVER, R. (1972). Sand and Sandstone. Springer-Verlag, Berlin, 241 pp.

PIEREN PIDAL, A.P. (2000). Las sucesiones anteordovícicas de la región oriental de la provincial de Badajoz y área contigua de la de Ciudad Real. Tesis de la Universidad Complutense de Madrid. 379 pp.

PRICE, J.R., VELBEL, M.A. (2003). Chemical weathering indices applied to weathering profiles developed on heterogeneous felsic metamorphic parent rocks. Chemical Geology, 202, 397-416.

PUELLES, P. (2004). Deformación, metamorfismo y exhumación de las granulitas de alta presión de la Bacariza (Complejo de Cabo Ortegal, NO de España). Nova Terra, 23, 411 pp.

RACZEK, I., JOCHUM, K.P., HOFMANN, A.W. (2003). Neodymium and Strontium Isotope Data for USGS Reference Materials BCR-1, BCR-2, BHVO-1, BHVO-2, AGV-1, AGV-2, GSP-1, GSP-2 and Eight MPI-DING Reference Glasses. Geostandards Newsletter, 27, 173–179.

RICHARD, P., SHIMIZU, N., ALLÈGRE, C.J. (1976). $^{143}Nd/^{146}Nd$, a natural tracer: an application to oceanic basalts. Earth and Planetary Science Letters, 31, 269–78.

RODRÍGUEZ ALLER, J. (2005). Recristalización y deformación de litologías supracorticales sometidas a metamorfismo de alta presión (Complejo de Malpica-Tuy, NO del Macizo Ibérico). Nova Terra, 29, 410 pp.

RODRÍGUEZ ALONSO, M.D., PEINADO, M., LÓPEZ-PLAZA, M., FRANCO, P., CARNICERO, A., GONZALO, J.C. (2004). Neoproterozoic–Cambrian synsedimentary magmatism in the Central Iberian Zone (Spain): geology, petrology and geodynamic significance. International Journal of Earth Sciences, 93, 897–920.

ROSER, B.P., KORSCH, R.J. (1986). Determination of tectonic setting of sandstone-mudstone suites using SiO_2 content and K_2O/Na_2O ratio. Journal of Geology, 94, 635-660.

ROSER, B.P., KORSCH, R.J. (1988). Provenance signatures of sandstone-mudstone suites determined using discriminant function analysis of major-element data. Chemical Geology, 67, 119-139.

RUBIO-ORDÓÑEZ, A., GUTIÉRREZ-ALONSO, G., VALVERDE-VAQUERO, P., CUESTA, A., GALLASTEGUI, G., GERDES, A., CÁRDENES, V. (2015). Arc-related Ediacaran magmatism along the northern margin of Gondwana: Geochronology and isotopic geochemistry from northern Iberia. Gondwana Research, 27 (1), 216–227.

RUBIO PASCUAL, F.J. (2013). Evolución tectonotermal varisca del Sistema Central en Somosierra - Honrubia. Nova Terra, 44, 364 pp.

SÁNCHEZ MARTÍNEZ, S. (2009). Geoquímica y geocronología de las ofiolitas de Galicia. Nova Terra, 37, 351 pp.

SÁNCHEZ MARTÍNEZ, S., ARENAS, R., FERNÁNDEZ-SUÁREZ, J., JEFFRIES, T.E. (2009). From Rodinia to Pangaea: ophiolites from NW Iberia as witness for a long-lived continental margin. In: Murphy, J.B., Keppie, J.D., Hynes, A.J. (Eds.), Ancient Orogens and Modern Analogues. Geological Society of America, Special Paper 327, 317–341.

SAN JOSÉ, M.A., PIEREN, A.P., GARCÍA HIDALGO, F.J., VILAS, L., HERRANZ, P., PELÁEZ, J.R., PEREJÓN, A. (1990). Central Iberian Zone: ante-Ordovician stratigraphy. In: Dallmeyer, R.D., Martínez García, E. (Eds.), Pre-Mesozoic Geology of Iberia. Springer, Berlin Heidelberg New York, 147–159.

SANTOS ZALDUEGUI, J.F. (1995). Geocronología y geoquímica isotópica de diferentes unidades de los complejos alóctonos de Cabo Ortegal y Malpica-Tuy (NO de España). Nova Terra, 11, 177pp.

STAMPFLI, G.M., VON RAUMER, J., BOREL, G.D. (2002). The Palaeozoic evolution of pre-Variscan terranes: From peri-Gondwana to the Variscan collision. In Martínez-Catalán, J.R., Hatcher, R.D., Arenas, R. and Díaz García, F. (eds.), Variscan Appalachian Dynamics: the building of the Upper Paleozoic basement. Geological Society of America, Special Paper 364, 263-280.

STAMPFLI, G.M., BOREL, G.D. (2002). A plate tectonic model for the Paleozoic and Mesozoic constrained by dynamic plate boundaries and restored synthetic oceanic isochrons. Earth and Planetary Science Letters, 196, 17–33.

STAMPFLI, G.M., HOCHARD, C., VÉRARD, C., WILHEM, C., VON RAUMER, J. (2013). The formation of Pangea. Tectonophysics, 593, 1–19.

SUN, S., McDONOUGH, W.F. (1989). Chemical and isotopic systematics of oceanic basalts: implications for mantle composition and processes. In: Sauders, A.D., Norry, M.J. (Eds.), Magmatism in the Ocean Basins. Geological Society, Special Publication 42, 313–345

TALAVERA, C. (2009). Pre-Variscan magmatism of the Central Iberian Zone: chemical and isotope composition, geochronology and geodynamic significance. Tesis Universidad de Granada.

TALAVERA, C., MONTERO, P., MARTÍNEZ POYATOS, D., WILLIAMS I.S. (2012). Ediacaran to Lower Ordovician age for rocks ascribed to the Schist–Graywacke Complex (Iberian Massif, Spain): evidence from detrital zircon SHRIMP U–Pb geochronology. Gondwana Research, 22, 928–942.

TAYLOR, S.R., McLENNAN, S.M., McCULLOCH, M.T. (1983). Geochemistry of loess, continental crustal composition and crustal model ages. Geochimica et Cosmochimica Acta, 47, 1897-1905.

TAYLOR, S.R., McLENNAN, S.M. (1985). The Continental Crust: Its Composition and Evolution. Blackwell, Oxford, 312 pp.

UGIDOS, J.M., ARMENTEROS, I., BARBA, P., VALLADARES, M.I., COLMENERO, J.R. (1997a). Geochemistry and petrology of recycled orogen derived sediments: a case study from the Upper Precambrian siliciclastic rocks of the Central Iberian Zone, Iberian Massif, Spain. Precambrian Research, 84, 163-180.

UGIDOS, J.M., VALLADARES, M.I., RECIO, C., ROGERS, G., FALLICK, A.E., STEPHENS, W.E. (1997b). Provenance of Upper Precambrian/Lower Cambrian shales in the Central Iberian Zone. Spain: evidence from a chemical and isotopic study. Chemical Geology, 136, 55-70.

UGIDOS, J.M., BILLSTRÖM, K., VALLADARES, M.I., BARBA, P. (2003). Geochemistry of the Upper Neoproterozoic and Lower Cambrian siliciclastic rocks and U–Pb dating on detrital zircons in the Central Iberian Zone, Spain. International Journal of Earth Sciences, 92, 661–676.

VALLADARES, M.I., BARBA, P., UGIDOS, J.M., COLMENERO, J.R., ARMENTEROS, I. (2000). Upper Neoproterozoic–Lower Cambrian sedimentary successions in the Central Iberian Zone (Spain): sequence stratigraphy, petrology and chemostratigraphy. Implications for other European zones. International Journal of Earth Sciences, 89, 2–20.

VERMA, S.P., ARMSTRONG-ALTRIN, J.S. (2016). Geochemical discrimination of siliciclastic sediments from active and passive margin settings. Sedimentary Geology, 332, 1–12.

VIDAL, G., JENSEN, S., PALACIOS, T. (1994a). Neoproterozoic (Vendian) ichnofossils from Lower Alcudian strata in central Spain. Geological Magazine, 131 (2), 169–179.

VIDAL, G., PALACIOS, T., GÁMED-VINTANED, J.A., DÍEZ BALDA, M.A., GRANT, S.W. (1994b). Neoproterozoic–early Cambrian geology and paleontology of Iberia. Geological Magazine, 131 (2), 729–765.

WINCHESTER, J.A., MAX, M.D. (1989). Tectonic setting discrimination in clastic sequences: an example from the late proterozoic Erris Group, NW Ireland. Precambrian Research, 45, 191–201.

WHITE, W.M. (2015). Isotope Geochemistry. 1st ed. Wiley-Blackwell, 496 pp.

WILSON, S.A. (1997). Data compilation for USGS reference material BHVO-2, Hawaiian Basalt. U.S. Geological Survey, Open File Rep.

WRONKIEWICZ, D.J., CONDIE, K.C. (1987). Geochemistry of Archean shales from the Witwatersrand Supergroup, South Africa: source-area weathering and provenance. Geochimica and Cosmochimica Acta, 51, 2401–2416.

ZAVALA, C., ARCURI, M. (2016). Intrabasinal and extrabasinal turbidites: Origin and distinctive characteristics. Sedimentary Geology, 337, 36–54.

El estudio geoquímico e isotópico de las series metasedimentarias del Macizo Ibérico ofrece una valiosa aproximación al contexto geodinámico presente durante su sedimentación, así como a la procedencia de los materiales terrígenos que se depositaron en cuencas próximas al Cratón del Oeste de África, permitiendo la reconstrucción del paleomargen de Gondwana durante la transición Ediacarense - Cámbrico.

Metagrauvacas de las Unidades Alóctonas Superiores en la localidad de Redes (A Coruña). Excursión del proyecto IGCP-497, “The Rheic Ocean - its origin, evolution and correlatives” (julio de 2007).